



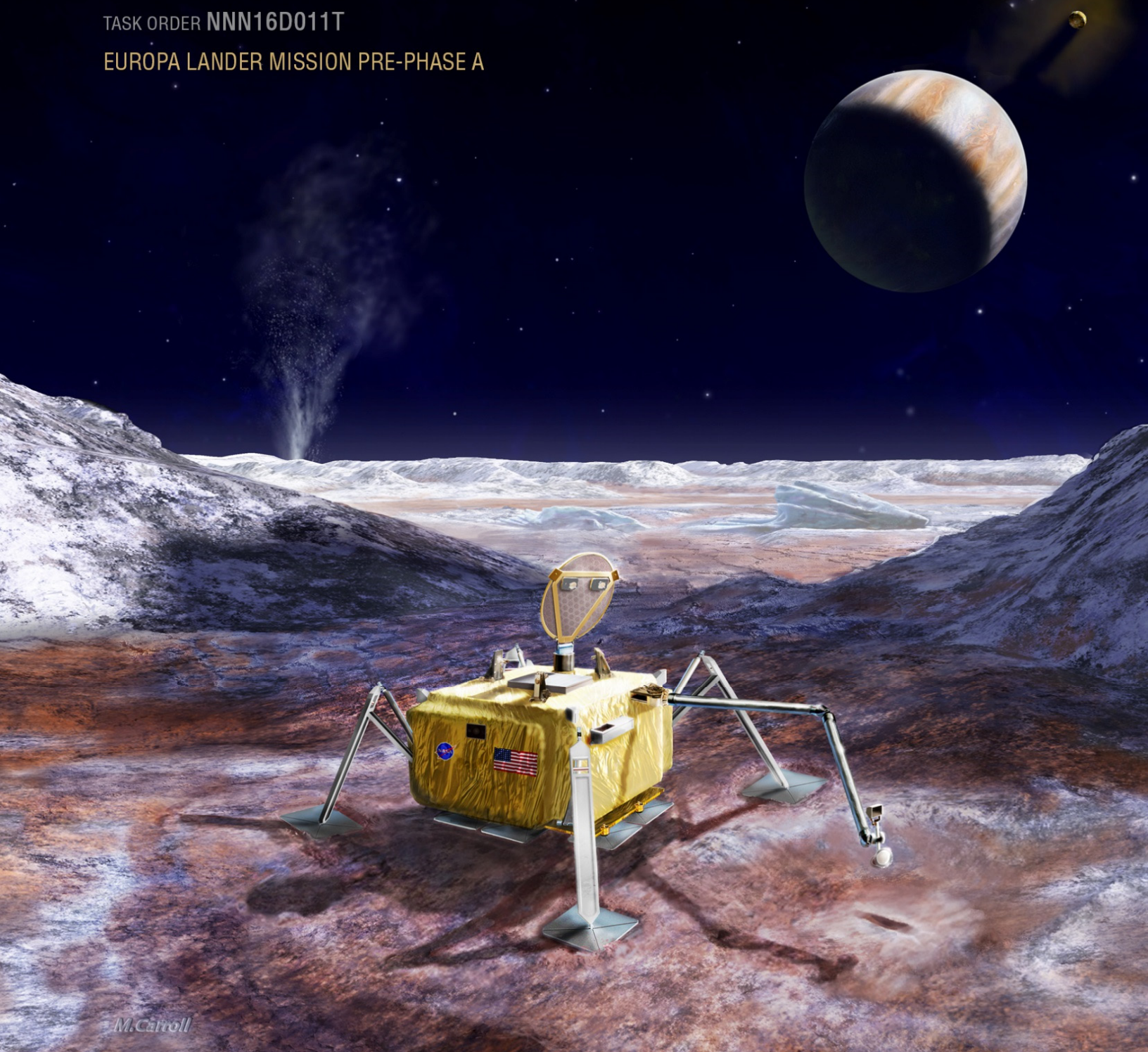
EUROPA LANDER STUDY 2016 REPORT

EUROPA LANDER MISSION

JPL D-97667

TASK ORDER NNN16D011T

EUROPA LANDER MISSION PRE-PHASE A



EUROPA LANDER MISSION CONCEPT TEAM

Science Definition Team *(affiliations provided in Chapter 1)*

Co-Chairs: Dr. K. P. Hand, Prof. A. E. Murray, Dr. J. B. Garvin,

Dr. W. B. Brinckerhoff
Prof. B. C. Christner
Dr. K. S. Edgett
Prof. B. L. Ehlmann
Dr. C. R. German
Prof. A. G. Hayes

Dr. T. M. Hoehler
Prof. S. M. Horst
Prof. J. I. Lunine
Prof. K. H. Nealson
Dr. C. Paranicas
Prof. B. E. Schmidt

Dr. D. E. Smith
Prof. A. R. Rhoden
Dr. M. J. Russell
Prof. A. S. Templeton
Dr. P. A. Willis
Dr. R. A. Yingst

Project – Science

Jet Propulsion Laboratory, California Institute of Technology

Hand, K. P. Cable, M. L. Hofmann, A. E. Pappalardo, R. T.
Phillips, C. B. Craft, K. L. (APL-JHU) Nordheim, T. A.

Project – Engineering

Jet Propulsion Laboratory, California Institute of Technology

Goldstein, B., Sabahi, D., Thurman, S. W., Dooley, J. A., Sell, S. W., Krajewski, J. A., Sukhatme, K. G., Syvertson, M. L.

Arakaki, G. A.	Dubord, L. A.	Kokorowski, M	Roberts, E. T.
Avila, A.	Elliott, J.O.	Kulkarni, T. P.	San Martin, A. M.
Bailey, E. S.	Ellyin, R.	Lam, R. L.	Shiple, M. D.
Bauer, B. A.	Estabrook, P.	Lancaster, J. D.	Shiraishi, L. R.
Beckwith, K. G.	Ewell, R. C.	Landau, D.	Skulsky, E. D.
Bhandari, P.	Frick, A.	Laubach, S. L.	Smith, M. W.
Bolotin, G. S.	Greco, M. E.	Lin, J. C.	Spaulding, M. D.
Boykins, K. T.	Harris, J. R.	McElrath, T. P.	Stehly, J. S.
Brandon, E. J.	Heverly, M. C.	Montgomery, R. H.	Tan-Wang, G. H.
Bugga, R. V.	Ilott, P. A.	Murphy, J.	Thompson, A.
Burns, B.	Johnson, B. A.	Park, E. L.	Truong, H. D.
Carr, G. A.	Jun, I.	Parker, J. M.	Warner, N. Z.
Chen, Y.	Kawata, J. M.	Ratliff, J. M.	Yahnker, C. R.
Cook, B. T.	Kipp, D. M.	Reeves, G. E.	Young, M. E.
Davis, G. L.	Klesh, A. T.	Reiz, J. M.	Zimmer, A. K.
DeBruin, K. J.			

Applied Physics Lab, Johns Hopkins University (APL-JHU)

Magner, T., Adams, D., Bedini, P., Mehr, L., Sheldon, C., Vernon, S.

Bailey, V.	Haapala-Chalk, A.	Kahler, F.	Roth, D.
Briere, M.	Hartka, T.	Murray, K.	Schwartz, P.
Butler, M.	Holdridge, M.	Napolillo, D.	Wolfarth, L.
Davis, A.	Hong, A.	Norkus, M.	
Ensor, S.	Hunt, J.	Pfisterer, R.	
Gannon, M.	Iskow, J.	Porter, J.	

Goddard Space Flight Center

Cardiff, E. H. Davis, A. Grob, E. W.

Marshall Space Flight Center

Adam, J. R. Betts, E. Norwood, J.

NASA HEADQUARTERS

This report was initiated through a task order request from, and subsequently delivered to, the following officials at NASA Headquarters:

C.S. Niebur (Program Scientist)
J.S. Salute (Program Executive)

J.L. Green (Director, Planetary Sciences Division)
D.C. Schurr (Deputy Director, Planetary Sciences Division)

T.H. Zurbuchen (Associate Administrator, Science Mission Directorate)
J.M. Grunsfeld (*retired*, Associate Administrator, Science Mission Directorate)

ACKNOWLEDGEMENTS

The Science Definition Team would like to thank the following individuals for their help with the report: E. Turtle, M. Bentley, M. Voytek, D. Bass, C. Conley, D.E. Pugel, R. Bhartia, R. Lorenz, D. Beaty, M. Panning, C. Sotin, F. Naderi, C. Elachi, D. McCleese, C. Chyba, D. O'Handley, and G. Soffen.

Cover art by Michael Carroll.

RECOMMENDED BIBLIOGRAPHIC CITATION

Hand, K.P., Murray, A.E., Garvin, J.B., Brinckerhoff, W.B., Christner, B.C, Edgett, K.S, Ehlmann, B.L., German, C.R., Hayes, A.G., Hoehler, T.M., Horst, S.M., Lunine, J.I., Nealson, K.H., Paranicas, C., Schmidt, B.E., Smith, D.E., Rhoden, A.R., Russell, M.J., Templeton, A.S., Willis, P.A., Yingst, R.A., Phillips, C.B, Cable, M.L., Craft, K.L., Hofmann, A.E., Nordheim, T.A., Pappalardo, R.P., and the Project Engineering Team (2017): Report of the Europa Lander Science Definition Team. Posted February, 2017.

CONTENTS

EUROPA LANDER MISSION CONCEPT TEAM	I
NASA HEADQUARTERS.....	II
ACKNOWLEDGEMENTS.....	II
RECOMMENDED BIBLIOGRAPHIC CITATION.....	II
CONTENTS.....	III
EXECUTIVE SUMMARY.....	V
1 INTRODUCTION	1-1
2 HISTORICAL CONTEXT: SEARCHING FOR SIGNS OF LIFE IN OUR SOLAR SYSTEM.....	2-1
3 BENCHMARKS FOR BIOSIGNATURE DETECTION: EARTH AS A BRIDGE TO OCEAN WORLDS	3-1
4 SCIENCE OF THE EUROPA LANDER MISSION.....	4-1
4.1 Goal 1: Biosignatures & Signs of Life	4-3
4.1.1 Objective 1A: Detect & Characterize Any Organic Indicators of Past or Present Life.	4-4
4.1.2 Objective 1B: Identify & Characterize Morphological, Textural, or other Indicators of Life. .	4-22
4.1.3 Objective 1C: Detect & Characterize Any Inorganic Indicators of Past or Present Life.	4-38
4.1.4 Objective 1D: Determine the Provenance of Sampled Material.....	4-43
4.2 Goal 2: Habitability via in situ Analyses	4-54
4.2.1 Objective 2A: Characterize the non-ice composition of Europa's near-surface material to	
determine whether there are indicators of chemical disequilibria and other environmental	
factors essential for life.	4-55
4.2.2 Objective 2B: Determine the Proximity to Liquid Water and Recently Erupted materials at	
the Lander's Location.....	4-61
4.3 Goal 3: Pathfinding For Future Exploration	4-71
4.3.1 Objective 3A: Observe the properties of surface materials and sub-meter-scale landing	
hazards at the landing site, including the sampled area. Connect local properties with	
those seen from flyby remote sensing.	4-74
4.3.2 Objective 3B: Characterize dynamic processes of Europa's surface and ice shell over the	
mission duration to understand exogenous and endogenous effects on the physicochemical	
properties of surface material.	4-85
4.4 Science Traceability Matrix	4-97
4.5 Model Payload	4-97
4.5.1 Sampling Strategy & Allocations.....	4-101
4.5.2 Context Remote Sensing Instrument	4-102
4.5.3 Microscope for Life Detection	4-111
4.5.4 Vibrational Spectrometer	4-115
4.5.5 Organic Compositional Analyzer.....	4-119
4.5.6 Geophysical Sounding System.....	4-123
4.5.7 Lander Infrastructure Sensors for Science (LISS)	4-126
5 FRAMEWORK FOR LIFE DETECTION & ASSESSING POTENTIAL BIOSIGNATURES.....	5-1
6 LANDING SITE RECONNAISSANCE AND ACCESS CONSIDERATIONS.....	6-1
7 PLANETARY PROTECTION	7-1

8	PAYLOAD SCIENCE SUPPORT CAPABILITY	8-1
8.1	Introduction	8-1
8.1.1	Design Drivers and unique challenges compared to past missions.....	8-1
8.1.2	Sampling System output characteristics	8-1
8.1.3	Instrument Sample Processing Front Ends	8-2
8.2	Sampling System.....	8-2
8.2.1	Sampling system heritage missions.....	8-3
8.2.2	Sampling System Overview	8-4
8.2.3	Description of the Sampling System	8-5
8.3	Sampling Workspace.....	8-6
8.4	Sample Characteristics.....	8-7
8.5	Sampling System Operations	8-7
9	SURFACE OPERATIONS CONCEPT.....	9-1
9.1	Introduction	9-1
9.2	Surface Energy	9-1
9.2.1	Terminology	9-2
9.3	Surface Mission Timeline.....	9-3
9.4	Strategy for science-in-the-loop.....	9-7
9.4.1	Monitoring Tal	9-7
9.4.2	Sample Tal.....	9-7
9.5	Fault tolerance, automation, and robustness of surface phase	9-8
9.5.1	Lander Fault Tolerance.....	9-8
9.5.2	Instrument Fault Tolerance	9-9
10	LANDER MISSION CONCEPT.....	10-1
10.1	Mission Overview.....	10-1
10.2	Integrated Spacecraft and Carrier Element Overview	10-2
10.3	Lander Spacecraft Conceptual Design	10-3
10.4	Mission Operations	10-4
10.4.1	Launch/Cruise.....	10-4
10.4.2	JOI and Jupiter Tour	10-5
10.4.3	Deorbit, Descent, and Landing	10-5
10.4.4	Lander and Carrier during Surface Phase	10-7
10.5	Systems Engineering.....	10-8
10.5.1	Environments	10-8
10.5.2	Planetary Protection Implementation	10-10
11	REFERENCES	11-1
	APPENDICES	1
A.	Acronyms and Abbreviations	A-1
B.	Science Definition Team Findings	B-1

EXECUTIVE SUMMARY

The Europa Lander Science Definition Team Report presents the integrated results of an intensive science and engineering team effort to develop and optimize a mission concept that would follow the Europa Multiple Flyby Mission and conduct the first in situ search for evidence of life on another world since the Viking spacecraft on Mars in the 1970s. The Europa Lander mission would be a pathfinder for characterizing the biological potential of Europa's ocean through direct study of any chemical, geological, and possibly biological, signatures as expressed on, and just below, the surface of Europa. The search for signs of life on Europa's surface requires an analytical payload that performs quantitative organic compositional, microscopic, and spectroscopic analysis on five samples acquired from at least 10 cm beneath the surface, with supporting context imaging observations. This mission would significantly advance our understanding of Europa as an ocean world, even in the absence of any definitive signs of life, and would provide the foundation for the future robotic exploration of Europa.

Jupiter's moon Europa is a prime target in our exploration of potentially habitable worlds beyond Earth. Europa, which is approximately the size of Earth's moon, very likely harbors a global, ~100 km deep, liquid water ocean beneath its relatively thin (<25 km) ice shell. This ocean exists today and it has possibly persisted for much of the history of the solar system. Europa's ocean is probably in contact with a rocky, silicate seafloor, which may lead to an ocean rich in the elements and energy needed for the emergence of life, and for potentially sustaining life through time. **Europa may hold the clues to one of NASA's long standing goals – to determine whether or not we are alone in the universe. The highest-level science goal of the mission presented here is to search for evidence of life on Europa.**

Critically, the Europa Lander mission would advance our scientific understanding of fundamental aqueous and geochemical processes in the solar system, independent of whether or not signs of life are discovered on Europa. **The second science goal of the mission is**

to assess the habitability of Europa via in situ techniques. As part of this goal, measurements would be conducted that could help remove ambiguities associated with detecting signs of life, and these same measurements would also help determine the composition of the sampled surface material, and the proximity of the lander to any subsurface liquid water. These measurements would serve to constrain the composition of Europa’s ocean and its relationship to the ice shell and rocky sea-floor.

The third and final goal of the mission is to characterize the surface and subsurface to enable future robotic exploration. Through this goal the measurements of the first two goals would be framed in the broader context of Europa as a potentially active and dynamic ocean world, and the measurements associated with this goal would ensure that future robotic missions could explore across Europa’s landscape, or deeper within the ice shell and ocean. The measurements made as part of the three Europa Lander science goals would also **extend and enhance the remote sensing observations of the Europa Multiple Flyby Mission (EMFM)** by performing in situ analytical investigations of Europa’s surface materials and ice shell, thereby providing valuable ground-truth measurements.

The science Goals of the Europa Lander mission concept (**Figure 1**) address three of NASA’s “Big Questions” (NASA, 2017a) that currently motivate planetary exploration:

1. How did life begin and evolve on Earth, and has it evolved elsewhere in the Solar System?
2. What are the characteristics of the Solar System that lead to the origins of life?
3. Are we alone?

In addition, the mission concept goals and objectives are directly traceable to multiple science priorities described in the 2011 Decadal Survey *Vision and Voyages for Planetary Science in the Next Decade 2013–2022* (NRC, 2011). Detailed science objectives flow directly from the

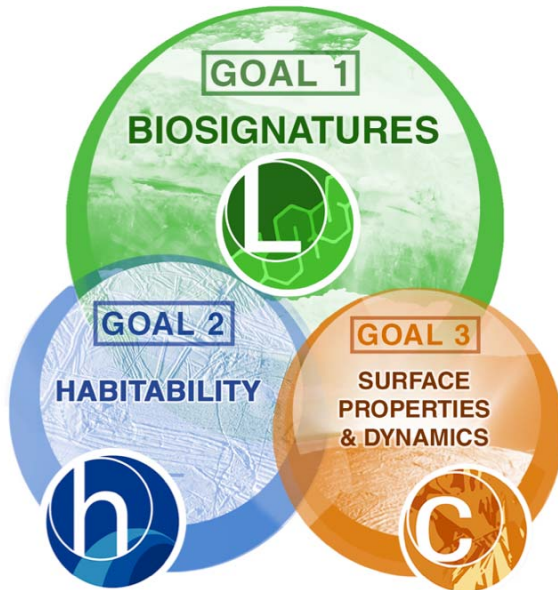


Figure 1. The Europa Lander Science Goals are distinct, but significant overlap in objectives and measurements leads to a highly capable, integrated instrument payload. Goal 1 is the highest priority and addresses the search for life (‘L’) and biosignatures. Goal 2 is the second priority and focuses on assessing the habitability (‘h’) of Europa. Goal 3 is the third priority and targets surface properties and dynamics for understanding the context (‘c’) for future robotic exploration.

Table 1. The Europa Lander Science Traceability Matrix (STM) Goals, Objectives, and Notional Instruments are outlined in summary form below. Dark blue and dark gray boxes indicate which instruments in the Baseline model payload address each Objective. The gray column indicates engineering sensors that are not strictly part of the science payload (e.g., descent imaging and LIDAR topography), but which the SDT identified as important for the complete science return of the lander mission.

Goals		Objectives	Notional Instruments					
			OCA	MLD	VS	CRSI	GSS	LISS
BIO-SIGNATURES	1. Search for evidence of life on Europa.	1A. Detect and characterize any organic indicators of past or present life.	Dark Blue	Dark Blue	Dark Blue	Dark Blue	Dark Blue	Dark Blue
		1B. Identify and characterize morphological, textural, or other indicators of life.	Dark Blue	Dark Blue	Dark Blue	Dark Blue	Dark Blue	Dark Blue
		1C. Detect and characterize any inorganic indicators of past or present life.	Dark Blue	Dark Blue	Dark Blue	Dark Blue	Dark Blue	Dark Blue
		1D. Determine the provenance of sampled material.	Dark Blue	Dark Blue	Dark Blue	Dark Blue	Dark Blue	Gray
SURFACE HABITABILITY	2. Assess the habitability of Europa via in situ techniques uniquely available to a lander mission.	2A. Characterize the non-ice composition of Europa's near-surface material to determine whether there are indicators of chemical disequilibria and other environmental factors essential for life.	Dark Blue	Dark Blue	Dark Blue	Dark Blue	Dark Blue	Dark Blue
		2B. Determine the proximity to liquid water and recently erupted materials at the lander's location.	Dark Blue	Dark Blue	Dark Blue	Dark Blue	Dark Blue	Gray
SURFACE PROPERTIES AND DYNAMICS	3. Characterize surface and subsurface properties at the scale of the lander to support future exploration.	3A. Observe the properties of surface materials and sub-meter-scale landing hazards at the landing site, including the sampled area. Connect local properties with those seen from flyby remote sensing.	Dark Blue	Dark Blue	Dark Blue	Dark Blue	Dark Blue	Dark Blue
		3B. Characterize dynamic processes of Europa's surface and ice shell over the mission duration to understand exogenous and endogenous effects on the physicochemical properties of surface material.	Dark Blue	Dark Blue	Dark Blue	Dark Blue	Dark Blue	Dark Blue

Instruments: Organic Compositional Analyzer (OCA), Microscope for Life Detection (MLD), Vibrational Spectrometer (VS), Context Remote Sensing Instrument (CRSI), Geophysical Sounding System (GSS), Lander Infrastructure Sensors for Science (LISS). Gray = LISS engineering sensors (Descent Imaging and LIDAR, thermal sensor(s), telecom, etc.)

high-level mission goals, as shown in the abbreviated science traceability matrix (**Table 1**; full version provided in **Chapter 4**).

For each science objective, a generic notional instrument is indicated that would be capable of acquiring the types of measurements required. The mission concept could be successfully conducted using a range of science payload configurations, in which different instrument types from these generic classes are integrated. However, in order to demonstrate the overall scientific and technical viability of the Europa Lander mission concept, two example payload configurations (Baseline and Threshold) were developed in detail, based on flight-proven technologies that could be adapted to Europa conditions. These example model payloads fit within the currently-established engineering constraints of the Europa Lander mission concept, and achieve the Baseline and Threshold level science requirements.

The high-level Europa Lander mission concept architecture was defined, for the purpose of the Science Definition Team (SDT) activity, by NASA HQ and the JPL Europa Lander pre-project team. These design requirements include the following: the lander would

be launched by a Space Launch System (SLS) rocket separately from the EMFM and would include a Carrier Relay Orbiter (CRO) spacecraft to support data relay to and from the Europa Lander; the EMFM would only serve as a back-up telecommunications link. The Europa Lander, therefore, would be a stand-alone surface mission, operating independently of the precursor EMFM, but guided by landing site reconnaissance enabled by the EMFM.

Several power systems were considered for the Europa Lander, with the final determination that primary batteries would provide for sufficient lifetime on the surface to achieve the Baseline science requirements. **Table 2** provides a summary of key mission parameters.

Primary batteries provide 45 kWh of energy, supporting operations in the mission design presented here. Several surface operations scenarios were considered, yielding a range of surface lifetimes from approximately 20 to 40 days on Europa's surface. Importantly, due to Europa's harsh radiation environment, the lifetime of the supporting CRO would be limited to ~30 days in orbit around Europa, thus making a longer-lived lander mission difficult to justify. **The lifetime of the lander is 20+ days on Europa's surface, for a Baseline surface phase operations scenario in which five samples (each acquired from 10 cm below the surface), are processed, analyzed, and the data uplinked/downlinked through the CRO to Earth.** The Baseline scenario provides for schedule margin on sample acquisition, and for science team ground-in-the-loop operations to determine which samples to acquire.

The Europa Lander mission concept provides 42.5 kg for the Baseline science instrument payload (32.3 kg without recommended margin). With the exception of the Context Remote Sensing Instrument (CRSI), all instruments are held within a vault that provides radiation shielding. The centerpiece instruments for characterizing any potential signs of life are:

1) an Organic Compositional Analyzer (OCA), which in the Baseline model payload is a Gas Chromatograph-Mass Spectrometer (GC-MS) **capable of achieving a 1 picomole per gram of sample limit of detection for organics,**

Table 2. Summary of key science and engineering parameters for the Europa Lander mission concept.

Parameter	Value
Science payload mass (with margin)	42.5 kg
Number of samples to be collected for in situ analyses	5 (Baseline scenario)
Required sampling depth capability	10 cm
Required minimum sample volume	7 cubic centimeters per sample
Limit of detection for organics	1 picomole in a 1 gram sample
Limit of detection for cells or cell-like structures	0.2 microns, at a concentration of 100 cells per cubic centimeter of ice
Duration of surface science phase	20+ days (Baseline scenario)
Energy source	45 kWh from primary batteries
Radiation shielding	Provided by central vault, with exception of externally-mounted context remote sensing
Data link to Earth	Provided by dedicated Carrier Relay Orbiter (CRO)
Data volume capability	> 4 Gbits from Europa via CRO
Launch vehicle	Space Launch System
Target launch date	2024-2025

2) a microscope system (referred to as the Microscope for Life Detection, MLD) **capable of distinguishing microbial cells as small as 0.2 microns in diameter, and as dilute as 100 cells per cubic centimeter (cc, or equivalently 1 mL) of ice.** In the Baseline model payload this capability is to be addressed by a combinations of spectroscopy and atomic force microscopy (AFM) or optical light microscopy (OM), and,

3) a Vibrational Spectrometer (VS), which in the Baseline model payload is a Raman and Deep UV fluorescence spectrometer **capable of characterizing both organic and inorganic compounds down to a level of parts per thousand by mass.**

Along with the analytical suite for detailed analyses of samples, the Europa Lander model payload also includes a pair of color stereo imagers for examining the landing site in 3-D (including capabilities for characterizing surface composition), and a seismic package for determining Europa's ice shell and ocean thickness through acoustic monitoring of cracking events in the ice shell.

In the brief sections below, summaries are provided of the science investigations within each high-level goal.



Science Goal #1 is to Search for Evidence of Life on Europa. No singular measurement would provide sufficient evidence for the detection of life on Europa; rather, the conclusion that evidence of **life had been detected would require multiple lines of evidence, from different instruments, on a set of samples examined across a variety of spatial scales.** Through the combination of the OCA, VS, MLD, and CRSI, the model payload for the Europa Lander presents at least nine different and complementary possible lines of evidence for signs of life in samples collected on Europa. These measurements range from detecting and characterizing organic compounds, to looking for cell-like structures, to determining if the samples originate from within Europa's ocean or other liquid water environments. The organic chemical analyses are specifically targeted to reveal the broadest possible range of signatures produced by life, including analysis of molecular type, abundance, and chirality. Spectroscopic analyses of samples provide the inorganic and geochemical context of the samples, and enable discrimination between material native to Europa (endogenous) and materials that may have been externally delivered (exogenous, e.g., from micrometeorites), or processed by Europa's radiation environment. Collection of five separate samples, each of at least 7 cc total volume, provides for repeated measurements, ensuring redundancy and robustness of results. Detection limits for measurements targeting evidence of life were established by comparison to several extreme, nutrient limited environments on Earth (**Chapter 3**). Importantly, the model payload and measurements defined for Goal 1 generate highly valuable scientific results even in the absence of any signs of life.



Science Goal #2 is to Assess the habitability of Europa via in situ techniques uniquely available to a lander mission. If the measurements from Goal 1 reveal potential biosignatures, then it is important to understand the geochemical context for habitability, and the proximity of the landing site to habitable regions within Europa's ice shell and ocean. However, if the measurements of the samples and landing site reveal no definitive biosignatures, then it becomes essential that ambiguous or null results are understood in the broader context of Europa's habitability. Investigations of habitability include characterizing the non-ice composition of Europa's near-subsurface to discern indicators of chemical disequilibria and other key environmental features that are essential to support life. In addition, Goal 2 addresses the need to understand the relationship of the landing site and samples to any liquid water, i.e., a subsurface ocean or regions within the ice shell. Goal 2 investigations are achieved primarily through measurements made by the VS, GSS, and CRSI, with some contributions from the MLD and OCA. Significantly, the in situ measurements made by the lander would link nested observations across multiple scales to the observations of the EMFM. The local-scale observations (submicron to decameter) of the lander would provide 'ground truth' measurements that would permit refined interpretation of remote sensing data across the surface of Europa.



Science Goal #3 is to Characterize surface and subsurface properties at the scale of the lander to support future exploration. The Europa Lander mission concept described in this report is a 'pathfinder' for the exploration of Europa, and potentially many other ocean worlds of the outer solar system. As a stationary, relatively short-lived mission, this spacecraft would survey the landscape and probe the subsurface (acoustically) to determine the physical and chemical conditions on, and within, Europa. These measurements would then feed forward into designs of future robotic vehicles that would explore across the surface, or down into the subsurface. The nature of the landing environment, mobility hazards, and (near) surface physical properties within the workspace accessible to the lander's robotic arm, are all key characteristics to observe and directly quantify as part of Goal 3. Investigations include characterizing textural, structural and compositional heterogeneities in surface and near-surface materials through measurements of the samples (with the VS, MLD, and OCA), and through observations of the terrain, from the lander workspace to the horizon and into the ice shell (with the CRSI and GSS). In addition, tidal and other dynamic motions would be investigated over the surface mission duration by monitoring the lander's position with respect to the CRO. Goal 3 also leverages engineering support data from the descent hazards imaging LIDAR and descent imaging systems (on the Powered Descent Vehicle that delivers the lander safely to the surface) and from the robotic arm and accelerometers on the lander. These datasets would help further constrain the ice shell properties, and span the image resolution gap from flyby images to surface images collected by the lander CRSI. The combination of these multi-scale measurements would aid in understanding the physical and mechanical properties of the ice shell and any associated regolith, and would directly support future robotic exploration.

The science addressed by the three Goals leads to a **fully integrated mission concept and model payload that would enable a diverse approach to the search for potential biosignatures, bringing together morphological, organic, chiral, and inorganic**

The Europa Lander mission concept is designed to achieve ground-breaking science. The SDT is confident that a payload matching or exceeding the requirements described herein could potentially reveal signs of life on Europa.

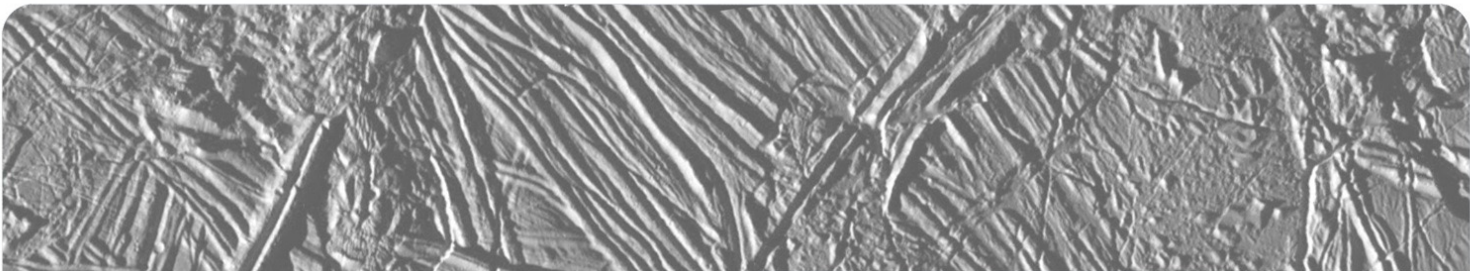
indicators of life, all within a well-quantified geological context. Chemical analyses of samples collected directly from Europa's near surface layer would provide for characterization of organics at the picomole-per-gram level of sampled material, which is an improvement of approximately **nine orders of magnitude over those possible by means of remote sensing capabilities.** Quantitative high-resolution imaging observations from lander instruments would span scales from fractions of micrometers to decameters (0.2 microns to tens of meters) to provide in situ context for sampled materials, local geology, and surface properties. This roughly **seven orders of magnitude enhancement in spatial resolution** over the EMFM would provide key insights into the properties of Europa's ice shell and any subsurface liquid water. Further, the acoustic sounding measurements would provide unique and complementary measurements to those performed by the radar, magnetometer, and plasma instruments which would be flown on the EMFM.

The scientific and technical approach of the Europa Lander mission concept presented in this study provides a robust, yet conservative, strategy for the first landed mission to search for signs of life on an ocean world. Several key findings from this study, related to the path forward for this mission, are presented on the following page, and in **Appendix B.**

The science return possible from the model payload is such that **if life is present in Europa's ice at a level comparable to one of the most extreme and desolate of environments on Earth (Lake Vostok ice) then this mission could detect life in Europa's icy surface.** The combination of detection methods, detection limits, and scales of observations provided by the model payload and mission concept combine to make this possible. In the absence of any signs of life, this mission is also designed to generate an incredibly valuable dataset about the chemistry of Europa's ice shell, its putative ocean, and the geological, geophysical, and chemical context for habitability. Either of the above outcomes is of fundamental scientific value to understanding the prospects for life in the solar system, and our place in it.

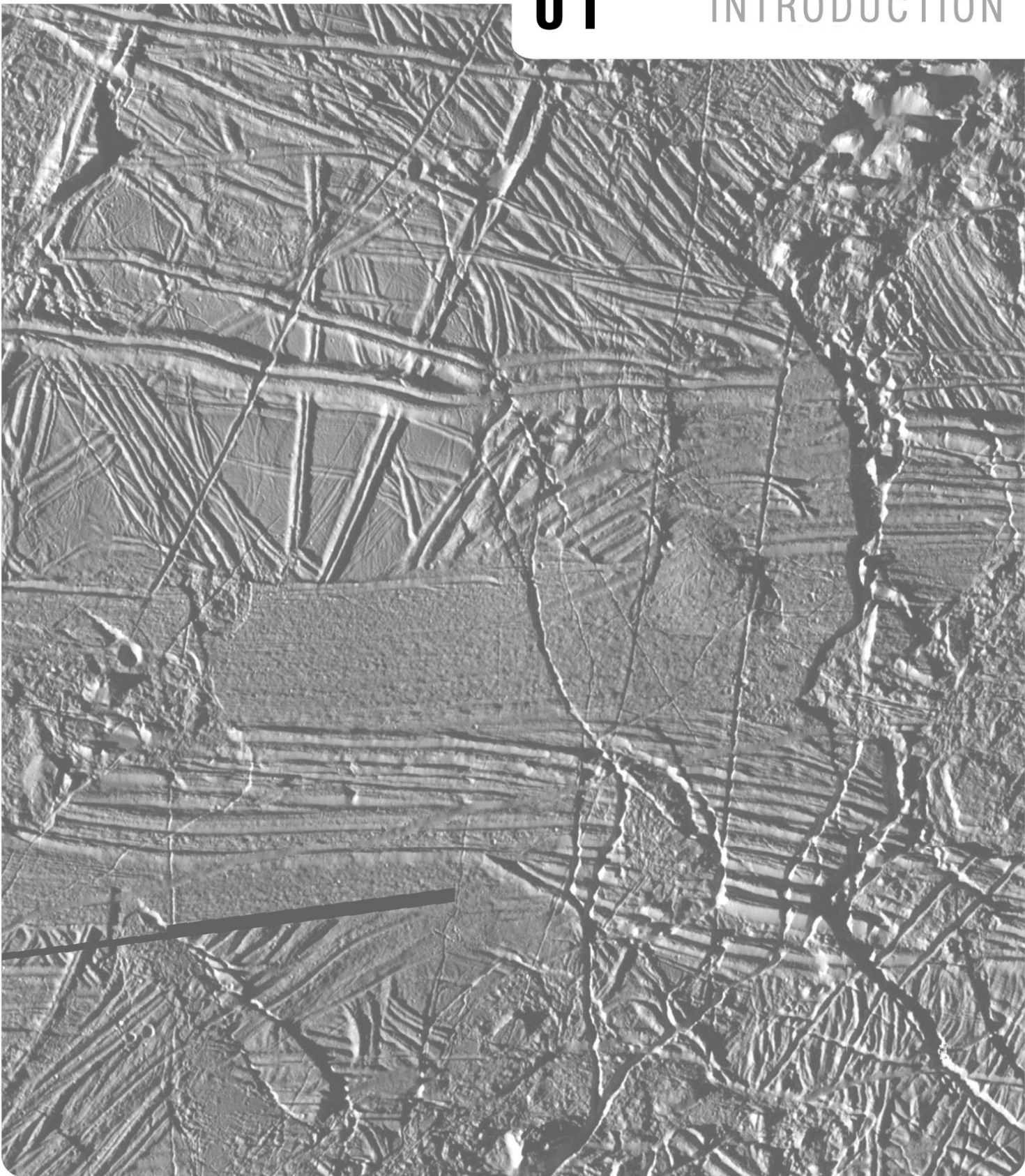
Key Findings of the Science Definition Team

- **The SDT strongly recommends early coordination and integration of the instrument payload.** Sample handling, processing, and analyses would benefit significantly from optimization of sample-related operations, which could yield more efficient energy expenditure, resource allocation (mass, power, volume), and ultimately increase science return of the mission.
- **The SDT strongly recommends a close coupling between the Europa Lander Science Team, Project Science, and Project Engineering so as to optimize the potential science return from engineering subsystems and sensors on the Europa Lander mission spacecraft.** Engineering data from the Powered Descent Vehicle (during DDL landing operations), and from the lander engineering instruments and subsystems (during and after landing), supports multiple SDT goals and should be captured and returned to Earth as scientific datasets (which eliminates the need for additional science payload mass). A Deorbit, Descent and Landing (DDL) working group of scientists could be assembled to work closely with the Europa Lander Project to optimize science return from these assets.
- **NASA’s in situ search for life in our solar system would benefit from increased investments in advancing miniaturized microscope technologies for robotic spaceflight missions, specifically targeting evidence of life.**



01

INTRODUCTION





1 INTRODUCTION

Structure of the Report

This report focuses on the science of a mission concept for landing on the surface of Europa. For any mission concept, however, science and engineering must be closely coupled, as the science return of a mission is enabled, or limited, by engineering capabilities.

The first seven chapters of this report detail the science, and science considerations, of the mission concept. **Chapters 2 and 3** provide some scientific background and context. **Chapter 4** then details the Goals, Objectives, Investigations, and Measurement Requirements of the mission concept, culminating with the Model Payload. **Chapters 5, 6, and 7** describe several aspects of the mission that incorporate additional engineering considerations, such as surface sampling, landing site reconnaissance, and planetary protection. **Chapters 8, 9, and 10** then go into detail on the engineering behind the mission concept and architecture.

While scientists reading this report would likely benefit from reading the report from the beginning forward, engineers may prefer to start at **Chapter 10** and work backward. Throughout the science chapters, however, references are made to some of the engineering capabilities of the mission, and thus readers may benefit familiarizing themselves with **Chapters 8, 9, and 10** before reading the report in full.

Introduction to the Science Definition Team

In June of 2016 NASA initiated a Pre-Phase A mission concept study for a soft lander to the surface of Europa for the purpose of in situ analyses of samples of the surface and shallow subsurface (also referred to as the ‘near-subsurface’). As part of this effort, NASA convened a Science Definition Team (SDT) to provide scientific guidance to the mission study.

The Co-chairs selected for leadership of the SDT were Dr. James Garvin of NASA Goddard Spaceflight Center, Dr. Alison Murray of the Desert Research Institute in Reno, Nevada, and Dr. Kevin Hand of the Jet Propulsion Laboratory, California Institute of Technology. Working with Dr. Curt Niebur (Program Scientist) and Joan Salute (Program Executive) of NASA Headquarters, a team of 18 additional scientists were selected to join the SDT. The full team is listed in **Table 1.1**.

On June 1, 2016, the SDT held a kick-off meeting, followed by weekly video conferences throughout the June through December 2016 timeframe. Face-to-face meetings of the

SDT were held at JPL on July 12–13, 2016, and August 8–10, 2016. In addition, throughout the process several 4-hour videoconferences and working group meetings were held.

Europa Lander 2016 Charter & Goals

The science goals for the Europa lander study, as detailed in the SDT Charter, were targeted to be ideally suited for the unique science enabled by in situ surface exploration. These prioritized goals are:

- 1) Search for evidence of biomarkers and/or signs of extant life.
- 2) Assess the habitability (particularly through quantitative compositional measurements) of Europa via in situ techniques uniquely available by means of a landed mission.
- 3) Characterize surface properties at the scale of the lander to support future exploration.

The SDT was tasked to work as an integral part of the broader Pre-Phase A study effort to formulate a detailed mission concept that appropriately balances science return, cost, and risk. Specifically, the SDT was asked to:

- Work closely and seamlessly with the engineering and design personnel as a single team to define a feasible and scientifically valuable and viable lander mission concept;
- Define a hierarchy of science objectives and derived measurements that is responsive to the three prioritized goals above and traceable to the broader

Table 1.1. Europa Lander Science Definition Team members.

Name	Institution
Dr. Will Brinckerhoff	NASA Goddard Space Flight Center
Prof. Brent Christner	University of Florida
Dr. Ken Edgett	Malin Space Science Systems
Prof. Bethany Ehlmann	California Inst. of Technology
Dr. James Garvin (Co-chair)	NASA GSFC
Dr. Chris German	Woods Hole Oceanographic Institution
Dr. Kevin Hand (Co-chair)	Jet Propulsion Laboratory, California Inst. of Technology
Prof. Alexander Hayes	Cornell University
Dr. Tori Hoehler	NASA Ames Research Center
Prof. Sarah Horst	Johns Hopkins University
Prof. Jonathan Lunine	Cornell University
Prof. Alison Murray (Co-chair)	Desert Research Institute & Univ. of Nevada, Reno
Prof. Ken Nealson	University of Southern California
Dr. Chris Paranicas	Applied Physics Laboratory, Johns Hopkins University
Prof. Britney Schmidt	Georgia Institute of Technology
Dr. David Smith	Massachusetts Institute of Technology
Prof. Alyssa Rhoden	Arizona State University
Dr. Mike Russell	Jet Propulsion Laboratory, California Inst. of Technology
Prof. Alexis Templeton	University of Colorado, Boulder
Dr. Peter Willis	Jet Propulsion Laboratory, California Inst. of Technology
Dr. R. Aileen Yingst	Planetary Science Institute

scientific questions and objectives in the most recent NRC Planetary Decadal Survey and the Outer Planets Assessment Group Goals document;

- Develop a Science Traceability Matrix that flows from the top-level science goals above through science objectives and derived measurements, culminating in functional requirements and capabilities for the flight system and payload;
- Define, in partnership with the broader study team, the concept of operations for the surface mission;
- Advise the flight system engineers on the most probable resource and accommodation needs of the science payload; and
- Consider a variety of potential (strawman) science instruments that fully address the SDT-defined science objectives, providing at least one strawman payload that can be accommodated within the resource and other constraints of the flight system as a proof of concept. At the proper time NASA will determine the final science payload for the lander mission.

The SDT reported on its progress on a regular basis to NASA HQ management. An initial draft of engineering requirements derived from science measurements was delivered to Project Engineering on August 16, 2016. A summary report was delivered to NASA HQ and the Program Office on September 30th, 2016, a final briefing took place at NASA HQ on December 9, 2016, and the final report was delivered on February 7, 2017.

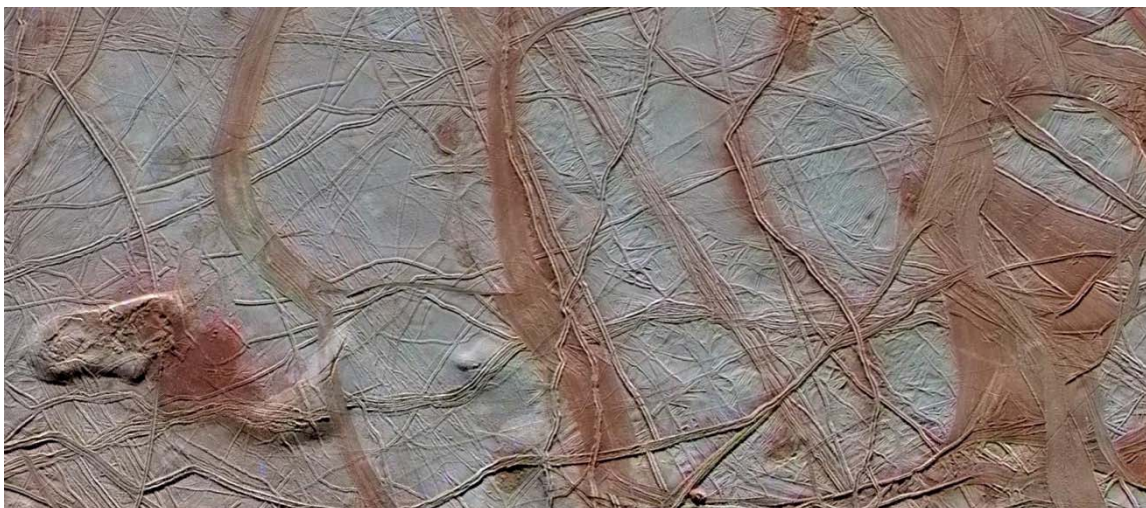


Figure 1.1. Enhanced-color image mosaic from *Galileo* showing crosscutting lineae, multiple wide, dark bands where the surface has spread apart (right), and chaos regions (left) where the surface has been disrupted into blocks of material. Image is approximately 200 km wide. Solar illumination is from the upper left.

Presentations by the Europa Lander co-chairs were also made at the OPAG meeting in Flagstaff, AZ, on August 11, 2016, and at the CAPS meeting in Irvine, CA, on September 15, 2016.

Relevance to NASA Goals

As described in the 2011 NRC Decadal Survey *Vision & Voyages for Planetary Science in the Decade 2013-2022*, a motivating goal of planetary exploration is the discovery of habitable environments and life on alien worlds. The motivation of the exploration of Europa, as mentioned in the survey, is explicitly habitability – the report states: “Because of this ocean’s potential suitability for life, Europa is one of the most important targets in all of planetary science.” The 2011 Decadal Survey explicitly mentions that a lander would enable scientific opportunities simply not possible from a flyby or orbital mission. The report states “A key future investigation of the possibility of life on the outer planet satellites is to analyze organics from the interior of Europa. Such analysis requires [...] a lander ...” and “...a lander will probably be required to fully characterize organics on the surface of Europa.”

The goals and objectives of the current Europa Lander mission concept are linked to the science priorities for outer solar system exploration and the search for habitable environments as described in the 2011 NRC Decadal survey (**Table 1.2**). Europa exploration was also listed as a high priority in the previous 2003 Planetary Decadal Survey *New Frontiers in the Solar System: An Integrated Exploration Strategy*. This study mentioned the “Europa Astrobiology Lander” as a future mission concept, which would allow the study of organic chemistry and possible biosignatures from a landed station. With its on-board chemical analysis suite and 10 cm sampling depth, that mission concept was similar to the current Europa Lander.

The science goals of the Europa Lander mission address three of NASA’s “14 Big Questions” for planetary exploration. In addition, NASA’s 2014 Science Plan¹, as part of the planetary science strategy, lists “Is there life beyond Earth” as one of the three fundamental science questions guiding solar system exploration, and includes “Explore and find locations where life could have existed or could exist today” as one of five science goals that help guide the Planetary Science Division’s science and research activities.

¹ Section 4.3 of https://smd-prod.s3.amazonaws.com/science-green/s3fs-public/atoms/files/2014_Science_Plan_PDF_Update_508_TAGGED.pdf

Table 1.2. Relevance of Europa Lander Goals and Objectives to the 2011 Vision and Voyages Decadal Survey science themes, goals, and motivating questions.

Europa Lander		Decadal Survey		
Goal	Objectives	Themes & Goals	Questions & Objectives	
1. BIOSIGNATURES	1. Search for evidence of life on Europa.	Crosscutting Theme 2: Planetary Habitats	Priority Question 6: Beyond Earth, are there contemporary habitats elsewhere in the solar system with necessary conditions, organic matter, water, energy, and nutrients to sustain life, and do organisms live there now? <i>... "a lander will probably be required to fully characterize organics on the surface of Europa "</i>	
			Priority Question 4: What were the primordial sources of organic matter, and where does organic synthesis continue today?	
		Satellite Science Goal 3: What are the processes that result in habitable environments?	1B. Identify and characterize morphological, textural and/or other indicators of life.	Objective 4: Is there evidence for life on the satellites? Question 1. Does (or did) life exist below the surface of Europa or Enceladus? <i>"A key future investigation of the possibility of life on the outer planet satellites is to analyze organics from the interior of Europa. Such analysis requires [...] a lander"</i> <i>"Studies of the plume of Enceladus and any organics on the surface of Europa (or in potential Europa plumes) may provide evidence of biological complexity even if the organisms themselves are no longer present or viable."</i>
			1C. Detect and characterize any inorganic indicators of past or present life.	
1D. Determine the provenance of sampled material.	Satellite Science Goal 3: What are the processes that result in habitable environments?	Objective 2: What are the sources, sinks, and evolution of organic material? Question 3: Are organics present on the surface of Europa, and if so, what is their provenance?		

Europa Lander		Decadal Survey	
Goal	Objectives	Themes & Goals	Questions & Objectives
2. SURFACE HABITABILITY 2. Assess the habitability of Europa via in situ techniques uniquely available to a lander mission.	2A. Characterize the non-ice composition of Europa's near-surface material and determine whether there are indicators of chemical disequilibria and other environmental factors essential for life.	Satellite Science Goal 3: What are the processes that result in habitable environments?	Objective 3: What energy sources are available to sustain life? Question 1: What is the nature of any biologically relevant energy sources on Europa? <i>"Important directions for future investigations ...include (1) measurement of the oxidant content."</i>
	2B. Determine the proximity to liquid water and recently erupted materials at the lander's location.	Satellite Science Goal 1: How did the satellites of the outer solar system form and evolve?	Objective 3: How are satellite thermal and orbital evolution and internal structure related? Question 8: What is the thickness of Europa's outer ice shell and the depth of its ocean? Objective 4: What is the diversity of geologic activity and how has it changed over time? Question 5: Has material from a subsurface Europa ocean been transported to the surface, and if so, how? <i>"...in situ measurements from the surface would provide additional information on the surface composition and environment and the subsurface structure"</i>
		Satellite Science Goal 3: What are the processes that result in habitable environments?	Objective 1: Where are subsurface bodies of liquid water located, and what are their characteristics and histories? Question 1: What are the depths below the surface, the thickness, and the conductivities of the subsurface oceans of the Galilean satellites?

Europa Lander		Decadal Survey		
Goal	Objectives	Themes & Goals	Questions & Objectives	
3. SURFACE PROPERTIES AND PROCESSES	3. Characterize surface and subsurface properties at the scale of the lander to support future exploration.	3A. Observe the properties of surface materials and sub-meter-scale landing hazards at the landing site, including the sampled area. Connect local properties with those seen from flyby remote sensing.	Crosscutting Theme 3: Workings of Solar Systems	Priority Question 10: How have the myriad chemical and physical processes that shape the solar system operated, interacted, and evolved over time?
		3B. Characterize dynamic processes of Europa's surface and ice shell over the mission duration to understand exogenous and endogenous effects on the physicochemical properties of surface material.	Satellite Science Goal 2: What processes control the present-day behavior of these bodies?	Objective 3: How do exogenic processes modify these bodies? Question 4: How are potential Europa surface biomarkers from the ocean-surface exchange degraded by the radiation environment?
			Satellite Science Goal 1: How did the satellites of the outer solar system form and evolve?	Objective 4: What is the diversity of geologic activity and how has it changed over time? Question 5: Has material from a subsurface Europa ocean been transported to the surface, and if so, how?
			Satellite Science Goal 2: What processes control the present-day behavior of these bodies?	Objective 1: How do active endogenic processes shape the satellites' surfaces and influence their interiors? Objective 3: How do exogenic processes modify these bodies?



02

HISTORICAL CONTEXT



2 HISTORICAL CONTEXT: SEARCHING FOR SIGNS OF LIFE IN OUR SOLAR SYSTEM

The search for life beyond Earth is a pursuit plagued by its own premise: We seek signs of life elsewhere in part to better understand biology and life as fundamental processes, yet to

search for life we need well-defined measurements as to what life is, and what life does. We currently have no succinct definition for life (Cleland and Chyba, 2002), and we are thus left with a combination of hypothesis testing and discovery-driven measurements.

“Life is the hypothesis of last resort.”

– C. Sagan et al. (1993)

Without at least an operational definition for life it is difficult to establish a universally accepted set of criteria for a positive or negative detection of life. Numerous definitions have been presented throughout the literature, including ones that emphasize physiological, biochemical, genetic, metabolic, and thermodynamic attributes, but all such definitions fail to be universally applicable (Sagan, 1970; Chyba and McDonald, 1995; Chyba and Phillips, 2002). A classic “textbook” definition for life is that it is “a self-sustained chemical system capable of undergoing Darwinian evolution” (Joyce, 1994). Though this definition may be sufficiently broad so as to be universal, operationally it is of little utility. As Chyba and Phillips (2002) point out, “How long do we wait to determine if a candidate entity is ‘capable of undergoing Darwinian evolution?’”

The search for life beyond Earth is in part a search to define life and biology. Constrained to the one known tree of life and biochemistry that we find here on Earth, we are, for the time being, limited to definitions that rely on a convergence of parameters that serve as signs of life, or biosignatures. **Here we define the term *biosignature* as a feature or measurement interpreted as evidence of life. To discover life beyond Earth is to amass a body of evidence, generated from multiple complementary measurements and multiple samples, such that the only remaining interpretation of the evidence is that biological processes were, and are, responsible for the observations.**

Lessons learned from Viking

A rigorous in situ search for signs of life on another world has only been conducted once (by two spacecraft) on another planet. The twin Viking Landers touched down on the martian surface on July 20th and September 3rd of 1976 (**Figure 2.1**). They landed using the ~100 meter per pixel imagery of the Mariner 9 spacecraft and the tens of meters per pixel imagery of the

Viking Orbiters. The landers were focused largely on finding signs of extant life in the martian soil, not evidence of past life as preserved in the rock record. The experiments and instruments were designed at a time when the fields of genetics and microbial ecology were just starting to piece together the major branches of life on Earth. By almost all accounts, the Viking Landers were ahead of their time and pushed the frontier of our understanding of biology. Though some have argued that the Viking missions were “failures” for not having discovered life on Mars, and thus stalled any

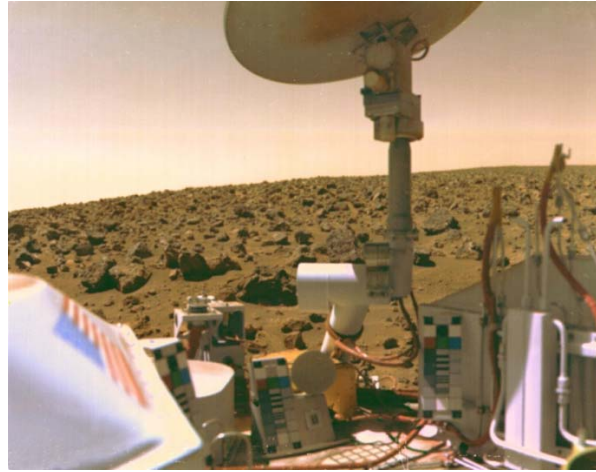


Figure 2.1. The surface of Mars' Utopian Plain as seen from the Viking 2 Lander in 1976. Viking marked humankind's bold first steps in the in situ search for life beyond Earth.

future Mars exploration, this is a poor read of history. The Viking Landers were operationally and scientifically a tremendous success – any “failure” to find life is not on the mission, but rather on the past and present habitability of Mars itself. And of course, we cannot levy science requirements on the worlds we explore. The technical success of the Viking missions has echoed throughout all subsequent Mars missions that have sought to investigate the habitability of Mars: no strong signs of past or present life have yet been observed and thus the Viking measurements still hold as a valid interrogation of martian habitability.

Each of the Viking Landers had a biology payload consisting of three experiments: the gas exchange experiment involved incubating soil samples with nutrients to prompt growth and gas exchange; the labeled release experiment used ^{14}C -labeled nutrients to monitor production of ^{14}C -gases evolved from the inoculated soil; and the pyrolytic release experiment examined incorporation of ^{14}C into solid biomass within the soil (Klein et al., 1972; Klein, 1978). This ‘biology’ payload was centered around a definition of life that prioritized metabolic indicators of extant life; the measurements targeted effects that living organisms have on the chemistry of their environment. Were it not for the results from the gas chromatograph mass spectrometers (GC-MS) on the landers, the results from the biology payload may have been ambiguous. However, the GC-MS measurement of an upper limit of organics present at no more than parts-per-billion in the soil made the putative metabolic chemistry nearly impossible to interpret as the result of carbon-based life (Biemann et al., 1977). Significantly, a biochemical definition – i.e., one in which detecting the building blocks for life are a critical cross-check for potential biosignatures – outweighed a metabolic definition (Chyba and Phillips, 2002). This concept of a biochemical definition was first introduced in Lovelock’s seminal 1965 paper “*A Physical Basis for Life Detection Experiments?*” (Lovelock, 1965) and later described by McKay as the *Lego™ Principle* (McKay, 2004). The great strength of this approach is that it allows us to search for life as we know it, as *well as for life as we don’t*. It has continued to guide analyses of

the Viking data and provide a framework for future missions (Nealson, 1997; Navarro-González et al., 2006; Biemann, 2007; Parnell et al., 2007; Navarro-González et al., 2010).

Working from the lessons of the Viking mission and considering a path forward for assessing potential biosignatures on Europa, Chyba and Phillips (2001) proposed the following approach for future robotic searches for life:

- 1) If the payload permits, conduct experiments that assume contrasting definitions for life.
- 2) Given limited payload, the biochemical definition deserves priority.
- 3) Establishing the geological and chemical context of the environment is critical.
- 4) Life-detection experiments should provide valuable information regardless of the biology results.
- 5) Exploration need not, and often cannot, be hypothesis testing. Planetary missions are often missions of exploration, and therefore the above guidelines must be put in the context of exploration and discovery-driven science.

The Europa Lander Science Definition Team developed an investigation strategy and mission concept that aligns directly with the above approach. As detailed in subsequent chapters, the model payload works in service to all five of the above considerations, ensuring that even in the absence of any potential biosignatures, valuable science is still conducted.

The initial search for signs of life on Europa will largely take the form of a biochemical search – both via remote sensing and with in situ analyses conducted by the lander. The Europa Multiple Flyby Mission (EMFM; **Figure 2.2**) will be able to identify sites of recent or compelling geological activity, and sites that are chemically interesting in the context of biosignatures (e.g.,

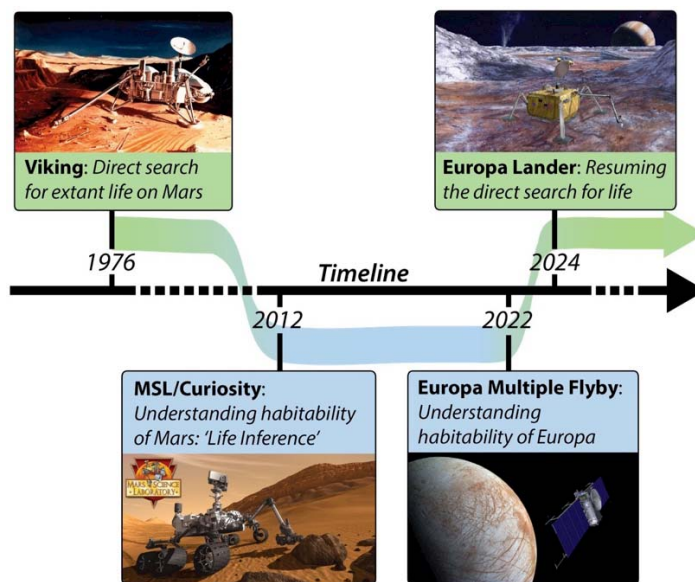


Figure 2.2. The Europa Lander resumes NASA's direct search for life beyond Earth, following on the EMFM's detailed assessment of Europa's habitability.

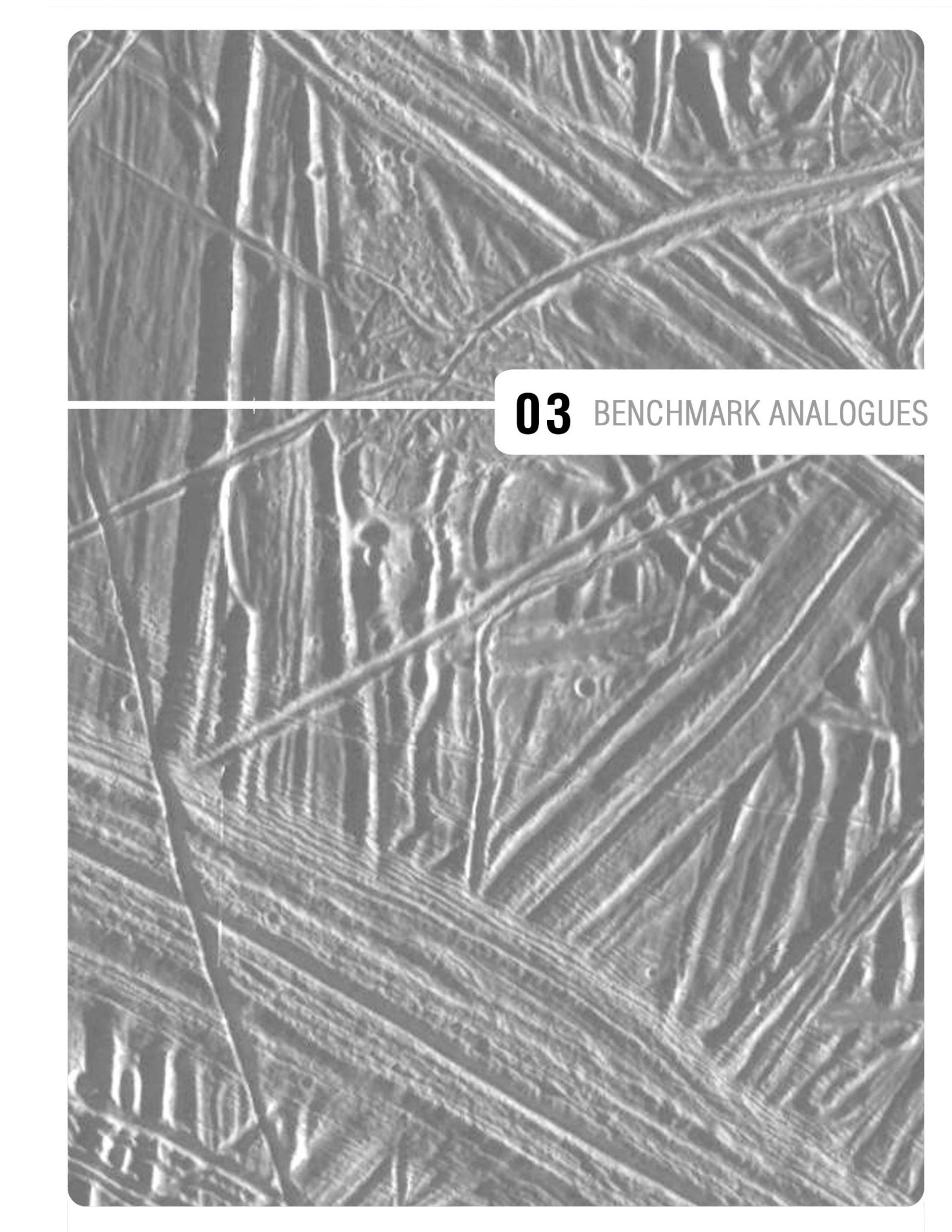
by mapping organics). **Given that the availability of liquid water is likely not a limiting factor for life on Europa, the search for endogenous carbon-containing compounds becomes the critical next step in searching for biosignatures.** Landing site selection based on Europa flyby reconnaissance is detailed in **Chapter 6**, but here we provide a brief description of how the search for biosignatures and establishing landing site context are closely coupled. Results from the Viking Landers, and subsequent Mars missions, have established how critical such context is, especially in light of a non-detection of biosignatures. For the case of points (3) and (4) in the list above, Figueredo et al. (2003) recommend several geological criteria that can be used to guide the search for biosignatures on Europa's surface. In assessing a variety of surface units such as chaos regions, bands, ridges, craters, and plains, they prioritize the following:

- 1) Evidence for high material mobility,
- 2) Concentration of non-ice components,
- 3) Relative youth,
- 4) Textural roughness (providing a possible shield from the degrading effects of radiation – though obviously complicating engineering considerations for a lander),
- 5) Evidence for stable or gradually changing environments.

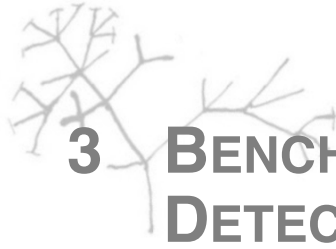
From these criteria Figueredo et al. (2003) highlight recent, low-albedo bands that fill interplate gaps as having very high potential for biosignatures. Smooth, salt-rich plains also rank very high, as do chaos regions that show evidence for melting and/or material exchange. Impact craters and ridges were ranked as moderate environments for hosting biosignatures, however, impact events could deliver abiotic compounds that complicate biosignature detection.

Finally, for completeness we note that a spacecraft designed for the study of the Jupiter and the Galilean satellites did indeed discover life on an inhabited world. The Galileo team detected signs of life on Earth during the Galileo spacecraft's Earth flyby, prompting Sagan et al., (1993) to declare that as we move forward with our search for life beyond Earth it is imperative that we proceed with caution, and adhere to the mantra that **“Life is the hypothesis of last resort.”**

The Europa Lander Science Definition Team adopted this mantra. In so doing the SDT generated a suite of investigations, and a mission concept, that could provide enough compelling information such that all other possible explanations are insufficient, and life is the only hypothesis that remains.



03 BENCHMARK ANALOGUES



3 BENCHMARKS FOR BIOSIGNATURE DETECTION: EARTH AS A BRIDGE TO OCEAN WORLDS

Earth Analogues for Europa's Ice Shell & Ocean

The search for life and habitable environments beyond Earth is grounded in the limits of life we know – and have studied – here on Earth (Nealson, 1997; Rothschild and Mancinelli, 2001; Shock and Boyd, 2015). Our search is focused on single-celled organisms (microbes), as they are more

pervasive in space and time on Earth than multi-cellular life, and single-celled life is an evolutionary prerequisite for multi-cellular life. The microbial biosphere on Earth is remarkably wide-reaching and diverse, occupying essentially every niche available, provided that the environment permits adequate regulation of material and energy exchange.

To guide the Science Definition Team's assessment of detection limits and measurement requirements for the Europa Lander, several "benchmark" ecosystems on Earth were considered as useful analogues for the ice and ocean environments of Europa. Total biomass, cell abundances, and organic content as measured in these environments served as useful metrics for potential biosignatures on Europa.

Here we briefly discuss three types of environments that were determined to be particularly relevant to conditions predicted for Europa:

- 1) the aphotic (removed from sunlight) deep polar oceans,
- 2) cold, deep brines, and
- 3) subglacial liquid water environments.

This discussion focuses on habitats disconnected from photosynthetic processes in which microorganisms of the domains Archaea and Bacteria, the smallest forms of eukaryotes, and phages (i.e., bacterial and archaeal viruses) thrive. The levels of organic carbon and associated characteristics for these environments reflect productivity and resource availability and

"Life on Earth is more like a verb. It repairs, maintains, recreates, and outdoes itself."

– L. Margulis

thus also inform biosignature detection thresholds. **Table 3.1** provides a summary of these key parameters.

Deep Polar Ocean Environments

Deep oceans, and the polar oceans in particular, are relevant Earth systems for establishing benchmarks for biosignature detection as they are cold, energy-limited, and ice-covered for much, if not all of the year, yet they harbor abundant chemosynthetic and heterotrophic microbial life at the base of the food web, in addition to other eukaryotic single and multicellular life forms in the water column and benthos.

A detailed understanding of the distribution of life forms in Earth's ocean, seafloor sediments, and ocean crust environments has become increasingly possible over the past 20

Table 3.1. Earth benchmark sites help establish detection levels to ensure that the Europa Lander model payload could detect signs of life across a variety of possible conditions. Guiding requirements for levels of detection for organic carbon, cell densities, and size ranges are shown in bold.

	Lake Vostok (Subglacial)			Lake Vida (Salty)		Winter Circumpolar Deep Water (Deep Ocean) ⁴
	Accretion Ice (Type I) ¹	Accretion Ice (Type II) ¹	Glacial Ice ¹	Brine ^{2,3}	Ice ³	
Organic carbon (μM)	65	35	16	64,700	n.a.	41 ± 3
DFAA (nM); DFAA % Org. Carbon	1-45; ≤ 0.006-0.17%	50-174; 0.08-0.49%	20-62; 0.6 – 1.2 %	n.a.*	n.a.	88 ± 16 ; 0.7 ± 0.1 %
Total Asp (nM)	15-49	8	11-39	n.a.*	n.a.	n.a.
DF L-Asp (nM)	6-10 [^]	n.d.	10 ^{^^}	n.a.*	n.a.	3-9 [#]
Cell density (cells mL ⁻¹)	260	80	120	49,000,000	444,000	30,000 to 100,000
Microbial size (μm)	~0.3 - 3.0	~0.3 - 3.0	~0.3 - 3.0	0.1-1	~0.5 - 2	0.2 – 1

Abbreviations: n.a., not available; n.d., not detected; DFAA, dissolved free amino acids; Asp, aspartic acid, and aspartate.

* DFAA and individual AA determinations are not available, although the protein content of the brine is high (~18% of DOC) in Lake Vida, so individual AA concentrations are expected to be very high compared to the accretion ice or ocean values. [^]at 3572 and 3605 m below surface; ^{^^}at 2610 m below surface. [#]Data from deep (>1000 m) seawater from Central North Pacific and Sargasso Sea (Kaiser and Benner, 2008) are similar to levels in Circumpolar deep waters (individual AA levels are not published). Cell density values for winter circumpolar deep water at 750 m from northern Antarctic Peninsula (n=32) provided by AE Murray. ¹Christner et al., 2006; ²Murray et al., 2012; ³Kuhn et al., 2014, ⁴Shen et al., 2016.

years largely due to advances in molecular biology and environmental genomic technology. Microbial life is globally distributed in Earth's oceans, and in general, cell abundances decrease with depth below the photic zone, through the oxygen minimum zone, and down to the deep ocean by about two orders of magnitude (Orcutt et al., 2011). On the seafloor, the ocean-sediment interface is an important region for biogeochemical transformations, and despite severe energy-limitation, the sediment-hosted subsurface biosphere that extends to great depths below this interface hosts a greater number of cells than does the oceanic water column above it (Whitman et al., 1998; Jorgensen and Marshall, 2016).

Globally, Bacteria and Archaea cell abundances in seawater are estimated at 3.1×10^{28} and 1.3×10^{28} cells, respectively, with the Bacteria-affiliated SAR11 currently being estimated as the most abundant (2.4×10^{28} cells; Giovannoni, 2017) and the Archaea-affiliated Thaumarchaeota falling not far behind (1.0×10^{28} cells; Karner et al., 2001). The third most abundant microbial group is *Prochlorococcus* (a Cyanobacteria clade affiliated with the Bacteria domain), which are distributed primarily between 40°S to 40°N latitude at depths of 100 to 200 m. *Prochlorococcus* are the most abundant photoautotrophic microbe in the ocean ($2.9 \pm 0.1 \times 10^{27}$ cells; Flombaum et al., 2013). **Photosynthesis is likely a very limited niche on Europa, so we focus here on chemosynthetic organisms, which significantly contribute to carbon cycling in the dark regions of Earth's oceans.** The non-photosynthetic marine Thaumarchaeota are primarily distributed below the photic zone to the depths of the abyssal ocean (Karner et al., 2001), and in the polar regions they can occupy surface waters in the ice-covered ocean during the dark winter periods (e.g., Murray and Grzymiski, 2007). Thaumarchaeota have ammonia-oxidizing, chemoautotrophic metabolisms and thrive throughout low energy parts of the ocean (e.g., Ingalls et al., 2006; Alonso-Saez et al., 2010).

Consideration of microbial-cell sizes for these key groups of Bacteria and Archaea in our own ocean helped guide the Science Definition Team's assessment of the resolution that would be required in order to obtain images of cells within a sample collected by the lander. Thaumarchaeota, Alphaproteobacteria-affiliated SAR11, and *Prochlorococcus* are all very small: 0.5–0.9 μm (Könnecke et al., 2005), 0.37–0.89 μm (Rappe et al., 2002), and 0.5–0.8 μm (Partensky et al., 1999) in their longest dimensions, respectively. **The dominance of sub-micron sized plankton in Earth's ocean drives detection level benchmarks for signs of life in Europa's subsurface down to resolve 0.2 μm cells.**

With respect to organic content of ocean waters and using those concentrations as figures of merit for detection limits, the SDT focused on deep ocean water in polar environments. The Circumpolar Deep Water (CDW), which surrounds the continent of Antarctica, is relatively salty and warm ($\sim 2\text{--}4^\circ\text{C}$) compared to Antarctic surface waters which are -1.8 to -2°C . At 750 m depth in the CDW in the Northern Antarctic Peninsula region, the levels of dissolved organic carbon ($41 \pm 3 \mu\text{M}$), individual amino acids (e.g., aspartic acid and asparagine; 3–5 nM), enantiomeric characteristics (relatively high levels of D-amino acids, $\sim 30\text{--}37\%$;

Shen et al., 2016), and biomass levels (averaging $7.4 \pm 3.2 \times 10^4$ cells mL⁻¹; n=32; personal communication, A. Murray) are indicative of a low-energy ecosystem, yet the signs of life are clear (**Table 3.1**). The deep waters of the Southern Ocean provide signs-of-life benchmarks for organic carbon and individual amino acids levels, as well as patterns of amino acid racemization found in natural environments.

Salt-rich (Brine) Environments

Aphotic, concentrated brines of varying salt compositions exist in many isolated locations on Earth – nearly all of which support microbial life, albeit substantially challenged in some cases by low water activity (Stevenson et al., 2015). Several large low-latitude brine systems lie in pools or basins in the Mediterranean, Red and Black Seas, and in the Gulf of Mexico. The Mediterranean deep brines are derived from a combination of evaporated seawater and dissolution of evaporites, and range from NaCl-brines in most of the basin to a MgCl₂ – dominated brine in Discovery Basin. The deep brines host cell densities ranging from $1.9\text{--}15 \times 10^4$ cells mL⁻¹ (van der Wielen et al., 2005). The brine environments in the Gulf of Mexico support dense microbial mat and sediment communities (Kellogg, 2010) and are thought to occur where deep subsurface brines are introduced to the seafloor along salt diapir-associated faults (Joye et al., 2005). Many of these deep marine-derived ocean (and inland ocean) systems harbor diverse microbial communities supporting autotrophic and heterotrophic assemblages often associated with methanogenesis, methane oxidation, and sulfur redox cycling.

Cold, icy brines pose additional constraints as the limits of cellular physiology are challenged by temperature and salinity. Nevertheless, diverse and active microbial assemblages have been reported. The most pervasive cold brines are those produced in sea ice that covers the polar oceans (**Figure 3.1**). Though microbial life in sea ice brines is fueled by photoautotrophic metabolism, the brines support large (e.g., in the Arctic $2 \times 10^5\text{--}2 \times 10^8$ cells mL⁻¹, Collins et al., 2008) and diverse heterotrophic bacterial populations (e.g., Bowman et al., 1997; Brinkmeyer et al., 2003; Bowman et al., 2012) that persist through long, dark winters in high-latitude oceans where photosynthesis is restricted.

The high latitude terrestrial cryosphere also hosts a number of unusual cold, NaCl brine systems at both poles (e.g., Forte et al., 2016). In the Canadian High Arctic, subzero brine seeps discharge at several sites where microbial life has been characterized, and metabolisms such as sulfate reduction and methane oxidation have been studied at temperatures as low as -20°C (Perreault et al., 2007; Niederberger et al., 2010; Lamarche-Gagnon et al., 2015). As another example, in Antarctica a large subglacial brine system that has an outlet at the face of Taylor Glacier – called “Blood Falls” (**Figure 3.2**) – hosts iron-rich mineral deposits and bacteria-dominated populations supported by chemolithoautotrophic metabolisms at densities measured to be approximately 6×10^4 cells mL⁻¹ (Mikucki et al., 2009). To the north of the

Taylor Valley lies Victoria Valley, where Lake Vida, a ~50 m deep frozen lake harbors a geochemically rich -13°C liquid brine system which permeates the ice through fissures and cracks below 16 m (**Figure 3.2**). The microbial assemblage found within Lake Vida is moderately diverse and is dominated by **ultrasmall cells $\sim 0.2\ \mu\text{m}$ in diameter ($48.5\text{--}61.4 \times 10^5\ \text{cells mL}^{-1}$)**, in addition to larger $\sim 0.5\ \mu\text{m}$ diameter cells ($0.1\text{--}0.6 \times 10^5\ \text{cells mL}^{-1}$); Murray et

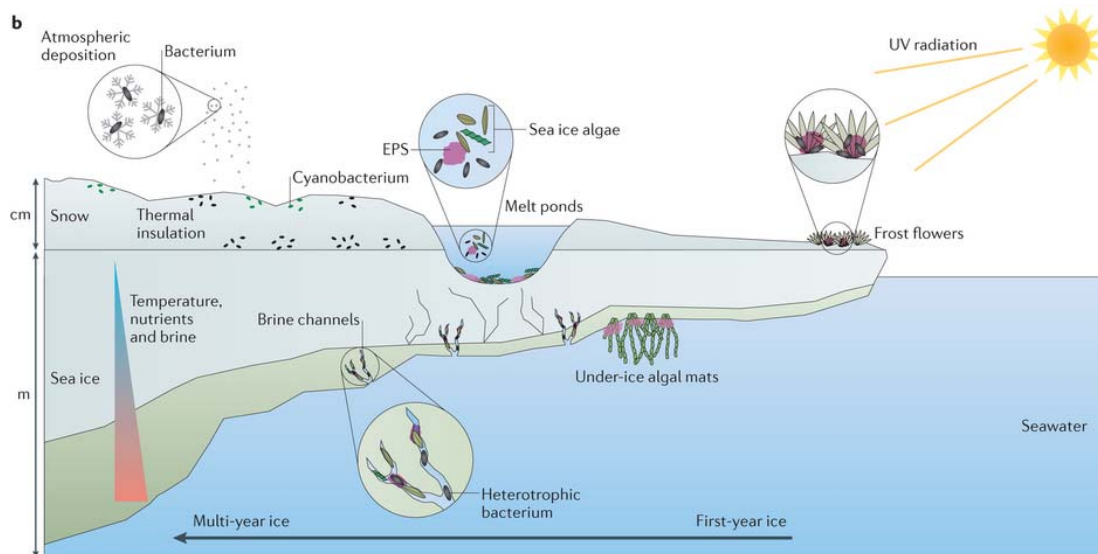


Figure 3.1. Snow and sea ice microbial habitats associated with ice-ocean interfaces on Earth (from Boetius et al., 2015). Heterotrophic bacteria inhabit all regions of snow and sea ice. Sea ice algae have been found in large aggregates at the bottom of melt ponds, and at the sea ice-ocean interface where filamentous diatoms (*Melosira arctica*) form large colonies. Diatoms in particular have pigmentation in the visible range that result in brightly colored bands in sea ice, while in snow on top of the sea ice, snow algae carotenoid pigments can be observed on the snow surface. High cell numbers at the interfaces between sea ice and seawater, snow or atmosphere have been attributed to higher primary productivity (e.g., in under-ice mats of diatom algae) and higher concentrations of brine or nutrients (e.g., brine channels and frost flowers).



Figure 3.2. Habitable aphotic subglacial brine systems in Antarctica. **Left:** “Blood Falls” at the shear zone of Taylor Glacier is the red surface expression of iron, sulfur, and organic compounds from a deep subglacial brine (Mikucki et al., 2009). **Right:** Ice over Lake Vida in Victoria Valley hides a -13.4°C brine in an ice-entrained aquifer in the lake ice below 16 m, which continues down into the permafrost at least 50 m below the lake surface (e.g., Dugan et al., 2015; Image: H. Dugan).

al., 2012). Despite the low temperatures, and potentially other limiting conditions, protein biosynthesis rates in Lake Vida brine were determined to be sufficient to support maintenance levels of metabolism (Murray et al., 2012).

Cold and saline ecosystems provide valuable context for detecting signs of life on Europa in a few dimensions. For example, isolated brine systems on Earth point to bacterial and archaeal survival under a wide variety of temperature and salinity conditions, including those beyond the established water activity levels that limit life (i.e., to 0.631; Yakimov et al., 2015). Furthermore, microbial survival over sustained periods at very low temperatures points to long-term cold survival (e.g., Lake Vida has been isolated for ~4000 years at -13.4°C , 18.5 m deep in the lake ice; Murray et al., 2012). Importantly, the low temperature limits of growth for microbes have recently been measured to extend down to at least -20°C (Clarke, 2014). Finally, cells common to extreme environments are known to be ultrasmall and either exist as ultramicrobacteria, or they reduce cell size as a response to environmental stresses (e.g., Roszak and Colwell, 1987; Kuhn et al., 2014). **For the Europa Lander mission concept, a lower limit benchmark for cell size should be $0.2\ \mu\text{m}$ or smaller to best support the ability to physically detect life.**

Antarctic Subglacial Lakes

Nearly 400 subglacial lakes have been identified in Antarctica (Wright and Siegert, 2012), and recent data from subglacial Lake Whillans implies that chemosynthetic microbial ecosystems may be widespread in the deep subsurface aquatic environments beneath polar ice sheets (Christner et al., 2014). Accretion ice that formed at the base of the East Antarctic Ice Sheet, over Subglacial Lake Vostok (SLV), offers the best available analogue on Earth to assess how geomicrobiological investigations of the ice can be used to infer chemical and biological conditions within the source water body. SLV exists beneath ~4 km of ice (**Figure 3.3**); has a surface area and volume of ~14,000 km² and ~5400 km³, respectively; and the lake has a maximum depth of ~800 m (Kapista et al., 1996; Studinger et al., 2004). Variation

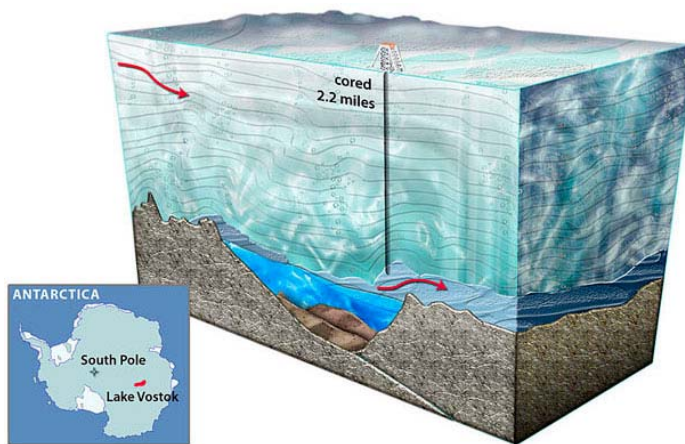


Figure 3.3. Diagram of Subglacial Lake Vostok, the largest of the subglacial lakes on the continent. The inset map shows the location, in red, of the lake. As the ice sheet moves over the lake, water is frozen onto the bottom of the ice sheet, and this ice has been sampled through a drilling program conducted by the Russian Antarctic Program (Source: Nicolle Rager-Fuller / NSF).

in the ice sheet thickness over SLV (from ~3900 to ~4200 m) significantly affects the pressure melting point of water such that glacial ice melts into the lake in the north, whereas ice accretion occurs in the southern portion of SLV (Wüest and Carmack, 2000). This process has been confirmed through analysis of samples from the basal portion of the Vostok ice core (below depths of 3,539 m), which has a chemistry and crystallography distinct from the overlying meteoric ice (e.g., low electrical conductivity, large ~1 m ice crystals (Jouzel et al., 1999)), and horizons with sediment inclusions (Simões et al., 2002; Souchez et al., 2002; Royston-Bishop et al., 2005).

Examination of ice samples from the deepest depths of the Vostok ice core has revealed two distinct categories of accretion ice (De Angelis et al., 2004). Accretion ice Type I (3539 m to 3609 m), contains 2–3 orders of magnitude more solute than accretion ice Type II (below depths of 3610 m), as the former forms by freezing of waters above an embayment of the main lake (**Table 3.2**). Accretion ice Type II forms by freezing over the lake proper, and therefore, is likely to be most analogous to ice formed by ocean water freezing to the base of Europa’s ice shell (e.g., Priscu and Hand, 2012). Biogeochemical and microbiological studies indicate that the accretion ice contains low concentrations of most major ions, microbial cells, and DNA (Priscu et al., 1999; Karl et al., 1999; Christner et al., 2006). Particles in Type II ice (3612 m) are at lower concentrations ($1.2 \times 10^4 \text{ mL}^{-1}$) than observed in meteoric ice, and the mode size of biotic particles in samples of Type II ice (as determined by flow cytometry) was $0.7 \mu\text{m}$ (Christner et al., 2008). Direct counts of DNA-containing cells by fluorescence microscopy in the SLV accretion ice were also dominated by cells $<1 \mu\text{m}$ in diameter, and the presence of aggregated populations and/or attachment of small cells to larger mineral particles was more commonly observed in samples of Type I ice compared with Type II ice (B. Christner, pers. comm.). Impurities (i.e., solutes, cells, particles, and gases) in SLV’s surface waters are rejected from the ice lattice during crystal formation (e.g., Killawee et al., 1998), and this means that the concentration of particular impurities in the source can be inferred if the degree of ice-water partitioning is known. Using ice and water column data from a permanently ice-

Table 3.2. Biomass, non-purgeable organic carbon (NPOC), and major ion concentrations in ices formed from subglacial Lake Vostok (Type I and II ice, see text and Christner et al. [2006] for details). Also shown are comparisons to average values for glacial ice and surface seawater. Cell densities and organic content measured in environments such as Lake Vostok served as a benchmark for measurement requirements and detection limits during the Europa Lander Science Definition Team study.

Constituent	Biomass (cells mL ⁻¹)	NPOC ($\mu\text{mol L}^{-1}$)	Concentration ($\mu\text{mol L}^{-1}$)						Total dissolved solids (mmol L ⁻¹)
			Na ⁺	K ⁺	Ca ²⁺	Mg ²⁺	Cl ⁻	SO ₄ ²⁻	
Type I Ice	260	65	22	0.32	6.8	5.8	17	9.1	0.061
Type II Ice	83	35	0.92	0.13	0.98	0.15	0.94	0.15	0.0033
Glacial ice (avg)	120	16	2.4	0.40	1.09	0.36	2.8	1.8	0.0088
Surface sea- water (avg)	$0.05\text{--}5 \times 10^5$	40–80	48,000	10,000	10,000	54,000	560,000	28,000	710

covered dry valley Antarctic lake, Christner et al. (2006) derived partitioning coefficients to estimate impurity concentrations in water at the ice-water interface of SLV's southern basin (Table 3.2).

Subglacial lake accretion ice is a highly relevant analogue for Europa through the demonstration that both cellular life, organic carbon, and inorganic materials can become entrained in overlying ice. **Subglacial Lake Vostok's Type II accretion ice serves as a valuable benchmark for the low limits of cell density, where a detection threshold of 100 cells per mL has been established (Table 3.1).**

Application to Europa: Energetic considerations to support life

The search for signs of life on Europa requires complementary lines of evidence, and is tethered to samples of a defined reference material. In the previous sections, we described analogue reference environments and samples. Here, we extend the geochemical conditions of some of those environments to models for Europa and calculate the projected biosignature levels based on a range of modelled conditions.

These terrestrial benchmark materials were chosen both because (a) they more closely approximate the physical settings to be investigated on Europa than do other inhabited environments on Earth, and (b) they are low energy systems, and are among the most oligotrophic – that is, the most sparsely populated by living organisms – such that they constitute a conservative design for benchmarks to establish criteria for biosignature detection. **It must be acknowledged, however, that there is likely to be no perfect analogue for the european environment to be found on Earth, and hence experiments to search for signs of life and their protocols must be designed to the greatest extent possible to function in unanticipated environments.**

One key difference between Earth and possibly every other liquid-water-bearing body in our solar system is the magnitude of biologically usable energy flux into the liquid water environment, a difference that could directly affect the quantity and quality of evidence for life. Most of the features that are proposed as biosignatures ultimately result from life's unique utilization of energy to mediate chemical and physical processes with speed, specificity, and selectivity. As such, and as described below, it can be expected that the abundance of life and the quantity and quality of biosignatures present in a given system would depend on the flux of energy into that system.

On Earth, the direct availability of sunlight within the habitable environment means that our biosphere is supported by an energy flux many orders of magnitude larger than is possible in any of the other liquid water-bearing environments in our solar system. A recent

conservative estimate of the global flux of biologically-accessible energy on Europa (Vance et al., 2016), normalized per unit volume of ocean water, is in the range of 10^{-15} to 10^{-13} W per L, for a 100-km deep ocean with low to moderate seafloor activity. The solar energy entrained into photosynthesis on Earth, at approximately 10^{-6} W per L, represents a volume-normalized energy flux to the biosphere that is 7–9 orders of magnitude larger. Significantly, our concept of what an inhabited world “looks like”, and the nature and abundance of the biological signal in the chosen design reference materials, is fundamentally linked to this larger energy flux. **Ocean worlds such as Europa may be inhabited, but the energy regime in which they operate could yield a significantly different “fingerprint” of life on such worlds.**

The influence of energy flux on biosignatures can be evaluated through reference to the two basic purposes into which life partitions energy flux:

1. *Life expends energy to sustain existing biomass in a metabolic-steady state (metabolically functional but not growing).*

Efforts to quantify “maintenance energy” have yielded a wide range of estimates that depend partly on the organism in question, partly on its metabolic status, and partly on the conditions in its host environment (Hoehler and Jørgensen, 2013). However, adopting a value of 5×10^{-18} W cell⁻¹ – derived from a study of aerobic organisms adapted for tens of millions of years to one of Earth’s most oligotrophic settings (Røy et al., 2012), and therefore presumably representing exceptionally energy-efficient cells – equates to a global euroman ocean average of 2×10^2 to 2×10^4 cells L⁻¹ if all available energy were utilized only to maintain standing biomass (**Figure 3.4**). These numbers must be taken in context: there is no way of knowing whether the maintenance energy associated with euroman cells would be comparable to that of Earth’s organisms, and a bulk average, as calculated here, cannot adequately capture the heterogeneity in biomass density that is likely to characterize any real population.

However, taking these numbers at face value is instructive: the upper end of this range approaches the cell density of approximately 100 per mL in our design reference material. The lower end of the range would still equate to a global biosphere approaching 10^{24} cells, but represents a case in which life on an inhabited Europa might go undetected by an investigation that seeks extant cells. This case underscores the importance of both seeking independent lines of evidence and including investigations that can help to establish the detailed environmental context required to interpret a possible non-detection of life.

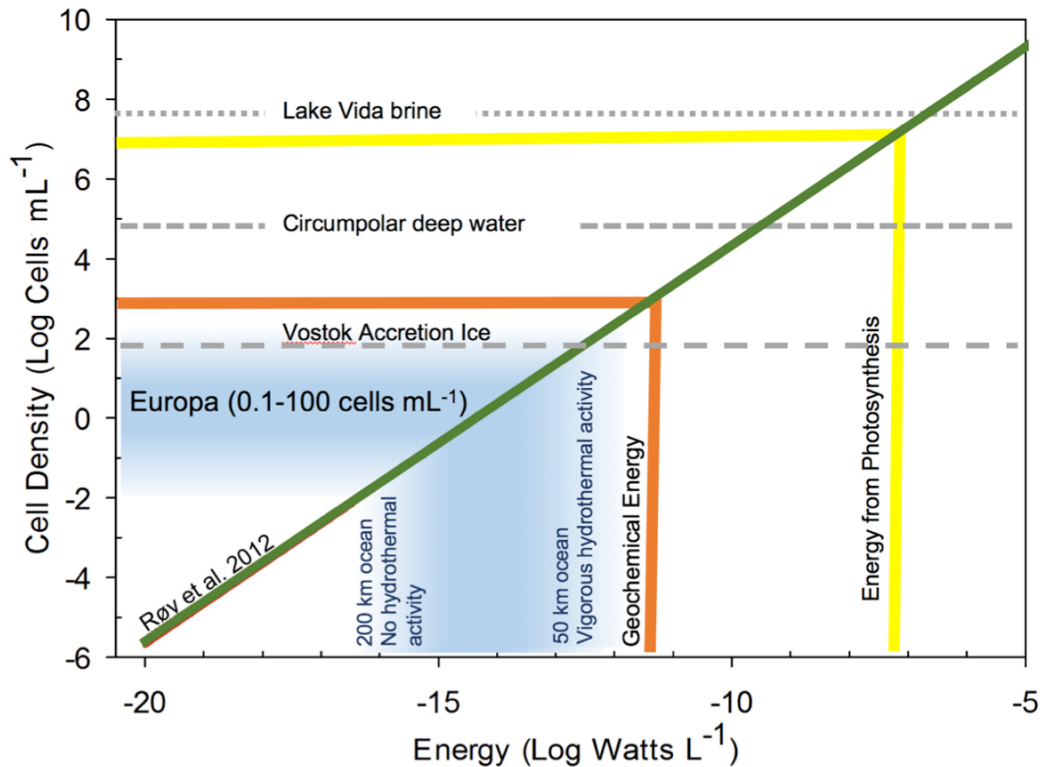


Figure 3.4. Cell density supported in steady state vs. energy flux (green line), calculated on a volume-normalized basis from cell-specific maintenance energy requirements reported in Røy et al., 2012 (derived from aerobic cells in ancient, energy-poor deep ocean sediments). Points of reference from Earth: horizontal dashed lines indicate average cell density in Type II accretion ice from Subglacial Lake Vostok (83 cells mL^{-1} ; Christner et al., 2006), circumpolar deep water ($7.4 \pm 3.2 \times 10^4 \text{ cells mL}^{-1}$, average of 32 samples at 750 m; source: A. E. Murray), and Lake Vida brine (average of $5.5 \times 10^7 \text{ cells mL}^{-1}$; Murray et al., 2012). Photosynthesis line (yellow) indicates the flux of chemical energy (as organic carbon + O_2) provided by oceanic photosynthesis, as a global ocean average (total oceanic productivity/global ocean volume). The Geochemical Energy line (orange) is an estimate of modern global oceanic chemical energy provision (as chemical reductant flux into an aerobic ocean), based on the calculations of McCollom and Amend (2005). The shaded blue bands indicate a range of energy flux estimates for Europa (Hand et al., 2009; Vance et al., 2016), across a range of ocean volumes (50 km deep to 200 km deep). Using the Røy et al. (2012) conversion of energy to biomass, the corresponding average cell abundances within Europa's ocean would be in the range of 0.1 to 100 cells mL^{-1} of ocean water. Though Europa may harbor significant chemical energy, the large volume of the ocean could lead to a high level of biomass dilution. Life, however, typically concentrates around interfaces of chemical disequilibrium, and thus dilution of biomass throughout the ocean may not be an accurate assumption.

2. Life expends energy to synthesize new biomass.

An end-member case in which new biomass is created at the energy-limited rate and the corresponding cells are immediately destroyed (so that the energy partitioned to cell maintenance is minimized) establishes an upper bound on the rate at which biological material can enter the dissolved (bulk ocean) pool. This rate, in conjunction with the rate at which

organic material is removed from the dissolved pool by chemical, physical, or biological mechanisms, determines the concentration at which biologically-derived materials could be present as dissolved components in ocean water. Because the rate of removal and the factors controlling that rate are unknown for Europa, it is more useful to think of the energy-constrained biosynthesis rate as determining the residence time, τ , of material in a given pool, when the concentration within that pool is specified: $\tau = [i]/R_i$ (where $[i]$ and R_i are the bulk ocean concentration and global rate of production of a specified compound or pool, i).

For example, using a biosynthetic energy requirement of 150 kJ per gram of new biomass synthesized (an average value for aerobic microorganisms on Earth; Heijnen and van Dijken, 1992), the estimated energy fluxes on Europa would equate to biosynthesis rates of 0.6–30 pg biomass per liter per year. At these levels, $\tau = 2 \times 10^{10}$ to 4×10^8 years for biologically-derived bulk dissolved organic carbon for a seawater concentration equivalent to Earth's deep ocean (40 μM). At the high end of this range, total dissolved organic carbon in Europa's ocean could have reached Earth-like levels during the first 10% of the ocean's history, and would have turned over 10 times during the entire age of the ocean; at the low end of the range, concentrations would have risen to approximately 8 μM by present day. Note that this is for bulk organic carbon. Compounds that comprise a smaller fraction of the bulk ocean organic content than the fraction they comprise in biomass (e.g., amino acids) could have a correspondingly shorter residence time.

For example, aspartic acid comprises 13 wt. % of an “average” protein, which in turn comprises about 55% by weight of the biomass in an Earthly *E. coli* cell. For a bulk ocean aspartic acid concentration of 1 nM, $\tau = 3 \times 10^6$ to 6×10^4 years. In either case, **the ocean of Europa could accumulate levels of amino acids comparable to the individual free amino acid concentrations in Earth's deep ocean water over timescales that are very short compared to the age of the ocean on Europa.** Again, these calculations are based on energy-biomass and biomass composition relations that are applicable to Earth organisms, and it is uncertain how applicable they may be in quantitative terms to putative europian life. Nevertheless, it is important to consider the implications of long residence times for life detection.

In general, a longer residence time means that biologically-derived material has a longer period to undergo diagenetic processes or be consumed, and it is noteworthy that the organic composition of bulk dissolved organic carbon in Earth's oceans differs considerably from that of fresh biological matter. Moreover, in the specific case of amino acids, a longer residence time means that racemization (abiotic inter-conversion between the D and L forms) acts on the pool to a greater extent, with a correspondingly greater loss of the biological signal of enantiomeric excess. In the case of an aspartate residence time $\tau = 6 \times 10^4$ years, spontaneous racemization at 260 K of a pool supplied continuously with enantiomerically pure material would yield a steady-state enantiomeric excess of 50% (e.g., 75% L-aspartate and 25% D-aspartate).

Summary

Benchmark environments on Earth provide a useful guide for how variations in environmental conditions affect habitability, biological activity, and ultimately biosignature type, size, and concentration. **On and within Europa, life might concentrate at the interfaces, such as the seafloor or ice-water interface.** Hydrothermal activity may power life, much as it does on Earth's seafloor, and oxidants within Europa's ice may help provide compounds to power life on Europa. Liquid water regions within the ice shell itself may also support life. **Materials from the ocean could be entrained into Europa's ice shell or plumes, leading to potential biosignatures within the ice fractures, ice blocks, and plume materials.** **Figure 3.5** provides an artistic representation of Europa in cross-section. Various processes, from the seafloor to the surface are indicated, providing an integrated perspective on how the seafloor, ocean, and ice shell could yield biosignatures detectable on the surface by a landed spacecraft.

In the chapter that follows, the science Goals, Objectives, and Investigations of the Europa Lander mission concept are described in detail, followed by a description of the model instrument payload. Throughout the descriptions of measurement requirements, reference is made back to the Earth analogue environments presented here.

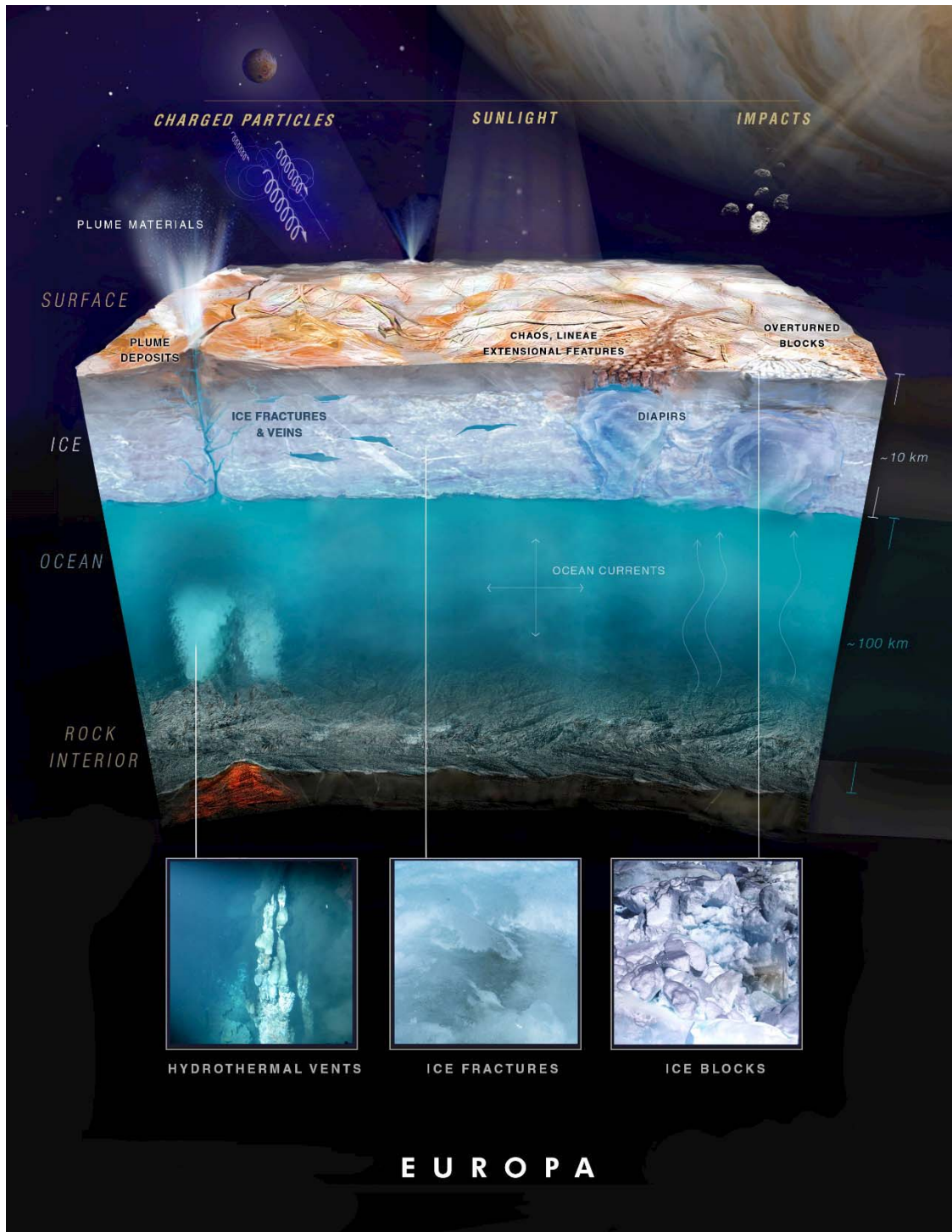
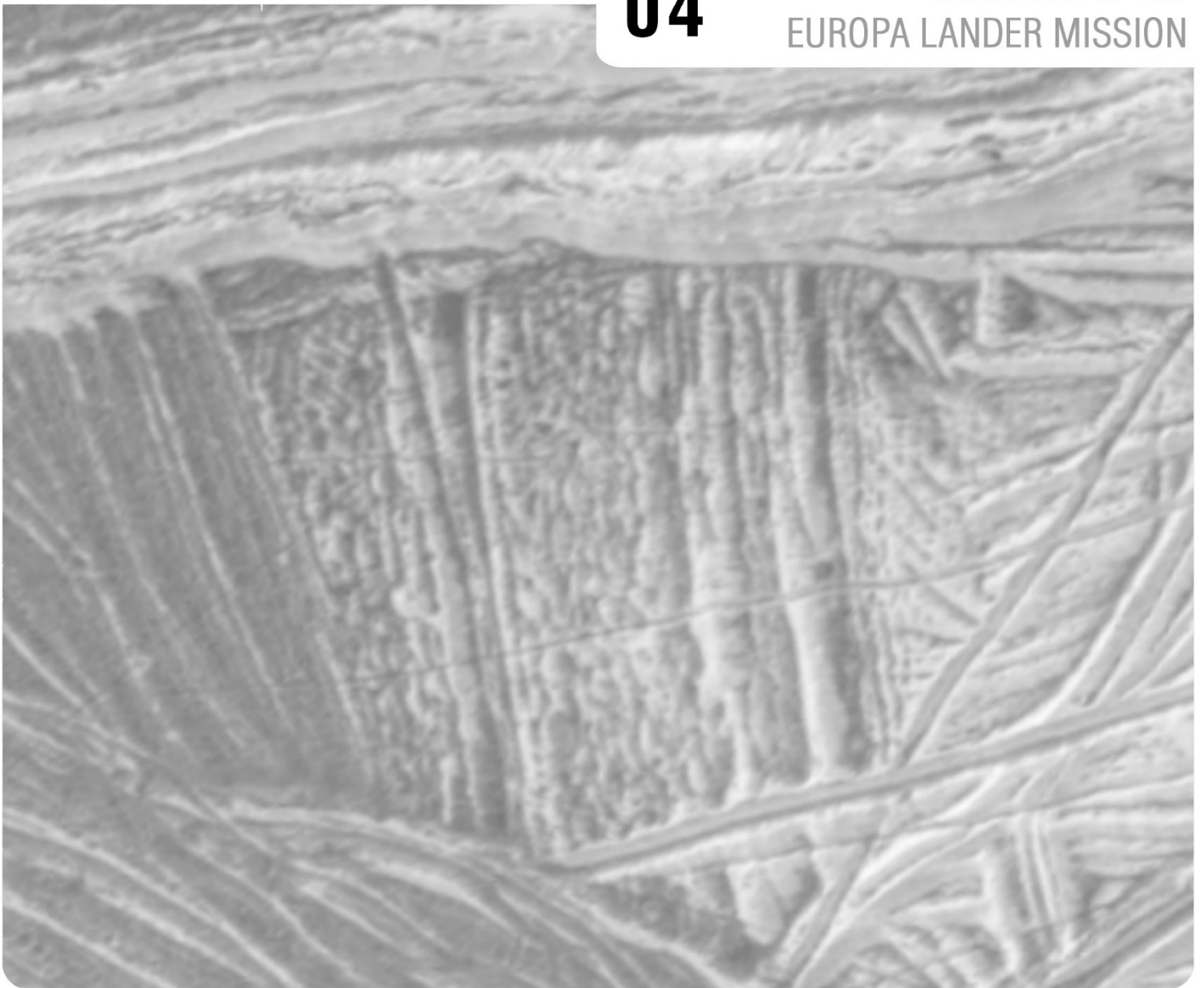


Figure 3.5. Artistic representation (not to scale) of Europa in cross-section showing processes from the seafloor to the surface. Boxes indicate potentially habitable sites such as hydrothermal vents, and regions on and within the ice shell that could harbor biosignatures. This diagram shows an integrated perspective of how the seafloor, ocean, and ice shell could yield biosignatures detectable on the surface by a landed spacecraft.



04

SCIENCE OF THE
EUROPA LANDER MISSION



4 SCIENCE OF THE EUROPA LANDER MISSION

The science of the Europa Lander mission is organized into three Goals that are ranked in priority order: **1) Search for evidence of life on Europa,** **2) Assess the habitability of Europa via in situ techniques uniquely available to a landed mission,** and **3) Characterize surface and subsurface properties at the scale of the lander to support future exploration.** The Science Traceability Matrix (**Table 4.4.1**) provides traceability from the Lander Goals, Objectives, and Investigations to measurement requirements, model payload, and mission requirements.

The high-level Goals and Objectives of the Europa Lander mission concept are shown in **Figure 4.1** as a circle of connected science investigations, each of which plays an important role in the scientific success of the mission.

Critically, **scientific success cannot be, and should never be, contingent on finding signs of life** – such criteria would be levying requirements on the results of an experiment. Rather, **scientific success is defined here as achieving a suite of measurements such that if signs of life are present in samples collected from the near-subsurface of Europa’s ice shell they could be detected at levels comparable to those found in benchmark environments on Earth** (Chapter 3). Furthermore, if no potential biosignatures are detected, the science return of the mission must significantly advance our fundamental understanding of Europa’s chemistry, geology, geophysics, and habitability.

In the sections that follow, we detail the science rationale of each Goal and the Objectives and Investigations within that Goal. The Goals, Objectives, and Investigations then feed into measurement requirements and example Baseline and Threshold model payloads for the Europa Lander mission concept. In some cases, the measurement requirements and implementation options are described at the Investigation level, in other cases they are described at the Objective level.

The Science Traceability Matrix (**Table 4.4.1**), provided towards the end of the chapter, charts the traceability between the Goals, Objectives, and Investigations to measurement requirements and mission functional requirements. Details of the model payload are provided

in section 4.5 of this chapter, and a coordinated approach for surface phase operations, including sample acquisition and analyses, is provided in **Chapter 5**. Additional information on sampling and mission operations to support science can be found in **Chapters 8** and **9**.

Finally, we emphasize that while the Europa Lander mission concept described here would follow on the Europa Multiple Flyby Mission (EMFM), and leverage results from that mission (especially for landing site selection, **Chapter 6**), none of the science of the Europa Lander mission requires interaction with the EMFM.

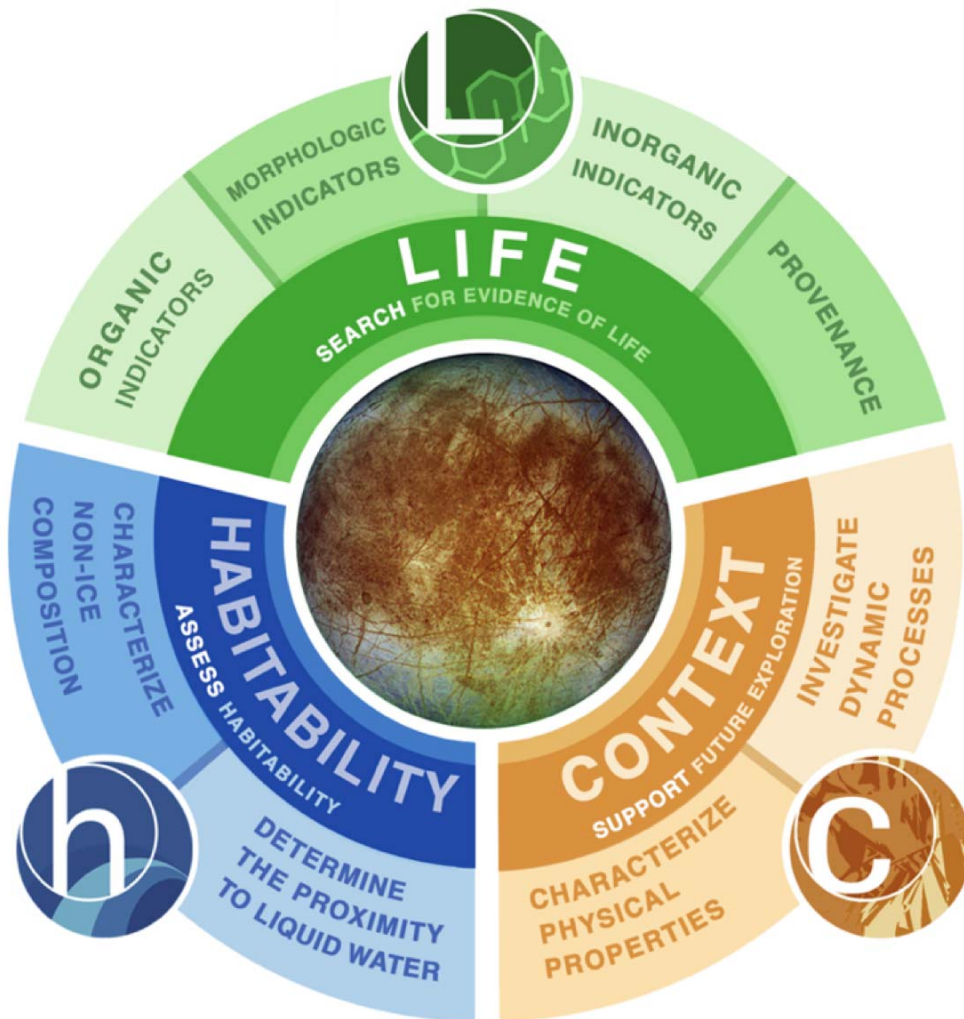


Figure 4.1. Science Goals and Objectives of the Europa Lander mission concept. In terms of priority order for science, Goal 1: Search for evidence of life (L) ranks highest, followed by Goal 2: Assess habitability (h), which is then followed by Goal 3: Support future exploration (c). Within each Goal are the high-level Objectives, represented as a fan across each Goal.

4.1 GOAL 1: BIOSIGNATURES & SIGNS OF LIFE



Goal 1 for the Europa Lander is to search for evidence of life on Europa. Biosignatures are features or measurements interpreted as evidence of life. No single line of evidence is sufficient for concluding that life has been detected. A robust detection of life requires several complementary and redundant biosignatures. Through nine distinct but related investigations, each of which represents at least one biosignature, the Europa Lander will enable the study of the surface and near-subsurface of Europa such that if biosignatures are present at levels comparable to the benchmark environments (Chapter 3), then life could be detected.

The first of the four Objectives (A, B, C, D) within Goal 1 focuses on the search for, and characterization of, organic compounds. Objective 1A emphasizes the importance of a biochemical definition for life: Is there carbon on Europa and if so, does the population of carbon compounds reveal any signs of biological processes?

As emphasized in the NASA Astrobiology Strategy (NASA, 2015), the fidelity of life detection benefits greatly from strategies that target measurements of multiple, distinct biosignatures. Objectives 1B and 1C of Goal 1 are highly complementary to the biosignature measurements within Objective 1A. Objective 1B targets morphologic evidence for life, while Objective 1C examines samples for biominerals. Lastly, Objective 1D addresses sample provenance and the context that is required for interpretation of the physical and chemical data generated in Objectives 1A, 1B, and 1C.

By developing a detailed, and integrated, understanding of the chemical, physical, and geological nature of the landing site and samples collected directly from the near-subsurface, the Europa Lander mission presents a set of complementary investigations that could detect signs of life, and which are robust to false positives and ambiguous results.



4.1.1

OBJECTIVE 1A: DETECT AND CHARACTERIZE ANY ORGANIC INDICATORS OF PAST OR PRESENT LIFE.

The purpose of Objective 1A is to seek evidence of biological activity by detecting and characterizing the organic composition of the sampled material. Within Objective 1A are three Investigations (1A1, 1A2, and 1A3) that target several complementary indicators of biological activity (**Figure 4.1.1**).

Life affects the organic chemistry of a system through production of biomolecules, consumption of organic substrates, and through the generation of metabolic intermediates and end products. Abiotic processes can also yield a diverse inventory of organic compounds, including many species that are utilized in the biochemistry of Earth's life. The challenge is therefore to distinguish molecules of uniquely biological character from a background of abiotic organic chemistry.

Organic chemistry in Earth's environments contains many features that allow such distinction to be made, but **three general properties of life as it occurs on Earth best serve as a framework for identifying extraterrestrial organic biosignatures: (i) biologically catalyzed reactions generally occur with significantly greater specificity, selectivity,**

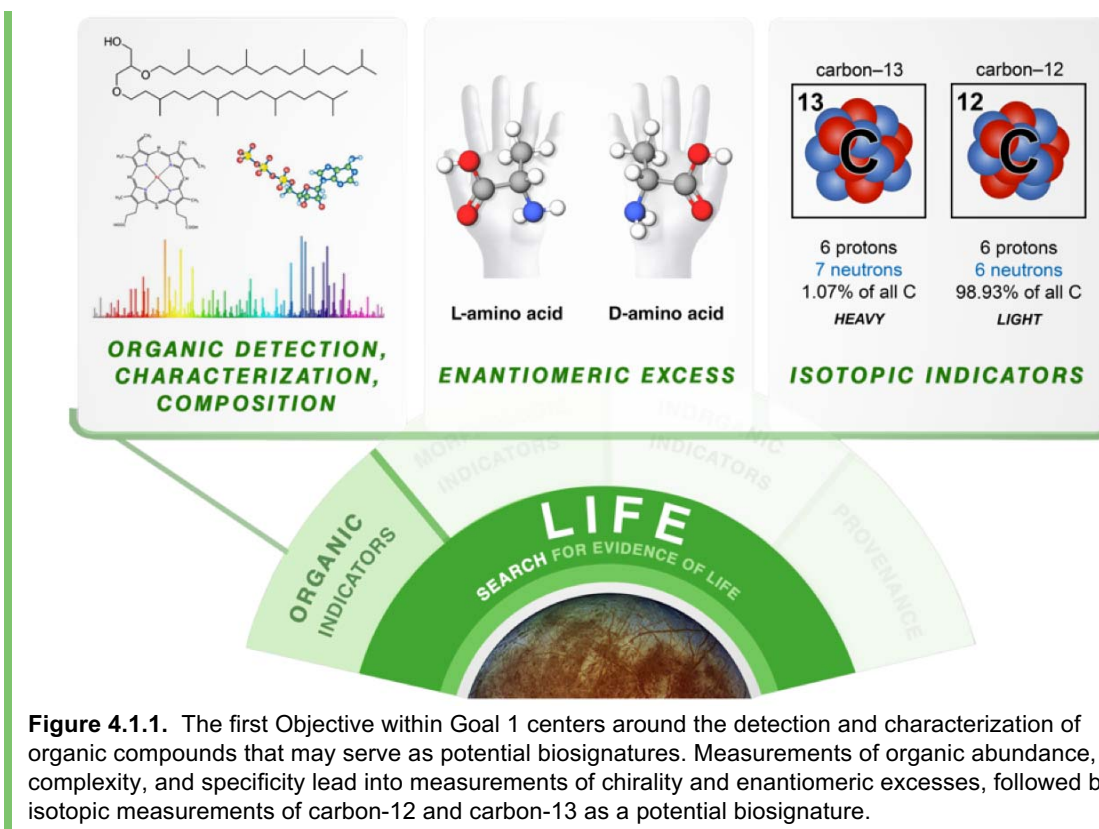
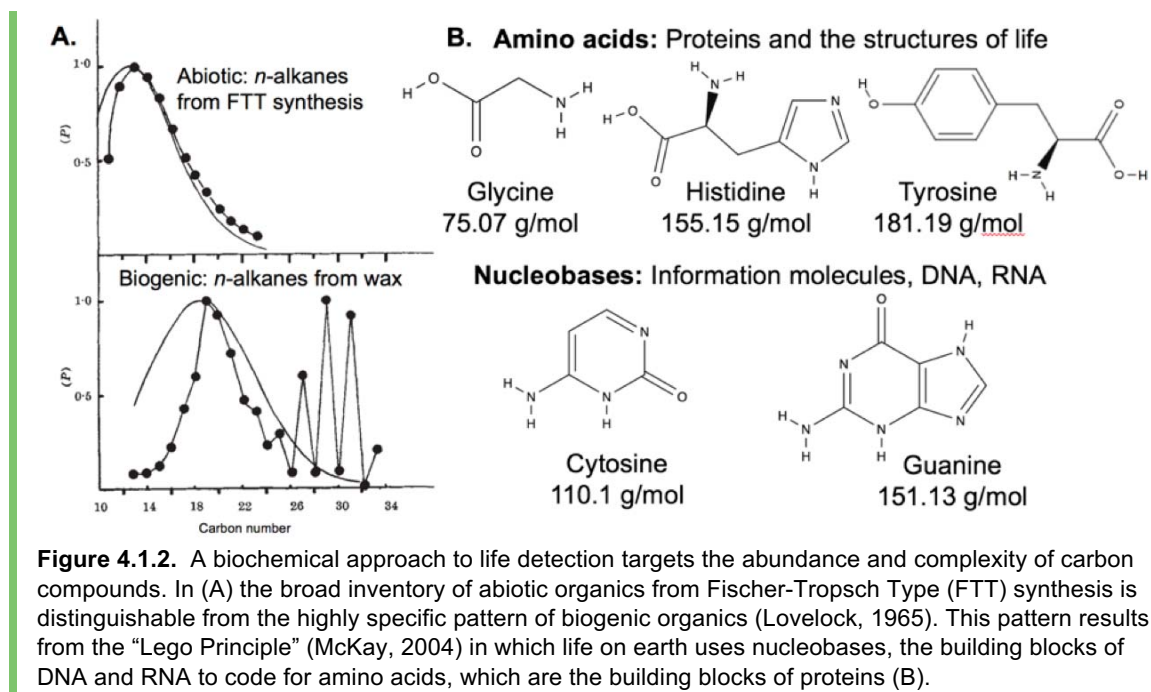


Figure 4.1.1. The first Objective within Goal 1 centers around the detection and characterization of organic compounds that may serve as potential biosignatures. Measurements of organic abundance, complexity, and specificity lead into measurements of chirality and enantiomeric excesses, followed by isotopic measurements of carbon-12 and carbon-13 as a potential biosignature.

and speed than the corresponding abiotic reactions; (ii) life invests energy repeatedly and in a specific fashion in order to yield otherwise thermodynamically unfavorable products, including specific (non-random) polymer sequences; and (iii) biosynthesis pathways may rely on repetition of specific molecular motifs, such as 2-carbon acetyl units (CH_3CO) or 5-carbon isoprene units, resulting in non-thermodynamic distributions among end products (over-representation of sub-unit multiples, relative to the molecular distribution resulting from abiotic synthesis). To the extent that these properties may be common to biological systems in general, they represent a set of “rules” with which to predict or identify diagnostically biogenic features in organic chemistry, even if generated by biochemistries that differ from life on Earth (Figure 4.1.2) (Lovelock, 1965; McKay, 2004).

Investigation 1A1: Determine the abundances and patterns (i.e., population distributions) of organic compounds in the sampled material, with an emphasis on identifying potentially biogenic characteristics.

Evidence of biogenicity of organic compounds should be sought in the patterns both within and among molecules. Life invests energy into the synthesis of specific structural, functional, and information-carrying molecules whose presence or relative abundance can be indicative of life processes (Peters et al., 2005; Summons et al., 2008; Eigenbrode, 2008). Abiotic processes generally produce samples containing smooth distributions of molecular properties, e.g., following a Poisson distribution as a function of compound mass. In contrast, biological processes create complex discretized distributions as a result of the specificity required to build the ordered structures of life (Figure 4.1.2 and Figure 4.1.3).



Some of the molecules synthesized by life – for example, some alkaloids, steroids, and pigments – are, given the current state of knowledge, uniquely biogenic. Such compounds contain a complexity of structure and/or diversity of chemical motifs that would be highly improbable to achieve outside of a biological system, with evidence of biogenicity therefore lying in a single compound rather than in patterns of relative abundance among compounds. The simple presence of such molecules, if demonstrably endogenous, would provide strong evidence for life; therefore, they represent attractive biosignature targets (Summons et al., 2008).

Importantly, a search for diagnostically biogenic molecules need not exclusively target the complex “biomarker” molecules known from life on Earth; indeed, it is questionable whether those same molecules, which represent highly specific and evolved features of our biochemistry, could be expected to emerge from a separate origin of life. Rather, the preferred approach is to assess molecular complexity in more general terms (e.g., Li and Eastgate, 2015; Böttcher, 2016), in order to encompass compounds that are not found in biochemistry on Earth, but whose features may nonetheless indicate uniquely biological character.

For example, Cronin (2016) has developed an approach to calculate complexity based on the number of unique synthetic pathways represented in the structural fragments or components of an overall molecular structure. When defined in this fashion, complexity is an intrinsic property of the molecule and its calculation does not require external calibration. Moreover, because the complexity metric is based on the identification of unique fragments and substructures, the algorithmic determination of complexity in known structures has an analytical counterpart – based on successive molecular fragmentation with mass spectral analysis – that does not require the structure of the parent molecule to be uniquely identified. The clear advantage in such an approach is that it is fully “agnostic” with respect to the specifics

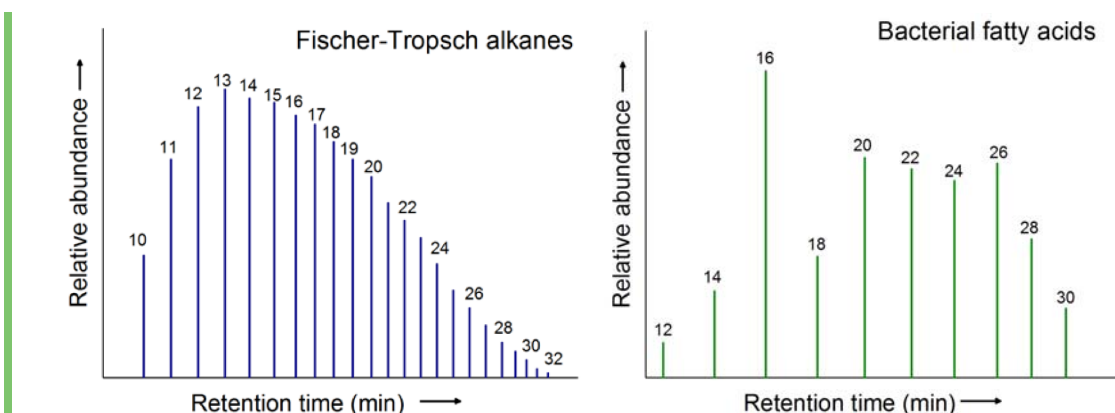


Figure 4.1.3. Left: Gas chromatogram of reaction products of Fischer-Tropsch synthesis, a non-biological process, showing the broad, non-specific production of organics. In contrast, the gas chromatogram on the right shows the specificity associated with biological processes, in particular the fatty acid fraction from a bacterial extract (Hartgers et al., 2000). Numbers above each line indicate total number of carbon atoms in the molecule associated with each peak.

of biochemistry: it seeks a generic manifestation of life's unique capability for complex molecular synthesis without assuming prior knowledge of a particular biochemistry.

Patterns among molecules can also provide evidence of biogenicity. For example, carboxylic and amino acids, as individual compounds, can be formed abiotically and have been identified in a variety of extraterrestrial materials. In these cases, it is not merely the presence, but rather the **relative distribution of molecular types that specifies a biogenic origin**. Here we detail the specific cases of carboxylic acids and amino acids as “Lego™ blocks”, and how specificity and distributions among these compounds could serve as a strong biosignature on the surface of Europa. We also highlight metabolic products resulting from biological processes as an important class of compounds that could serve as a biosignature.

Carboxylic Acids. The distribution of carbon chain length in populations of carboxylic acids differs markedly in biological samples relative to abiotic. Biological carbon chains are generally built up two – or in the case of Archaea, five – carbon atoms at a time, which leads to the observed biological “Lego™ blocks”. These products include the phospholipid fatty acids (PLFAs), which have specific chain lengths and give cellular membranes their structure. PLFAs serve as powerful indicators of life through the highly non-random pattern of carbon numbers and chain lengths (Balkwill et al., 1988; Costello et al., 2002; Lester et al., 2007; Steger et al., 2011). As a specific example, the two-carbon biosynthetic pathways of Bacteria and Eukaryota leads to the prevalence of even-numbered chains in biologically derived materials, while abiotic synthesis yields a smoother distribution of even- and odd-numbered chain lengths (**Figure 4.1.3**).

Amino Acids. The processes that govern the production of amino acids, and the resulting pattern in the distribution of those acids, differ markedly in biological and abiotic systems (e.g., Creamer et al., 2016). The production source can be determined using different analytical approaches, supporting the utility of amino acid types and distributions as a biosignature (Dorn et al., 2003). Life on Earth uses 22 amino acids, while over 70 have been detected in meteorites (Lu and Freeland, 2006, Cronin and Pizzarello, 1983; Ehrenfreund and Charnley, 2000); about 500 members of this chemical class are known (Gutiérrez-Preciado et al., 2010). **Abiotically produced amino acids have abundance distributions driven by thermodynamics and kinetics** (Higgs and Pudritz, 2009), in sharp contrast to **biotic amino acid distributions that are driven by functionality**.

Several amino acids (Alanine [Ala], Aspartic acid [Asp], Glutamic acid [Glu], Glycine [Gly], Leucine [Leu], Serine [Ser], and Valine [Val]) are abundant in both biological samples (Lobry, 1996) and in CM2 and CR2 carbonaceous chondrite meteorites (Cronin, 1983; Shimoyama, 1985; Martins et al., 2007ab; Pizzarello and Holmes, 2009; Cobb and Pudritz, 2014). However, terrestrial proteinogenic amino acids include representatives (e.g., Histidine [His])

that, potentially owing to the complexity of synthesis, are not found in meteorites. The meteoritic amino acids, however, include several that are found sparingly or not at all in biological material on Earth (e.g., alpha-Aminoisobutyric acid [α -AIB], Isovaline [Iva], beta-Alanine [β -Ala], and gamma-Aminobutyric acid [GABA]; **Figure 4.1.4**).

Within the pool of amino acids that are common to biology on Earth and meteorite samples, relative ratios and the composition of amino acids can further differentiate biotic and

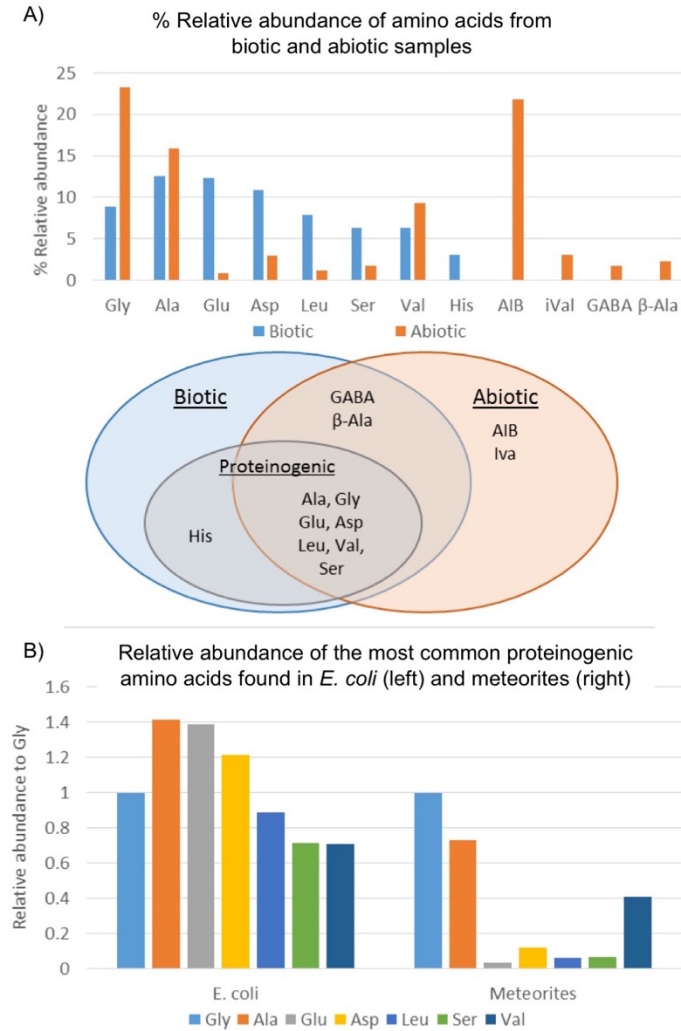


Figure 4.1.4. A) Relative abundance of amino acids that occur most frequently in abiotic and biotic samples. B) Relative abundance of the proteinogenic amino acids with respect to Gly. Data for the *E. coli* values comes from averaging concentrations reported in Aubrey, 2008; Lobry and Gautier, 1994; Nishikawa and Ooi, 1982. Data for meteorites comes from averaging concentrations of amino acids reported for CM2 (Cronin and Pizzarello, 1983; Shimoyama et al., 1985) and CR2 (Martins et al., 2007ab; Pizzarello and Holmes, 2009). Figure reproduced with permission of authors from Creamer et al. (2017).

abiotic samples. In particular, **higher molecular weight (mass >100 Da) amino acids are over-represented in terrestrial biological samples relative to meteorite samples**, where thermodynamic factors favor a prevalence of low molecular weight species (Higgs and Pudritz, 2009; **Figure 4.1.4**). It is important to note that although on Earth a set of 22 amino acids are used by life, extraterrestrial life could use a different set of building blocks.

Metabolic Products.

Metabolism can leave an imprint on organic chemistry through consumption of substrates and generation of either end-products or chemical intermediates. In some cases, rates of substrate metabolism can be higher than those of biosynthesis on a molecule-for-molecule basis, particularly for low energy (e.g., methanogenic) metabolisms or for populations characterized by maintenance metabolism rather than active growth. As such, metabolic intermediates and end-products (e.g., methane) can potentially be much more abundant than the biomolecules of

the life that generated them. However, the end-products of metabolism may also be less diagnostic because many such molecules – e.g., methane, hydrogen sulfide, nitrogen, carbon dioxide, and others – are also formed through a variety of abiotic processes. In such cases, the imprints of life’s catalytic speed and/or selectivity must serve as evidence of biogenicity, and it becomes important to accompany abundance measurements with stable isotope ratio (i.e., Investigation 1A3) and broader physical and geochemical context measurements (Objectives 1B/1C/1D; Goal 2).

Metabolic intermediates may represent a target class in which molecules are more abundant than the products of biosynthesis and also potentially less ambiguous than metabolic end-products. The conversion of substrates to end-products in biological systems often occurs in multiple steps – either as part of a biochemical pathway within a given organism or, as often occurs in Earth’s anaerobic ecosystems, by the sequential action of different metabolic groups of organisms operating in consortia. The formation of chemical intermediates during these multi-step processes creates the potential for ‘leakage’ of compounds that, relative to the ultimate (equilibrium) end-products, may be either more difficult to make abiotically or may remain in disequilibrium relative to local environmental conditions. The nitrous oxide formed during biological denitrification and the acetate passed between organisms in Earth’s organic-fueled anaerobic ecosystems are respective examples. To encompass such targets requires a capacity to discern compounds whose abundance, relative to the broader context of local organic chemistry, cannot be accounted for by abiotic mechanisms. For this, an analytical approach capable of broadly characterizing the organics of the sampled material, rather than a focus on a few specific targets, is necessary.

Measurement Requirements & Implementation Options

Underlying “rules” that give rise to molecular patterns, such as observed in biochemistry on Earth, are expected to be a general feature of biological systems reflected in any alternative biochemistry that might be encountered on Europa. Hence, the analytical approach for this investigation is to search for individual compounds that have no known abiotic origin, *and* for specific patterns and distributions within compound classes atypical of abiotic processes. The specific requirements to address Investigation 1A1 are:

- **Determine the presence, identities, and relative abundances of amino acids, carboxylic acids, lipids, and other molecules of potential biological origin (biomolecules and metabolic products) at compound concentrations as low as 1 picomole in a 1 gram sample of europian surface material.**

- **Determine the broad molecular weight distribution to at least 500 Da (Threshold) and bulk structural characteristics of any organics at compound concentrations as low as 1 picomole in a 1 gram sample of european surface material.**

The first requirement targets definitive identification of individual compounds and/or suites of compounds that could represent biomolecules or metabolic intermediates and end products. The stated detection requirements are set at a level that would allow quantification of free amino acids at the concentrations (low nM) typically observed in Earth reference materials, such as deep ocean water or Lake Vostok accretion ice (**Chapter 3**).

The second requirement addresses the need for a broad characterization of the pool of any organics in the sampled material. This does not require definitive identification of individual compounds; rather the intent is to identify patterns in the overall distribution of compounds within the sample that may be consistent with a biological origin. Such patterns could derive, for example, from the number of compounds present overall, the appearance of clusters or concentrations of compounds in specific regions of chemical space, ratios of specific molecular compositions (e.g., ratios of CHOS/CHO or CHNOS/CHNO; Yakimov et al., 2015), or the overall mass envelope of compounds, each of which can be diagnostic of biological synthesis and processing and differ markedly from the distributions observed in abiotic extraterrestrial materials (e.g., Schmitt-Kopplin et al., 2010).

In addition, assessment is required of the bulk structural characteristics of the sampled material – for example, a prevalence of specific functional groups, branching patterns, or molecular fragments that might serve to indicate biogenic character. Detection requirements are set by the same benchmark as stated above. The mass range of 500 Da encompasses amino acids, nucleobases, sugars, fatty acids and other classes of potential molecular biosignatures, as well as oligomers of those compounds and a wide range of (abiotic) compounds found in carbonaceous meteorites.

Investigation 1A1 is addressed by high-sensitivity compositional analysis of acquired surface samples. This is achieved generically in the Baseline and Threshold mission concept model payloads (**Chapter 4.5**) with a Separation-Mass Spectrometer (S-MS) system capable of broadly characterizing molecular composition to low (sub-parts per billion by weight) limits of detection, both to identify key compounds and to characterize any patterns in the distribution of groups of organics (**Figure 4.1.5**). The “front-end” separation capability disperses compounds into structural groups, including isomers, enabling subsequent identification of individual molecules and molecular weight distribution patterns by mass spectrometry over a wide effective dynamic range. The inclusion of separation functionality additionally enables analysis of enantiomers (required by Investigation 1A2), which cannot be accomplished solely by MS. The driving performance requirements for this S-MS system are as follows.

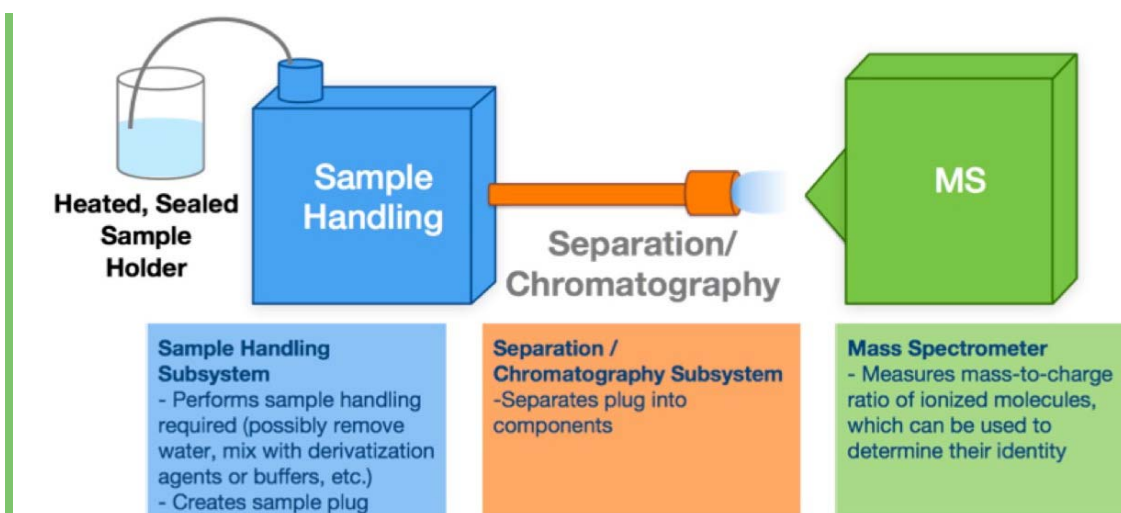


Figure 4.1.5. Schematic of the Baseline Separation-Mass Spectrometry (S-MS) instrument for organic chemical and amino acid analysis, including three primary instrument subsystems required.

Requirement 1: Limit of Detection (LOD)

The primary driving functional requirement of the model payload S-MS system is the analysis of individual organic compounds such as amino acids at levels as small as 1 picomole in a 1 gram sample. This level provides a high probability of detecting a variety of amino acids and other organic species in a conservative model of a European ocean-derived, ice-rich sample. In the case where the sample collected is primarily water ice, 1 gram \sim 1 mL. Hence for these samples, the limit of detection (LOD) requirement is a water-based molarity $M \sim 1 \text{ pmol mL}^{-1} = 1 \text{ nmol L}^{-1} = 1 \text{ nM}$. With the nominal molecular mass of water of 18 g mol^{-1} , this molarity corresponds to a mole fraction of 18 parts per trillion (ppt). As a mass fraction, for a reference mass m , this corresponds to m ppt by weight. For the amino acid Serine (Ser) at 105.09 Da, for example, this LOD would correspond to 105 ppt = 0.105 ppb by mass.

Requirement 2: Molecular Identification

The model payload S-MS system must be capable of identifying individual compounds and/or suites of compounds, including structural isomers where this is pertinent to distinguishing biotic and abiotic origins, over a wide range of molecular masses. The required mass range of at least 500 Da is set to capture a wide range of molecular structures that are diagnostic, either individually or in their broad distribution, of biotic and abiotic origin. These include amino acids, lipids (fatty acids, prenols), sugars, nucleobases, polycyclic aromatic hydrocarbons (PAHs) and related structures, and potential oligomers; as well as the myriad smaller catabolic products discussed above. A mass range higher than 500 Da (e.g., kDa range) would be of interest for detection of polymers (e.g., peptides), larger PAHs, and macromolecular carbon compounds, but does not drive the present requirement. If a particular implementation of this requirement involves inducing chemical reactions between target analytes and

adducts, such as with derivatization, then the *instrumental* mass range would naturally need to be increased to take this into account. Depending on the capabilities of the separation system, within the complete analytical chain, various mass resolution modes of operation could be applied; at least “unit” resolution across the mass range is necessary to assign a *nominal mass* to each compound, fragment, or isotope. Note: additional details on identification of amino acids are given in Investigation 1A2.

Requirement 3: Molecular Abundance

The model payload S-MS system must be able to determine the relative abundances of potentially related groups of compounds to establish significant patterns such as even-odd biases, distinct, non-equilibrium molecular weight distributions, isomeric preference, etc. For this requirement the relative abundance must be determined to within a relative standard deviation (RSD) of no more than 20% to confidently capture differences such as those shown in **Figures 4.1.3** and **4.1.4**. Note: the relative abundances of chiral amino acid enantiomers have a more stringent requirement stated in Investigation 1A2.

Sample Handling Requirements

To accomplish this Investigation, S-MS further levies requirements on the Europa Lander sample acquisition and delivery system. At a minimum, the system must be capable of delivering a solid sample of at least 1 cm³ volume into a receiving vessel inside the payload vault for subsequent processing by the S-MS. Following sample delivery under high vacuum conditions, the vessel must be hermetically sealable to retain any volatiles that are passively or actively released from the sample. Furthermore, the vessel must be temperature controlled to limit sample loss, to meet the volumetric requirement, at least for the period of time prior to closure of the hermetic seal. Additional requirements would likely be levied by the particular S-MS implementation. These may include accommodation of additional features and functions of the vessel assembly itself, such as temperature and pressure control, interface with plumbing manifold(s), and/or particulate filtration; as well as potential system-level requirements such as delivery of an organic free blank or other control deemed necessary for the science. As one example implementation, the vessel could be instrumented to permit temperature- and pressure-controlled lyophilization of the sample, with water vapor evolved from an ice matrix passing through a valved port (for subsequent processing or simply for venting), leaving a solid particulate residue in the vessel that would be available for inspection and chemical analysis.

S-MS Implementation Options

The model payload S-MS instrument could be based upon gas chromatography mass spectrometry (GC-MS), liquid chromatography mass spectrometry (LC-MS), capillary electrophoresis mass spectrometry (CE-MS), other “hyphenated” separation protocols, or any combinations thereof. Nearly all classes of mass analyzer, such as quadrupole, ion trap, time-of-

flight, are capable of addressing the MS requirements within the molecular analysis measurement objective. Various MS systems may also offer design flexibility to enable additional, enhanced Europa lander science, such as direct analysis of neutral or ion composition of the near-surface atmosphere/exosphere, or spatially resolved sample analysis using focused laser or other beam ionization.

Investigation 1A2: Determine the types, relative abundances, and enantiomeric ratios of any amino acids in the sampled material.

Some compounds employed in Earth's biochemistry – for example, sugars and most amino acids – are chiral. Chiral compounds can exist in either of two configurations (enantiomers) that represent non-superimposable mirror images of one another (**Figure 4.1.6**). In the case of amino acids, known abiotic mechanisms of synthesis generate nearly equal amounts of the two possible enantiomers (D and L). In meteorites, the D and L forms are generally also present in approximately equivalent amounts, although excesses of the L enantiomer ranging from 1–15% have been observed among the α -methyl amino acid series (Pizzarello, 2006) and up to 21% for the non-proteinogenic amino acid isovaline (Elsila et al., 2016). In an analysis of the Tagish Lake Meteorite, unusually large L-enantiomeric excesses ranging from 43–45% were reported for glutamic acid in which the $\delta^{13}\text{C}$ -content confirmed its meteoritic origin (Glavin et al., 2012).

In contrast, biological materials on Earth are composed almost exclusively of the L-enantiomer (D/L ~ 0.02 ; Aubrey, 2008) and recent work suggests that such homochirality is required for the proper folding and function of proteins in biochemistry across the three domains of life on Earth. For this reason, it is suggested that **a large enantiomeric excess (ee) in multiple different amino acid types would constitute strong evidence for biology** (Halpern, 1969; Kvenvolden, 1973; Bada et al., 1996; Bada and McDonald, 1996).

Bacteria however, also incorporate non-proteinogenic D-amino acids (aspartic acid, asparagine, glutamic acid, glutamine, serine, and alanine) as components of bacterial biomolecules such as peptidoglycan, polypeptide, teichoic

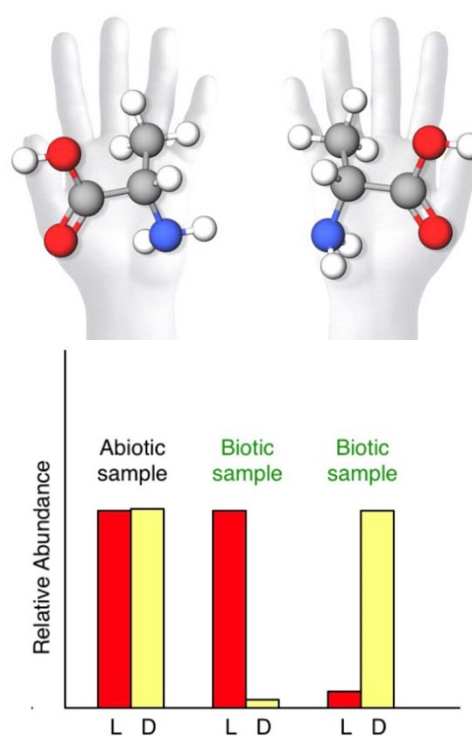


Figure 4.1.6. Chirality of alanine, represented artistically as the left- (L) and right- (D) handed versions. Biological use of predominantly one form of chiral molecules, i.e., one enantiomer (L or D), may provide a highly diagnostic biosignature.

acid, lipopolysaccharide, lipopeptide, siderophore, and as free D-forms in the cell (Kaiser and Benner, 2008). In the deep Pacific and Atlantic oceans (below 1000 m) the D-forms of these amino acids are well-represented in unfiltered seawater (%D = 13–21%), which represents a mix of biological particles, bacterial cellular debris (contributing to dissolved organic material in deep seawater), and diagenetic material. The higher proportions of D-forms are limited to the subset of amino acids used in non-ribosomally synthesized molecules, whereas the representation of L-forms are heavily weighted across other amino acids in seawater samples (McCarthy et al., 1998).

Given the opportunity to sample Europa’s near surface materials, characterization across a suite of amino acids offers the advantage of detecting pervasive biosignatures if present, compared to a limited subset. This investigation is further strengthened when conducted in conjunction with an analysis of the type and relative abundance of amino acids, as described in Investigation 1A1. **The combination of three complementary lines of analysis – type, abundance ratios, and enantiomeric ratios of amino acids – would collectively yield compelling evidence of a biologically altered system** (Creamer et al., 2017), even for a biochemistry that utilized only D-enantiomers, or a different library of amino acids (McKay, 2004).

Measurement Requirements and Implementation Options

Measurement requirements associated with chirality focus primarily on amino acids in the sampled material. To achieve measurements that could be interpreted as evidence of life, the following capability requirements must be met:

- **Detect and identify (at 1 nM LOD) at least four of the following amino acids: Ala, Asp, Glu, His, Leu, Ser, Val, Iva, Gly, β -Ala, GABA, and AIB, with at least one from each representative class (abiotic, biotic, proteinogenic). Note that for chiral amino acids, limit of detection is 1 nM for each of the two different chiral forms.**
- **Quantify abundances of all amino acids detected relative to glycine at an accuracy of better than or equal to 2%.**
- **Quantify enantiomeric excess (ee) of at least three proteinogenic amino acids, one abiotic amino acid, and histidine, with an accuracy of 5% or better.**

Clearly the above requirements cannot be met if no amino acids are detected, but the mission must have the capabilities to perform such analyses in the event that sufficient concentrations of amino acids are present.

To give increased confidence in the ability to identify potential biosignatures in European samples, analyses are required on multiple amino acid types and chiralities. Additionally, the relative standard deviation (RSD) of species quantitation needs to be smaller than measurements described earlier in Investigation 1A1. This more stringent requirement is due to the need to precisely determine the value of the enantiomeric excess (ee) for each amino acid type, where (ee) is calculated as:

$$ee_L = (L-D)/(L+D),$$

where L and D are the concentrations of each enantiomer. As detailed above, enantiomeric excesses of up to nearly 20% have been measured in meteorites, and thus in order to maximize the chances of correctly identifying an enantiomeric excess associated with life, it is desirable to have an RSD value for measured abundances significantly smaller than this value. For example, if measurements of ee had uncertainties of 20%, it would be conceivable that the measurement system, even if capable of detecting a range of amino acids at the detection limits specified, would be incapable of recognizing a chiral excess produced by living processes, which have been measured in the range of 20-100% in terrestrial samples. An accuracy of 5% or better on select proteinogenic and abiotic amino acids is required on the ee measurement to ensure a strong basis for a biogenic, or abiogenic, interpretation of chirality.

Investigation 1A2 is addressed by high-sensitivity compositional analysis of acquired surface samples. This is achieved in our model payload generically with a Separation-Mass Spectrometer (S-MS) system, as described in Investigation 1A1, which would be capable of determining the abundances of individual stereoisomers of key chiral compounds. However, since the different stereoisomer forms of amino acids have identical sizes and charge, and differ only in their geometries, the S-MS system for these measurements must also incorporate chiral selectors (CS) into its separation media in order to create the chiral environment necessary for separating the two enantiomeric forms from one another. These chiral selectors can either be bonded to the surfaces or walls of the stationary phase (separation column or capillary, as is the case for LC-MS or GC-MS), or they can be dissolved in the fluid used to perform separations (in empty capillaries, as is the case for CE-MS).

For GC-MS, this measurement system would be capable of receiving solid samples and selectively reacting the amino acids present in the sample with volatilization agent molecules that produce amino acid complexes exhibiting a significant vapor pressure such as MTBSTFA (Stalport et al., 2012; Zampolli et al., 2007; Kaspar et al., 2008; Waldhier et al., 2010). These volatile amino acid adduct species can then be analyzed by GC-MS. The compounds are heated such that they enter the gas phase, where they traverse a heated chiral gas column such as Chirasil-L-Val (L-Val-tert-butylamide modified polydimethylsiloxane). Interactions of the volatile amino acid adduct compounds with chiral centers on the column

wall give rise to the separation between amino acid enantiomers. For LC-MS or CE-MS systems, fluids containing amino acids are passed through either a coated, packed, or bare walled capillary directly. In the case of LC-MS, chiral selectors are added to the “stationary phase” used for separations, namely the surface of the column walls, or to surfaces of materials used to pack the separation column. For CE-MS, which utilizes bare glass capillaries, chiral selectors can be dissolved in the separation fluid (giving rise to a “pseudo-stationary phase” such as a micelle; Simo, et al., 2010). As with Investigation 1A1, this “front-end” separation capability disperses compounds into their isomeric forms, enabling subsequent identification and relative quantitation of individual molecules by mass spectrometry over a wide effective dynamic range. The inclusion of the separation functionality with chiral-sensitive retention specifically enables analysis of enantiomers that cannot be accomplished solely by MS.

Investigation 1A3: Determine whether the carbon stable isotope distribution among organic and inorganic carbon is consistent with biological activity (Baseline only).

Biological processes have the potential to impart a diagnostic signature on the stable isotope ratio of compounds utilized in metabolism or biosynthesis (Figure 4.1.7). The purpose of this investigation is to measure such signatures in the stable isotope ratio of carbon compounds in the sampled material.

The isotopes of a given element differ slightly in the strength of the bonds they form. As a consequence, lighter isotopes may react at slightly higher rates, with the products of such reactions becoming preferentially enriched in the lighter isotope and the residual reactants becoming increasingly enriched in the heavier isotope as the reaction progresses. Although such kinetic isotope effects occur in both abiotic and biological processes, the highly selective nature of enzymatic activity often amplifies the effect to such an extent that biologically produced materials – both biomolecules and the products of catabolism – can be distinguished by virtue of their stable isotope composition (Northrup, 1981). This effect is well studied for carbon, and often creates “signatures” that are commonly used to distinguish abiotic from biotic sources of carbon on Earth (Peters et al., 2005; Lollar et al., 2006).

On Europa, a set of measurements at a single site could have few, if any, points of comparison (though the EMFM may make some isotopic measurements of materials from sputtering and plumes), and the isotopic composition could be subject to environmental conditions that have no direct analogue on Earth, such as radiation processing. Nevertheless, **were an isotopic excursion to be observed, it could serve as a useful potential biosignature**, especially if combined with measurements detailed in Investigations 1A1 and 1A2 (see e.g., Lollar et al., 2006). For this reason, the carbon isotope measurements are included as Baseline, but not Threshold measurements.

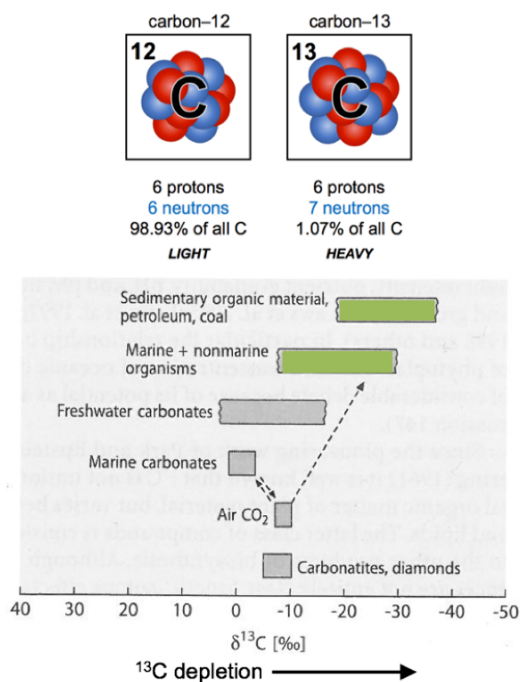


Figure 4.1.7. Biological modification of the relative ratio between carbon-12 and its stable isotope carbon-13 could serve as a useful potential biosignature. On Earth, geological, atmospheric, and biological processes yield a complex, but informative framework for interpreting the carbon-13 signature (bottom plot from Hoefs, 2004).

The imprint of kinetic isotope fractionation, whether biotic or abiotic, is reflected in the differing isotopic compositions of reactant and product pairs, rather than in the stand-alone composition of a single compound. Evidence of such fractionation should ideally be established by isotope ratio measurements made on known reactant-product pairs, but this may be largely impractical for a system in which the specifics of carbon-cycling reactions are not known. Lacking such capability, the investigation should instead establish “isotopic context” by determining $^{13}\text{C}/^{12}\text{C}$ in a diversity of compound classes (e.g., aliphatic hydrocarbons, amino acids, PAHs, and CO_2) with sufficiently low uncertainties to identify potentially significant differences among them. At a minimum, this requires that measurements be made on at least two different carbon compounds or pools of carbon. Ideally, such measurements should encompass the major (most abundant) pools, including representatives of the re-

duced and oxidized fractions, as well as any compound-specific analyses that may be tractable. Measurements made on a diversity of pools may also be important in addressing the potential for abiotic false positives. Specifically, some abiotic processes – e.g., Fischer-Tropsch Type carbon reduction reactions under hydrothermal conditions – have been shown to yield fractionations within the “life-like” range (Horita, 2005; McCollom and Seewald, 2007). Isotope ratio measurements made on pools that both target and exclude the products of such reactions could help in avoiding potential isotopic false positives.

Isotopic analysis offers both benefits and challenges. **Stable carbon isotope ratios can potentially be highly resilient to diagenesis, even over long time scales and large environmental perturbations.** For Europa, this resiliency may serve to preserve biosignatures in materials that experience radiation processing, but work remains to be done to understand fractionation under such conditions. Significant challenges exist that are inherent to constraining carbon-cycling context in sufficient detail to support a unique interpretation of measured isotope signatures, and in accounting for the full spectrum of endogenous and exogenous processes that could affect the isotopic composition of carbon in the system. **Comparison of isotope ratios across different compounds nevertheless holds great potential to yield insight into global scale processing of carbon, even if evidence of biology is**

not identified. Furthermore, the EMFM will obtain isotopic measurements of carbon-containing compounds, be they sputtered or ejected in plumes, and measurements by the lander would provide highly valuable ground-truth for such measurements.

The factors detailed above suggest that the utility of carbon isotopic investigations is to support other lines of evidence for biogenicity rather than to serve as stand-alone evidence for life. This view is in line with that of the Mars 2020 study (Mustard et al., 2013), which ascribed a relatively low level of confidence in stable isotope measurements as stand-alone indicators of biogenicity.

Measurement Requirements and Implementation

The combined measurement requirement resulting from Investigation 1A3 is to:

- **Measure the carbon stable isotope composition of multiple compounds, compound classes, or pools of carbon, with a relative standard deviation of no greater than 5‰ (5 per mille) in each measurement. Note that to achieve such measurements for organic compound concentrations as low as 1 pmol per gram, the LOD would need to be 10 fmol per gram or better to measure $^{13}\text{C}/^{12}\text{C}$ in a C1 compound (Baseline only).**

This measurement would determine the $^{13}\text{C}/^{12}\text{C}$ distribution in hydrocarbons or other organics, and any additional pools of carbon (such as oxidized carbon in the form of CO_2 or carbonate), to look for isotope discrimination that could be consistent with biological synthesis.

The samples would be obtained and passed into a mass spectrometer and/or other possible analytic devices to determine the isotopic ratios of the various species. The observables include either the overall average isotope ratio of all carbon atoms present (relative to some known carbon sample), or individual isotope ratio mass spectra of the different carbon containing compounds present (i.e. compound-specific isotope analysis, or CSIA).

It cannot be known *a priori*, with certainty, what precision is required in isotope ratio measurements to identify potentially biogenic character in sampled materials on Europa, but reference to Earth suggests the value of an ability to distinguish differences of ten per mil among different pools of carbon. On Earth, such precision would clearly resolve: (i) isotopic differences between reactants and products arising from kinetic isotope effects in a diversity of (though not all) biosynthetic pathways (Hayes, 2001) and catabolism; (ii) Earth's bulk organic and inorganic pools, which differ by approximately 20‰ due to the isotope fractionation associated with photosynthetic biosynthesis (Des Marais, 2001); and (iii) the clustering, within

a relatively narrow range, of C isotope ratios in a diversity of Earth's organics, relative to the broader distribution observed in meteorite organics (Pizarello, 2006).

Investigation 1A3 is addressed by high-precision isotopic analysis of carbon-bearing compounds in acquired surface samples. Isotope analysis of other elements could also be highly valuable for interpretation of the C-isotope results for biology, or for investigations into Europa's planetary origin and evolution. However, such investigations are beyond the science scope of the Europa Lander; the requirements are driven solely by the need to measure the $^{13}\text{C}/^{12}\text{C}$ distribution. Sample analysis for the carbon isotopic signature is achieved in the model payload with a Stable Isotope Analyzer (SIA), which includes stable isotope mass spectrometry as a core capability, but which may also incorporate other approaches such as tunable diode laser spectroscopy for high-precision analysis of selected species. The top-level Investigation 1A3 requirement leads to three individual driving requirements on the SIA, as follows:

Requirement 1: Measurement Uncertainty

To distinguish fractionations of 10‰, C isotope ratio measurements must be made with a relative standard deviation (RSD) of no greater than 5‰ within each C pool. This requirement assures that SIA-measured values separated by as little as 10‰ are highly unlikely, in terms of statistical uncertainty at 1 RSD, to be erroneous measurements of the same true ratio.

Requirement 2: Analytical Breadth

To interpret a C isotopic fractionation measurement in the environment, $^{13}\text{C}/^{12}\text{C}$ of compounds from at least two reservoirs must be measured by the SIA – one nominally abiotic and one potentially biotic. Abiotic compounds would best be so-identified by other means. These could include CO or CO₂ in surface ice or as sputtered into the exosphere (and thus measurable by the EMFM) or minerals such as carbonates ($-\text{CO}_3$), from which biotic C molecules would have fractionated $^{13}\text{C}/^{12}\text{C}$. Potentially biotic compounds include all those targeted for detection in Investigation 1A1 such as amino acids, aliphatic and aromatic hydrocarbons, carboxylic acids, etc. Here the meaning of biotic includes compounds for which $^{13}\text{C}/^{12}\text{C}$ results from biological reactions; that is, not necessarily a biomolecule *per se*.

Isotopic analyses of more than two C compounds or sources would expand the scientific scope in terms of more fully understanding the context of fractionation effects within the european environment (i.e., dispersion among abiotic compounds) as well as strengthening any conclusions about biology (i.e., dispersion among potentially biotic compounds, of various C-numbers, when correlated to fractionation of other elements such as D/H). As such, a broad molecular isotopic analysis capability would add substantial value to the overall mission.

This requirement serves to emphasize that potential isotopic biosignatures are reflected in their distinction from a European planetary background. One commonly applied method to measure the carbon isotope ratios of all C-bearing compounds present, which minimizes sample handling, would be to simply combust all carbon compounds present and measure isotope ratios of carbon dioxide produced relative to a known standard sample (e.g., Kramer and Gleixner, 2006). However, it will not be possible to compare the isotopic composition of the diverse pools of carbon that may exist within the sample, at least not without more specialized pre-separation of the carbon provided to the mass spectrometer for analysis.

Requirement 3: Limit of Detection (LOD)

Precise quantitation of $^{13}\text{C}/^{12}\text{C}$ of individual organics is challenging given their likely trace concentrations and the low ($\sim 1.1\%$) relative natural abundance of ^{13}C . A compound at a bulk concentration of 1 part per billion by weight (ppbw) would therefore occur in its heavier (^{13}C -containing) forms at concentrations as low as ~ 0.01 ppbw, for single-carbon species (CO_2 and C1 organics). Higher C-number species contain greater proportions of heavier C (e.g., 0.06 ppbw for a C5 organic). In a mass spectrometer, where signal intensities are directly correlated to abundance, this would ideally ease the signal-to-baseline (S/B) requirement for the ^{13}C contribution.

However, in natural samples, overall signal intensities are often found to decrease with increasing C-number (increasing molecular weight), somewhat countering this benefit. For a mass spectrometer-based measurement, to “see” the ^{13}C contribution, the ultimate limit of detection must be substantially lower, on the order of 1%, of the concentration of the compound in the sample. For organic compound concentrations as low as 1 pmol g^{-1} as stated above, the LOD would need to be at most 10 fmol g^{-1} to measure $^{13}\text{C}/^{12}\text{C}$ in a C1 compound. Alternatively, a higher sample concentration would correspondingly relax the LOD requirement for isotopes.

Ideally, the SIA capability would offer sufficient margin on this threshold to achieve a limit of quantitation (LOQ) that enables statistical averaging of multiple integration periods (individual measurements). In cases where absolute concentrations are too low, higher effective S/B could be achieved by co-adding spectra from multiple, structurally-associated organics to obtain $^{13}\text{C}/^{12}\text{C}$ for a putative ensemble.

Stable Isotope Analyzer (SIA) Implementation Options

The SIA implementation involves a mass spectrometer, with any required front-end sample processing functionality, capable of measuring the full range of potential C-bearing compounds with sufficient fidelity to quantify the distribution of $^{13}\text{C}/^{12}\text{C}$ values as described above. The mass range for stable isotope analysis should be at least 100 Da in order to be able

to capture up to C6 hydrocarbons, smaller amino acids, and other species, in addition to myriad lighter compounds. The mass resolution must be at least sufficient to resolve the isotopes of each C-bearing compound, that is, unit mass separation, while potential isobaric interferences may be addressed as required by various approaches. Front end processing may involve various methods to extract and/or partition the target analytes into the various types or pools, such as use of a hydrocarbon trapping method, or a scrubber to capture CO₂ or other gases, for later release.

To perform compound-specific isotope analysis on relatively small, volatile organics, the front end may be “simply” a method for controlled heating and release of gases directly from the collected sample. For larger, more complex organics, measurements typically require additional sample processing, including possibly derivatization, sample combustion, and/or gas or liquid separations. For example, in the case of the measurements of phospholipid fatty acids, one standardized method includes extraction and preparation of lipids using methods developed by Bligh and Dyer (1959). This treatment involves extraction of samples in a phosphate buffer/methanol/chloroform mixture, followed by decanting and evaporation of the chloroform phase to reveal dry lipids. These lipids would then be subjected to a methylation or derivatization process. Finally, the processed sample would be passed through a gas chromatograph (GC) before mass analysis, and results compared to a standard mixture that is used to correct for deviations in the carbon isotope ratios introduced by the carbon added via methylation or derivatization protocols (Miltner et al., 2004).

The SIA functionality and specifications are thus potentially very similar to those required by the S-MS for Investigations 1A1 and 1A2, and it is expected that a single system could address most or all measurements. Where the mass spectrometer system is unable to meet particular isotopic requirements due to LOD (S/B) or precision concerns, or where there are strong arguments for having supplementary or corroborative measurements of some isotope ratio, the SIA may benefit from inclusion of a spectroscopic isotope capability, such as a tunable diode laser absorption spectrometer focused on selected gases such as CO, CO₂, or CH₄. Such techniques can often achieve LODs and uncertainties, for pre-selected analytes, well below those reached by a typical mass spectrometer system, under flight mission constraints. The SAM investigation on MSL is an example of a mass spectrometer and a tunable laser spectrometer sharing common solid sample and gas processing systems (Mahaffy et al., 2012).

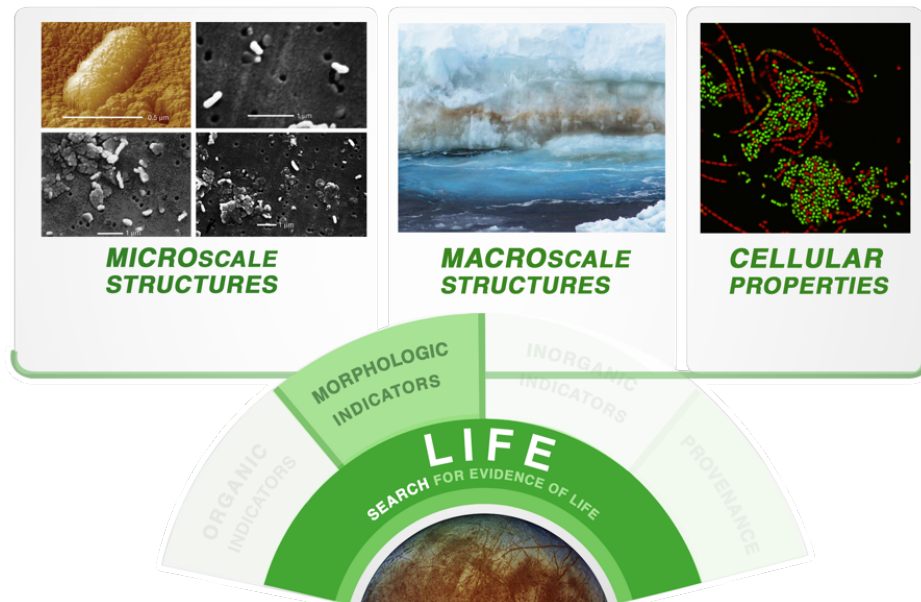


Figure 4.1.8. The second Objective within Goal 1 focuses on the observation of microscopic and macroscopic indicators of potential biosignatures. At the smallest scale this includes the detection of cells and other features potentially connected to biological processes. At the larger scale this Objective includes the observation of formations or layers within the ice and landing site material that could be indicative of biological processes.



4.1.2

OBJECTIVE 1B: IDENTIFY AND CHARACTERIZE MORPHOLOGICAL, TEXTURAL, OR OTHER INDICATORS OF LIFE.

Detecting and characterizing microscopic and macroscopic structures to search for evidence of life in Europa's near surface is the focus of Objective 1B (**Figure 4.1.8**). Observations of morphology across many spatial scales are highly complementary to Objective 1A. Direct signs of life can be discerned through observation of active or inactive life forms, deposits, or other biogenic structures (Baross et al., 2002; Domagal-Goldman et al., 2016). **Earth's most diverse and ancient life forms appear in a limited spectrum of morphologies that are recognizable using microscopy, and in some cases, detectable using macroscopic imagery. Thus, morphologic features can be used to recognize both extant and extinct life.**

Investigation 1B1: Resolve and characterize microscale evidence for life in collected samples.

Characterization of non-ice materials collected by the lander at the microscopic scale would serve as a critical component of life detection and biosignature analyses. **Observation of sam-**

ples at the scale of microscopic organisms on Earth could provide direct physical evidence for life, if present. Conversely, if no physical structures of life are detected, such measurements would provide useful information for the interpretation of results from Objective 1A and 1C.

Visual identification of cell-like structures is by itself not a definitive biosignature. Microscopy can provide ambiguous results, but observations can be strengthened when paired with measurements that probe the properties of microscale features (e.g., via fluorescence, spectroscopy, or other biosignature detection approaches). In the event that the biochemical search for evidence of life reveals interesting molecules, patterns, and distributions of organics, Investigation 1B1 addresses the potential to identify physical features from which the potential biosignatures may be derived, including cells.

Most of the prokaryotes in Earth's biosphere are smaller than 1 μm in diameter (**Figure 4.1.9**) and for this reason, the history of invention in microscope technology largely parallels the development of microbiology as a discipline. Antony van Leewenhoek published the first description of a marine microorganism (van Leewenhoek, 1677) based on observations he made with a single lens, short focal length $\sim 200\times$ magnification microscope that resolved objects as small as $\sim 1.5 \mu\text{m}$ (Porter, 1976). In effect, our current understanding of the ubiquity, diversity, and role of microorganisms in Earth's ocean has resulted from efforts initially motivated by the “wee animalcules” Leewenhoek reported within seawater.

Although the use of flow cytometry has increased in marine microbial ecological studies over the last few decades, its strength is in particle enumeration and detection of (auto)fluorescent pigments in photosynthetic organisms. **Microscopy is still the most robust approach for characterizing the morphology, size, and abundance of planktonic microorganisms.**

Members of the Bacteria and Archaea display a range of rather simple morphologies (e.g., coccus, rod, vibrio, spirillum, or filament). Shape alone is typically not informative for inferring relevant species characteristics, nor is shape diagnostic of evolutionary origin. Cell size and shape, however, are important determinants of the surface-to-volume ratio, with larger ratios (e.g., cells of small diameter) facilitating significantly higher rates of substrate/product diffusion into, and out of, the cell.

In addition to the typical optical and fluorescence-targeted techniques used to image single cells, cell clusters, and microbial biofilms, microorganisms may also be detected using non-invasive, label-free imaging (**Figure 4.1.10**). These techniques include atomic force microscopy (AFM) and optical methods that can provide specific and sensitive imaging of microbial cells, even when they are associated with salts, minerals, or other solid phases (Fischer et al., 2016).

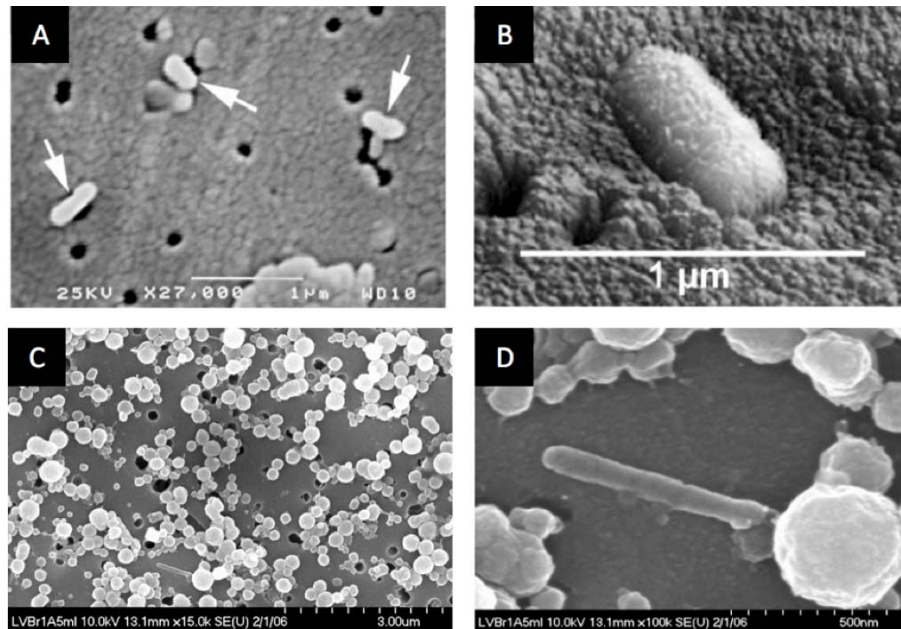


Figure 4.1.9. Examples of Terrestrial bacteria in icy habitats ranging in size from 0.1 to ~0.8 microns. Cells from Subglacial Lake Vostok accretion ice microbiota were imaged with SEM (A) and AFM (B) (Priscu et al., 1999). Brine collected from the lake ice at Lake Vida contains a dense microbial population comprised of cells varying in size imaged with SEM (C), including a population of ultrasmall cells on the order of 0.2 microns. Different morphologies are apparent at higher magnification that were 0.4–0.7 microns in longest dimension (Kuhn et al., 2014; Image: Murray et al., 2012).

More recently, spectroscopic techniques have been integrated with microscopy. For example, infrared (IR) spectroscopy can be used to obtain signals of proteins, lipids, polysaccharides, and other carbohydrates in the cellular biomass in the 600 cm^{-1} to 4000 cm^{-1} range. Common targets include the C=O and C-N stretching vibrations associated with amide I and amide II groups (Schmitt and Flemming, 1998). Similarly, Raman spectroscopy can produce distinct spectroscopic signatures for these same classes of cellular components (in the deep UV or near IR; Butler et al., 2016). Raman spectroscopy can be used to not only detect organisms on the basis of vibrational bonding, but also to resolve differences between various strains or species, or to differentiate vegetative cells from spores (e.g., Rösch et al., 2005).

Another relatively new approach to image cells uses Deep-UV (DUV) laser-induced detection of native fluorescence can be used to image single cells in a microscope, with the appropriate optics, for excitation and transmission below 300 nm to generate an intrinsic fluorescence response to proteins, nucleic acids, amino acids and aromatics (Bhartia et al., 2010), enabling the imaging and enumeration of cells.

Measurement Requirements and Implementation Options

In situ analyses for microscale evidence of life require consideration of both size and abundance of any potential biogenic features. Based on the cell-size distribution of microbial life in Earth's ocean, ice sheets, and polar brines (**Chapter 3; Figure 4.1.10**), measurement requirements were established for analyses of Europa's near-subsurface material.

Investigation 1B1 focuses on observation of microscale features in samples collected from Europa's surface and/or near-subsurface, leading to the following requirement:

- Search for cells and other microstructures in the sample that are 0.2 micron or larger in their longest dimension.

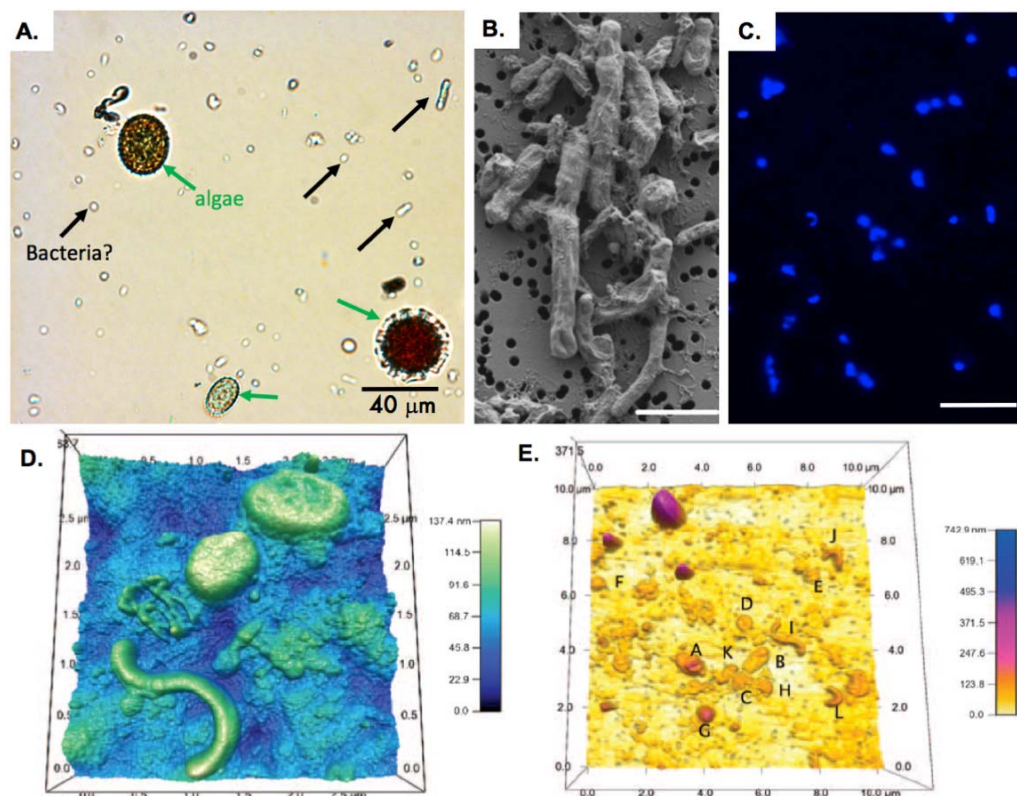


Figure 4.1.10. Micrograph examples of snow, ice, and marine bacteria. (A) Light microscopy at 400× magnification of snow bacteria and algae (Murray, AE unpub.); (B) scanning electron micrograph of prokaryotic cells from Last Glacial Maximum period (23.4–19.9 kyr before 1950 CE). White scale bar is 1 μm. Santibáñez et al. 2016; (C) epifluorescence micrograph (1000×) of Antarctic marine bacteria stained with a DNA-binding dye (DAPI, 4,5-diamino-phenolindole) and filtered onto a 0.2 micron nucleopore membrane filter. Scale bar is ~10 μm (Murray, AE, unpub.); (D, E) Atomic force microscope images of natural marine bacteria from coastal (D) and off-shore (E) samples recovered on 0.2 micron Anodisc filters. Scale bar shows the z-axis, indicating tens nm-resolution (Malfatti et al., 2010).

In the Baseline and Threshold mission, the model payload capability for this investigation is referred to as the Microscope for Life Detection (MLD) instrument. For the Baseline investigation a spectroscopy and deep UV enhanced microscope capability is integrated, enabling imaging and chemical mapping. This instrument is referred to in the model payload as the spectrometer-enhanced microscope. Investigation 1B1 could be addressed in the Threshold mission with high resolution microscopy. Several existing technologies are available that could meet these requirements, details of which are provided below.

Requirement 1

The detection sensitivity of microscale features (i.e., cells and other microstructures) must be at least 0.2 microns (**Figure 4.1.11**). Cells in this size range include the majority of cellular life forms on Earth. Life forms including ultrasmall or starved cells (e.g., Litchfield, 1998) and viruses (including bacteriophages) can be even smaller than ~ 0.1 microns in their longest dimension. **Resolving submicron-sized microorganisms can be improved by use of fluorescent dyes that bind to macromolecules**, allowing even viruses to be viewed with an epifluorescence microscope. Higher resolving power that can directly image such structures can be achieved with advanced microscopic technologies such as atomic force microscopy (AFM) or scanning electron microscopy (SEM). Although flight-qualified microscopes have not yet been used for life detection, the AFMs flown on the Phoenix and Rosetta Missions provided quantitative relief images of soil and dust particles at micron to nanometer resolution. Both systems could be capable of imaging cells in the size range of the Investigation 1B1 measurement requirements.

Requirement 2

The second measurement requirement concerns detection of microscopic structures that are dilute in the native sample matrix. The most relevant Earth reference site to Europa's ice shell that has been well-studied is accretion ice from sub-glacial Lake Vostok (SLV), which has minimum abundances of $\sim 10^2$ cells mL^{-1} in the accretion ice (ice melt equivalent; Christner et al. 2006; see **Table 3.2**). Such concentrations are also broadly representative of cell densities in ice sheets on Earth.

Given the potential for cells and microscale features to be small and dilute the requirement for sample collection leads to a threshold sample volume of 5 cubic centimeters (cc) of ice, or 5 grams equivalent of non-

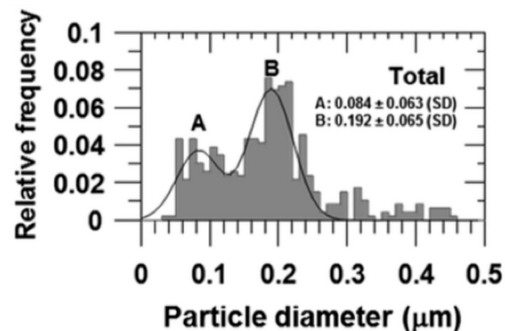


Figure 4.1.11. Histogram of microbial cells and unidentified particles collected from within the brine of Antarctica's Lake Vida. The 0.2 μm mode are microbial populations, whereas the 0.1 μm mode may have contributions from inorganic particles (Kuhn et al., 2014).

ice material. To detect particle densities at a level of 100 cells per mL, a minimum of 5 cc would provide at least two particles per observation on a 1 mm diameter filter with a field of view of 100×100 microns (**Figure 4.1.12**).

Sample Handling Considerations

The architecture of the sample handling and preparation system will, by necessity, depend on the instrumentation used. However, it is clear that **the ability to concentrate microscale features could greatly enhance detection of morphological signs of life if they are in low-abundances and dispersed in a dilute matrix of material from Europa's near-subsurface.** Given that material collected from Europa could range from predominantly water ice, to salt dominated, to an as-yet-to-be-discovered surface composition (e.g., organic “tholins”), some degree of phase change of the collected sample may be necessary to achieve the requirements detailed above. Including a phase change from solid-to-liquid (through solubilizing salts and/or adding a combination of heat and pressure to change the phase from ice to liquid) is one way to potentially filter or concentrate small, potentially biogenic materials onto a target for microscopic observations.

Finally, specific instrumentation designs should include concepts for evaluation of experimental controls (blanks), fluid handling for additions of aqueous solvents, and/or molecular stains that need to be integrated.

MLD Implementation Options

Microscopes have not yet been used for life detection beyond Earth, but they have been important components of planetary research missions (**Figure 4.1.13**). High resolution imaging systems were developed for spaceflight operations (e.g., MAHLI; Edgett et al., 2012), and optical microscopes (OM) were flown (though not operated) on the Beagle 2 Lander (Thomas et al., 2004) and on the Rosetta Philae mission (Bibring et al., 2007ab). On Philae a near IR hyperspectral imager (the Comet Infrared and Visible Analyser, CIVA), was coupled

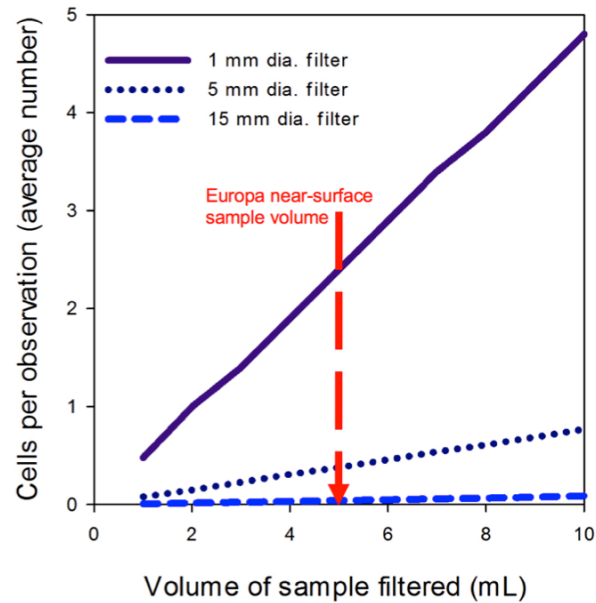


Figure 4.1.12. Effect of sample volume and filter area on average number of cells per 100 micron by 100 micron observation. Filtering to concentrate cells is highly advantageous for detecting cells in low biomass environments, such as Lake Vostok. For the case shown, a 5 mL volume of Lake Vostok ice is used as a proxy for a Europa sample, and the filter size serves to greatly enhance cell counts per observation.

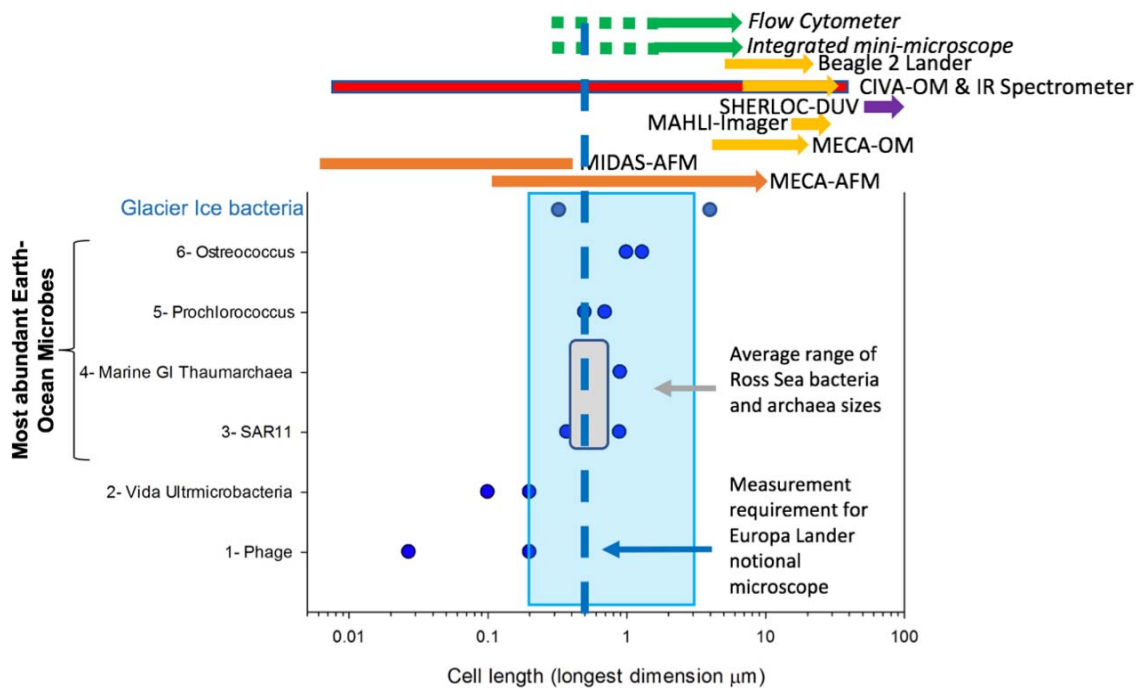


Figure 4.1.13. Distribution of microbial sizes common in Earth's Ocean (blue box highlights 0.2–3.0 micron range) and glacier ice in relation to microscopy technologies, several of which have flown in space. Orange arrows represent atomic force microscopes (AFM); Gold: Optical Microscopy (OM); Purple: native deep UV fluorescence detection spectroscopy; Red: infrared spectroscopy coupled to optical microscope; Green fluorescence-based stain detection technologies that have not yet flown in space.

to the OM. A microscope-spectrometer was also developed and launched for the Phobos-Grunt mission (Korablev et al., 2010).

Two missions have flown and successfully used atomic force microscopes (AFM) including Phoenix (MECA; Hecht et al., 2008; Goetz et al., 2010; Pike et al., 2011) and Rosetta (MIDAS; Riedler et al., 2007; Bentley et al., 2016). In addition, electron microscopes have been developed for spaceflight missions (e.g., Gaskin et al., 2012), but have not yet flown.

Microscope technology has seen many advances, and has diversified over the past 25 years, making high resolution imaging accessible in a variety of small (e.g., Ghosh et al., 2011) and automated (e.g., Swalwell et al., 2011) platforms that are used to address science and technology needs across fields including biology, geoscience, and materials science. Several different microscope technologies could potentially serve the purposes of meeting requirements specified in Investigation 1B1. A partial list of implementation options that could be used are summarized in **Table 4.1.1**.

Table 4.1.1. Implementation options for microscopy technologies with flight experience as well as several emerging technologies (OM: Optical microscopy; DUV: Deep Ultraviolet; AFM: Atomic Force Microscopy; SEM: Scanning Electron Microscopy). All technologies except #1 and #8 could likely be compatible with Investigation 1B1 measurement requirements.

Microscope Technology	Flight hardware	Biosignature detection strengths	Biosignature detection challenges
OM – visible wave length ¹	Y	Potentially the simplest and most universal implementation option.	Lack of high resolution <1.0 micron; false positive risk potential.
OM – fluorescence microscopy ²	N	Fluorescent stains target biomolecules (proteins, lipids, nucleic acids); stain enhances cell detection beyond the Nyquist limit.	Requirement to add molecular stain(s) to sample challenges implementation.
OM – DUV Fluorescence ³ / Raman ⁴	N	Detection of naturally fluorescent compounds (e.g., aromatic amino acids); Raman spec. provides compositional information.	Relies on biosignatures that utilize fluorescent amino acids.
Flow Cytometry ⁴	N	Use of multiple lasers for detection; detection limit meets 100 cells per mL in liquid ⁴ ; May be compatible with DUV detection	Requires fluids and added molecular stains for fluorescence detection, challenging implementation.
AFM ⁵	Y	High resolution (nm), can detect textures and reveal 3-D information; softness-hardness (e.g. turgor pressure) etc.; capability enhanced with OM ⁶	Moderate false positive risk mitigated by AFM mechano-sensing capability.
SEM ⁷	N	High resolution (nm), can detect textures and reveal 3-D information.	Moderate risk of false positives.
Microspectroscopy ⁸	Y	Combined technologies provide visible and spectral biosignature detection (Raman or IR).	Visible detection has same limits as OM.
High Resolution (500 μ m) Context Remote Sensing	Y	Biosignature detection for macroscopic life forms; living or fossils, that leave non-random structures or biomineral patterns.	Risk of false positives; Definitive interpretation is challenging.

Footnotes: 1) Yingst et al., 2016; 2) Ghosh et al., 2011; 3) Bhartia et al., 2010; 4) Santibanez et al., 2016; 5) Hecht et al., 2008; 6) Bentley et al., 2016; 7) Gaskin et al., 2010; 8) Bibring et al., 2007ab.

The primary implementation strategy is that image capturing resolution be sufficient to characterize particles at least 0.2 microns in size and at abundances of 100 cells per mL (or cc) in a 5 cc sample. Implementation options would potentially require a sample processing system to interface with the sample observation technology. There are a variety of options for processing, including phase change possibly using pressure to move the ice to a liquid, followed by sample concentration.

Investigation 1B2: Resolve and characterize the landing site for any macroscale morphological evidence for life (Baseline only).

Investigation 1B2 targets organisms that produce macroscopic biomarkers. These biomarkers could be products of biosynthesis, such as pigments as seen in Antarctic sea ice (e.g., **Figure 4.1.14(A)**), or the result of colonial or filamentous growth forming larger structures visible by camera or optical microscopy. Some **potential signs of extant/extinct life that might manifest as morphologic indicators include colonies of microbial cells; biofabrics, in the form of concentrations of organics and spatial arrangements of minerals; particulate**

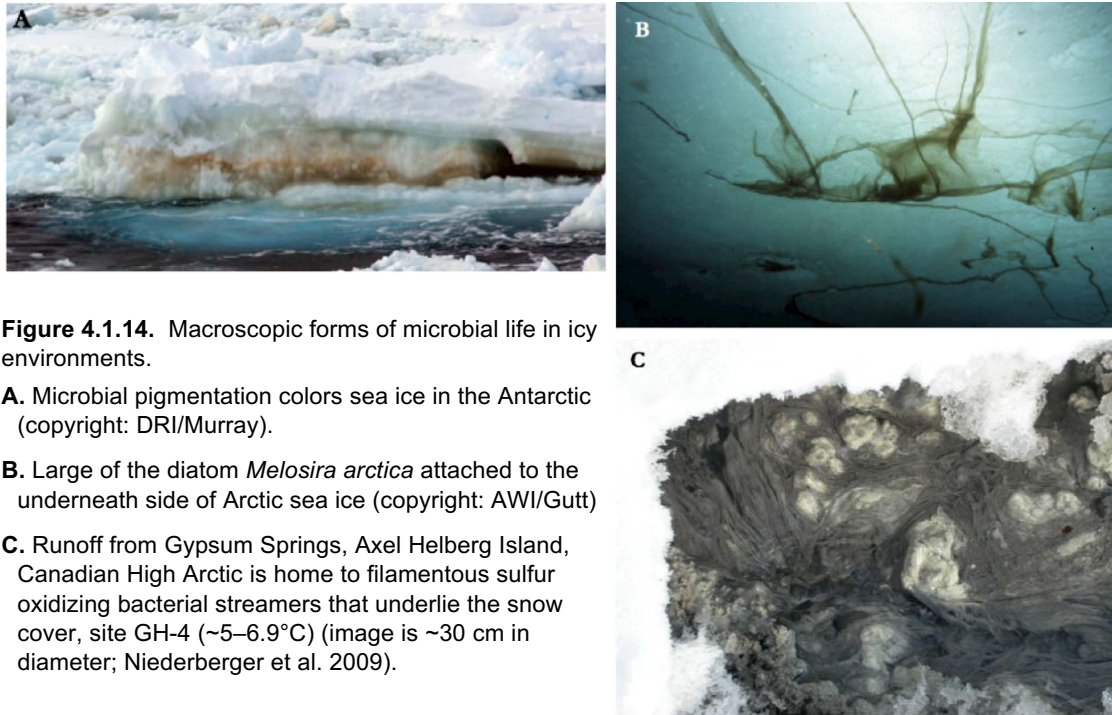


Figure 4.1.14. Macroscopic forms of microbial life in icy environments.

A. Microbial pigmentation colors sea ice in the Antarctic (copyright: DRI/Murray).

B. Large of the diatom *Melosira arctica* attached to the underneath side of Arctic sea ice (copyright: AWI/Gutt)

C. Runoff from Gypsum Springs, Axel Helberg Island, Canadian High Arctic is home to filamentous sulfur oxidizing bacterial streamers that underlie the snow cover, site GH-4 (~5–6.9°C) (image is ~30 cm in diameter; Niederberger et al. 2009).

matter coupled to organic components; or discolorations in the ice that could represent entrapped biomass (e.g., Watanabe et al., 1990).

For example, at the sea ice–ocean interface in the Arctic, large filamentous strands of the diatom *Melosira arctica* grow into the water (Boetius et al., 2015), while part of the “biofilm” is attached to the ice (**Figure 4.1.14 (B)**). While many macroscopic filamentous microbial forms on Earth are phototrophic (using light as energy), numerous environments – including polar icy environments – have been found to harbor macroscopic chemoautotrophic communities that generate macroscopic structures (**Figure 4.1.14(C)**; e.g., Niederberger et al., 2009).

In addition, **biomineralization reactions between microbial life and the geosphere can result in incorporation of microorganisms into the geological record as body fossils or casts that can appear macroscopic** (>1 mm in scale). Certain biofabrics such as microbiolites (e.g., stromatolites, thrombolites) and biofilms may also be large enough to be resolved at the 100 μm scale, if not larger depending on the habitat. Whether comparable structures could form within, or at the base of Europa’s ice shell is uncertain (Hand, 2010), but the observation of macroscopic morphological features could serve as a compelling biosignature, especially when coupled with detailed organic and inorganic chemical analyses (Summons et al., 2011).

At smaller scales, morphological expressions of life may include individual cells (Investigation 1B1) as well as cellular products, such as extracellular polymeric substances (EPS),

microbially-induced sedimentary structures and associations of cells, such as colonies, biofilms, and smaller bioconstructions (Farmer and Des Marais, 1999; Summons et al., 2011; Westall et al., 2015). Mineral permeation or encapsulation of cellular structures may occur within brines and minerals such as silica, iron oxides (e.g., Kuhn et al., 2014), barite (Stevens et al., 2015), salts such as halite; or microbes may be preserved in ice (Christner et al., 2003). Biomineralization studies at low temperatures are limited, as are studies in cold brines, though recent efforts have documented biomineralization of elemental sulfur at 4°C (Gleeson et al., 2011), and calcium carbonate at -15°C (Mykytczuk et al., 2016).

Because there is significant overlap between abiotic and biotic processes, direct observation of structures resulting from biomineralization is best used as an “early warning” of putative biosignatures for which deeper interrogation would be required (Investigation 1C1; Summons et al., 2011).

On Earth, the structures and features described above can be spatially variable over areas smaller than tens of centimeters, and samples acquired from a given workspace volume could be similarly heterogeneous (e.g., Potter-McIntyre et al., 2014). Thus, in the search for macroscopic indicators of past or present life on Europa, it is important to both image the surface at resolutions sufficient to reveal morphologic evidence for past or present life, and to provide the broader contextual information needed to interpret the sampled surface material.

Measurement Requirements and Implementation Options

Imaging at appropriate resolutions in the workspace is an important component of selecting the most promising samples for collection. Some morphologic indicators of life can be detected by a camera that images in the visible wavelengths, at resolutions sufficient to resolve mm-scale variability, but other structures may require finer scales. Colors or pigmentation of Europa’s near surface could enhance detection of macroscopic biosignature, thus requiring lower levels of resolution, if the biomarkers are abundant and dense. Even with reconnaissance images from the EMFM, we will have no *a priori* knowledge of what fine scale is ideally suited to Europa’s surface.

Working from analogous structures on Earth, however, resolving 2 mm-spaced parallel laminations in a microbial mat would require resolutions of at least 1 mm per pixel. Thus, the recommended sensitivity is to resolve regions within ~2 m of the lander at 2 mm in color, leading to the following measurement requirement:

- **Identify objects as small as 1 mm within the lander workspace (~2 m), in color.**

To provide context for a potential biosignature observable in the workspace or landscape, overall imaging should include a continuum of resolutions from the intermediate- and highest-resolution flyby images down to the micron-scale. For example, a block of material visible at meter-scale (flyby) resolution that is hypothesized to have been brought up from the ocean should ideally be resolvable at the grain-scale level on the ground, so that the morphologic features of the block could be identified and characterized, and its origin confirmed. To accomplish this, the landscape to the horizon should be resolvable from 1–10 mm per pixel (i.e., resolve cm-dm scale features). This would enable features the size of large blocks, tentatively identified from flyby images, to be characterized at the textural level. Resolution within the workspace at the hundreds of microns to millimeter per pixel scale would permit connecting local features to far-field context images, so that, for example, accreted biofabrics that discolor surface ice could be preliminarily identifiable from 10 m away and fully resolved in the workspace.

The resolutions above are necessarily based on analogy with known morphologic indicators of life. Depending on the technology implemented, the microscale imaging of Investigation 1B1 could also potentially target the 10 to >100 micron-scale level with optical microscopy (part of the model payload inside the lander vault), thereby providing additional supporting observations.

To implement the range of spatial scales to be observed, allocation was made in the model payload for two cameras with radiation-hard detectors, placed external to the vault and approximately one meter above the surface of Europa. Camera separation in the mission concept is approximately 20 cm, enabling stereo imaging. Finally, the surface phase of the mission must ensure that images can be acquired during the european day such that the sun angle is sufficiently high to illuminate cracks, blocks, and sampling sites.

Investigation 1B3: Detect structural, compositional, or functional (SCF) indicators of life (Baseline only).

While Investigation 1B1 may provide observations of cell-like structures, standard imaging alone cannot determine if a given structure is, or was, life. For this reason, a second line of evidence is incorporated into the Baseline mission to further probe candidate cells for evidence that distinguishes abiotic particulates from microbial cells. This could include detecting indicators of viability (e.g., membrane integrity and potential), structural properties of cell envelopes, redox chemistry consistent with metabolism, or detecting biosynthesized molecules.

Microbes and biogeochemical materials from Europa's ocean could become incorporated into the ice shell (**Figure 3.5**) through processes similar to those observed in subglacial Lake Vostok (Christner et al., 2006). No organism would be expected to survive direct expo-

sure to the cold, vacuum, and harsh radiation environment of Europa's surface (see e.g., Nedwell, 1999, Tuorto et al., 2014, for psychrophile limits; Paranicas et al., 2009, for Europa surface conditions).

However, ancient ice on Earth (100,000 to 750,000 years old) contains microbes that can be revived with nutrients after extended periods of quiescence (e.g., Bidle et al., 2007; Christner et al., 2003), so the preservation of viable cells within Europa's ice cannot be disregarded outright. Microorganisms that get transported to the surface via ice shell dynamics would incur damage at rates that depend on local conditions. Rapid burial in fresh plume deposits, or becoming encased in salt deposits, serve as two examples of processes that might shield cells, at least for geologically short periods of time. Such organisms would potentially persist in a state of metabolic dormancy, or alternatively, cells could lose viability (i.e., die) and their constituents would then become preserved in the ice. **Were cells and additional organic biosignatures to be detected, some form of additional "metabolic" or biophysical biosignature (as described below) could prove quite powerful, and it would be highly complementary to other lines of evidence.** Biosignatures contingent on metabolic

activity must be sensitive to detect minimal rates, such as those operating in Earth's cryosphere and deep subsurface environments (Price and Sowers, 2004; Hoehler and Jorgensen, 2013). The possibility of long lags in the initiation of metabolic activity, and growth in Earth's icy environments (e.g., >30 days; Christner et al., 2003), would also limit the ability to detect metabolism in a short duration Europa mission lifetime.

Although detection of metabolism could be a strong biosignature, a given assay design is heavily biased towards microbes with a specific physiology and tolerance to a defined range of environmental parameters. A lesson learned from the labeled release experiments on the Viking missions (Klein et al., 1972; Klein 1978; Mazur et al., 1978) is that ambiguous results may be obtained if proper context is not available. As a result, it is critical to consider more

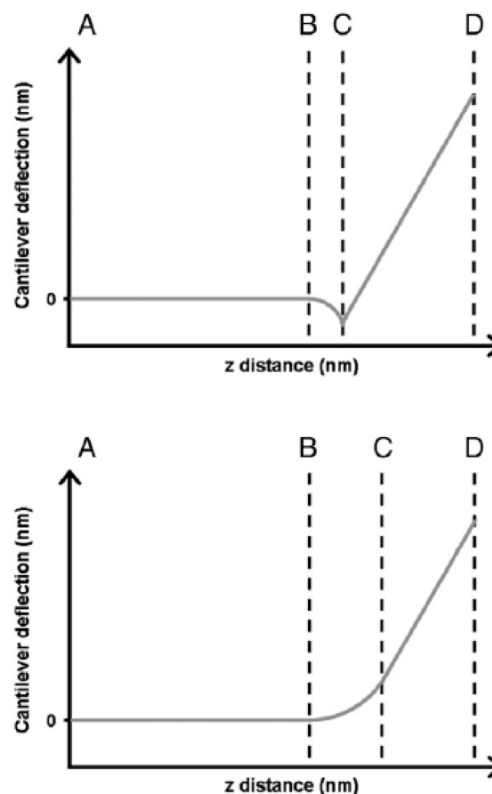


Figure 4.1.15. Model distance-deflection curves, consisting of three sections: the section between A and B, where the tip is yet to contact the surface, the non-linear section between B and C, where the tip first contacts the surface and attraction (top) or repulsion events (bottom) occur, and the linear section between C and D, where the tip is in full contact with the surface. The gradient of the latter section is dependent on the hardness of the sample; essentially hard samples have a gradient of 1, softer samples between 0 and 1. Source: Webb et al. (2011).

universal approaches that provide information on biological structures and textures, as well as the chemical, molecular, and functional composition of any putative european organisms. For example, a number of microscopic approaches provide structural and compositional information, or indications of function such as physiological and metabolic activity. Thus, measurements that could support this investigation while also addressing measurements in Investigation 1B1, are important to consider. Below are just three examples of microscopic approaches for biosignature detection that could fulfill the science of Investigation 1B3:

1) The biophysical properties of particle (cell) surfaces can be determined using atomic force microscopy (AFM). AFM can be used to image cell substructures such as nanotubes, pili, flagella, and blebs (Alsteens, 2012). When used in ‘force’ spectroscopy mode, AFM can sensitively measure biomechanical forces between individual molecules or cellular turgor, hardness, and elastic properties (**Figure 4.1.15**; Dorobantu et al., 2012; Webb et al., 2011). AFM can be used to image samples under any conditions, including a liquid medium, which allows dynamic cell processes to be investigated (e.g., whole cell, intracellular molecular motion, or cell division; Kasas et al., 2015). Finally, this technique can be used to estimate specific interactions and generate force-distance curves using cantilevers baited with various compounds (Liu and Wang, 2010).

2) Fluorescently-stained biopolymers or autofluorescent compounds are sensitive and potentially definitive approaches for detecting microbial cells. Biopolymer-targeted fluorescent stains provide information on cellular composition by binding to specific target molecules. They also provide information related to cellular physiological properties by revealing membrane integrity, membrane potential, and cellular enzymatic activity. Native fluorescence of naturally occurring biomolecules such as cofactors, aromatic amino acids, flavin nucleotides, and photosynthetic pigments can also be used for imaging cells. The wavelength of excitation/emission varies as a function of the molecular structure, which can be highly diagnostic for biomolecules. For example, targeting autofluorescence at deep UV (DUV)

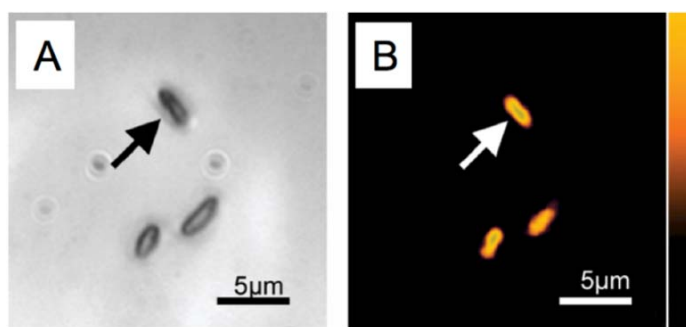


Figure 4.1.16. Label-free imaging of bacterial cells on gypsum surface. A. White-light illuminated visible image that contains three putative bacterial cells. B. Deep-UV native fluorescence image of same field as shown in panel A showing objectives that correlate to bacterial cells. Source: Bhartia et al. (2010).

wavelengths (<250 nm) excites aromatic amino acids and can be used to distinguish microbial cells in environmental samples, including in ice samples and glacial ice boreholes (**Figure 4.1.16**; Bhartia et al., 2010; Price et al., 2009; Salas et al., 2015).

Microscopic detection of microbial cells in aquatic and icy ecosystems on Earth most commonly

uses fluorescent molecules that react with or bind to specific cellular macromolecules (i.e., lipids, proteins, and nucleic acids). There are also fluorescence-based approaches that detect membrane integrity, respiratory activity, and electrochemical potential. Movement of any substance into or out of a cell requires passage through the membrane, an essential barrier that prevents charged inorganic/organic compounds that comprise life from escaping into the exterior milieu. Therefore, methods that detect breaches of cellular integrity have been used widely to differentiate dead cells from those that are potentially viable (i.e., have intact cellular membranes), including cryosphere habitats such as Antarctic sea ice (Martin et al., 2008) and Subglacial Lake Vostok (Christner et al., 2006). This assay can be performed by filtering and staining the cells on nucleopore filters followed by epifluorescence microscopy or using flow cytometry (e.g., Berney et al., 2007). Such approaches have been used to detect activity in bacterial cells in winter Arctic sea ice at temperatures as low as -2°C (Junge et al., 2004). A significant caveat, however, with these approaches (especially the use of fluorescent dyes) is that they may pose Earth-centric biases. Ideally, SCF assays should target universal properties that are consistent with life, though not impose requirements of nucleic acid-based information systems, for example, as assays of membrane integrity or electrochemical potential. Alternatives that target native fluorescence may be less Earth-centric, representing a viable option to meet the goals of this investigation.

3) Spectral characterization of microscale features can provide information on chemical composition associated with a putative cell. Microspectroscopy is an advanced non-destructive approach that uses either Raman or Fourier transform infrared spectroscopy to map composition at the microscale to visible or fluorescent microscopy images that provide

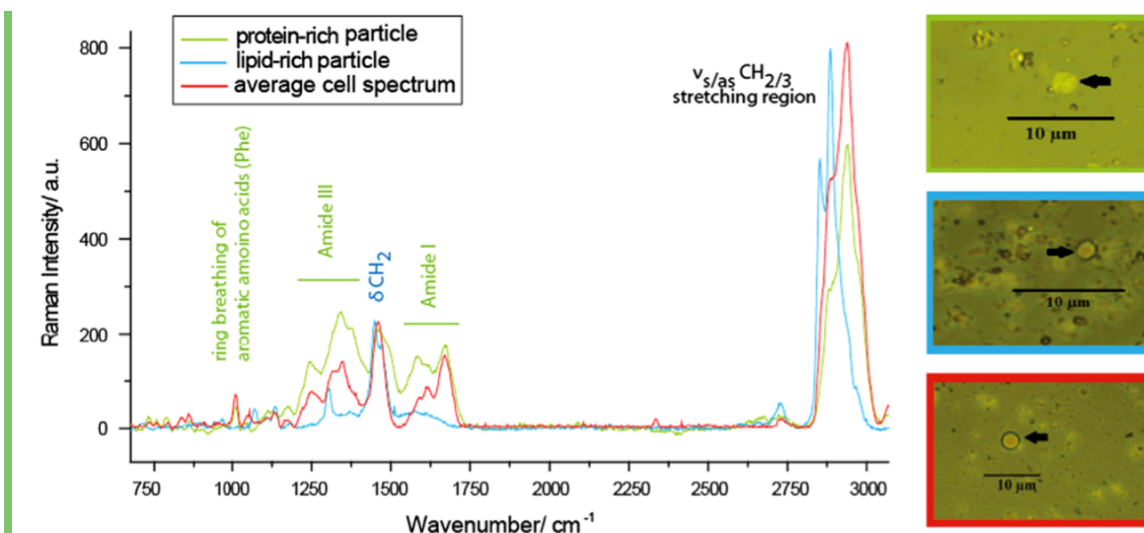


Figure 4.1.17. Microspectroscopy of microbial cells (*Methanosarcina soligelidi* SMA-21) showing coupled composition measurements from Raman spectra (left) and confocal microscope images (right). Small particles within the images at right were targeted with Raman to determine biogenicity, and to characterize specific biomolecules. Source: Serrano et al. (2014).

distinguishing characteristics of the molecules interrogated (e.g., Tang et al., 2013). These techniques can be used with minimal sample preparation to reveal the chemical composition of cellular components (**Figure 4.1.17**). A variant of Raman – resonance Raman spectroscopy – uses UV excitation of macromolecules for robust detection of biomolecules and minerals (Tarcea et al., 2007). Raman microspectroscopy has been used to detect cells in halite fluid inclusions (Winters et al., 2013), and to distinguish microbial cells (e.g., via lipids and other organics) amongst mineral background (Serrano et al., 2014; Ménez et al., 2012). A microscope-IR hyperspectral imaging spectrometer was flown on the Rosetta Philae Lander Mission (CIVA-M; Bibring et al., 2007ab), and an IR “videomicrospectrometer” was developed for the unsuccessful Phobos-Grunt Mission (Korablev et al., 2007).

All of the above measurements could significantly enhance the model payload capability for distinguishing small structures that look like microbial cells, from false positive abiotic structures. Furthermore, several of the measurements described could provide compelling evidence of organisms that were recently, or currently, viable and metabolically active (i.e., alive).

Measurement Requirements and Implementation Options

The investigation to reveal SCF properties associated with microscale particles collected in Europa’s near-subsurface, leads to the following measurement requirement:

- **Measure structural, compositional, and/or functional properties (such as biophysical or mechanical properties, native autofluorescence, or micro-spectroscopic signatures), associated with microscale particles in the sampled material (Baseline only).**

As detailed above, a variety of options exist for addressing the measurement requirement of Investigation 1B3. In the Baseline model payload, the Microscope for Life Detection (MLD) addresses both investigations 1B1 and 1B3. In addition, the model payload instrument could also bridge the gap in resolution between microscale and macroscale features detected in Investigation 1B2 using Context Remote Sensing imaging. Several additional considerations flow from the requirement above:

Requirements [see 1B1 for expanded discussion]:

The same imaging requirements established for Investigation 1B1 apply for Investigation 1B3: 0.2 μm resolution and a detection sensitivity of 100 cells per mL in a 5 cc sample from Europa’s near-subsurface. If these requirements are met and putative cells are identified in 1B1, the purpose of 1B3 is to then provide supplementary structural, compositional, or functional data that would facilitate interpretation of observations based solely on microscopic

imaging. The working sample allocation concept is that the same processed 5 cc sample interrogated in Investigation 1B1 is used for this investigation. There may be variants on this theme that would be consistent with mission operations.

Sample Handling:

If the same instrumentation is used to address investigations 1B1 and 1B3, the sample handling requirements are identical. Ice samples would need to be warmed and pressurized for liquid handling, allowing particulates in the melt water to be concentrated by pressure filtration or vacuum onto a filter; microfluidic operations may be necessary to add stains and substrates to the sample. Thus, the ability for liquid operations with the sample (through phase change if the sample has water ice, or through adding liquid to an evaporite/salt sample) may be required, depending on technique employed.

SCF Implementation options:

Several SCF enabling technologies were described above. Below are two more detailed examples of SCF options that include detection of mechanical properties of particles observed, and demonstrating that microscale features are comprised of organic compounds or biominerals. Many additional options exist, but given limited payload allocation (**Chapter 4.5**), it is critical that implementation of this investigation be considered as an enhancement to other model payload capabilities.

Implementation option 1:

Characterization of microscale particle biophysical properties using AFM. There are several applications of AFM beyond sample topographical analysis that can provide evidence for life-associated structural and/or functional properties in the particulate fraction of a sample. The requirements for determining mechanical properties involve a set of capabilities that employ AFM to record force distance curves that unveil the mechanical and adhesive properties of a particular object.

An example set of experimental steps would include: i) immobilize particles on a substrate (also required for topographical imaging); ii) flood substrate with solution (e.g., phosphate buffered saline); iii) localize particles; iv) select particle(s) for force measurement, and v) apply force and record deflection of cantilever to generate a force-distance curve for several individual particles – sufficient to generate statistically testable data sets (>5 measurements) – and/or at multiple locations across the X-Y plane to generate a spatially resolved map of microbial physio-chemical properties (see Dorobantu et al., 2012). The AFM must be internally calibrated and able to analyze procedural controls that can be used to determine background levels of contaminating particles and cells.

Implementation option 2:

Spectral and Deep UV characterization of microscale features. This composition-based assay would require a spectrometer-enhanced microscope for life detection that meets the measurement requirements above (and for 1B1). Experimental preparation requires sample concentration to minimize search space and maximize signal-to-noise. By combining the capabilities of particle visualization with spectroscopy and native fluorescence detection, particles composed of organic molecules or associated with biominerals could be spatially linked. The compositional mapping must enable detection of possibly biogenic features as small as 0.2 microns.



4.1.3

OBJECTIVE 1C: DETECT AND CHARACTERIZE ANY INORGANIC INDICATORS OF PAST OR PRESENT LIFE.

Microscopic life could be detected through its strong association with inorganic materials. Inorganic solutes can serve as critical sources of free energy (e.g., coupled reductants and oxidants required for metabolism) and comprise metabolic waste products that are generated as chemical disequilibrium is dissipated.

Dissolved inorganic species also commonly associate with the surfaces of microbial cells and extracellular exudates, giving rise to the formation of minerals through biologically influenced pathways (Zegeye et al., 2005; Fu et al., 2016; Ngwenya, 2016). Inorganic materials also act as substrates for syntrophic communities of organisms (Vindedahl et al., 2016). Not surprisingly, much of the biomass in any environmental system is also localized to aggregates of mineral particles in contact with the aqueous phase.

Objective 1C seeks evidence of extant or fossil biology by identifying the composition of the non-ice inorganic materials, including any minerals present in ice collected near Europa's surface (Figure 4.1.18). This objective addresses whether the detected minerals (i) encapsulate and preserve intact cells or cellular components (such as organic acids, proteins, carbohydrates, lipids) or (ii) record chemical, morphological or isotopic evidence that they formed as a direct result of microbiological activity. **In the search for evidence of life on Europa, biominerals could serve as a powerful biosignature, particularly if found in association with biogenic organic compounds.**

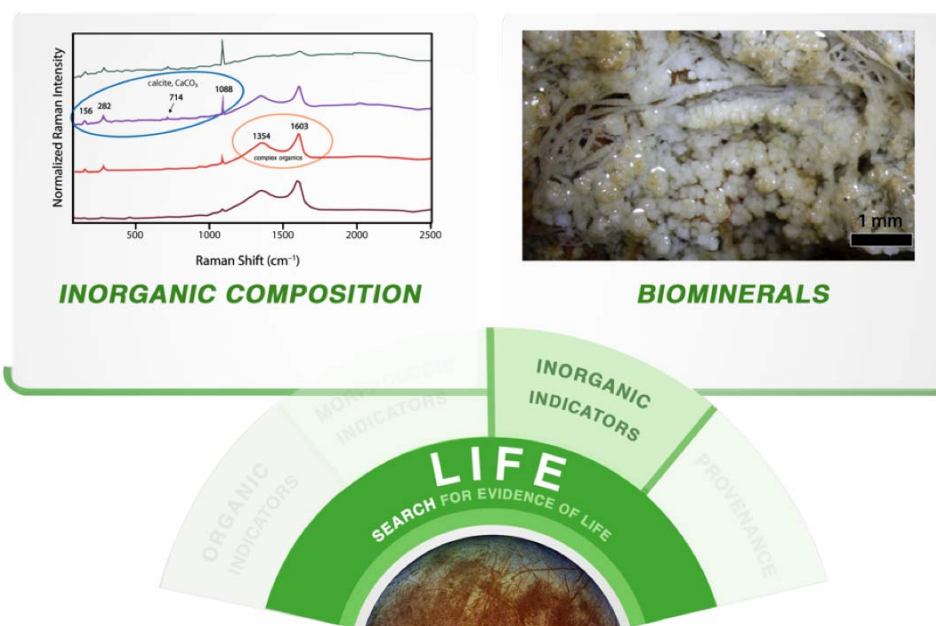


Figure 4.1.18. The third Objective within Goal 1 targets inorganic indicators of life. Potential biosignatures include evidence from inorganic components within the sampled material of minerals created by, or precipitated from, biological processes.

Investigation 1C1: Detect and characterize any potential biominerals.

Europa's ocean may contain dissolved salts, silica(tes), and gases that reflect a history of water/rock interaction between the ocean and rocky mantle; to date we know only that the ocean must be salty (e.g., Khurana et al., 2009). If there is an active biosphere, we could expect microorganisms to exert measurable chemical effects on their environment and to potentially overprint the abiotic ocean geochemistry through both the dissipation of redox disequilibria and the generation of solid and gaseous products of metabolism (e.g., Shock and Boyd, 2015). Therefore, it is important to measure the inventory of inorganic chemical species, including minerals that may have been produced as a direct or indirect result of biological activity.

Several classes of potential mineral products are well known to permineralize or encapsulate cells, such as silica, salts (e.g., carbonates, halite, gypsum), sulfides, and iron oxides, enhancing cellular preservation. Certain phyllosilicates, oxyhydroxides, and “green rust”-type structures also complex with organic matter (Braterman et al., 2004). The mineral component of the ice may also play a critical role in preserving organic biogenic molecules by protecting them against Europa's radiation environment and presence of strong oxidants in the ice matrix (cf., Phoenix et al., 2001).

Biomining is the production of intracellular or extracellular mineral particles with properties distinct from materials produced through abiotic reactions (Templeton and Benzerara, 2015). Properties include mineral composition, shape, size, magnetic and electrical properties of nanoparticles, and microscale mineralization features. Biominerals can be formed within cellular microcompartments, or through nucleation on cell surfaces or extracellular organic polymers (see e.g., Banfield and Nealson, 1997; Banfield et al., 2000). **Figure 4.1.19** provides one example of a sulfate biomineral produced by filamentous, sulfide-oxidizing microbes.

Any analysis of the inorganic mineralogy of samples, and its interpretation as a putative biomineral or product of biological activity, would be significantly more compelling were it coupled with the successful analysis of the distribution of organic molecules as described in Objective 1A (e.g., **Figure 4.1.20**). Minerals known to bind organic matter (e.g., Fe(II/III)-



Figure 4.1.19. An evident biomineral – modern barite-mineralized bacterial filaments (linear features) within authigenic barite crusts sampled from the margins of the Dead Crab Lake brine pool within the Gulf of Mexico. Photo adapted from Stevens et al. (2015).

oxides and hydroxides), or to preserve microbe-mineral interfaces, are a prime target for life detection (Bascomb, 1968).

Microorganisms have a high surface-area to volume ratio and possess charged surfaces. The charge of exposed surface functional groups (e.g., carboxyl, amino, and hydroxyl) drives interactions with inorganic ions, leading to the localized growth of minerals that are supersaturated under in situ conditions (Douglas, 2005). In addition, organic molecules such as proteins can serve as

precipitation nuclei. The properties of the organic molecule can control crystal nucleation, orientation, size and phase (Lowenstam and Weiner, 1989), giving rise to distinctive “biominerals”. The carbohydrate and protein fraction of the cellular interfaces are then encapsulated in the precipitates, such that the resulting biominerals may contain up to a few percent of glycoproteins, proteoglycans, and polysaccharides (Decho, 2010).

Continued precipitation reactions can lead to permineralization of the cells, preserving intracellular features, as well as the organic components associated with the cell surface, sheath, or membranes. Pathways of Fe and Si permineralization are well known to result in excellent preservation of cellular materials, organics, and morphologies of single cells or biofilms (Parenteau and Cady, 2010). However, even when pseudomorphs and fossilized colonies of microorganisms exist within a mineral sample, it can be difficult and controversial to observe

and verify their properties (Westall et al., 2015). **To be recognized as evidence of life, microbial biominerals or fossils must contain chemical and structural attributes uniquely indicative of microbial cells or cellular or extracellular processes** (Cady, 2002). Detailed mineralogical characterization that combines chemistry, morphology and provenance is required (Douglas, 2005).

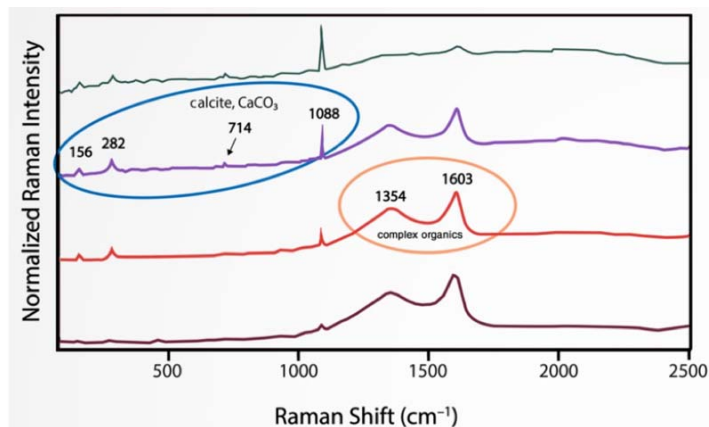


Figure 4.1.20. Raman spectra of black shales containing different relative concentrations – as indicated by relative peak intensities – of calcite (CaCO_3) and “kerogens” (complex organic molecules). Such measurements could help discriminate abiotic chondritic organics from biogenic organics. Modified from Tuschel (2013).

Minerals that often provide robust biosignatures are carbonates found within “microbialites”, where it can be shown they contain bacterioform morphologies and organic matter rich in aromatic functional groups and peptide bonds (e.g., Benzerara et al., 2006). Oceanic phosphorite deposits also often contain strong evidence of fossilized microorganisms, as biomorphs preserved in carbonate fluoroapatite and pyrite (Cosmidis et al., 2013).

Although few studies have explored microbial biomineralization by organisms within salt deposits, this type of cellular encapsulation may also occur in salt deposits, such as sulfate deposits that may be detected on Europa. Cockell et al. (2010) showed that biologically induced mineralization, cellular encapsulation and entrapment in gypsum could occur. Douglas and Yang (2002) have also proposed that sulfur minerals such as rosickyite represent biomineralization within gypsum crusts from Death Valley. Similarly, rosickyite that was considered to be a putative biosignature was also detected in elemental sulfur deposits forming at a Europa analogue spring system in the Canadian High Arctic (Gleeson et al. 2012; though, see also Cosmidis and Templeton, 2016).

Given that mineral deposits such as gypsum can provide protection from UV, desiccation, and redox reactions, it is possible that similar sulfate mineralization could play a critical role in protecting organics from radiation damage or exposure to strong oxidants and radicals on Europa. Complicating the interpretation of sulfur minerals, however, is the fact that iogenic sulfur implanted on Europa leads to a radiolytic sulfur cycle, generating sulfates and sulfur polymers (Carlson et al., 2002).

Measurement Requirements and Implementation Options

There is one key measurement requirement resulting from Investigation 1C1:

- **Identify potential biominerals, such as SiO₂ or carbonate filaments/structures, magnetite, and iron sulfides, at levels of a few to hundreds of parts per thousand by mass.**

The identification of any inorganic components at the level of a few to hundreds of parts per thousand level ensures that exogenous chondritic material containing silicates, and radiolytically processed sulfur, could be measured and potentially discriminated from endogenous minerals, after volatiles and excess water is removed from the sample (see e.g., Johnson et al., 2004, for exogenous fluxes).

For measurements of non-ice materials within samples extracted from the near-surface of Europa, many techniques could serve to address this requirement. Vibrational spectroscopic techniques were determined to be the most advantageous as they provide a non-destructive capability and can also yield measurements of organics that are highly complementary to the S-MS measurements detailed in Objective 1A.

Infrared (near- to mid-IR) or Raman spectroscopic measurements could detect and discriminate multiple classes of minerals and inorganic constituents in sampled ices, as well as in concentrated ice residues (Figure 4.1.20). These techniques are non-destructive and utilize the fact that electronic transitions and/or vibrations and rotations of components of the mineral structures occur at discrete wavelengths and can be measured. Raman scattering provides the added advantage of being able to “see” through ice, due to the small scattering cross-section of water molecules. Infrared or Raman measurements are complementary to destructive measurements within a mass spectrometry system because they provide some characterization of the structure of organic and inorganic compounds prior to their volatilization into gases for GC-MS analysis.

Spectroscopic measurements could be made of the sample in bulk or by micro-spectroscopy to measure the composition of subsamples. An advantage of micro-spectroscopy of inorganic constituents is that it enables assessment of sample compositional heterogeneity with detection thresholds on a per-pixel, or per-spot, basis rather than for the bulk sample. For example, micro-spectroscopy might detect organomineral associations by recognition of spectral evidence of C-H and amine groups co-located only with silica and not in other portions of the sample, indicating possible permineralization products. Similarly, coupling of visible microscopy at the sub-micron scale with the IR or Raman spectroscopy at larger spot sizes provides simultaneous textural and compositional information making mineral identification more definitive. For example, detection of rosickyite, a sulfurous mineral that has been known

to be associated with microbial biofilms (Douglas and Yang, 2002) would benefit from a combined microscopic-spectroscopic investigation.

The Baseline model payload for the mission concept includes spectroscopic imaging of the samples, such that compositional associations between any inorganic and organic materials could be identified. For the Threshold model payload, point spectroscopy of the bulk sampled material is sufficient.



4.1.4

OBJECTIVE 1D: DETERMINE THE PROVENANCE OF SAMPLED MATERIAL.

A critical part of assessing sampled material for potential biosignatures is to determine the place and time of origin of the material, i.e., the provenance. **Is the sampled material representative of the subsurface ocean, or other liquid environments within the ice? How long has the material *not* been a part of the ocean? How long has the material been exposed to the harsh surface environment of Europa, and how has surface processing modified the fingerprint of any endogenous chemistry?** Ultimately, the purpose of this objective is to **determine whether there is a connection between the samples collected and Europa’s potentially habitable ocean**, or liquid water environments within the ice shell.

Two Investigations within this Objective serve to address sample provenance (**Figure 4.1.21**). The first focuses largely on the geological history while the second targets the chemical history. Europa’s geology and chemistry are closely coupled, and thus each investigation contains aspects of both processes. Importantly, Objective 1D provides substantial overlap with investigations in Goal 2. In Goal 1, the focus of provenance is on understanding the context of any potential biosignatures, whereas in Goal 2 the focus is on understanding the landscape in the broader context of Europa’s habitability. Though similar in implementation, these are two distinctly different questions.

Investigation 1D1: Determine the geological context from which samples are collected.

Whether it is a rover on the surface of Mars (e.g., Grotzinger et al., 2012) or a drill site in Antarctica (e.g., Gramling, 2012), experience has demonstrated that the provenance of collected samples is critical to understanding the implications of any in situ analysis. This is particularly important in the search for extant or past life, as provenance may be traceable to an environment (e.g., subsurface ocean) that could harbor life.

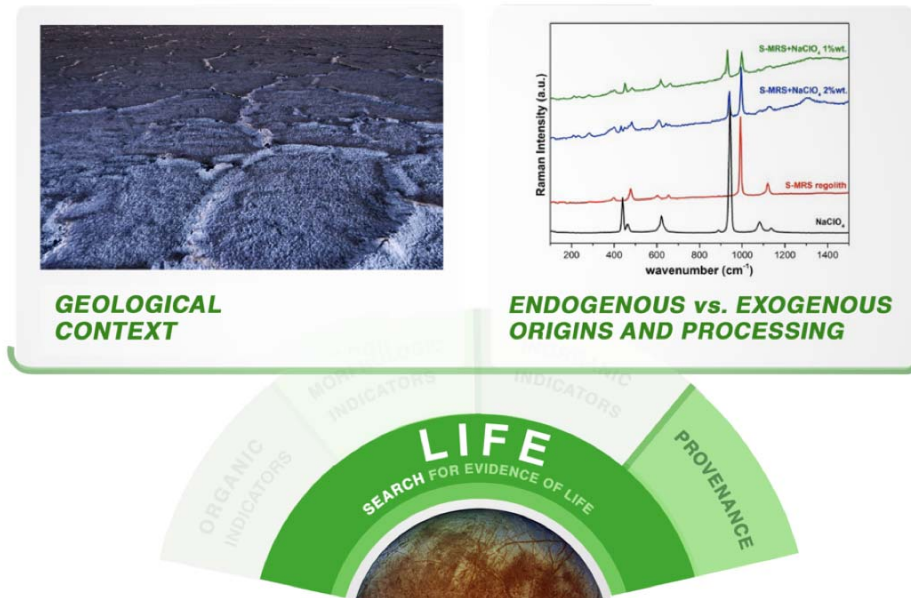


Figure 4.1.21. The fourth and final Objective within Goal 1 addresses the provenance of sampled materials and how the geological and geochemical context informs the assessment of any potential biosignatures.

Determining sample provenance requires understanding the geologic context from which samples are collected, as well as any in situ modification that has occurred since emplacement. Europa has a varied and complex surface geology that chronicles a variety of geomorphic and geochemical processes (e.g., **Figure 4.1.22**). The habitability of Europa cannot be decoupled from these processes, which govern both the evolution of the ice shell and the communication between the surface and interior. Observed geomorphic units on Europa’s surface include impact craters, ringed basins, a wide variety of tectonic ridges and bands that crisscross the surface, chaos terrain, smooth dark plains, cliff faces, putative flows, and hints of even more complex and varied terrain awaiting discovery by higher resolution images (Greenley et al., 2004).

Of particular importance for life detection are features indicative of exchange processes with liquid water (Figure 4.1.23), because such sites indicate potential exchange between the surface (where measurements can be made but the environment is hostile to life) and the subsurface ocean or liquid water regions (where life may reside). Low-albedo surfaces near ridges, ridge complexes, and lenticulae could be associated with cryovolcanism (Fagents, 2003; Fagents et al., 2000; Prockter and Schenk, 2005). Chaos terrain may be related to diapiric upwelling (Collins and Nimmo, 2009), perched water (Michaut and Manga, 2014; Schmidt et al., 2011), or disaggregation due to melting of the surface (Greenberg et al., 1999; Collins et al., 2000; Nimmo and Giese, 2005). Double ridges may indicate intrusions of near-surface liquid water (Dombard et al., 2013; Johnston and Montesi, 2014), eruptions (Fagents, 2003),

or direct extrusion of recently frozen ocean water by fractures opening and closing under tidal stresses (Greenberg et al., 2003). Some smooth regions at the margins of ridges and small chaos features have also been interpreted as fluid flows (Fagents, 2003). Little is known about Europa's surface at small scales, but steep slopes at decameter scales (Schenk, 2009) and decimeter-decameter roughness from ablation (Hobley et al., 2013) have been suggested.

Composition is also a key tracer of geological context (Carlson et al., 2009).

At least three discrete endmember compositional units have been identified using spacecraft data and ground-based telescopes (Carlson et al., 1999ab; 2002; 2009; Dalton et al., 2012; Grundy et al., 2007; Brown and Hand, 2013; Fischer et al., 2015). Some bands and chaos regions have distinctive spectral properties that could be the fingerprint of subsurface exchange (e.g., Shirley et al., 2010; Dalton et al., 2012; Fischer et al., 2015). **Figure 4.1.24** shows one example from Galileo imagery and spectroscopy of co-located geological and chemical features that may indicate recent activity. Furthermore, chloride salts from an interior ocean have been proposed as a candidate material for the dark yellow-brown color of Europa's surface within geologically young regions (Hand and Carlson, 2015).

Over timescales of decades, initially amorphous ice may change into crystalline ice, so regions of amorphous ice would indicate either recently condensed sublimated/plume material or recent radiation processing (Hansen and McCord, 2004; Carlson et al., 2009). The presence of radiolytic products, such as SO₂, O₂ and H₂O₂, could also potentially serve to differentiate between older and younger materials. Thus, the spatial, topographic, and compositional relationships between these features and the landing site could help constrain the interaction between collected samples and any shallow or deep liquid water, as well as provide a relative history of when the sample was transported to the surface.

Many of the surface features and geologic units described above would be mapped and characterized during the EMFM at the meter to tens of meter scale, which will be essential for advancing our understanding of surface processes on Europa, and for landing site selection (**Chapter 6**). **To accurately assess the specific geological context of samples collected,**



Figure 4.1.22. Europa's enigmatic chaos region, Thera Macula (image is ~70 km × 85 km), rests slightly below the level of the surrounding plains. The curved fractures along its boundaries indicate that Thera may have collapsed in the recent past and could be ongoing (see Schmidt et al., 2011). The difference in colors may indicate an endogenous origin for the reddish-brown material within Thera. Credit: NASA/JPL

however, the lander needs images of - and potentially compositional information about - the landing site and workspace at the decimeter to micron scale.

For Mars, some lessons from coupled orbiter-lander observations are clear. Decameter compositional data and decimeter-scale imaging data enabled discoveries and a level of understanding of landing site geologic history not attainable with lower resolution data. Experience with the High Resolution Imaging Science Experiment (HiRISE) shows that decimeter-scale images provide key information on geologic processes (volcanism, tectonism, fluvial, etc.). This is especially true if coupled with compositional information (e.g. decameter scale images from the Compact Reconnaissance Imaging Spectrometer for Mars, CRISM) and physical properties information (e.g., decameter scale images from the Thermal Emission Imaging System) to discriminate units not discernible in color data alone.

Landed investigations by the Mars Exploration Rovers (Spirit and Opportunity) and Mars Science Laboratory (Curiosity) demonstrate the importance of linking regional-scale orbital data on geomorphology and composition with high resolution ground-based images in order to identify the best locations for in situ analysis and provide regional geologic context to determine sample provenance (Grotzinger et al., 2012; Squyres et al., 2004a; Squyres et al., 2004b; Arvidson et al., 2014).

For geological context on Europa, a comparable approach would entail a multi-scale image campaign that combines meter-scale images from the Europa Imaging System (EIS),

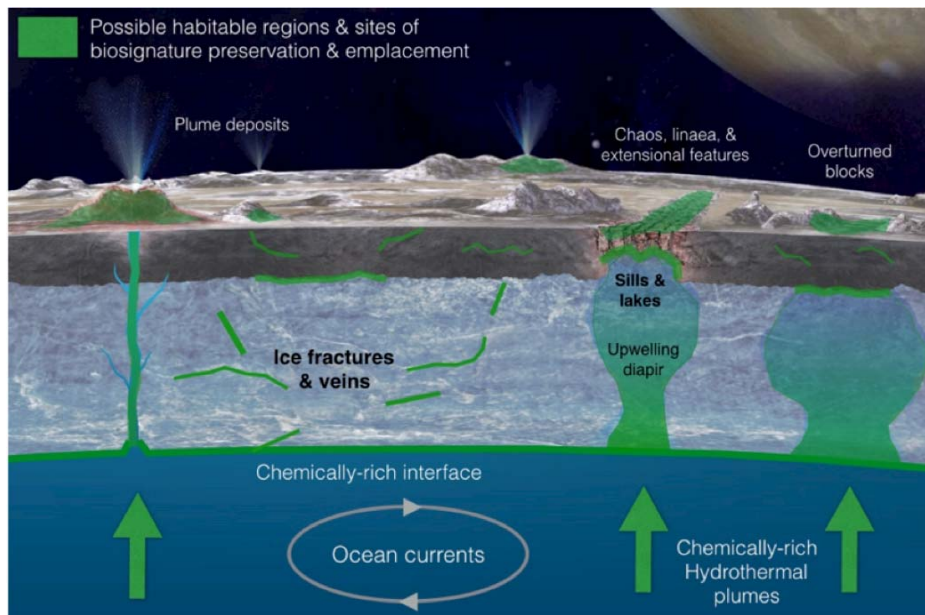


Figure 4.1.23. Potential biosignatures on Europa's surface would likely have a geological context associated with processes that deliver material from the ocean to the surface. Examples include extensional features, plumes, diapirs, sills, and perched lakes. Overturned ice blocks in chaos regions could also reveal geologically young, endogenous material.

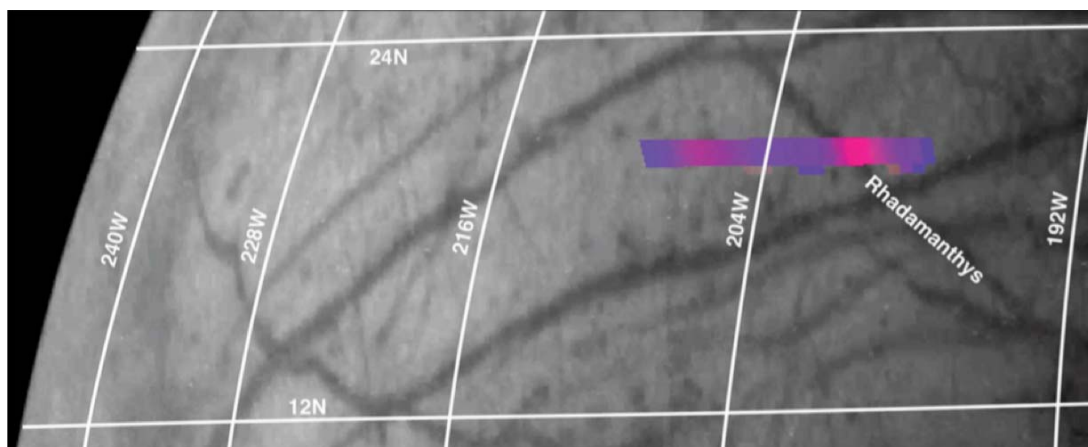


Figure 4.1.24. Numerous sites of proposed geological activity on Europa also show compositional differences with the surrounding terrain, as indicated by this overlay of spectral data onto Rhodamanthys lineae (Dalton et al., 2012). Blue corresponds to the surface brightness at $0.7 \mu\text{m}$, indicating more water ice, while red is the brightness at $1.5 \mu\text{m}$, indicating a higher abundance of hydrated materials – possibly endogenous salts.

decameter-scale compositional maps from MISE, and decameter scale thermophysical properties information from E-THEMIS on the EMFM. The Europa Lander would then interrogate the surface over a work volume substantially smaller than that resolvable in flyby data. Hence, regional grayscale or color mosaics at the decimeter-scale generated by the lander during descent, and mm-scale images of the sample work volume obtained from the model payload CRSI on the lander would be critical to completing the link to the regional context established from orbit.

Measurement Requirements and Implementation Options

Determination of sample provenance involves interpretation of landforms and materials evident at a range of observing scales. For the Europa Lander samples, this involves relating sample extraction sites (i.e., excavation holes) to their local, regional, global, and temporal context. Achieving this investigation requires:

- Identify features as small as 1 mm at the sampling sites, in color.
- Identify features as small as 1 mm in the lander workspace (~2 m), and as small as 1 cm in the landing zone (~5 m), in color.
- Identify features in the landing zone (~5 m) as small as 50 cm, in color, to bridge the gap between lander and flyby resolutions.

Implementing this set of requirements would involve high spatial resolution color images, collected by the model payload CRSI of the work volume at a resolution better than the size scale of the bulk volume of the samples (1 cc each for OCA and VS, 5 cc for MLD). For the sake of this study this a ~3–5 mm chip size was defined to be the largest discrete sample produced by the acquisition system, leading to a 1 mm per pixel resolution for observing chips and materials within the workspace. This capability would permit identification of lateral and vertical textural properties, and their variations, at the scale of the sample. Imaging of the surface, covering terrain adjacent to the lander and out to the horizon with near 360° CRS panoramas, with resolutions ranging from millimeter to meter scale respectively is required.

For the Baseline investigation, additional information on workspace heterogeneity that informs sample provenance includes information on compositional heterogeneity (e.g., salt hydrate type and concentration, organics presence/concentration, evidence of the products of radiation processing) or ice grain size. Color or spectral information sufficient to recognize compositional heterogeneities in the work space should be acquired. Increased spatial resolution (sub-mm) would also improve the characterization of textural context. **An important aspect of the Baseline capability is the opportunity for an enhanced, and more informed, sample acquisition strategy in which compositionally compelling sites in the workspace could be targeted directly. This is a key consideration for sampling during a short-lived mission.** CRS color mosaics, coupled with EMFM data and chemical measurements of sampled materials, is the minimal means (Threshold model payload) by which to discriminate heterogeneities in sample provenance. Sampling sites must be imaged before and after sampling with sufficient solar illumination so as to reveal any potential color differences. Collection of images at night was considered, as the radiation environment may excite fluorescent or luminescent materials (Sparks et al., 2010), but there is no requirement for such imaging. In the mission concept, the surface phase of operations permits science ground-in-the-loop decision making for collection of the five Baseline samples (see **Chapters 5, 8, 9**).

In addition to science CRSI data products, there could be an opportunity to image the landing zone at <50 cm per pixel by storing and eventually downlinking the descent imaging system data of the landing site. Such data would be of high science value and must be prioritized. This would not be a science instrument product, but a science team should be established to work closely with the descent phase engineering team.

Investigation 1D2: Characterize the chemistry of the near-subsurface to determine the endogenous versus exogenous origin of the sample, and any surface processing of potential biosignatures.

To achieve a high degree of confidence in the interpretation of any of the previously detailed measurements as potential biosignatures, **it is critical to establish if the provenance of the**

sampled material is endogenous, i.e., derived from the ocean or other potentially habitable liquid water environments within the ice shell. Samples in which organics and other materials of exogenous origin are present would complicate the search for life. As described in Investigations 1A2 and 1A3, the specific population of compounds, such as amino acids, could serve as a discriminating measurement for exogenous versus endogenous organics. However, basic measurements of the mineralogy and radiation processed materials on Europa's surface would also be a critical part of determining an endogenous versus exogenous provenance.

Several exogenous processes affect Europa's surface and could serve to mask the fingerprint of any endogenous chemistry (Figure 3.5). Impacts (large and small), photolysis (primarily from solar UV), and radiolysis (from energetic electrons, protons, and ions in the jovian magnetosphere and solar wind, Figure 4.1.25) are just three of the most important processes.

The composition of the micrometeorite flux is assumed, based on existing data, to be approximately cometary or chondritic, while that from Io is estimated to be basaltic to ultramafic plus volcanic gas species like sulfur and chlorine (for reviews, see e.g., Johnson et al., 2004; Carlson et al., 2009). Sodium, magnesium, and SO₂ from Io also reach the surface of Europa (e.g., Hall et al., 1994; Bagenal et al., 1985; McEwen et al., 1998), but the sodium around Europa exceeds the iogenic source rate, thus implying an endogenous source (Brown and Hill, 1996; Brown, 2001; Johnson et al., 2002; Johnson et al., 2004). Magnesium, however, which may also be delivered from the ocean to the surface, has not been found in Europa's tenuous atmosphere, down to an upper limit column density of $2 \times 10^{10} \text{ cm}^{-2}$, at a distance of 8.8 Europa radii south of Europa (Horst and Brown, 2013).

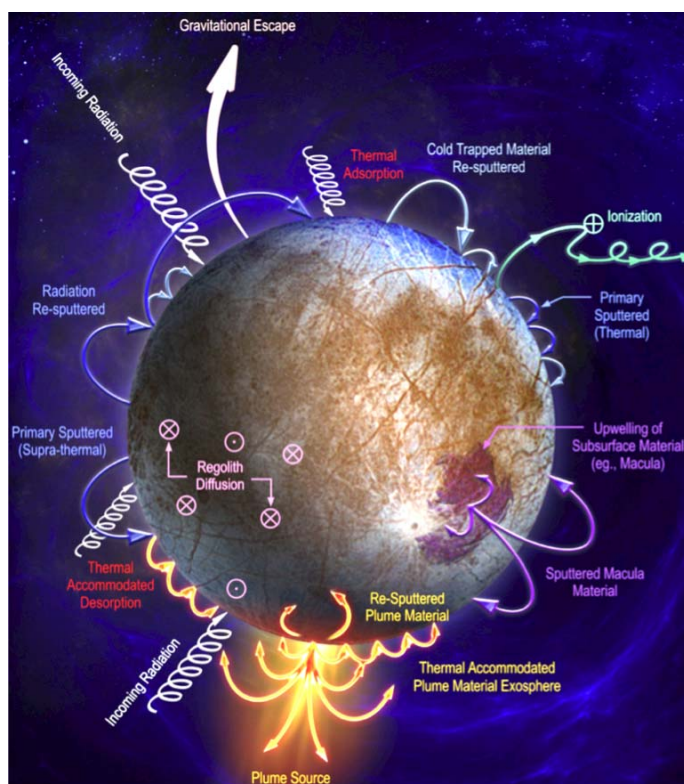


Figure 4.1.25. Europa's surface is heavily modified by sputtering and radiolysis that occurs as a result of the $\sim 125 \text{ mW m}^{-2}$ of charged particle irradiation, most of which (>75%) is from energetic electrons (Cooper et al., 2001). Note, the observation of plumes on Europa remains tenuous. Image: Teolis et al. (2017).

Impacts not only deliver exogenous materials, they also “garden” the surface, generating overturn and mixing within the surface regolith. The impact gardening depth as a function of Europa’s average surface age ($\sim 10^7$ years), is estimated to be about one centimeter (Bierhaus et al., 2005; Moore et al., 2009). Thus, on average, exogenous materials could be expected to be mixed in with endogenous materials down to a depth of a centimeter.

Radiation processing modifies endogenous materials, and the ions and neutrals that impact Europa’s surface also serve as a source of sulfur, oxygen, hydrogen, carbon, as well as several additional species delivered from Jupiter, Io, and the solar wind (Cooper et al., 2001; Cohen et al., 2001; Johnson et al., 2004). Sputtering by ions and neutrals leads to erosion of Europa’s surface at a rate of approximately $0.016 \mu\text{m}$ per year (Cooper et al., 2001), or about a centimeter over the average surface age. Photolysis and radiolysis (primarily by energetic electrons that penetrate much deeper than ions and neutrals), results in the destruction and reorganization of molecular bonds, as well as the scavenging of compounds by radicals produced by dissociation of H_2O (Johnson and Quickenden, 1997). Compounds that have been observed on Europa’s surface, and that are produced via photolysis and radiolysis, include H_2O_2 , O_2 , CO_2 , SO_2 , H_2SO_4 -hydrates, and several sulfur allotropes (see e.g., Carlson et al., 2009).

Distinguishing between exogenous and endogenous processes, based on composition, leads to the need to be able to characterize chondritic materials and radiolytically produced materials, as they serve as the hallmark of exogenous processes. If such materials are found in the sampled material, then any observed potential biosignatures must be interpreted with greater caution as exogenous chemistry and processes could mask the true endogenous chemistry. Importantly, even with significant radiation processing of endogenous organics, biosignatures could still be distinguishable from abiotic organics (Sundararaman and Dahl, 1993; Hand et al., 2009; Hand and Carlson, 2012).

Along with characterizing exogenous materials and processes, such as silicates from Io and micrometeorites, and oxidants from radiolysis, the lander should also be able to characterize endogenous materials that would be indicative of the subsurface ocean or other liquid water environments. Measurement of salts (e.g., NaCl , KCl , MgCl_2 , carbonates, and sulfates) and other minerals that could be hard to explain as being of exogenous origin should be targeted. In addition, minerals that could serve as indicators of ocean pH and redox state should also be targeted (Zolotov and Shock, 2001; Zolotov and Shock, 2004; Hand et al., 2009; Pasek and Greenberg, 2012). Several examples include sulfides, iron and aluminum oxides, phyllosilicates, sulfates, silica, phosphates, carbonates, and green rust, all of which have the potential to record geochemical and potentially biological processes. As detailed in Goal 2, such measurements would also help guide an assessment of the habitability of Europa’s ocean.

Interrelationships between multiple samples – exclusive of assumptions of the composition of exogenous materials would also provide very useful information. For example, if a potential organic biosignature of interest is found in multiple samples, and its concentration is inversely correlated with the concentration of H_2O_2 , a product of radiation, then an endogenous origin might be favored. If this sample was also positively correlated with salts, and endogenous origin would be further supported.

Finally, information could also be obtained by studying composition as a function of depth, comparing the composition of materials in the uppermost centimeters - most subject to radiation processing and exogenous delivery - to the composition of material collected from several centimeters below the surface. This could be accomplished with samples from multiple depths, or with context remote sensing of the vertical heterogeneity of the surface upon disturbance of the surface and exposure of materials from depth by the sample handling system.

Measurement Requirements and Implementation Options

Characterizing the endogenous versus exogenous chemical history of the sample provenance leads to the following measurement requirement:

- **Identify salts, radiation products (e.g., H_2O_2 , CO_2 , O_2 , SO_2 , S_n), silicates (anhydrous and hydrous), metals, and metal hydroxides, if present, at levels of a few to hundreds of parts per thousand by mass.**

Hydrogen peroxide has been measured on Europa at concentrations from near zero to 0.13% by number relative to water (Carlson et al., 1999a; Hand and Brown, 2013). Oxygen may be present at levels as high as a few percent by number abundance (Spencer and Calvin, 2002; Hand et al., 2007), and carbon dioxide has been measured to be present at levels of at least several hundreds of parts per million by number (Hand et al., 2007; Hansen and McCord, 2008). These measurements were all made from the Galileo spacecraft, or with ground-based telescopes, and thus likely represent low-end estimates for local concentrations since the spatial resolution of these observations averaged tens to hundreds of square kilometers. To assess the role of exogenous radiolytic processing within the sampled material, the lander instrumentation should thus be able to identify and quantify the concentrations of any known radiolytic products, such as peroxides, oxygen, carbon dioxide (which could also have an endogenous source), sulfur dioxide, and/or sulfur allotropes at the level of a few to hundreds of parts per thousand by mass.

Salts may be present in Europa's ocean at the levels of tens of parts per thousand to hundreds of parts per thousand by mass (Zimmer et al., 2004; Hand and Chyba, 2007), and brine pockets could serve to concentrate salts and other minerals even further. **To measure**

salts as an indicator of endogenous chemistry thus requires a sensitivity down to the parts per thousand level for candidate ocean salts (e.g., Kargel et al., 2000; Zolotov and Shock, 2001). Exogenous silicates and other chondritic materials delivered from micrometeorites and larger impacts may yield globally averaged concentrations of parts per thousand to tens of parts per thousand by mass, depending on regolith mixing, and thus the detection limits for these materials are also established at the parts per thousand level (Johnson et al., 2004; Pierazzo and Chyba, 2002).

The measurements required for this investigation are fundamentally inter-instrument, and inter-sample, as both the vibrational spectrometer (VS) and the organic compositional analysis instrument (e.g., S-MS) of the model payload could characterize volatiles and inorganic compounds. Measurements made by the VS of ices should be acquired at temperatures close to the ambient temperature of the European surface so that volatiles are retained for possible spectroscopic detection. Most of the radiolytic compounds listed above are infrared active, however molecular oxygen is not. It is critical that a suite of radiolytic compounds are targeted, but not all compounds may be uniquely identifiable with a singular technique. Molecular oxygen, for instance, could be measured with the OCA if not the VS.

The Baseline model payload capability includes spatially resolved Raman or IR microspectroscopy of samples as part of the VS and/or MLD, in addition to the OCA. If spatially resolved, organic-mineral, mineral-mineral, and mineral-organic-ice associations could be mapped in the sample. This would be a powerful means to determine whether potential organic and inorganic biosignatures are co-associated. There is no specific requirement for the scale of spatial resolution; rather, the signal-to-noise on the detection limits for a given technique should be the driving parameter.

The Baseline CRS instrument includes compositional capabilities to resolve vertical and lateral variations in ice chemistry, possibly revealing the presence/absence of salts, hydrates, and radiolytically produced compounds in the workspace. Infrared, color, and/or spectroscopy at high spatial resolution (millimeters) would enable determination of the distribution of species in the sampling area, thus providing a powerful indicator of exogenous vs. endogenous origin. This could be implemented with camera filters, or spectroscopic capability, on the Context Remote Sensing instrument.

The Threshold model payload employs the VS (e.g., infrared or Raman) to identify and characterize both radiolytic compounds and minerals of exogenous and endogenous origin. The threshold configuration is a point spectrometer that interrogates the sample once it has been introduced into the payload vault. Color imaging with the CRS instrument is sufficient to collect a sample.

Gardening, Sputtering, Radiation Processing, and Sampling Depth

To access endogenous samples that have the smallest exogenous influence, the lander must collect material from below Europa's surface at a depth where exogenous processing is predicted to be reduced. Gardening and sputtering occur to a depth of ~1 cm over the average surface age of Europa (Moore et al., 2009). Radiolysis, primarily from energetic electrons and their secondary bremsstrahlung particles, reaches deeper into Europa's surface than the gardened and sputtered regolith and thus driving the sampling depth requirement.

Paranicas et al. (2002) computed dose-depth curves for charged particles for a limited number of equatorial locations. They found that below about 1 mm the energetic electrons begin to dominate the accumulated dose. Furthermore, they predicted that secondary bremsstrahlung photons would affect the dose down to 1 m or more. Using a GEANT4 simulation, Nordheim et al. (2017b) modelled spatially resolved dose versus depth patterns for the saturnian moons, and extended that work to Europa (Nordheim et al., 2016; 2017a). That work also considered the time required for the radiation dose to reach 100 eV per 16-amu at different points on the surface, and at different depths. A dose of 100 eV per 16-amu (~60 Grad) is generally considered sufficient to destroy every bond (e.g., in a water molecule or hydrocarbon) several times, thus yielding a radiation processed sample (Cooper et al., 2001).

Results from Nordheim et al. (2017a) show that **the surface is heavily irradiated down to depths of 10 cm over ~10⁷ years (Europa's average surface age) around the apex points of the leading and trailing hemispheres.** However, at higher latitudes on both hemispheres, the radiation dose is significantly reduced. The lowest radiation doses are expected at latitudes >40° on the trailing hemisphere apex, and >65° latitude on the leading hemisphere apex. In these lower dose regions, the dose at depth is dominated by protons, and material is processed down to depths of approximately a few cm. These less-irradiated regions extend to lower latitudes as one moves away from the meridians at 90°E and 90°W.

Based on these results, **the Europa Lander must be able to sample to a depth of 10 cm (in solid ice), such that if the most scientifically compelling sites are found in the higher radiation regions, the lander could access material beneath the heavily radiation-processed material.** As a corollary to this, if the landing site is outside of the leading and trailing hemisphere radiation "lenses" then sampling to a depth of ~2 cm could be sufficient for acquiring "pristine" endogenous material. Sampling to depths of 10 cm represents a conservative scenario; it is the greatest depth at which material over the leading and trailing hemisphere lenses could be expected to be heavily radiation processed, for a timescale of 10⁷ years. Clearly, targeting young surfaces could help to ensure collection of fresh, unprocessed material. Furthermore, acquiring samples from deeper than 10 cm, though not required, could be advantageous for accessing unprocessed material. Additional considerations for landing site selection are provided in **Chapter 6**.



4.2 GOAL 2: HABITABILITY VIA IN SITU ANALYSES

Goal 2 for the Europa Lander is to assess the habitability of Europa via in situ techniques uniquely available to a lander mission. If the measurements from Goal 1 reveal potential biosignatures, then it is important to understand the geochemical context for habitability, and the proximity of the landing site to habitable regions within Europa's ice shell and ocean. Alternatively, if no biosignatures are identified as part of Goal 1, then it becomes critical that ambiguous or null results are understood in the context of the landing site, and the broader context of Europa's habitability: Did the materials investigated derive from Europa's ocean or other potentially habitable regions? Does a null result at the landing site apply to all of Europa?

Two Objectives were defined by the SDT to address Goal 2. The first focuses on how Europa's composition informs habitability, and the second focuses on the relationship of the landing site and samples to any subsurface liquid water environments (**Figure 4.2.1**). In the sections below, detail is provided for each of these Objectives, and the Investigations and Measurement Requirements are developed for those Objectives.

Significant crossover exists between Goal 1 and Goal 2, particularly with respect to compositional measurements, but the scientific utility of each measurement is in service to a distinctly different Goal. The detection of biosignatures (Goal 1) necessitates a past or presently habitable environment. **A habitable environment, however, could well be devoid of life if conditions for the origin of life were not satisfied. In other words, life requires habitability, but habitability does not require life. Understanding Europa's habitability is thus a critical aspect of addressing any ambiguous results that may arise when attempting to measure biosignatures in Europa's surface material.** Much of the discussion within the SDT about Goal 2 focused on this key issue and question: If we do not find any signs of life at the landing site, which measurements would best constrain our understanding of Europa's habitability – or lack thereof – and the relationship of the sampled material to potentially habitable regions within Europa?

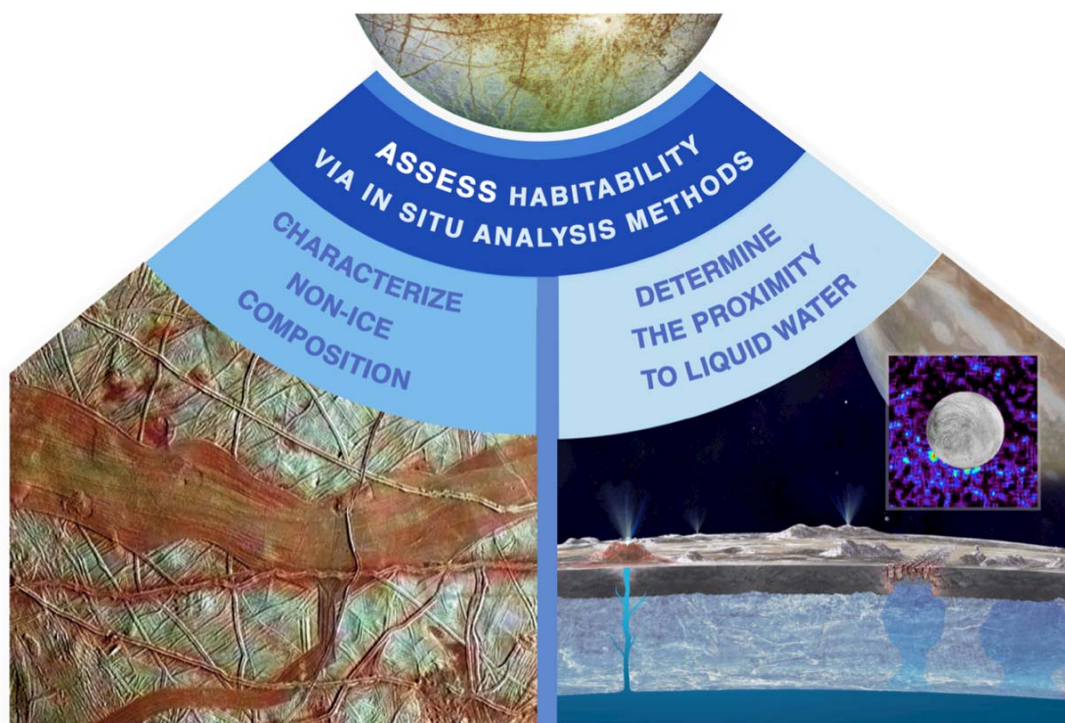


Figure 4.2.1. Goal 2 is focused on assessing the habitability of Europa through in situ analyses that inform our understanding of the non-ice composition, assessing whether sampled materials were derived from an ocean, and helping determine the proximity of the lander to liquid water.



4.2.1

OBJECTIVE 2A: CHARACTERIZE THE NON-ICE COMPOSITION OF EUROPA'S NEAR-SURFACE MATERIAL TO DETERMINE WHETHER THERE ARE INDICATORS OF CHEMICAL DISEQUILIBRIA AND OTHER ENVIRONMENTAL FACTORS ESSENTIAL FOR LIFE.

Liquid water is a necessary, but not sufficient, condition for life as we know it. Though Europa may harbor two to three times the volume of all the water found in Earth's oceans, its ocean could still prove inhospitable for life if the environmental and chemical conditions present are inadequate in providing the elements and free energy needed to build and power life.

To better understand and interpret the results from measurements made as part of Goal 1, it is important that measurements of the biogeochemical context for habitability be made. Figure 4.2.2 highlights just a few of the elements and compounds important for determining whether Europa's ocean and/or ice shell are capable of supporting life. The lander should search for, and where possible quantify, the concentration of many of these compounds (e.g., Table 4.2.1) at sensitivities that are orders of magnitude better than the

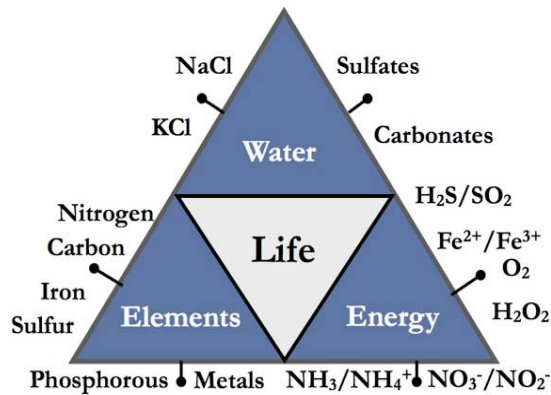


Figure 4.2.2. Keystones for habitability include liquid water, the elements to build life, and the energy needed to power life. To better understand Europa's habitability, the Europa Lander must measure the chemical composition of samples to search for compounds related to habitability, several of which are shown for each keystone.

remote sensing capabilities achievable from the Europa Multiple Flyby Mission (EMFM). In the case that the investigations of Goal 1 lead to finding signs of life, Goal 2 is essential to understanding the habitats and mechanisms that sustain life. Even if Goal 1 fails to return a positive result, our Goal 2 activities would still need to answer two distinct but important questions: 1) Were the samples we collected related to or derived from any underlying ocean or other body of water in the first place? 2) If they were, do we have any evidence that the ocean or water was habitable, or, conversely, uninhabitable?

In the case of an ambiguous or null result from Goal 1, the lander should provide valuable information even in the absence of life. Chemical measurements to determine habitability would be particularly significant in the absence of detections of signs of life, as they are crucial to determining if the samples analyzed were originally derived from a habitable niche (NRC, 2000). **If biosignatures are not detected at the landing site, it is critical to understand the extent to which a non-detection is indicative of an ocean devoid of life, or just a localized region or methodological issue in which the samples provide a false-negative.**

Within Objective 2A there are two closely related Investigations. The second Investigation is not part of the Threshold science mission; it is only in the Baseline mission. These two Investigations are described together in the section that follows. Measurement requirements follow at the end of this section.

Investigation 2A1: Determine the extent to which the habitability of Europa's ocean and liquid water environments can be inferred from surface non-ice materials as sampled and imaged.

Investigation 2A2: Identify patterns of spatial variability (textural, compositional) that may relate to habitability, and inform sample collection (Baseline only).

The clearest indicator of any past or present oceanic chemistry on Europa would be the definitive determination of the presence or absence of salts such as chlorides, carbonates, and sulfates in the acquired sample. The presence of different salts and their

relative abundances could help reveal the extent to which Europa's ocean geochemically interacts with a silicate seafloor. For example, despite the compelling cases for sulfates within Europa's ocean (e.g., Kargel et al., 2000; McCord et al., 1999; Dalton et al., 2005), it would be challenging for a sulfate-rich ocean to persist if circulation through a rocky silicate seafloor is

ongoing. Magnesium and sulfate both get drawn down and fixed in salt minerals in this process, leaving the chlorides as the major dissolved salts. This is why Earth's ocean is predominantly NaCl (Holland, 1984; Krauskopf and Bird, 1995). A chloride-rich, sulfate-poor ocean would likely be indicative of ongoing water/rock interaction at the seafloor, whereas a sulfate-rich, chloride-poor ocean could indicate one of two scenarios: either a primordial, leached-composition or significant cycling with the ice shell and delivery of radiolytically-produced sulfate derived from sulfurous materials ultimately originating at Io.

A third key salt phase may be carbonate, as measurements of the concentration of carbon dioxide ice and carbonate-complexes of plume materials in Enceladus have been used to support suggestions of water-rock serpentinization reactions creating a high pH ocean (Zolotov, 2007; Glein et al., 2015). In addition, dissolved silica could be another product of interaction with a silicate crust, as has been suggested for Enceladus (Hsu et al., 2015), where nm-size silica, detected in the plume, could come from ongoing hydrothermal spring-type reactions at the silicate-ocean interface. Measurements of silica or of salts, such as sulfates, chlorides, and carbonates, would provide key insights into Europa's aqueous geochemistry, and consequently its habitability.

Along with salts, another potential constraint on Europa's endogenous chemistry would be the detection of metal hydroxides associated with iron, aluminum, and

Table 4.2.1. Possible compositional indicators of endogenous and exogenous processes for Europa.

Compound	Processes and Example Indicators	
	Endogenous	Exogenous
Inorganic	<ul style="list-style-type: none"> • Salts (NaCl, KCl, MgSO₄, Na₂Mg(SO₄)₂) • Metal hydroxides 	<ul style="list-style-type: none"> • Silicate-rich chondrites • Sulfur from Io (S₃, S₄, H₂SO₄)
Organic	<ul style="list-style-type: none"> • Hydrocarbon chains • Nitrogen compounds 	<ul style="list-style-type: none"> • Polyaromatic hydrocarbons (PAHs) • Carbonaceous chondrites
Volatiles	<ul style="list-style-type: none"> • H₂S, CH₄, NH₃, CO₂ 	<ul style="list-style-type: none"> • Radiolysis, photolysis • O₂, SO₂, CO₂, CO, H₂O₂

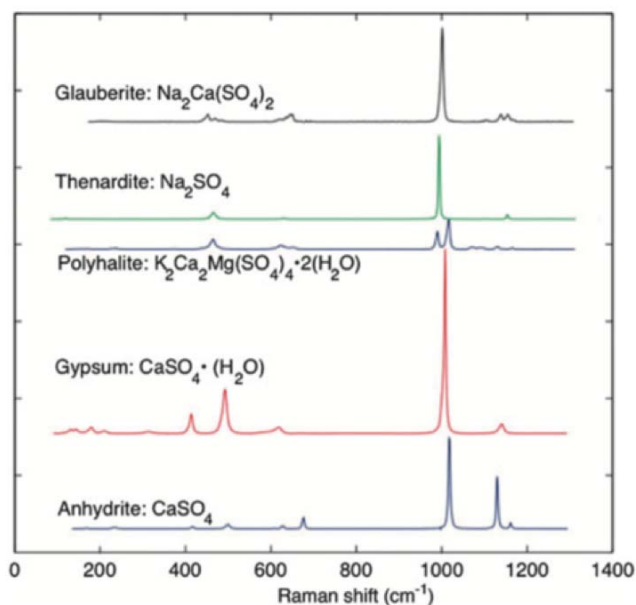


Figure 4.2.3. Example Raman spectra of several candidate salts relevant to Europa's chemistry (Downs, 2006).

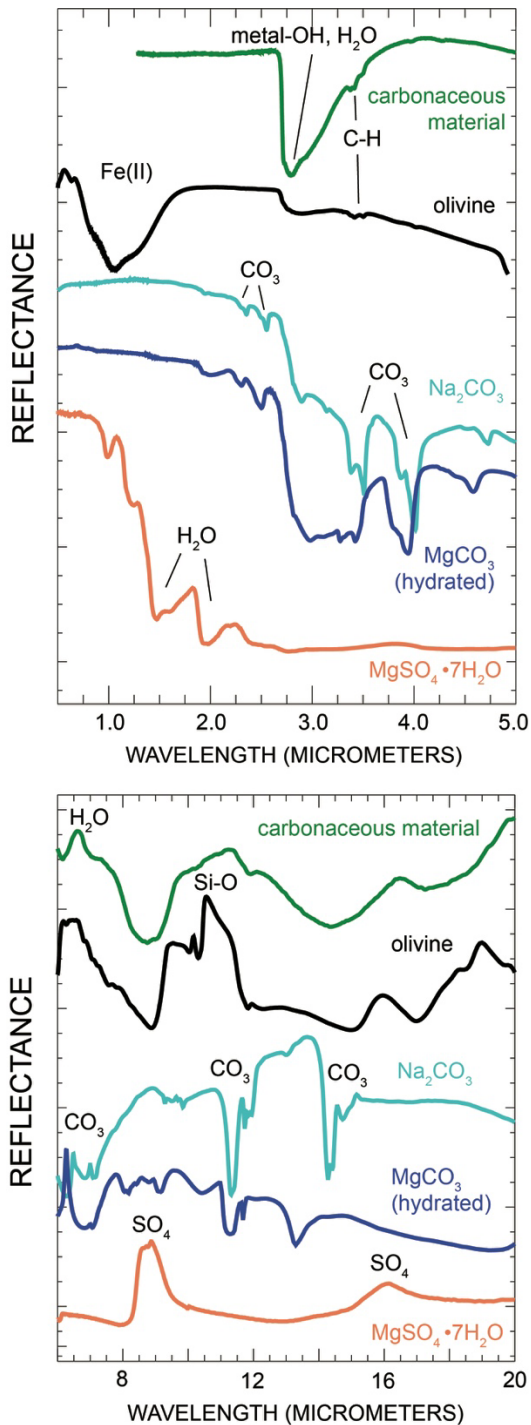


Figure 4.2.4. Example infrared spectra of select compounds relevant to Europa's chemistry (Courtesy B. Ehlmann).

magnesium. Depending on the pH and redox state of the ocean or subsurface liquid water, dissolved silica, Fe- and Al-bearing phases could be emplaced on the surface via a variety of processes (Stumm and Morgan, 1996; Hand et al., 2009). On Europa's surface, metal ions would likely oxidize to hydroxides and oxyhydroxides as a result of radiolysis.

In contrast, exogenous delivery of Fe- and Al-minerals would be in the form of silicates, oxides, and sulfides known to exist in chondrites (Lodders and Fegley, 1998). Anhydrous silicates such as olivine and pyroxene are not expected to be endogenous because they would not stay in suspension in water. Hydrated silicates (serpentine, smectites, and silica), also found in chondritic material, might form at the water-rock interface, though only sub-micron particles are likely to be entrained upward as far as the ice-water interface (e.g., silica as observed in Enceladus' plume (Hsu et al., 2015); Fe as transported across entire ocean basins on Earth (Fitzsimmons et al., 2017; Resing et al. 2015)).

Variations in the non-ice composition found on Europa's surface, and within the near-subsurface, are critical to understanding its ocean chemistry. **Figures 4.2.3** and **4.2.4** provide candidate spectra of select species relevant to Europa and their absorption features. By consideration of the concentrations of anions and cations in Europa's ice (excluding exogenous components), the pH of the underlying ocean can be predicted (e.g., Glein et al., 2015). Determination of parameters such as salinity and pH provides a framework for assessing Europa's habitability (Nealson, 1997; Hand et al., 2009) and could guide our understanding

of Europa's potential for hosting life (Shock and Boyd, 2015). **As a result, the assemblage of non-ice constituents and grain sizes of silicates and oxides present in the ice offers key information for discriminating between an exogenous origin (e.g., anhydrous silicates, coarse hydrated silicates) or endogenous origin (nanophase silica, oxyhydroxides, chlorides) of materials sampled.**

The habitability of Europa's ocean is also contingent on the availability of bio-essential elements and any chemical free energy to power life. On Europa, the chemistry and availability of nutrients are related to the water/rock ratio of silicate-water reactions and any geochemical cycling that provides the elements and energy needed to build and power life, some examples of which are shown in **Table 4.2.1** (Hoehler et al., 2001; Wackett et al., 2004). Along with the salts and minerals discussed above, detection and characterization of volatile compounds could provide an indication of hydrothermal activity (e.g., H₂S), radiolytic processes (e.g., H₂O₂), and any chemical energy available within the ocean and ice shell. Characterization of volatile species within the sample, when coupled with measurements of salts, minerals, and organics, could help determine the redox state of the ocean and ice shell, and possible metabolic processes (McCollom, 1999; Zolotov and Shock, 2003; Zolotov and Shock, 2004).

Measurement of volatiles known to be produced radiolytically (e.g., H₂O₂, CO₂, CO, SO₂, CH₄) would provide context for surface modification of endogenous and exogenous materials, and how these materials are - or are not - exchanged with the ocean (Raulin et al., 2010; Cassidy et al., 2010). Carbon- and sulfur-containing compounds such as CH₃SH and (CH₃)₂S should also be targeted as they could be indicative of radiation processing or biological waste, depending on the biosignature analyses from Goal 1 (see e.g., Pilcher, 2004; Vance et al., 2011). Much of the radiolytic modification is covered through Goal 1, but it is also relevant here because radiolytic volatiles may be important to the chemical energy budget of the ocean (Gaidos et al., 1999; Chyba, 2000; Hand et al., 2007), and to understanding the fate of any organics (Johnson and Quickenden, 1997; Moore and Hudson, 1998; Hand and Carlson, 2012).

Measurement Requirements & Implementation Options

The science of Investigations 2A1 and 2A2 lead to the following set of measurement requirements:

- **Determine the abundances of Cl-containing compounds, carbonates, sulfates, metal hydroxides, silica, and silicates, if present, at levels of a few to hundreds of parts per thousand by mass.**

- **Determine the abundances of volatiles such as H₂S, CH₄, O₂, H₂O₂, SO₂, CO₂, CO, CH₃SH, and dimethyl sulfide (DMS), if present, at levels of a few parts per thousand by mass.**
- **Determine variations in morphology of the lander workspace (~2 m) at 2 mm per pixel or better. Determine variations in composition of the landing zone (~5 m) at better than 1 decimeter per pixel (e.g., with color or spectral information). Determine variations in composition of the sampled material at better than 1 mm per pixel (Baseline only).**

To determine the endogenous nature of the sampled material the lander instrumentation must be able to identify salts such as chlorides, carbonates, and sulfates at the parts per thousand (ppt) level of detection, which is more than 30 times lower than the salinity of Earth's ocean. Europa's induced magnetic field necessitates a salty ocean with a minimum salinity comparable to Earth's ocean (Kivelson et al., 2000; Schilling et al., 2007; Hand and Chyba, 2007) and thus a ppt detection limit is justifiable based on available data. Metal hydroxides, silica, and silicates must also be distinguished at the ppt level.

To further determine the redox state of oxidant and reductant species in the sample, and to determine the extent of radiation processing, **compounds such as H₂S, CH₄, O₂, H₂O₂, SO₂, CO₂, CO, CH₃SH, and dimethyl sulfide must be measured at the level of tens of ppt**, which is at least an order of magnitude better than the remote sensing capabilities of the EMFM and provides information specific to the samples investigated for biosignatures.

In addition to characterizing the non-ice chemistry of each sample, the lander instrumentation may be able to identify lateral and vertical heterogeneities in ice composition at scales below the EMFM's tens-of-meter scale. The combination of multiple sample analyses with observations of the lander workspace, and surrounding terrain, would lead to an enhanced understanding of the landing site, and the relationship between the landing site and any subsurface habitable environments. Compositional differences are expected to exist vertically due to radiation processing and may exist laterally, depending on the spatial scale of heterogeneity of the processes that entrain ocean materials into surface ices.

The ability to characterize the surface and subsurface composition remotely, without direct sampling, would be useful for understanding the work space, aid in sample collection, and provide additional compositional information without requiring mobility. For example, organics could be present as reddish-brown material on or within water ice on Europa, and detailed chemical analyses of samples could be extended to the landscape of Europa if color and/or spectral information is collected. Further, the ability to spatially resolve compositional units, both within the sample collection area and in the terrain surrounding the lander, could help differentiate discoloration in radiation processed halide salts (Hand and Carlson, 2015) from radiation processed iogenic sulfur or endogenous organics. The more that measurements

capable of characterizing compositional differences could be extended out from the lander, the better the contextual information would be on the nature and history of materials at the landing site. A continuum of observations at multiple, nested scales, from overhead (from the EMFM and Europa Lander descent instrumentation) down to the micron-scale (within samples collected by the lander), would allow materials with compositions identified from flyby spacecraft instrumentation to be compared to ground truth from lander observations. Furthermore, once combined with regional compositional mapping from the EMFM, such ground truth measurements could be extended globally.



4.2.2

OBJECTIVE 2B: DETERMINE THE PROXIMITY TO LIQUID WATER AND RECENTLY ERUPTED MATERIALS AT THE LANDER'S LOCATION.

To understand the landing site and the samples that are analyzed by the lander, it is critical to characterize the path that the material took to arrive at the sampling location. In the event that biosignatures and signs of life are detected within the samples, understanding the connection of those samples to the ocean, or to liquid environments within the shell, provides an essential link between life and the habitable environment.

In the event that no signs of life are detected, understanding the connection between the ice shell and exchange processes within any habitable regions provides key context for **determining whether the non-detection of biosignatures resulted from an *unhabitable* ocean (or other liquid water environment), an *uninhabited* ocean, or from selection of a landing site that simply does not contain material from a region that is inhabited.**

Within Objective 2B there are four separate Investigations. Though these Investigations are closely related and, in some cases, use similar measurements, they are detailed individually in the text that follows. Measurement requirements follow at the end of this section.

Investigation 2B1: Search for any subsurface liquid water within 30 km of the lander, including the ocean.

The search for life on Europa is motivated in large part by the preponderance of evidence for liquid water beneath Europa's icy surface. The largest habitable region is likely a global ocean, separated from the surface by between three (e.g., Billings and Kattenhorn, 2005; Greenberg et al., 1998; Hand and Chyba, 2007) to ~25 km of ice (e.g., Schenk 2002; Pappalardo et al., 1998). In addition to the ocean, there are many possible reservoirs of liquid water, each tied to geologic hypotheses that have yet to be tested. Europa's surface and subsurface ice layers are sculpted by continuous geologic activity that has resurfaced the moon, including the generation and modification of fractures, ridge-building, the formation of chaotic terrains, and

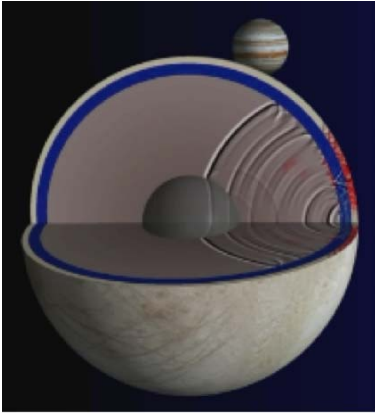


Figure 4.2.5. Artistic representation of seismo-acoustic waves traveling throughout Europa's ice shell, ocean, and interior (Image credit: S. Staehler).

bands formed through dilation, contraction, and possibly subduction of surface materials (Kattenhorn and Hurford, 2009; Collins and Nimmo, 2009; Prockter and Patterson, 2009; Kattenhorn and Prockter, 2014). Many of these processes imply that some liquid water must occur within the shell, and potentially in the near-subsurface (e.g., Schmidt et al., 2011, Dombard et al., 2013). Each of these processes may form potential habitable regions and can alter or destroy materials that move between the surface and subsurface, and thus could help inform the detection of biosignatures, or lack thereof, in samples analyzed by the lander. Based on available models and evidence, the ability to detect liquid water within 30 km of the lander, either radially (for water inclusions) or directly below (for the top of the ocean) should be sufficient.

Seismo-acoustic measurements provide a unique in situ technique for investigating Europa's subsurface and interior. Sound waves generated by natural geological activity (e.g. tidal flexing, ice fracturing, and impact events) propagate through solid materials (ice, silicates) and liquid regions (ocean, lakes, and sills) as seismic and acoustic waves (**Figure 4.2.5**). Depending on the energy of the event, the timing of the scattering and refraction of seismo-acoustic waves could reveal heterogeneities in the ice shell, the depth of the ice-ocean interface, and even the depth of the ocean-seafloor interface.

Due to the constant tidal flexing of Europa's ice shell, many sources of seismicity are expected over an 85-hour euroman day, with a variety of strengths (e.g., Rhoden et al., 2012; Schmerr et al., 2013). Lee et al. (2003) calculated arrival times and signal levels for a variety of distances between a geophone on Europa's surface and a tectonic event that creates a seismic signal near the surface, at some distance, R . **Figure 4.2.6** illustrates the propagation of waves through the ice and ocean, and the reflections back to the surface. The designation of "P", "S", and "C" indicate compressional waves in the ice shell, shear waves in the ice shell, and acoustic waves in the ocean, respectively. Travel times between reflections – and ultimately to the geophone or seismometer – are directly related to the ice-shell thickness and mechanical and material properties, and ocean or liquid reservoir depth. As the ice shell becomes thinner, thicker, or denser, the received waves become more closely clustered, or separated out, in time.

Cracking events are likely the dominant source of seismic activity on Europa. The depth to which these cracks propagate is proportional to the energy of the cracking event, and thus the strength of the seismic signal is related to the depth of ice along and through which the crack releases energy. Also shown in **Figure 4.2.6** is a seismo-acoustic time-range plot from Lee et al. (2003) for a 250 m cracking event within a 20-km convective ice shell (or

equivalently, a 10-m radius impactor). Travel times from an event at a given distance, R , to a detector for a variety of wave types are shown, along with the corresponding change in vertical and horizontal velocity.

The strength of the received signal also depends on the receiver-source separation. As detailed by Lee et al. (2003), Europa may be so active that small, shallow cracking events close to the lander could generate considerable noise which then masks the larger but more remote events that permit interrogation of Europa’s interior. Small near-surface events, however, radiate less energy, and the spectral distribution of that energy is broad and extends over high frequencies (>10 Hz). In contrast, larger cracking events in the ice shell release more energy and that energy is concentrated in a smaller, lower frequency (<10 Hz) bandpass. In their analyses, Lee et al. (2003) calculated that for a crack spacing of 100 km and with one shallow crack event occurring per minute, the ambient noise would create a velocity floor of -35 dB re $1 \mu\text{m/s}$. In the travel time plot shown in **Figure 4.2.6**, this ambient noise level corresponds to all of the colors from green to black on the dB color scale.

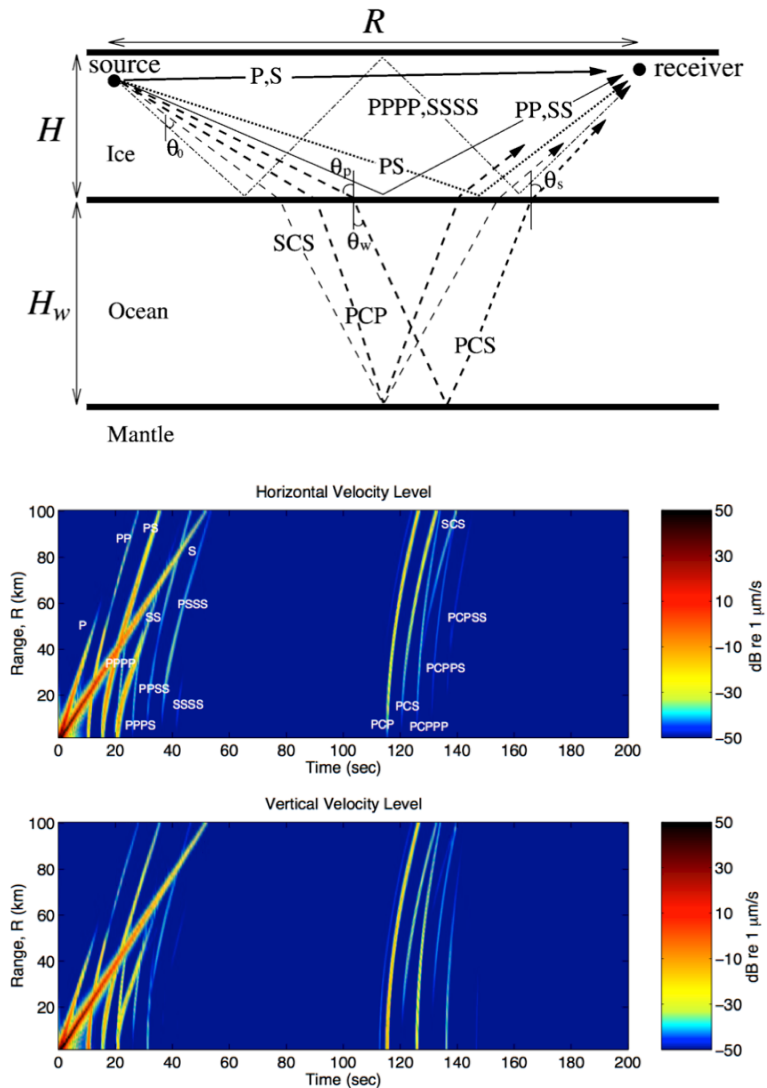


Figure 4.2.6. Goal 2B is designed to assess the habitability of Europa through in situ analyses that provide context for the chemical and biological analyses by determining the proximity of the lander to liquid water. Seismic waves, generated by energetic events such as ice fracturing, travel along the surface and through the interior and can be converted from one type of wave to another. Thus, their paths can be traced back through the ice shell, ocean and interior through the arrival time, energy, and waveform of the received signal, producing a three-dimensional picture of the satellite's interior. From Lee et al., 2003.

Importantly, the in situ seismo-acoustic investigation of Europa's interior would be highly complementary to the remote sensing ice penetrating radar (REASON) instrument on-board the EMFM. In situ measurements would serve as a valuable ground truth for these remote sensing observations since radar waves cannot penetrate through liquid water and are highly attenuated by warm or salty ice. Comparing the high resolution in situ seismic data for the landing site and surrounding region to ice penetrating radar on a global and regional scale would provide invaluable context for those measurements and enrich our understanding of the dynamics of Europa's ice shell that influence the habitability of the ice shell and ocean below.

Investigation 2B2: Search for evidence of interactions with liquid water on the surface at any scale.

Along with searching for subsurface liquid water environments, it is important that the lander search for geological evidence of the workspace and sampled materials having had interactions with liquid water. In particular, **determining whether the samples, or any nearby features, are the product of recent communication of liquid water with the surface is crucial for understanding if the samples were derived from a potentially habitable region in the subsurface.** This information provides both the context of samples acquired in the workspace from the robotic arm, and the context of features observed at the landing site that are relevant to potential biosignatures (Goal 1), and to assessing habitability (Goal 2). In the event of negative or ambiguous results for biosignature detection, such geological context for habitability and any connection to subsurface liquid water environments is critical, and serves as an important ground truth observation of assessments made with the EMFM.

Direct delivery of liquid water from a subsurface source to Europa's surface through a conduit in the ice shell is perhaps the most straightforward pathway for emplacement of unprocessed material that could be sampled by the lander. Interpretations of images from the Solid State Imager (SSI) camera on the Galileo spacecraft indicate that vigorous cryovolcanism is not a widespread resurfacing mechanism on Europa, however low-albedo smooth surfaces found in local topographic depressions have been interpreted as evidence for cryovolcanic flows (Fagents, 2003). Challenges inherent in moving liquid water upward through a

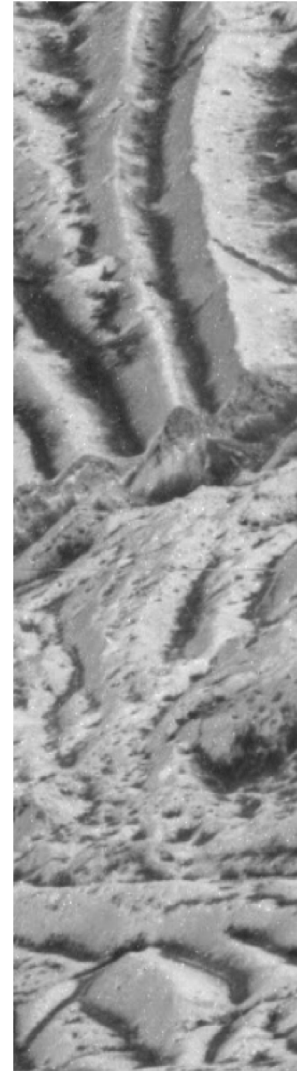


Figure 4.2.7. Mottled terrain on Europa as imaged at ~10 m/pixel reveals possible uplift, faulting, mass-wasting, exogenous processing, and possible structure within ridges (near center of image).

thick ice shell (e.g., Crawford and Stevenson, 1988; Nimmo and Manga, 2009) could make such conduits unlikely.

Alternatively, ice exposed on Europa's surface could have formed at the base of the ice shell from slow accretion of ocean water (e.g., Soderlund et al., 2014) or be derived from subsurface melt lenses (Sotin et al., 2002; Schmidt et al., 2011), brine zones (Head et al., 2002), dikes (Ojakangas and Stevenson, 1989ab), sills (Collins et al., 2009, Michaut and Manga, 2014, Craft et al., 2016), or cryovolcanic features (e.g., Fagents et al., 2000). Uplift and overturn within Europa's ice shell could then expose these materials on the surface (**Figure 4.2.7**). Similarly, dilational bands (Prockter et al., 2002), lenticulae, and chaos features could all provide mechanisms for transporting ice that was recently liquid water to the surface (Figueredo et al., 2002). Finally, large-grained ice blocks and talus along the flanks of ridges or ice cliffs – or along impact ejecta blankets – may provide a source of 'fresh' ocean or liquid water ice. The Europa Multiple Flyby Mission will help reveal much of this context, but once on the surface the direct inspection of the terrain at the meter-to-microns scale would help further establish the connection to any subsurface water.

At the landing site, and within the lander workspace, examples of possible morphological and compositional evidence for interactions with subsurface water could include observations of brine pockets and veins within the ice (which are mm- to cm-scale features on Earth), flow features derived from cryolavas, young deposits that have not been radiolytically processed, and/or fine-grained, salt-rich deposits indicative of plume activity. Thermal activity and diurnal heat anomalies could also reveal localized regions of subsurface water or a direct connection to the ocean. Use of the lander robotic arm for acquiring samples down to 10 cm would also enable observations into the shallow subsurface that could reveal some of the features described above.

Investigation 2B3: Search for evidence of active plumes and ejected materials on the surface.

The search for eruptive plumes is a key investigation for the EMFM as such sites could provide access to material derived directly from the ocean or liquid water regions within the ice shell. Were plumes to be observed by the flyby mission they would likely be considered of high scientific value for landing site selection. Due to the harsh radiation environment at Europa, pristine endogenous materials are more likely to be present and detectable in freshly erupted material, especially if that material has erupted along with liquid water. **Active plumes and vents provide a pathway for such materials to reach the surface and could be accessible to a lander.** Characterizing potential evidence of eruptions that may have occurred in the vicinity of the lander is, thus, critical to understanding the context of the sample. The frequency of eruptions, both spatially and temporally, as well as the scale of plume activity, also

have implications for the overall activity and habitability of the ice shell. Furthermore, observations of plumes feed forward to future missions that could sample plume material directly (e.g., fly-through sample collection).

The presence of active plumes on Europa has been hypothesized (e.g., Crawford and Stevenson, 1988), though these hypotheses have yet to be conclusively validated. Two kinds of plumes have been discussed in the literature: large-scale (hundreds of km high) and small-scale (tens of km high or less). Modeling of Ly-alpha emission from Europa's south pole, detected using the Hubble Space Telescope (HST; Roth et al., 2014b), suggested the presence of two 200-km-high plumes of water emanating from the southern, anti-jovian hemisphere (center of location range is 180°W). However, the plumes were not detected in more than 20 subsequent HST observations (Roth et al., 2014a). While no unambiguous evidence of plumes has been identified in older data sets (e.g., Phillips et al., 2000), two other independent methods of plume detection have recently identified signatures (**Figure 4.2.8**) that could be consistent with plumes (Sparks et al., 2016; Paganini et al., 2016).

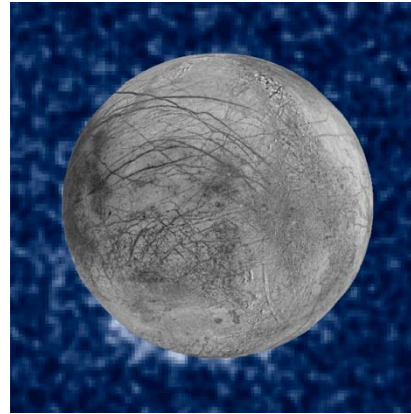


Figure 4.2.8. Hubble Space Telescope observations of Europa indicate that plumes may be active on Europa, and that plumes may be variable in space and time (Roth et al., 2014a,b; Sparks et al., 2016). This composite image shows candidate plumes in Europa's southern latitudes (courtesy NASA/Sparks et al./STSci).

The plume searches conducted thus far suggest that Europa's plumes are not tidally modulated (Roth et al., 2014a; Sparks et al., 2016), however some fractures on Europa correlate with the patterns of tidal stress throughout Europa's 85-hour orbit (e.g., Rhoden et al., 2010; Kattenhorn and Hurford, 2009; Rhoden and Hurford, 2013), and thus, smaller, time-variable plumes erupting from these fractures could be controlled by the tidal cycle (see e.g., Hedman et al. (2013) for Enceladus as a possible example). Small-scale plumes have been considered as a source of dark deposits (**Figure 4.2.9**) observed along some of Europa's lineaments, the margins of large chaos features, and surrounding small chaos and other topographic features (Fagents et al., 2003; Quick et al., 2013). Numerical modeling of the eruption process predicts plume heights between 2.5 and 26 km. A plume that can erupt material out to 10 km laterally from the source vent would have a height of 5 km if dispersed in a wide plume, and 21 km high in a narrow plume.

The Europa Multiple Flyby Mission will be capable of searching for plumes with several different instruments. Transient plumes of order 10 km or smaller, however, may be difficult to identify via remote sensing. **The Europa Lander offers a highly-complementary approach in which one specific region could be monitored for activity over several tidal cycles with surface observations.**

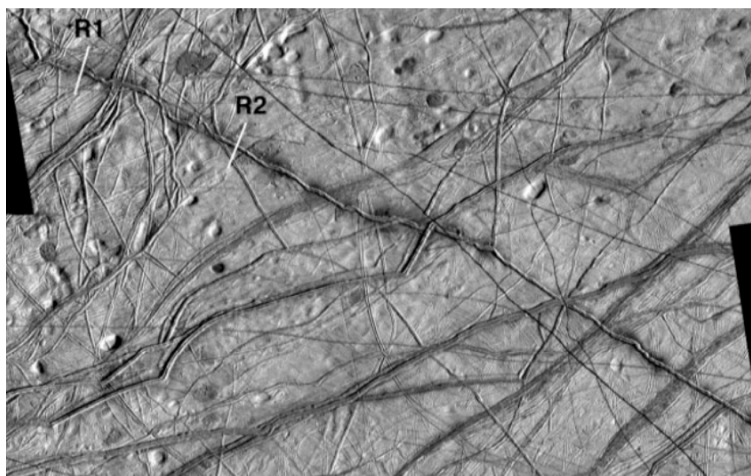


Figure 4.2.9. Dark deposits along Rhadamanthys Linea (seen bisecting the image from upper left to lower right; 230 m per pixel) could result from plume activity or cryovolcanism on Europa. The lines and notation of R1 and R2 indicate two of the many transects studied by Fagents et al., 2000.

In addition to searching for active plumes, geologically recent plume deposits on Europa's surface would also be of great interest. Though some features on Europa have been hypothesized to have a cryoclastic origin (e.g., Rhadamanthys Linea (**Figure 4.2.9**), see e.g. Belton et al., 1996; Fagents et al., 2000; Pinkerton et al., 2000), there have been no direct observations of cryovolcanic surface products. Ballistic plumes on airless silicate

bodies tend to be approximately umbrella-shaped and produce diffuse-edged haloes of tehptra centered around their fissure or point source. As a result, ejected particles may also tend to be deposited in zones of relatively homogeneous sizes within certain distances from the source vent. These geochemical, mechanical, and physical variations may appear as features with albedos, tones, or spectral signatures that contrast with that of the pre-existing terrain. Plume deposits on Europa may manifest as diffuse-edged features comprised of small (sub-mm to cm) particles that vary in size, shape, and/or mineralogy from the background

Observations of plumes from the surface of Europa could provide clear evidence of a connection between the sampled material and its origin from the plume, and ultimately from a region of liquid water. In addition, imaging of plumes by lander instrumentation could also yield information on plume structure and deposition patterns (Porco et al., 2014), which would be important for understanding the composition and origin of any ice grains sampled by the lander (Brilliantov et al., 2008; Schmidt et al., 2008; Postberg et al., 2011).

Investigation 2B4: Determine the depth of Europa's ocean (Baseline only).

As part of the Baseline mission the lander should constrain the depth to the ocean seafloor, provided seismic activity generates the acoustic sources needed to probe to seafloor depths of 100 to 200 km (e.g., the SCS, PCP, PCS reflections off the seafloor boundary in **Figure 4.2.6**).

Constraining the seafloor depth is an important component of characterizing the habitability of Europa’s putative global ocean. The seafloor could be the primary locale of geochemical disequilibrium, resulting from high or low-temperature hydrothermal activity (Gaidos et al., 1999, McCollom, 1999, Vance et al., 2016). The ocean-seafloor interface could also be the most habitable and biologically active region within the ocean. The chemical, and possibly biological, signatures of such hydrothermal activity could potentially be transported to the ice-water interface of the ocean, and subsequently up to the surface (Goodman et al., 2004). **By constraining the depth of the ocean, and the thickness of the ice shell, measurements from the lander would provide data needed to model exchange processes extending from the seafloor up to the surface.** Robotic vehicles may someday target the seafloor, and thus obtaining a measurement of the depth to the seafloor is also important for future missions (Goal 3).

Measurement Requirements & Implementation Options

To address the science detailed above, the measurement requirements for Investigations 2B1 through 2B4 are as follows:

- **Measure the thickness of the ice shell and locate any subsurface water by observing reflected body and/or surface waves from seismic events with 3-axis arrival information over a range of frequencies from 0.1–100 Hz (Threshold), or 0.1 to >100 Hz or better (Baseline only).**
- **Identify any surface morphologies/textures indicative of liquid water emplacement in the landing zone, including any compositional indicators of liquid water emplacement, and any thermal signatures of recent endogenic activity associated with liquid water.**
- **Acquire multi-temporal horizon imaging (high phase angle) to search for active plume discharge or surface change, over mission duration.**
- **Characterize any geologic and geomorphic evidence for local deposition from plume materials, such as arrival of new surface material, sloughing, plume ejecta, and non-ice composition.**
- **Measure the depth of the ocean by observing reflected body waves from seismic events covering frequencies from 0.1 to >100 Hz with 3-axis arrival information (Baseline only).**

Assuming vertical transport of ice or water from the ocean below is the most likely path for the material sampled by the lander to arrive at the surface, the farthest relevant source of water is the ice-ocean interface. For this reason, the minimum search volume for liquid

water is a 30-km radius half space below the lander. The ice could be thicker, but most models and evidence indicate a shell <30 km (see chapters in Pappalardo et al. (2009) for detailed reviews). Shallow acoustic reflections could be from liquid water zones within that space. Water could also reach the surface through narrow fissures, wider cracks, or large zones of brine saturated ice, all of which could provide seismic reflections revealing the ice shell structure. The lander instrumentation should be able to detect such reflections for features out to a 30-km radius from the landing site.

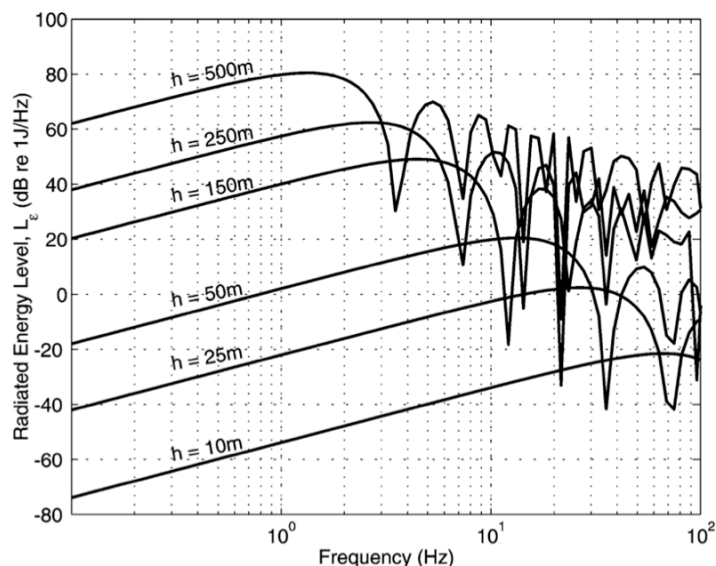


Figure 4.2.10. Energy and frequency response of simulated seismic events at depth, h , within Europa's ice shell (from Lee et al., 2003). Deeper cracks may occur less frequently, but they carry more energy and have peak energies in the range of ~ 0.5 – 10 Hz. Shallower, less energetic events have a peak spectral response at ~ 70 Hz.

The analysis from Lee et al. (2003) of the frequency and energy released by cracking events of a given depth below the surface is shown in **Figure 4.2.10**. Deeper events provide more energy and thus enable deeper probing through Europa's ice, ocean, and interior. If cracks open on Europa under every tidal cycle, several models indicate that the most frequent events would be to depths of about 50 to 150 meters (e.g., Hoppa et al., 1999; Leith and McKinnon, 1996; Rhoden et al., 2010; Kattenhorn and Hurford, 2009). Shallow local events (<100 m) could create the background energy above which the more energetic events, and their reflections, must be detected. Conveniently, the frequency distribution is a function of crack depth, h , and the peak amplitude scales as h^6 . As described in the text associated with **Figure 4.2.6**, reasonable estimates for background seismic noise (predominantly Rayleigh [surface] waves) lead to a noise velocity floor of -35 dB re $1 \mu\text{m s}^{-1}$. **To probe the ice shell to 30 km depth, and be separable from the background noise, seismo-acoustic monitoring should be conducted with a focus on deep energetic events (>100 m depth) and distinguishing those signals from shallow surface noise.** For these reasons, the Baseline requirement would monitor over 0.1 to >100 Hz, and the Threshold requirement would monitor over 0.1–100 Hz. Additional frequency range beyond 100 Hz could help ensure strong signal-to-noise performance for natural sources, and help discriminate spacecraft noise from geological events. Locally induced activity from the lander settling could also cause higher frequency noise. Further away, at high frequencies, shallow structure and rheological properties could be better constrained. At the low-frequency end of the spectrum, separating the noise from near-field shallow

events, and multiples of the initial reflections produced by deeper, more distant events, becomes possible. For both the Baseline and Threshold accommodation three-axis information is required and instrument accommodation would be within the instrument vault of the lander. The model payload allocation is for a single instrument. However, recent developments in seismometer and accelerometer technology may present a more optimized configuration, potentially providing the chance to carry multiple sensors in the allocation assumed for this mission concept (**Chapter 4.5**).

Given that both compressional and shear wave speeds in ice and water are hundreds of meters to kilometers per second, and that the total ice and water depth on Europa is <200 km (Anderson et al., 1998), seismo-acoustic echoes can be recorded within a few minutes after a source event. At a minimum, monitoring measurements should be made over the course of two european tidal cycles (7.1 Earth days) to capture the full response of Europa to diurnal stresses. Additional monitoring is desired to increase the chances of detecting larger, less frequent energy sources (e.g., large fractures or impact events) and to improve signal-to-noise in the event that no activity is detected over diurnal cycles.

To search for features indicative of liquid water emplacement from the decameter scale down to the sub-millimeter scale, repeat panoramas and stereo imaging should be collected to permit the creation of time-variable mosaics over the lifetime of the lander (~5.6 european days). Searching for active or recent plumes in the landing site region requires that the lander must, over the duration of the mission, collect images that would reveal evidence of injection/eruption of water at the surface via (a) eruptive plumes that might be visible in the sky as viewed at high phase angle, (b) injected into cracks that might open/close in response to tidal forces, and/or (c) deposition of new plume material in the visible landscape. Images should be collected across a diversity of true anomaly positions to determine if tidal cycles influence plume activity. Images sufficient to identify plume deposits are also desired. Eruptive plumes of water might form deposits with morphologic, textural, or tonal characteristics that might be identified at the dm- to cm-scale, similar to lunar pyroclastic glass beads. Constituent particles and grain sizes might range from sub-mm (comparable to lunar glasses, and particles collected by Cassini during Enceladus plume flybys (Postberg et al., 2011)) to 0.5–5 mm (average size range of Hawaiian basaltic glass droplets).

In the Baseline model payload the CRS instrument provides compositional information, as well as morphological details, about the landing site. Color filters or spectroscopic imaging capabilities of the workspace and/or landing zone would significantly improve the ability to remotely determine the distribution of potential plume materials, and other characteristics indicative of recent liquid water emplacement.



4.3 GOAL 3: PATHFINDING FOR FUTURE EXPLORATION

Goal 3 of the Europa Lander mission is to characterize surface and subsurface properties at the scale of the lander to support future exploration. These investigations focus on the surface properties and dynamic processes at Europa's surface. They would also provide context for understanding the science of Goals 1 and 2, and feed-forward into future exploration. The Goal 3 investigations would directly support the higher-priority Goal 1 and 2 objectives by providing a framework for their interpretation in a geologic and geophysical context. Importantly, the science of this goal would provide essential 'boundary conditions' to inform all future robotic missions. This approach has proven highly successful in the systematic exploration of Mars and the Moon.

Two overarching Objectives were defined by the SDT to address Goal 3. The first focuses on surface properties of Europa, and the second focuses on dynamic processes (**Figure 4.3.1**). In the sections below, detail is provided for each of these Objectives and the Investigations and measurement requirements developed to address the science. Significant crossover exists between Goal 3 and measurements defined in Goals 1 and 2, especially as it relates to chemistry and seismic measurements. The scientific utility of each measurement is, however, in service of a distinctly different Goal. Regardless of whether biosignatures are detected, Goal 3 would help characterize the surface properties and processes on Europa to provide geologic context for those results. Goal 3 also opens new opportunities for future exploration.

To enable future landings across a broad range of lander-scale terrain types and mechanical characteristics on Europa, or any similar "ocean world" planetary surface, the first landed missions should work in service to future pathways for scientific exploration. This should ideally be accomplished on the initial Europa Lander mission by quantitatively characterizing the europian surface in an integrated approach that opens new possibilities for the next stage of exploration. One important pathway through which Goal 3 works is in the coupling of flyby/orbital remote sensing data (e.g., from the EMFM) with landed ground-truth measurements. This approach has been used effectively as a key aspect of NASA's ongoing Mars Exploration Program. Mars Global Surveyor data guided Mars Exploration Rover (MER)

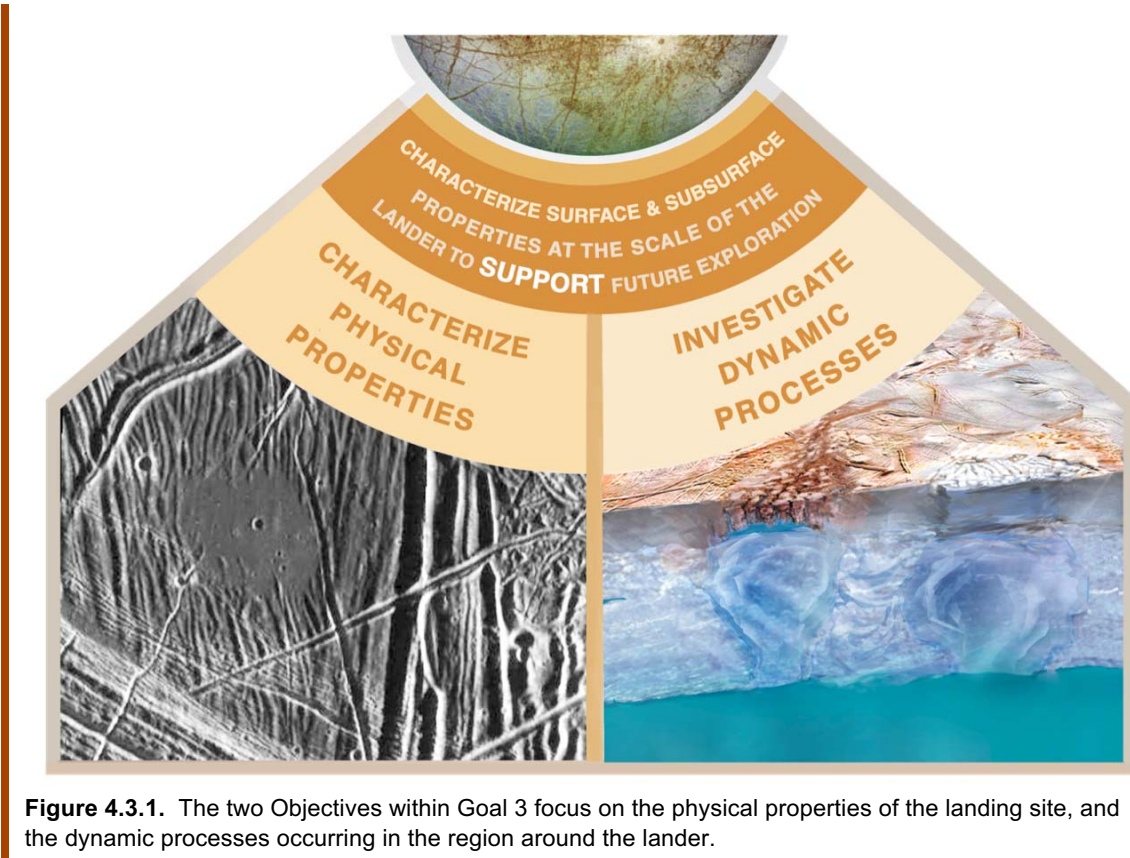


Figure 4.3.1. The two Objectives within Goal 3 focus on the physical properties of the landing site, and the dynamic processes occurring in the region around the lander.

landing site selection, and MER landed data then informed how Mars Reconnaissance Orbiter/ Mars Science Laboratory (MSL) would operate. Such coupling of capabilities provides a useful model for the future exploration of Europa, and other ocean worlds, more broadly.

The priorities within the science-driven Mars Exploration Program were twofold, first to increase lateral coverage using horizontal mobility or roving range, and second to investigate habitability through time by developing capabilities for stratigraphic analyses of exposed rock at local scales. **On Europa, our initial pathfinding Europa Lander may reveal that more lateral coverage is desired via horizontal mobility, or that the next steps require moving downward into Europa’s ice shell and interior.** Thus, the applied scientific and engineering supporting measurements from the Europa Lander mission must serve to provide boundary conditions for future phases of exploration on Europa and elsewhere, with particular emphasis on the search for evidence of life. Development of these “engineering boundary conditions” within Goal 3 would further support the aim of placing the keystone scientific measurements from Goal 1 and Goal 2 investigations into quantitative geological, geochemical, and geophysical context.

Goal 3 primarily supports applied science, engineering, and technology. The measurements from Goal 3 would feed forward to the future science exploration of Europa. If the Goal 1 (and related Goal 2) investigations find convincing evidence of life, then Goal 3 becomes essential for identifying where to find, and how to access, habitable regions within Europa. Future missions would target these habitats, and the quantitative characterizations from Goal 3 would help guide those future mission designs.

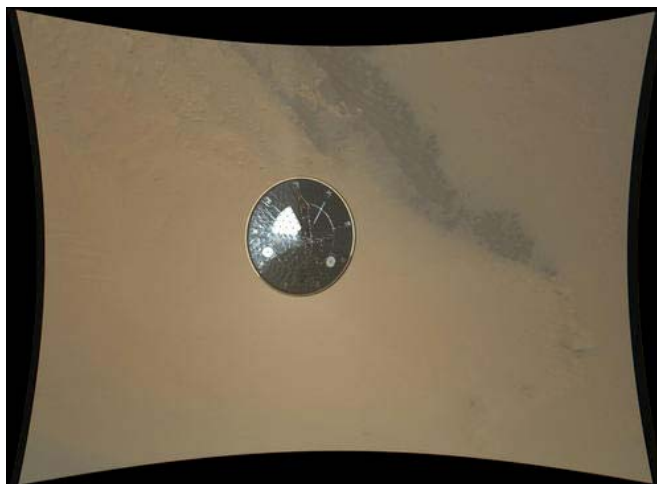


Figure 4.3.2. Image of the martian surface and heatshield as captured by the Mars Descent Imager (MARDI) during the landing of MSL/Curiosity. Similar images during the Europa Lander DDL phase could be of high scientific value. (Credit: MSSS/JPL/NASA).

Alternatively, if no signs of life are discovered (Goal 1), but Europa is deemed habitable (Goal 2), then results from Goal 3 – coupled with the EMFM data – would provide a set of ground-truth measurements that would help determine the prime targets for subsequent missions. Finally, if no signs of life are detected, and Europa is also determined to be inhospitable for life, then results from Goal 3 and the EMFM would be critical to guiding future science exploration priorities, for Europa and other ocean worlds. For all of these reasons, Goal 3 measurements support the longer time horizon of enabling the future exploration of Europa (see **Chapter 2** for more historical context on the search for life).

One of the key strengths of Goal 3 is that it leverages crossover with the engineering subsystems of the Europa Lander project, utilizing engineering-critical measurements to support science investigations. The De-orbit, Descent and Landing (DDL) system, for example, would provide high-resolution nadir-viewing descent imaging, extremely-fine-scale digital terrain models (DTM), and other measurements of the landing site during the lower altitude descent phase (**Figure 4.3.2**).

As another example, the lander’s robotic arm and sample acquisition device – which would allow the engineering team to precisely control arm motion and positioning as well as excavation operations – would also allow quantitative feedback to be gathered on the physical parameters of Europa’s surface, such as mechanical strength and compressibility. Furthermore, the thermal management system of the lander could also be used to characterize and quantify temperature changes and some of the thermal properties of Europa’s surface that occur over the mission lifetime (i.e., as has been done with missions to Mars dating back to Viking in the 1970s).

Thus, while Goal 3 does not represent a purely scientific goal, it would enable the Europa Lander mission (and NASA) to leverage engineering capabilities to yield unique, science-related measurements that also feed-forward into future exploration missions. This approach builds on the precedent and successful utilization of this strategy in the development of the Mars Exploration program, starting with the 1997 Mars Pathfinder mission and extending to the MER rovers and now MSL/Curiosity.



4.3.1

OBJECTIVE 3A: OBSERVE THE PROPERTIES OF SURFACE MATERIALS AND SUB-METER-SCALE LANDING HAZARDS AT THE LANDING SITE, INCLUDING THE SAMPLED AREA. CONNECT LOCAL PROPERTIES WITH THOSE SEEN FROM FLYBY REMOTE SENSING.

Objective 3A focuses on studying the properties of Europa’s surface at the landing site, including the immediate area surrounding the lander and the detailed properties of the sampling sites(s). These observations would allow local properties in the vicinity of the lander to be connected with remote sensing data taken by the Europa Multiple Flyby Mission. This objective has cross-cutting ties with Goal 1, Objective 1D, and with Goal 2, Objectives 2A and 2B.

Investigation 3A1: Characterize the physical properties of Europa’s surface materials through interaction with the sampling and landing system.

Investigation 3A1 is focused on studying and quantitatively characterizing the physical properties of Europa’s surface at scales not accessible from orbit or flyby altitudes. **To enable future exploration, it will be important to determine the properties of both loose surface materials (referred to as “fines” or “regolith”), and any solid surface materials (“icy shell material”).** For regolith, the aim is to measure the physical and mechanical properties of any loose, unconsolidated or weakly indurated fine-grained surface materials (i.e., typically with a size distribution finer than ~1 mm on average), which can be called regolith. (Note, as used here, the term regolith does not strictly require a genetic connection with ballistically-derived hypervelocity impact products, although impact processes are an important component). The lander should characterize the millimeter-to-decimeter textural, morphological, and structural attributes of this material as it exists on the topmost surface layer, and also fresh material as exposed by the sampling system. The mission should also characterize the physical and mechanical properties of any solid surface materials, which are assumed to be portions of icy shell material (i.e., bulk geologic materials including objects larger than centimeters in scale). The lander instrumentation should further characterize the millimeter-to-decimeter scale textural, morphological, and structural attributes of this material, as well as

measure the thermal properties of the surface over the duration of the mission. This investigation requires multi-scale and multi-temporal measurements.

Observations made by the Europa Lander model payload would depend on a variety of parameters, including the distance from the lander, solar illumination phase angle, and the geomorphology of the site (e.g., the terrain flatness relative to the horizon, and the presence of hills, ridges, fault scarps, boulders, ponded deposits of “fines”, and other local-scale topographic features). Millimeter-scale features would be observable nearest the lander with the CRSI, and decimeter-to-decameter scale features would be resolvable out to the horizon.

In addition, microscopic images of sampled materials could be visible at the micron to millimeter scale, albeit after processing by the sampling system to create mm-sized chips and smaller. The microscope could be a valuable tool for this objective because it might allow recognition of trapped gas bubbles, and possibly clathrates, in ice and/or deformation or melt zones. The sections that follow detail each of these physical parameter investigations.

Loose to weakly indurated fines (e.g., regolith, plume deposits, sublimation residues, and frosts)

Radar and thermal analyses of Europa’s surface are consistent with the interpretation that the surface is covered by at least patches of porous material (Moore et al., 2009, and references therein). Spectroscopic data suggest surface ice grain sizes of 20–100 μm , significantly larger than particulates in Giant Planets’ rings (Hansen et al., 2005). This, however, refers only to the remote-sensing-accessible layer at the very top of the surface (<100 microns). The size of surface materials likely changes with depth down to the 10 cm sampling depth.

In situ characterization of deposits from fines that have accumulated at the landing site from eruptive plumes, impact ejecta, tectonic processes, or processes associated with sublimation and cold-trapping of water and other compounds, is critical for future exploration. These materials may constitute much of the material that is sensible via remote sensing, and they could serve to mask the chemical and thermal properties of the materials they cover. Any future robotic vehicle would need to be designed to be capable of traversing through, or melting/drilling through, this material.

Characterizing the nature and physical properties of this fine-grained material (e.g., particle size distribution, porosity, compressive strength, and thermal conductivity), would feed forward into both future exploration and models of volatile transport and thermal behavior of the uppermost meters of Europa. Characterization of these properties would provide a critical boundary condition for crustal heat flow. The suite of observables includes indicators of layering, grain size and shape characteristics, and signs of fragment formation processes and induration (e.g., Moore et al., 2009).

Icy Shell Substrate Material

The ‘bedrock’ or ‘country rock’ of Europa is predominantly water ice, most likely mixed with a host of non-ice materials, as detailed in **Goals 1 and 2**. **Observations and characterization of the icy shell substrate material, or bedrock, is critical for future exploration because it is primarily this material through which any deep drilling or melting would occur. Furthermore, designing for mobility across Europa’s surface would likely require negotiating blocks, ridges, and faults of bedrock material.** For these reasons, it is important to observe any geomorphic and geologic textural and structural indicators of properties of the bedrock material (**Figure 4.3.3**).

At the small scale, these indicators include, but are not limited to, signs of deformation, phase changes, bubbles or veins in ice, and attributes of ice granularity that indicate metamorphism. These measurements require sub-cm spatial resolutions, most accessible through microscopic examination of the sampled materials.



Figure 4.3.3. Blocks of Arctic sea ice on Earth covered with snow. On Europa, blocks of ice could be created by tectonic activity and dynamic processes. Fine-grained material from plumes, sublimation and cold-trapping, sputtering, impacts, and other regolith-generating processes could coat blocks and ‘bedrock’. Image: K.P. Hand.

At the larger scale observables also include – depending on their presence/absence at the landing site – observations of matrix materials among blocks in chaos terrain, the rotation of chaos blocks, the presence of stratification (layering), and the presence of land-

forms created by sublimation of icy shell material (pits, dirt cones, topographic albedo segregation, penitentes, etc.). These measurements require centimeter-to-meter-scale spatial resolution images over a wide area, including both the area accessible to the sampling system and the broader-scale terrains surrounding the lander.

Along with panoramic scans obtained throughout the mission duration by the CRSI, the nadir-pointed, high-resolution descent imaging (from the DDL Phase Powered Descent Vehicle, see **Chapter 10**), and DTMs from the Active LIDAR Hazard Avoidance Imaging system, would provide the necessary observations. This combination of images and LIDAR data offers a multi-perspective, multi-scale set of observations for detailed characterization over fields of view that could extend from $\sim 300 \text{ m} \times 300 \text{ m}$ (from descent imaging) to immediately around the lander.

Temperature of the Surface

In addition to investigating Europa's loose, fine-grained material and solid surface material, the Europa Lander may also be able to measure some key aspects of the thermal properties of Europa's surface layer. The thermal management system, one of the lander's engineering subsystems, could determine the surface temperature over the duration of the mission. These measurements, likely to be made with engineering thermal sensors, would allow temperature changes and thermal properties of Europa's surface to be recorded. Establishing constraints, however limited, on the thermal conductivity of the uppermost layer, and potentially on local thermal gradients (from 0 to 10 cm at least), has been of noteworthy significance in prior studies of the lunar and martian surfaces, so there is precedent for utilizing such engineering support observations to study Europa. In addition, such measurements would provide important ground truth for existing telescopic and remote sensing measurements of Europa's surface temperature (Rathbun et al., 2010). Measurements of Europa's thermal boundary conditions would help constrain designs for future landing and mobility platforms, and melt/drilling systems for accessing the subsurface.

Measurement Requirements & Implementation Options

To address Investigation 3A1, the following measurement requirements must be met:

- **Measure physical and mechanical properties of surface "fines" and regolith (i.e., loose, unconsolidated or weakly indurated fine-grained surface materials). Characterize textural and structural attributes of this material at millimeter scales in the workspace, and as exposed by the sample extraction tool, and at decameter scales in the far-field (horizon).**
- **Measure physical and mechanical properties of solid surface materials (i.e., icy-shell material). Characterize textural and structural attributes of this material at millimeter-to-meter scales in the landing zone (~5 m), and at decameter scales in the far-field (horizon).**
- **Determine the temperature of the european surface at the landing site, to an accuracy of ± 5 K.**

Observations of fine, regolith-type material and solid icy shell substrate-type material would be made with the context remote sensing instrument (CRSI) and microscope (MLD) that are part of the Europa Lander model payload, and with engineering data from the spacecraft subsystems.

Parameters to be measured, for the fine, regolith-type material, could include: particle size distribution, bulk density, bearing capacity (strength), penetration resistance, cohesion, adhesion, coefficient of friction, grain morphology, and optical properties.

In the case of ‘bedrock’ solid icy shell substrate materials, parameters to be measured could include hardness, bearing capacity (strength), bulk density, particle size distribution and related spatial distribution of materials within large blocks and ridges, grain morphology, and melt properties. The temperature of the surface would be measured with engineering thermal sensors on the lander. Because these measurements address the nature of surface layer materials, these observations also tie directly to measurements detailed in Objective 1D: Determine the provenance of sample material.

This investigation would also address the relationship of the sampled materials to landforms that indicate the original emplacement mechanism, and subsequent tectonic and processing history. Surface geologic units and landforms in high resolution (<30 cm per pixel) descent images (and related DTMs from the DDL-phase hazards imaging LIDAR) and CRSI data would indicate whether the materials were substantially disrupted naturally, over time, or as a result of the powered descent of the lander (i.e., terminal DDL surface interactions). Furthermore, investigation of ice at the sub-cm scale would help determine mixing of the surface ices due to micrometeorite impacts (i.e., gardening; see Investigation 3B1). Such observations would also provide information needed for selection of future landing sites, and allow the first landing site to be used as a pathfinding ground-truth mission that enables extrapolation across Europa via coupling to regional and global scale datasets from the EMFM.

Investigation 3A2: Identify geomorphic features and their quantitative relief (topography) characteristics in the landing zone.

The information obtained from Investigation 3A2 would contribute to the design of future landing systems, including those that might provide deep subsurface access or horizontal mobility. Present-day knowledge of the nature of Europa’s surface at the scale of landers and landing systems is such that the first landing system (i.e. this mission concept, **Chapters 9 and 10**) is designed to be a stationary lander that is robust to a wide range of plausible surface environments.

This lander and its descent system would provide vital knowledge regarding the topography and geomorphic origin of the sub-meter-scale surface. For example, does the terrain include meter-scale slope or roughness elements – such as blocks, pits, domes, cracks, ridges, penitentes, mass wasted ice, or icebergs and rafts (e.g., Moore et al., 1996; Hobley et al., 2013) – that could be hazards to a landing system? While the EMFM Europa Imaging System (EIS)

would yield key information at ~ 1 m per pixel, **understanding finer scales would be essential for ensuring safe landings and operations for more complicated and capable future landers.**

For Mars, the ability to predict candidate landing site surface properties, and use them to quantitatively assess the probability of success for a particular landing or mobility system, has been evolving since the 1976 Viking landings. The martian case is aided by relevant Earth analogue experience (e.g., Golombek and Rapp, 1997) and continued refinement of our understanding of how meter-scale features observed in orbiter images relate to sub-meter-scale features and mobility hazards observed from the ground (e.g., Stack et al., 2016; Arvidson et al., 2016).

Similarly, future landers on Europa would need to rely on a combination of meter-scale images from EMFM EIS along with mm- to cm-scale images of the landing zone obtained from the CRSI on the lander described in this study. Nadir descent images and hazards avoidance LIDAR-based DTMs generated from this lander would further address this investigation (i.e., as required as engineering data during DDL).

This multi-scale imaging campaign would be used to understand the geomorphic context of the landing site and tie in situ observations to other locations on Europa's surface (e.g., if landing in chaos terrain, the observations might be broadly applicable to other chaos terrains, etc.). At Europa, presently only $\sim 10\%$ of the surface is imaged at a spatial scale better than ~ 300 meters per pixel. The EMFM will obtain near global coverage at 100 meters per pixel or better, with targeted locations imaged at pixel scales as fine as ~ 50 cm per pixel (i.e., feature identification resolution of 1–2 m) near closest approach. The Europa Lander would complement this dataset by providing a wealth of information at its landing site that would be tied to the EMFM's global imaging dataset. Geomorphic context from the EMFM, and ground truth measurements from the Europa Lander, would be especially important because – while reasonable Earth analogues exist for martian terrains – the Earth analogues for Europa's surface deviate considerably from the conditions on Europa (e.g., ~ 270 K at 0.1 MPa on Earth versus ~ 100 K at 10^{-7} Pa).

Necessarily, this investigation is limited to those geologic materials and landforms visible at the landing site, which may only be a subset of possible surface and near-subsurface materials that occur elsewhere on Europa. The data from this Europa Lander on the spatial scales of heterogeneity, e.g. relative to the reach of a sampling system, would determine whether robotic systems that can move landed hardware (i.e., horizontal mobility systems such as rovers) from an initial landing site to other promising surface or near-subsurface materials and sites are needed in future exploration.

Measurement Requirements & Implementation Options

The Investigation 3A2 science leads to the following measurement requirements:

- **Determine centimeter to decimeter slope and elevation distribution of the landing zone (~5 m).**
- **Characterize centimeter- to meter-scale geomorphic features (e.g., boulders, penitentes, frost deposits, sublimation residues, small impact craters, ejecta deposits, and pits) in the landing zone (~5 m).**

Quantification of the surface area abundance of meter- to decimeter topographic features is important for future landing site selection, landing system design, and mobility system requirements and specification. For example, when describing potential hazards to landing systems on Mars (Golombek et al. 2003, Golombek et al. 2012), concerns have included (a) terrain relief over an entire landing ellipse, (b) slopes at a length scale relevant to landing system design (e.g., slope at lander touchdown spot), (c) protrusion height and surface area abundance (e.g., block, rough surface), (d) radar reflectivity (for landing systems that use landing radar), and (e) whether the surface is load-bearing (e.g., so that landers or mobility systems do not sink into the surface). The combined capabilities of the EMFM and Europa Lander would help address many of these key points for a variety of regions on Europa's surface, thereby enabling future robotic mission. As part of the model payload on the Europa Lander, the Baseline (or Threshold) context remote sensing instrument would be the key instrument for addressing this investigation.

The slope and elevation distribution of the landing zone would be calculated from repeat stereo panoramas of the landing site and workspace, which would be used to construct digital terrain models (DTMs). The DTMs could be used to determine the macroscopic surface slopes at multiple scales and the centimeter to decimeter slope and elevation distribution of the landing zone. In addition, DTMs could also help determine the surface roughness at the landing site at multiple scales (the same scales as slope measurements), ranging from the size of the landing zone to the size of lander contact surfaces (e.g., landing pads and sampling system). **Figure 4.3.4** provides several examples – from Europa and from Earth – of how surface roughness changes with the scale of observations.

Data from the context remote sensing instrument, and DTMs produced from those data, could also be used to study the nature and abundance of topographic and geomorphic features, ranging from the centimeter to meter scale, in the vicinity of the lander. At meter to decimeter scale, images and DTMs could provide the landing zone surface height distribution with multiple-scale slope distribution functions. At the centimeter to meter scale, images and DTMs could be used to characterize the size, spacing, coverage, and morphology of features

such as boulders, pentitentes, frost deposits, sublimation residues, pits, small impact craters, and ejecta deposits.

At larger scales, landforms that could be observable with the CRSI include cracks, ridges, chaos blocks and matrix material, landslide (mass wasting) deposits, and talus. The way that these landforms interact, specifically their topographic relationships (e.g., superposition etc.), could reveal the sequence of the processes that emplaced them and, thus, reveal the geological evolution of the landscape.

Investigation 3A3: Characterize the chemical and mineralogical composition of the surface to inform future site selection.

As detailed in Goals 1 and 2, a variety of exogenous and endogenous compounds have been observed, or are expected, on and within Europa's ice shell. The addition of these compounds to water ice could lead to significant alteration of both the chemical and physical nature of the

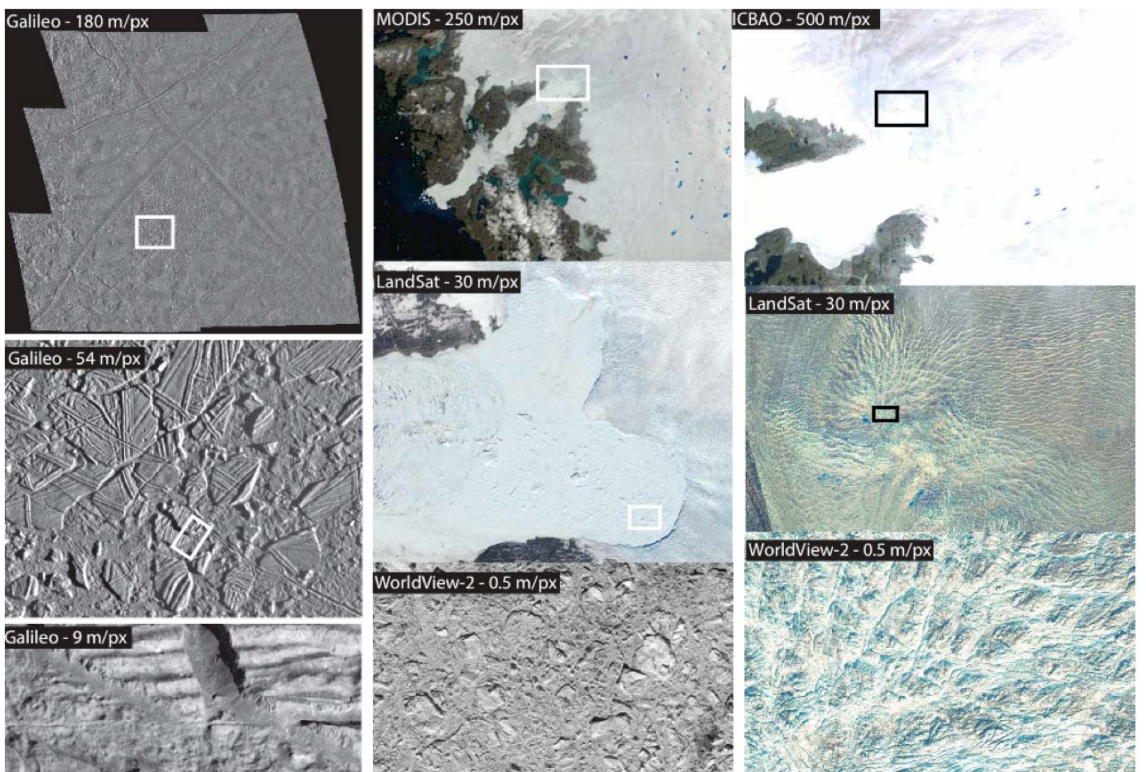


Figure 4.3.4. Comparisons of Europa's surface (left column) and Earth icy environments at similar spatial scales. At resolutions comparable to that of Galileo Solid State Imager (SSI), the surfaces of glaciers on Earth, physically affected by several similar processes, appear smooth. At higher resolution, dynamic fracturing, mass wasting, and other processes become clear, many of which can produce hazards for landed missions. Such features could be evaluated statistically through the REASON radar and E-THEMIS data from the EMFM, but without context and ground-truth measurements. Landed 3-D imaging, descent imaging, and DTMs would help clarify and resolve key scales relevant to understanding Europa. Image courtesy B. Schmidt and C. Walker.

European surface. Hence, knowledge of the resulting chemical and mineralogical composition of non-ice surface materials at the landing site would be essential for both future landing site selection, and overall design of future missions seeking to explore Europa. Regardless of the location chosen for a subsequent landed mission, this information would still be required.

For example, if the determination was made that the landing site selected for the first lander (this mission concept) should also be the landing site for a subsequent, more capable mission (e.g., with lateral mobility or ice-shell-melting technologies) then understanding the surface material properties would be critical for designing a spacecraft that could crawl across, rove over, or possibly even melt through, the ice shell. However, if the determination was made that the site selected for the first lander was not to be the site for the subsequent mission, then it would become imperative to be able to extend the in situ, ground truth measurements of the first lander to the flyby remote sensing data of the EMFM. In so doing the surface composition and properties of many candidate sites across the surface of Europa could be assessed for follow-on exploration.

Measurement Requirements & Implementation Options

Investigation 3A3 leads to the following measurement requirement:

- **Identify salts, radiation products, silicates, metals, and metal hydroxides, if present, at levels of a few to hundreds of parts per thousand by mass.**

This requirement is very closely aligned with the requirement set by Investigation 1D2 and reinforced in Goal 2, but without such stringent detection limits. This is the case because the focus of this investigation is for the design of future robotic spacecraft, and to improve site selection by providing ground truth measurements that could be coupled with compositional maps generated from EMFM data. By achieving detection levels of parts per thousand by mass, the Europa Lander would already exceed remote sensing detection limits for many compounds by at least an order of magnitude. Beyond the requirements already identified in Goals 1 and 2, one important radiolytically produced compound that should also be considered as part of these measurements – due to its corrosive potential – is sulfuric acid. Were a melt probe attempting to burrow into Europa’s ice, high concentrations of sulfuric acid in liquid phase with water could prove highly problematic. Finally, by measuring the composition and connecting that information with the geologic context, relative rates of change could be determined that would help inform how potential landing sites change over time (see previous section), and whether there is a risk associated with those changes over the decadal timescale of robotic exploration. In other words, if a landing site looks scientifically compelling and technically ‘safe’ right now, how will we know if it would still be good a decade from now?

The Baseline model payload CRSI instrument and VS instrument described in sections 4.1 and 4.2 (Goals 1 and 2, respectively) address the measurement requirements for this investigation. However, in the Threshold configuration the loss of compositional CRSI capabilities would decrease the ability to characterize the landing zone and broader landscape.

Investigation 3A4: Characterize the internal structure of Europa including ice shell thickness and depth of the ocean.

Europa's internal structure has been determined to first order from gravity and magnetic field observations made by the Galileo spacecraft (Anderson et al., 1998; Kivelson et al., 2000). Models from these observations imply an 80–170 km thick region of ice and ocean, overlaying a differentiated interior consisting of a silicate mantle and iron, or iron-sulfur, core.

Geologic constraints on the ice shell (Billings and Kattenhorn, 2005) place its thickness between ~3 km (e.g., Greenberg et al., 1998) and ~30 km of ice (e.g., Schenk, 2002, Pappalardo et al., 1998). The thickness of the shell may not be uniform across Europa's surface, with variations possible at different locations, although it is to be expected that any large differences in shell thickness would tend to flow laterally and not persist over geologic time scales (Stevenson, 2000). Furthermore, the thickness of the ice shell may change with time via secular cooling and freezing of the ocean (Nimmo, 2004), or from periodic heating and cooling events due to changes in Europa's orbit or rotational state (e.g., Hussman and Spohn, 2004; Bills et al., 2009). Such changes have implications for the long-term habitability of Europa's ocean and the creation and persistence of potential habitats within the ice shell.

Knowledge of the exact depth of the ocean, as only directly measureable through seismic sounding, could provide constraints on the salinity of Europa's ocean when coupled with the lander chemistry measurements, and orbiting magnetometry, and ice penetrating radar measurements from the EMFM. This is a key constraint on Europa's ocean's habitability, and it is also a very important consideration for assessing the feasibility of any future missions that would explore the ocean directly.

Any future exploration of Europa that targets the interior would require knowledge of the ice shell thickness and potentially the ocean depth; power systems and communication relays through these layers will be a premier technical challenge for the direct exploration of Europa's subsurface. The structure of the interfaces between the ice shell and ocean, and between ocean and seafloor, is also important to our understanding of the habitability of Europa, as these could be regions of concentrated chemical activity (e.g., hydrothermal vents).

Finally, understanding the geophysical processes that might drive any seafloor fluid flow and ocean currents will require constraints to a much higher fidelity than the tens of kilometers-scale that is currently available (e.g., from Galileo). While the EMFM will provide

new constraints on the ice and ocean thickness at a variety of scales, measurements of the ocean thickness would rely on inversions of gravity and magnetometer data, rather than direct measurements, as would be possible from the Europa Lander. As detailed in Goal 2, acoustic measurements could reveal the thickness of the ice shell and potentially the ocean thickness. Importantly, the only way to detect activity in the silicate mantle would be through active geophysical sensing of the interior by means of seismic activity measurements, which could be made uniquely through sensors on a landed mission.

Measurement Requirements & Implementation Options

The measurement requirement for Investigation 3A4 is as follows:

- **Measure acoustic signals of reflecting body waves over the lifetime of the surface mission, covering frequencies from 0.1 to >100 Hz with 3-axis arrival information (Baseline only).**

As in Objective 2B, this measurement requires observing seismic waves generated by ice shell cracking or impacts (if they should occur) that are then reflected and refracted through the ice shell, and in this case, the ocean and potentially deep interior. Measuring the ocean thickness (and potentially any interior structure) would require observing waves that travel through the ice shell, are refracted into the ocean, and then are either reflected by, or refracted into, the seafloor, and then returned. These signals are recognizable as transformed body waves. The strength of these signals declines with each refraction or reflection, and they require additional time after the initial event to scatter through Europa and arrive back at the lander. Such measurements likely require detailed characterization of the background noise in order to differentiate these potentially weak signals. For this reason, monitoring at higher frequencies (>100 Hz) over the mission duration is required. In order to record signals from a seafloor as deep as 100 km or more, and separate those results from background noise, seismo-acoustic monitoring should be conducted with a focus on deep energetic events (>100 m depth) to distinguish those signals from shallow surface noise. The Baseline requirement for this Investigation is monitoring over at least the range from 0.1 to >100 Hz, with monitoring of 3-axis arrivals.

In order to enhance the chance that such signals are detected, observing over the complete range of tidal-stress states of Europa, monitoring should take place over the course of two complete europan days (7.1 Earth days), or until at least five of these events are observed. Clearly, monitoring and observation of more events would provide the opportunity to characterize variability and increase resolution on the deep interior. As in Objective 2B, large seismic events would trigger higher frequency sampling to be recorded for 60- and 180-second

minimum windows to allow for the arrival of waves that have undergone reflection and refraction within Europa.



4.3.2 **OBJECTIVE 3B: CHARACTERIZE DYNAMIC PROCESSES OF EUROPA'S SURFACE AND ICE SHELL OVER THE MISSION DURATION TO UNDERSTAND EXOGENOUS AND ENDOGENOUS EFFECTS ON THE PHYSICOCHEMICAL PROPERTIES OF SURFACE MATERIAL.**

As a complement to the physical properties of Europa's surface studied in Objective 3A, Objective 3B focuses on the dynamic processes which modify Europa's surface. Such processes can be both endogenic and exogenic, and may be physical, chemical, or thermal in nature. Changes in Europa's surface are also possible over the short lifetime of the Europa Lander surface phase, due to tidal surface dynamics or even to local adjustments due to the landing event. In four separate investigations, Objective 3B covers this range of possibilities.

Investigation 3B1: Characterize the physical processes that affect materials on Europa (e.g., gardening).

Processes such as surface impacts of micrometeorites, thermal processing and thermally-induced fracturing, charged-particle exposure, mass wasting, erosion by sublimation, and solar-induced ablation all affect the physical properties of the top layers of Europa's surface (Moore et al., 2009). Such processes can be considered in terms of which are endogenic, caused by the internal activity of Europa itself, versus exogenic, processes that are solely external and reflect only on the surface characteristics of the icy satellite and not on its internal characteristics. It is also possible that changes may be observed over the course of a surface mission such as the Europa Lander, and careful monitoring of the surface for changes, and documentation of any such observed, would have important implications for our understanding of Europa's surface age, resurfacing rate, and degree of ongoing geologic activity. The Europa Lander mission would also be able to characterize macroscopic motions of surface materials that might yield insights into surface properties such as mechanical strength and cohesion.

Europa's regolith can be defined as the top loose surface layer, which is processed through bombardment by charged particles and through overturn by small impacts (primarily from micrometeorites) in a process called impact gardening (**Figure 4.3.5**). Europa's charged-particle irradiation (Paranicas et al., 2009) also serves to chemically modify the surface ice layer with increased penetration depths near the equator (**Figure 6.1**), and sputtering erosion can redistribute and remove material. Acceleration of charged particles by Jupiter's strong magnetosphere results in a surface energy flux that includes keV to MeV electrons, along with H^+ ,

O^{n+} , and S^{n+} ions. Sputtering by these charged particles may result in the erosion of 0.02 microns/year from Europa's surface (Johnson et al., 2009). While this rate is substantial enough to remove about a meter of surface material over the presumed 50 Myr surface age of Europa, it is slow enough that on the scale of a lander mission, it is unlikely to have any measureable effect or produce any visible changes in the area of the surface observed by the lander. However, as **Chapter 6** shows, radiation processing may have a large effect on the chemical state of europian surface materials, and this processing may vary with depth on scales observable by the lander and its ability to dig beneath the surface.

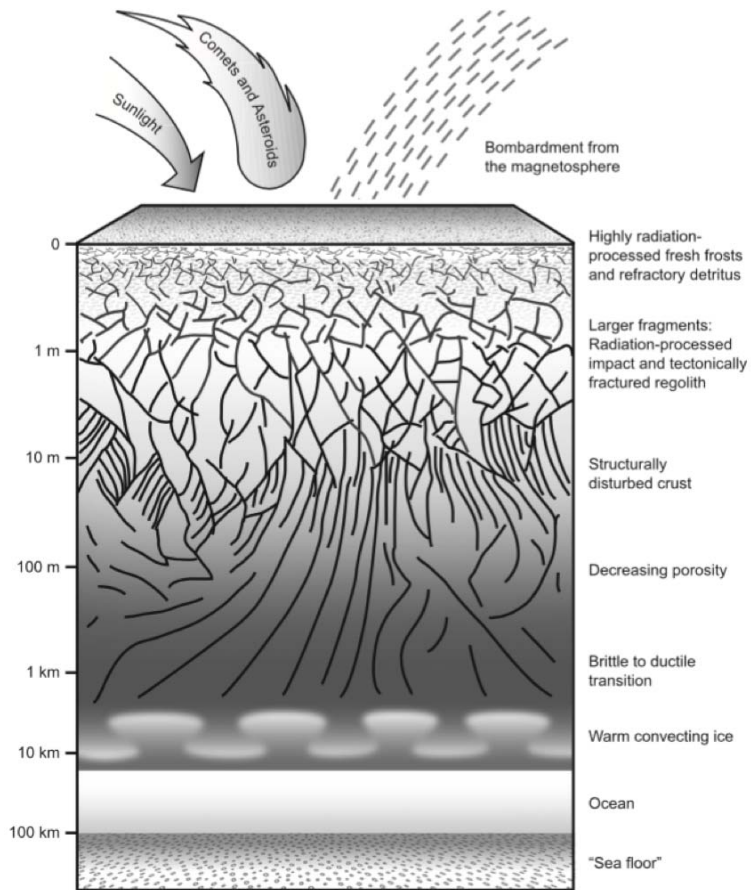


Figure 4.3.5. Hypothetical Europa cross-section diagram with a focus on surface processes (Moore et al., 2009). This diagram shows how exogenic processes such as sunlight, impacts, and radiation process the surface at different depths.

While gardening can produce a well-sorted regolith many tens of meters thick on a world like the Moon, a geologically-active world like Europa has a surface that is too young (~50 Myr vs. 4 Gyr for the Moon) to have developed such a thick layer. Europa's population of small craters is dominated by secondary craters from the handful of large primary craters on Europa's surface (Bierhaus et al., 2009), further complicating models of gardening. The best estimate of regolith depth from gardening is about 1 cm (Moore et al., 2009). While significant gardening is unlikely to be observed over the lander mission lander ($\sim 3 \times 10^{-15}$ impacts per minute per square kilometer, using the median impactor flux reported by Zahnle et al., 2003), evidence of small impacts in the area of the surface visible by the lander should be sought to help understand how such impacts change the surface materials.

Tectonic and thermal degradation also are likely to modify the surface of Europa (Moore et al., 2009). Thermal segregation occurs when ice sublimation causes motion of bright cold frost deposits upslope to ridge crests, leaving behind darker lag deposits in local topographic lows. Thermally-induced fracturing has been proposed as a dominant erosional mechanism on comet 67P-Churyumov-Gerasimenko (Vincent et al., 2016), and sublimation-driven erosion has been proposed for Callisto (Howard and Moore, 2008; White et al., 2016) and other worlds. Ablation structures have been proposed to develop with decimeter-to-meter scale separation at Europa's equator (Hobley et al., 2013). Over the course of a 20-day landed mission, average sublimation-driven down cutting rates reported by Spencer (1987) suggest that up to 0.5 mm of water ice could be removed or added from or near the sampling surface (note that rates would be significantly faster for more volatile substances such as CO₂).

Debris generation and mass wasting has been inferred from high-resolution Europa images (Sullivan et al., 1999), and this process could continue to produce fragmented regolith. Mass wasting and downslope motion is possible in the vicinity of the lander, particularly in response to the force of the impact on the local geology. Repeat observations would allow characterization of these and larger-scale movements such as motion of ice blocks or tectonic motion along pre-existing or newly-formed fractures at or near the landing site (Investigation 3B4).

While a full local-scale Digital Terrain Model (DTM, see **Figure 4.3.6**) of the immediate landing site would be produced to aid in selection of sample sites and precise navigation to those sites by the sampling system, repeat DTMs (i.e., computation of multiple DTMs over

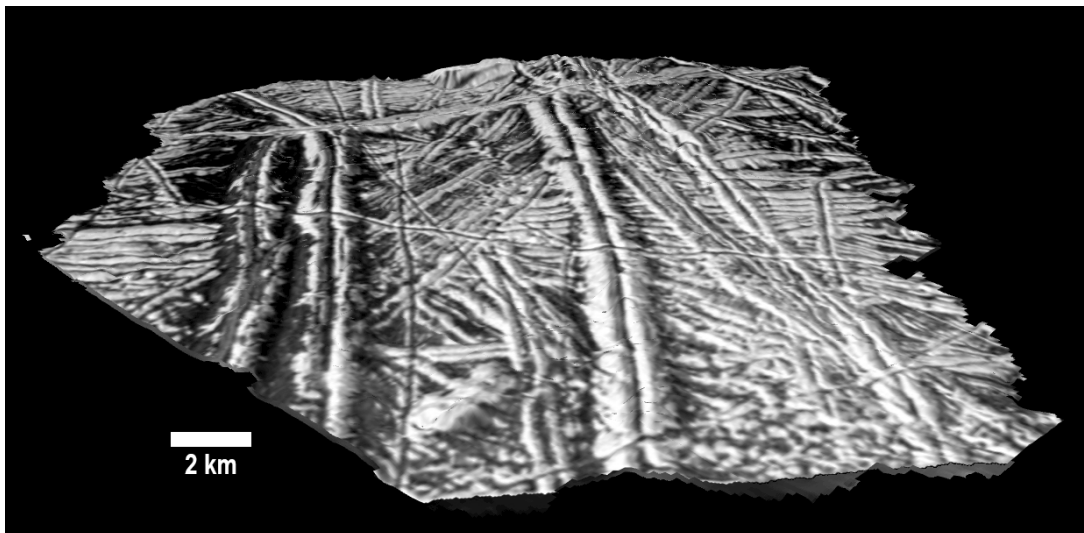


Figure 4.3.6. An example low-spatial resolution DTM of Europa generated from Galileo data. While stereo imaging opportunities with Galileo were limited, a few stereo views of the surface are possible in overlap areas. This image shows ridges near the Cilix impact crater. Ridge heights vary from 50–100 m tall, and the large ridge at the center of the image is 2 km wide. Credit: C.B. Phillips.

time of the same field of view) would allow the search for, and potential detection of, small-scale changes in the surface at the landing site. It is possible that such repeat DTMs would allow the detection of ongoing activity in the near surface, such as motion along a fault or fracture, downslope motion of surface material, or other forms of ongoing geologic activity.

Measurement Requirements & Implementation Options

The measurement requirements for Investigation 3B1 are as follows:

- **Identify changes to textural and structural attributes of surface "fines" over mission duration.**
- **Identify changes to textural and structural attributes of solid ice and mineral ice shell materials over mission duration.**

Repeated (CRS) images and other observations are required to document dynamic processes acting on the surface material in the immediate vicinity of the Europa Lander. Multiple high-resolution images, spectroscopic measurements, and other observations made with the Europa Lander's instrumentation could be compared in time sequences, using ratios and other techniques to isolate and quantify changes in color, texture, grain size, and other parameters of note.

Repeated DTMs of the landing site would allow for detection of larger-scale dynamic changes in the surface (Investigation 3B4); such DTMs could also be used to look for smaller-scale changes in the near vicinity of the lander due to mass wasting or other location motion.

Investigation 3B2: Characterize the chemical processes that affect materials on Europa (e.g., radiolysis).

Chemical processing of Europa's surface includes radiolysis, decomposition, oxidation, and other methods that modify and transform Europa's surface materials over both long and short timescales. In the case of radiation processing, the plasma in Jupiter's magnetosphere overtakes Europa in its orbit. The particles that make up the ion and electron plasma preferentially bombard the trailing hemisphere. However, there are two important exceptions: (1) approximately >24 MeV electrons, which, due to their strong gradient-curvature drift motion, have a net longitudinal motion that is opposite to Europa's and therefore preferentially bombard the leading hemisphere, and (2) energetic ions that can reach all points on the surface. As a result, models indicate that geography and landing site selection could have a significant influence on the radiation exposure that the Europa Lander spacecraft could be expected to experience. For this first mission, which is relatively short, radiation is unlikely to be a limiting factor for surface lifetime. However, for future missions that may need to operate for extended periods

(months to years), radiation exposure and total accumulated dose could severely limit spacecraft operations.

By making chemical analyses of Europa's near-subsurface, and possibly surface, materials, changes in the ice and non-ice materials could be measured, and the radiation environment assessed. As described in **Chapter 6**, for regions on Europa's surface that are within the leading and trailing hemisphere radiation 'lenses', it takes approximately 10^7 years to reach a dose of 100 eV per 16 amu down to a depth of 10 cm (Paranicas et al., 2002; Nordheim et al., 2016; 2017a; Patterson et al., 2012). While the timescales associated with radiolytic processing of silicate-rich material have been well documented, the timescales for radiation-induced albedo changes of fresh icy surfaces are not as well-known (Moore et al., 2007). If material within the lander's field-of-view is fresh, radiation darkening may be observed over the course of the landed mission. Details on radiation damage in, for instance, salts and fresh water ice, are provided in the discussions for Investigations 1D2 and 2A1.

The Europa Lander sampling system (see **Chapters 8 and 9**), which includes the excavation capability associated with the robotic arm, would be designed to expose materials to at least 10 cm depth beneath the outermost surface of Europa. Such exposures, whether in trenches or other styles of depressions, would expose materials for CRSI observations over time (i.e., before and after the excavation as part of sampling, and potentially over the longer term) to investigate potential cm-scale color changes of freshly-exposed materials (ices, fines, silicate-ice mixtures, salts, etc.).

The observation of both color changes and dynamic adjustments at fine (i.e., mm to cm) scales over time may also be tied to the physics of radiation processing of the newly exposed materials, which could affect their bulk mechanical properties. By measuring such phenomena over time, the observations of bulk materials could then be compared with results on the physical and chemical characteristics of samples made using the OCA, VS, and microscope. This integrated strategy for analyzing the sampled regions during the course of the mission would potentially add quantitative constraints on material properties, including compositional factors that extend beyond sampled materials.

Measurement Requirements & Implementation Options

Investigation 3B2 leads to the following measurement requirement:

- **Characterize changes in ice and other surface materials in the landing zone (~5 m) in response to landing and sample collection, over mission duration (e.g., color, morphology, and composition).**

The measurement requirements for this investigation closely parallel, and are a subset of, the requirements described for Investigation 1D2 and 2A1. The primary difference is that over the duration of the mission, the Baseline CRS should be used to monitor any possible radiation induced changes, such as discoloration of exposed salts or other materials. The Baseline model payload CRS would be able to measure variation in composition across the workspace and with depth via color imaging or spectroscopy. In the Threshold model payload, only color information is available for the determination of surface composition. The VS instrumentation enables detailed compositional analyses for measurement of radiation products (including O_2 , H_2O_2 , H_2CO_3 ; e.g., Carlson et al., 2013) in ices, thus providing an indication of the amount of radiation-induced chemical change. Specific compounds might also serve as indicators of maturation/diagenesis of materials in ice over time, e.g., disrupted zones in ice signifying changes in ice structure with pressure release as ices, and ice mixtures, are brought from depth to the lower-pressure surface environment (e.g., for water ice with CH_4 or NH_4 or other compounds; e.g., Sotin and Tobie, 2004). Measurements to characterize chemical indicators of ice processing would inform future landing site selection and, in the case of radiation processing, the design of robotic vehicles and sample extraction subsystems (e.g., deep drills, coring devices, etc.) that would interact with surface or subsurface materials.

Investigation 3B3: Characterize the magnitude of the thermal response at the landing site from the landing event and the lander surface operations (e.g., sampling).

Characterization of temperature changes of Europa's local surface at the landing site would help determine the thermal inertia and other physical parameters of the surface at scales not accessible from orbit. In addition, the response of the surface temperature to other operations of the lander, such as operation of the sampling system and activation of the instruments inside the lander's vault, could also be monitored by the thermal management system (provided such data is logged and stored for later transmission back to Earth). Similar surface thermal characterization has been performed on surface missions to Mars, dating back to the first Viking landers.

In addition to observing changes in temperature of the surface ice during the lander's mission, surface images from the CRSI would also be used to monitor changes in the appearance of nearby ice in the hours and days following the landing. The landing event may cause localized warming of the sub-lander ice immediately post-landing. As the surface cools to ambient temperature, changes in grain size and particle shapes are possible and may be visible in the immediate vicinity of the lander, at least in the mm-resolution CRSI images. Frost deposition on or near the lander is also possible as vaporized materials are redeposited. These, and other thermally-induced surface changes, would yield insights into surface material properties.

Measurement Requirements & Implementation Options

The measurement requirement for Investigation 3B3 is as follows:

- **Identify thermally-induced changes to the surface over mission duration. Monitor surface temperature to an accuracy of ± 5 K over mission duration.**

Surface temperature monitoring following the landing, and periodically throughout the surface mission, with an engineering thermal sensor would capture thermal information about Europa's surface. The thermal management system, one of the lander's engineering subsystems, would determine the surface temperature after touchdown, and periodically over the course of the lander's 20+ day mission. These measurements would likely be achieved with standard engineering thermal sensors such as one, or several, platinum resistance thermometers (PRTs), that are typically accurate to within 1 K.

In addition, repeated surface images taken by the CRSI could be compared for changes, some of which could be thermally-induced. As with other datasets taken specifically for change detection, repeated images should be acquired under conditions that match or complement the initial images as closely as possible in resolution, lighting, and viewing geometry.

Investigation 3B4: Characterize the three-dimensional surface dynamics of Europa and the local dynamic variability (potentially indicative of activity) at the landing site.

Likely decoupled from its solid mantle by the ocean, Europa's ice shell may be free to move and rotate (e.g. Geissler et al., 1998). It can be expected that any landing site would undergo both tidal and librational motion. The magnitude of the tidal motion would depend on the landing site location, the thickness of the ice shell (at the lander location), the depth of the ocean below the ice shell, and the proximity to water within the shell.

As one example, modeling results for Europa over the course of each 3.55-day orbit indicate that Europa is subject to tidal amplitudes ranging from 0.4 m in the mid-latitudes, to 56 m at the equator, assuming a tidal Love number (h_2) of 1.20 (Wahr et al., 2006). Over a 50 m baseline, spatial variability in tidal displacements can lead to differential surface slopes of up to 3.4×10^{-5} . Over a 1 km baseline, differential slopes can reach 6.7×10^{-4} . For comparison, these slopes are similar to gradients along flat-bedded terrestrial rivers, such as the Mississippi River (Church, 2006), and are not likely to drive mass wasting or collapse events. Even in the low gravity environment of comet 67P/Churyumov–Gerasimenko, boulders are static under the influence of local decameter-scale slopes of up to 10^{-1} in smooth terrain (Groussin et al., 2015). By comparison, the magnitude of the libration is dependent on the

thickness of the ice shell and the decoupling of the shell from the deep interior, with a half-amplitude between 0 and ~100 meters in longitude.

Considering other mechanisms for movement over diurnal timescales, fault-driven movement associated with ridge and/or band evolution could result in observable changes in the local terrain. Assuming an average strain rate of $2 \times 10^{-10} \text{ s}^{-1}$ for a thin ice shell over a hydrostatic ocean (Ojakangas and Stevenson, 1989ab) and an average spacing of 7 km between ridges on the surface (Culha et al., 2014), strike-slip motion along existing faults could be of order 0.5 m over a 3.55-day diurnal cycle.

Measuring the motion of the landed spacecraft during the nominal 20+ day lifetime of the mission could reveal activity in the ice shell, the relationship of the ice to the ocean, and its coupling to the interior, although it would not necessarily be possible to distinguish between the causes. In particular, resolving the libration of the ice shell from the amplitude of the tide would provide a constraint on how the ice shell flexes and responds to gravitational and oceanic tides. Observing any vertical displacement of the spacecraft with Europa's tidal motion, in comparison with predicted tidal motion for the site location, measurements of the ice shell thickness from the EMFM, landed sounding measurements, and ocean tidal models, could advance our understanding of the local and regional structure of the ice, and the behavior of the ocean below.

Measurement Requirements & Implementation Options

The measurement requirements to achieve Investigation 3B4 are as follows:

- **Obtain repeated stereo imaging to produce time-variable digital terrain models.**
- **Determine the time variable position of the lander over the surface mission duration by tracking the x,y,z position of the lander from the Carrier Relay Orbiter (CRO) spacecraft as well as from the CRO to Earth (e.g., via X-band at 0.1 mm per second over 10 seconds or longer) (Baseline only).**

To look for large-scale motions of the surface, repeat surface stereo imaging observations would be required. Small vertical scale topographic deflections at the landing site, and within the near-field accessible workspace, may occur at measureable scales over the mission duration. Regional deflections associated with the diurnal tidal cycle and the thickness of the ice shell may not propagate over 3.55 to 20+ day time scales, but local effects associated with proximity to liquid water or active geologic processes (faulting, plume vent activities, shallow liquid water migrations, etc.) may be detectable using methods demonstrated from landed spacecraft on Mars (e.g., Liebes and Schwartz, 1977).

Such techniques have been demonstrated recently on Mars using data from the Mars Curiosity Rover, as illustrated in **Figures 4.3.7** and **4.3.8**. DTMs could be produced from the stereo-imaging observations acquired by the Europa Lander CRSI located ~ 1 m above the local euroman surface with inter-ocular distance of ≥ 20 cm.

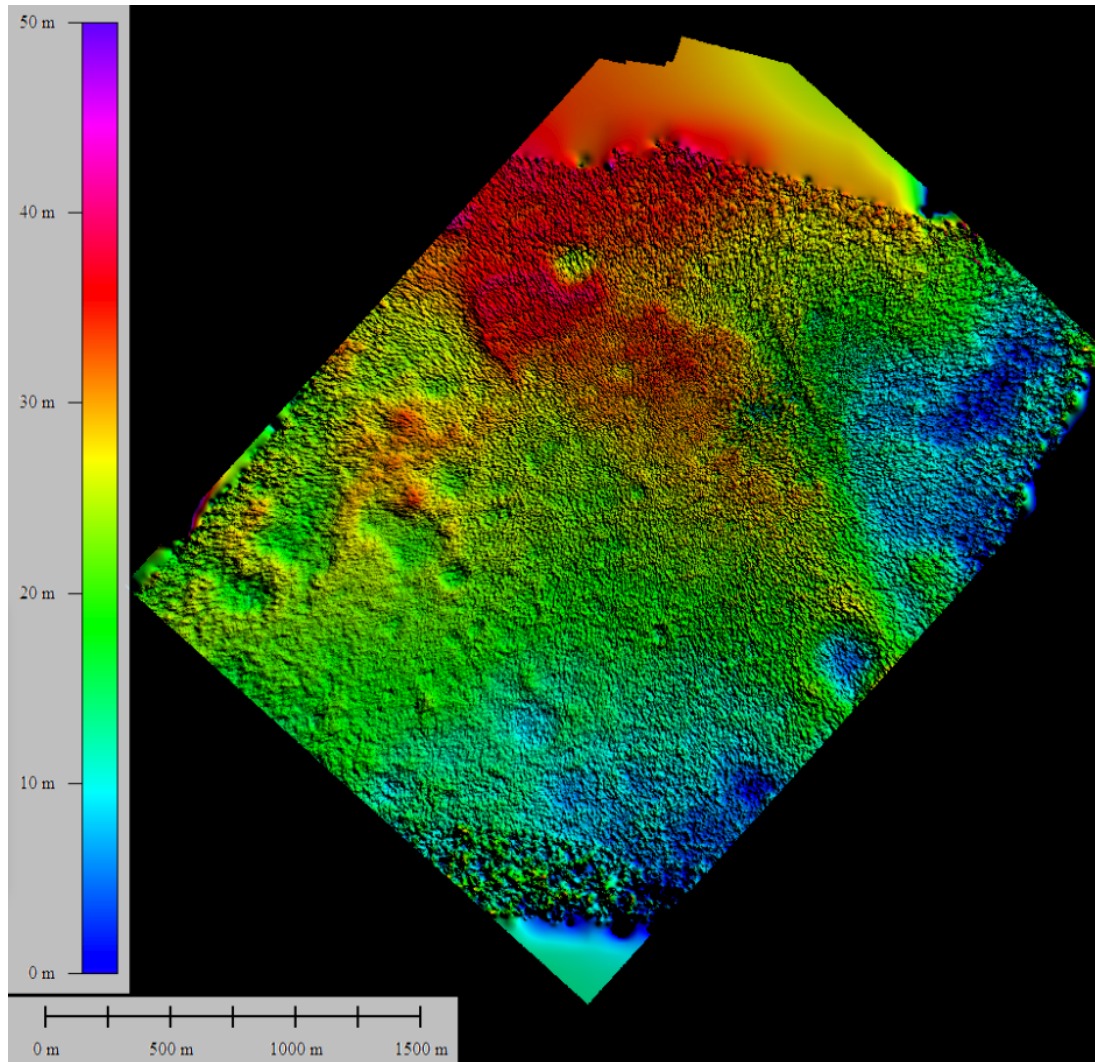


Figure 4.3.7. Digital Terrain Model (DTM) computed from terminal descent images from the MARDI instrument on the Mars Science Laboratory rover (*Curiosity*). The full DTM features a ground-scale distance of 1 m (horizontal grid scale) and offers better than 25 cm vertical resolution across a region approximately 2.5 km x 2.5 km centered on the *Curiosity* final touchdown position (“Bradbury Landing”) in Gale Crater, Mars. The MARDI descent images from ~ 2.5 km altitude down to 60 m above the local surface were used to construct this high resolution topographic map, using shape-from-motion feature matching algorithms. A DTM at finer scale than this could be constructed from terminal DDL phase descent images for the Europa Lander Mission, potentially with a horizontal grid scale as fine as 20-30 cm for the immediate touchdown position (300m x 300m). See e.g., Garvin et al. (2017ab) for more details of descent topographic imaging of planetary surfaces.

As part of Goal 3, acquisition of images to create multi-temporal DTMs for regions within the workspace (and perhaps in additional regions beyond the workspace) is recommended, if only as a secondary but independent approach for assessing the physical characteristics of the uppermost layer of the European ice shell in the vicinity of the lander. In this case, a DTM would be computed on the basis of CRSI stereo pairs (or as many multiple overlapping pairs as possible) for at least two test regions as close as possible to the lander base.

The initial post-landing CRSI imaging campaign would produce a *time 0* DTM for this purpose (for the accessible workspace). A sub-region of this workspace DTM could then be targeted for repeat DTM computation on the basis of CRSI stereo pairs on a diurnal cycle (~ 3.55 days) in order to produce a time-series of DTMs from immediately post-landing throughout the baseline 20+ day surface mission, with several discrete time-steps for cross comparison. All DTMs computed after the initial workspace survey would be co-registered to the “time 0 workspace DTM” using feature matching algorithms (Lowe, 2004), and then differential DTM measurements would be performed as a function of time. To minimize the impact of lander-induced adjustments from the initial post-landing workspace DTM (i.e., DTM-0) to all others in the time series, a higher-order polynomial surface could be removed from all DTMs in the time series so that only vertical deflections and variations due to Europa itself are observed.

On the basis of the time history of δz variations over a ~ 20 -day time period, boundary conditions for how the uppermost ice shell at the landing site is dynamically responding to regional stresses and strains could be developed. These constraints could be used in regional models of tidal responses of the ice shell. The vertical precision of the differential DTMs would be limited by viewing geometry and classical stereogrammetry methods, but is likely to be < 1 cm (ground scale distance) with ~ 2 mm vertical repeatability (Hayes et al., 2011; Garvin et al., 2017ab).

In order to derive the position of the lander and its motion over the mission duration, tracking of the lander by the CRO, as well as the CRO to Earth (X-band Doppler at 0.1 mm per second averaged over 10 seconds), should be leveraged. These observations should cover many different true anomalies to cover tidal variations. If the orbit of the CRO permits, daily observations at three geometries, of short duration, equally spaced, would provide a sufficient data set.

Equally important from a long-term perspective is the need to obtain the mean location of the lander in a body-fixed frame that could be compared with its position at some future time by a possible follow-on mission, thus providing a potential measurement of the ice shell plate motion. A combination of radio tracking of the lander, and perhaps even EMFM images, if still in operation, would be able to accomplish this measurement most effectively.

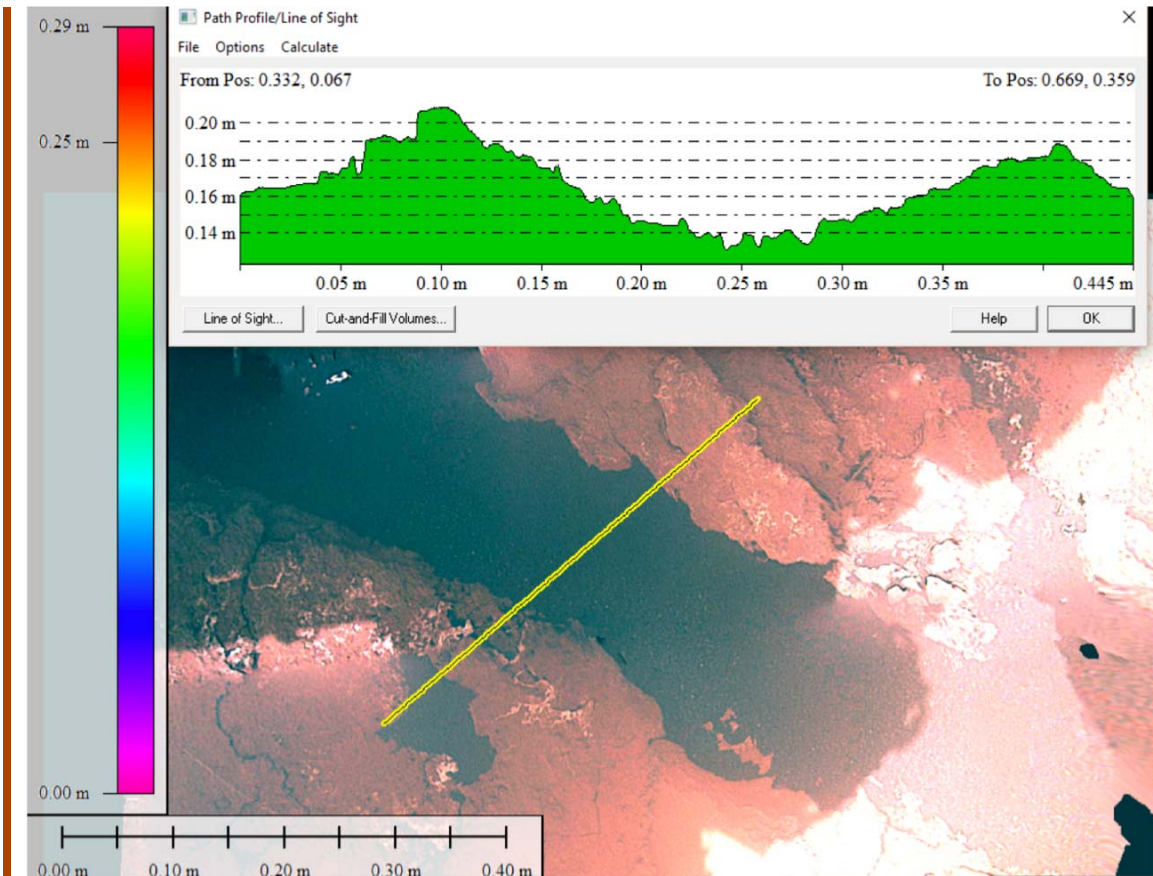


Figure 4.3.8. Topographic profile with <2 mm vertical resolution atop image of martian surface from MARDI (Sol 1512) as extracted from a 1 cm GSD DTM computed from MARDI stereo data. The Europa Lander CRSI would be able to produce DTM's at better than this quality for the near-field of the sampler-arm accessible Work Volume. Multi-temporal DTM's of better than this quality could thus allow measurement and detection of vertical and slope changes over time (Garvin et al., 2017ab).

4.4 SCIENCE TRACEABILITY MATRIX

The high-level Goals, Objectives, and Investigations of the Europa Lander mission flow into measurement objectives and a model payload, which serves as an example suite of instruments that could address the prioritized science investigations. **Table 4.4.1** is the Science Traceability Matrix (STM) that summarizes the flow from Goals to the model payload, and onto mission functional requirements (i.e., those that drive mission design and capability requirements).

4.5 MODEL PAYLOAD

Baseline and Threshold model payloads were developed on the basis of: (1) the science investigations and derived measurement requirements listed in the STM, and (2) an understanding that the available mass for science instruments on the pathfinding, first Europa Lander is highly constrained. **The total payload mass allocation, including Project-held margin, is 42.5 kg.** Each model payload element is comprised of a complement of instrument classes, from which specific instruments have been identified (**Table 4.5.1**). We note that **these model payloads are notional and exemplary only, intended to demonstrate the feasibility of a Europa Lander concept mission; more than one combination of instruments may indeed meet the measurement requirements and achieve the lander science goals while fitting within the mass, volume, power, and surface lifetime mission constraints.** The model payload also represents a highly complementary suite of instruments that address the measurement requirements of the mission in a robust, integrated approach to biosignature detection, habitability assessment, and pathfinding for future exploration. Summary tables are provided in **Table 4.5.2** (Baseline) and **Table 4.5.3** (Threshold).

Table 4.5.1. Baseline and Threshold model payloads for the lander. Elements housed within the radiation-protected vault are in white; elements outside of the vault are in orange.

Instrument Class [mass allocation, unmarginied], Total = 42.5 kg (with margin)	Model Payload	
	Baseline	Threshold
Context Remote Sensing Instrument (CRSI) [4.3 kg, includes shielding]	2 identical multi-filter, focusable, visible to near-infrared, stereo overlapping cameras with narrowband filters equivalent to those of the Europa Multiple Flyby Mission EIS cameras	2 identical RGB, fixed focus, stereo overlapping cameras
Microscope for Life Detection (MLD) [5.4 kg]	Deep UV resonance Raman and optical microscope with fluorescence spectrometer	Atomic Force Microscope (AFM) with optical context imager
Vibrational Spectrometer (VS) [5.4 kg]		Raman Laser Spectrometer (RLS)
Organic Compositional Analyzer (OCA) [16.4 kg]	Gas Chromatograph Mass Spectrometer (GC-MS) with Chirality Analysis and Stable Isotope Analyzer (SIA)	Gas Chromatograph Mass Spectrometer (GC-MS) with Chirality Analysis
Geophysical Sounding System (GSS) [1.2 kg]	Broad-band seismometer	3-axis geophone

Table 4.4.1. Europa Lander Science Traceability Matrix. Gray cells indicate capabilities not included in the Threshold mission concept. Instruments in italics are engineering sensors.

Goals	Objectives	Investigations	Measurement Requirements	Model Instrument	Mission Constraints/Reqs	
Goal 1: Search for evidence of life on Europa.	1A: Detect and characterize any organic indicators of past or present life.	1A1: Determine the abundances and patterns (i.e., population distributions) of organic compounds in the sampled material, with an emphasis on identifying potentially biogenic characteristics.	Determine the presence, identities, and relative abundances of amino acids, carboxylic acids, lipids, and other molecules of potential biological origin (biomolecules and metabolic products) at compound concentrations as low as 1 picomole in a 1 gram sample of europian surface material. Determine the broad molecular weight distribution to at least 500 Da (Threshold) and bulk structural characteristics of any organics at compound concentrations as low as 1 picomole in a 1 gram sample of europian surface material.	Organic Compositional Analyzer, Vibrational Spectrometer	Operations: Land on surface of Europa. Ability to collect samples from the surface of Europa. Ability to collect and transmit data of sample analyses to Earth, and provide for Ground-in-the-Loop science decisions on sampling strategy. Ability to determine time-variable position of lander from Carrier Relay Orbiter spacecraft.	
		1A2: Determine the types, relative abundances, and enantiomeric ratios of any amino acids in the sampled material.	Detect and identify (at 1 nM LOD) at least four of the following amino acids: Ala, Asp, Glu, His, Leu, Ser, Val, Iva, Gly, β-Ala, GABA, and AIB, with at least one from each representative class (abiotic, biotic, proteinogenic). Note that for chiral amino acids, limit of detection is 1 nM for each of the two different chiral forms. Quantify abundances of all amino acids detected relative to glycine (Gly) at an accuracy of better than or equal to 2%. Quantify enantiomeric excess (ee) of at least three proteinogenic amino acids, one abiotic amino acid, and histidine, with an accuracy of 5% or better.			
		1A3: Determine whether the carbon stable isotope distribution among organic and inorganic carbon is consistent with biological activity.	Measure the carbon stable isotope composition of multiple compounds, compound classes, or pools of carbon with a relative standard deviation of no greater than 5‰ (5 per mille) in each measurement. Note that to achieve such measurements for organic compound concentrations as low as 1 picomole per gram, the LOD would need to be 10 femtomole per gram or better to measure ¹³ C/ ¹² C in a C1 compound.	Organic Compositional Analyzer		
		1B: Identify and characterize morphological, textural, or other indicators of life.	1B1: Resolve and characterize microscale evidence for life in collected samples.	Search for cells and other microstructures in the sample that are 0.2 micron or larger in their longest dimension.		Microscope
	1B2: Resolve and characterize the landing site for any macroscale morphological evidence for life.		Identify objects as small as 1 mm within the lander workspace (~2 m), in color.	Context Remote Sensing Instrument		
	1B3: Detect structural, compositional, or functional indicators of life.		Measure structural, compositional, and/or functional properties such as biophysical or mechanical properties, native autofluorescence, or microspectroscopic signatures, associated with microscale particles in the sampled material.	Microscope, Vibrational Spectrometer		
	1C: Detect and characterize any inorganic indicators of past or present life.	1C1: Detect and characterize any potential biominerals.	Identify potential biominerals, such as SiO ₂ or carbonate filaments/structures, magnetite, and iron sulfides, at levels of a few to hundreds of parts per thousand (ppt) by mass.	Vibrational Spectrometer, Microscope	Instruments: Accommodate Organic Compositional Analyzer, Vibrational Spectrometer, Microscope, Context Remote Sensing Instrument and Geophysical Sounding System.	
	1D: Determine the provenance of sampled material.	1D1: Determine the geological context from which samples are collected.	Identify features as small as 1 mm at the sampling sites, in color.	Context Remote Sensing Instrument		
			Identify features as small as 1 mm in the lander workspace (~2 m), and as small as 1 cm in the landing zone (~5 m), in color.	Spacecraft Descent Imaging and LIDAR		
			Identify features in the landing zone (~5 m) as small as 50 cm, in color, to bridge the gap between lander and flyby resolutions.	Vibrational Spectrometer, Organic Compositional Analyzer		
	Goal 2: Assess the habitability of Europa via in situ techniques uniquely available to a lander mission.	2A: Characterize the non-ice composition of Europa's near-surface material to determine whether there are indicators of chemical disequilibria and other environmental factors essential for life.	2A1: Determine the extent to which the habitability of Europa's ocean and liquid water environments can be inferred from surface non-ice materials as sampled and imaged.	Determine the abundances of Cl-containing compounds, carbonates, sulfates, metal hydroxides, silica, and silicates, if present, at levels of a few to hundreds of ppt by mass. Determine the abundances of volatiles such as H ₂ S, CH ₄ , O ₂ , H ₂ O ₂ , SO ₂ , CO ₂ , CO, CH ₃ SH, and dimethyl sulfide (DMS), if present, at levels of a few ppt by mass.	Vibrational Spectrometer, Organic Compositional Analyzer	Sample Acquisition: Collect a minimum of 5 (Threshold 3) samples, comprised of at least 7 cubic centimeters (cc) of Europa surface material collected from 10 cm depth or more, from one or more sample sites (up to 5 for Baseline, 3 for Threshold).
			2A2: Identify patterns of spatial variability (textural, compositional) that may relate to habitability, and inform sample collection.	Determine variations in morphology of the lander workspace (~2 m) at 2 mm per pixel or better. Determine variations in composition of the landing zone (~5 m) at better than 1 decimeter per pixel (e.g., with color or spectral information). Determine variations in composition of the sampled material at better than 1 mm per pixel.	Context Remote Sensing Instrument, Vibrational Spectrometer	
2B: Determine the proximity to liquid water and recently erupted materials at the lander's location.		2B1: Search for any subsurface liquid water within 30 km of the lander, including the ocean.	Measure the thickness of the ice shell and locate any subsurface water by observing reflected body and/or surface waves from seismic events with 3-axis arrival information over a range of frequencies from 0.1-100 Hz (Threshold), or 0.1 to >100 Hz or better (Baseline).	Geophysical Sounding System		
		2B2: Search for evidence of interactions with liquid water on the surface at any scale.	Identify any surface morphologies/textures indicative of liquid water emplacement in the landing zone, including any compositional indicators of liquid water emplacement, and any thermal signatures of recent endogenic activity associated with liquid water.	Context Remote Sensing Instrument, <i>Spacecraft Descent Imaging and LIDAR, Engineering Thermal Sensor(s)</i>		
2B3: Search for evidence of active plumes and ejected materials on the surface.	Acquire multi-temporal horizon imaging (high phase angle) to search for active plume discharge or surface change, over mission duration.	Context Remote Sensing Instrument				
	2B4: Determine the depth of Europa's ocean.	Measure the depth of the ocean by observing reflected body waves from seismic events covering frequencies from 0.1 to >100 Hz with 3-axis arrival information.	Geophysical Sounding System			
Goal 3: Characterize surface and subsurface properties at the scale of the lander to support future exploration.	3A: Observe the properties of surface materials and sub-meter-scale landing hazards at the landing site, including the sampled area. Connect local properties with those seen from flyby remote sensing.	3A1: Characterize the physical properties of Europa's surface materials through interaction with the sampling and landing systems.	Measure physical and mechanical properties of surface "fines" and regolith (i.e., loose, unconsolidated or weakly indurated fine-grained surface materials). Characterize textural and structural attributes of this material at millimeter scales in the workspace, and as exposed by the sample extraction tool, and at decimeter scales in the far-field (horizon). Measure physical and mechanical properties of solid surface materials (i.e., icy-shell material). Characterize textural and structural attributes of this material at millimeter-to-meter scales in the landing zone (~5 m), and at decimeter scales in the far-field (horizon).	Context Remote Sensing Instrument, Microscope, <i>Spacecraft Descent Imaging and LIDAR, Sampling System</i>	Imaging: Provide for sufficient FOV and lighting conditions to image lander workspace and landing zone.	
			Determine the temperature of the europian surface at the landing site, to an accuracy of ±5 K.	<i>Engineering Thermal Sensor(s)</i>		
		3A2: Identify geomorphic features and their quantitative relief (topography) characteristics in the landing zone.	Determine centimeter to decimeter slope and elevation distribution of the landing zone (~5 m). Characterize centimeter- to meter-scale geomorphic features (e.g., boulders, penitentes, frost deposits, sublimation residues, small impact craters, ejecta deposits, and pits) in the landing zone (~5 m).	<i>Spacecraft Descent Imaging and LIDAR, Context Remote Sensing Instrument</i>		
		3A3: Characterize the chemical and mineralogical composition of the surface to inform future site selection.	Identify salts, radiation products, silicates, metals, and metal hydroxides, if present, at levels of a few to hundreds of ppt by mass.	Vibrational Spectrometer, Organic Compositional Analyzer		
	3B: Characterize dynamic processes of Europa's surface and ice shell over the mission duration to understand exogenous and endogenous effects on the physicochemical properties of surface material.	3A4: Characterize the internal structure of Europa including ice shell thickness and depth of the ocean.	Measure acoustic signals of reflecting body waves over the lifetime of the surface mission, covering frequencies from 0.1 to >100 Hz with 3-axis arrival information.	Geophysical Sounding System		
		3B1: Characterize the physical processes that affect materials on Europa (e.g., gardening).	Identify changes to textural and structural attributes of surface "fines" over mission duration.	Context Remote Sensing Instrument, Vibrational Spectrometer, <i>Sampling System</i>		
			Identify changes to textural and structural attributes of solid ice and mineral ice shell materials over mission duration.	Context Remote Sensing Instrument, Microscope, Vibrational Spectrometer, Organic Compositional Analyzer		
		3B2: Characterize the chemical processes that affect materials on Europa (e.g., radiolysis).	Characterize changes in ice and other surface materials in the landing zone (~5 m) in response to landing and sample collection, over mission duration (e.g., color, morphology, and composition).	Context Remote Sensing Instrument, <i>Engineering Thermal Sensor(s), Sampling System</i>		
		3B3: Characterize the magnitude of the thermal response at the landing site from the landing event and the lander surface operations (e.g., sampling).	Identify thermally-induced changes to the surface over mission duration. Monitor surface temperature to an accuracy of ±5 K over mission duration.	Context Remote Sensing Instrument		
		3B4: Characterize the three-dimensional surface dynamics of Europa and the local dynamic variability (potentially indicative of activity) at the landing site.	Obtain repeated stereo imaging to produce time-variable digital terrain models. Determine the time variable position of the lander over the surface mission duration by tracking the x,y,z position of the lander from the Carrier Relay Orbiter spacecraft (CRO) as well as from the CRO to Earth (e.g., via X-Band at 0.1 mm per s over 10 s or longer).	<i>Telecom (HGA to CRO)</i>		

Table 4.5.2: Europa Lander Baseline Model Payload. *Note that not all of the characteristics of the ‘similar instruments’ listed are relevant to the Europa Lander model instruments.

Instrument Class	Baseline Model Payload		
	Model Instrument	Characteristics	Similar Instruments*
Context Remote Sensing Instrument (CSRI)	<ul style="list-style-type: none"> Two identical multi-filter, focusable, visible to near-infrared, stereo overlapping cameras with narrowband filters equivalent to those of the EIS cameras on the EMFM 	<ul style="list-style-type: none"> Multispectral filter wheel spanning the 350–1050 nm range 34-mm fixed focal length, f/8 lenses with 21° x 15° FOV Camera heads: <ul style="list-style-type: none"> Mounted on the HGA, ≥1 m above the local european surface Spaced ≥20 cm apart with 2.5° toe-in Camera resolution: <ul style="list-style-type: none"> Minimum of 500 microns per pixel at distance of 2 m or more 	<ul style="list-style-type: none"> Mastcam-34 or -100 on MSL Mastcam-Z on Mars 2020 ChemCam on MSL SuperCam on Mars 2020
Microscope for Life Detection (MLD) + Vibrational Spectrometer (VS) <i>[combined instrumentation]</i>	<ul style="list-style-type: none"> Deep UV resonance Raman and optical microscope with fluorescence spectrometer 	<ul style="list-style-type: none"> Optical microscope (OM): <ul style="list-style-type: none"> Resolution appropriate to provide context imaging of samples FOV: 100 microns x 100 microns Co-boresighted to spectrometer Spectrometer <ul style="list-style-type: none"> Adjustable optical focus (depth of field ±12.5 mm) Rastered mapping of area co-registered with OM Raman shift: 150–3800 cm⁻¹ <ul style="list-style-type: none"> Sufficient range for minerals and organics Resolution: ~6 cm⁻¹ 	<ul style="list-style-type: none"> Context imager: <ul style="list-style-type: none"> WATSON on Mars 2020 Spectrometer: <ul style="list-style-type: none"> SHERLOC on Mars 2020 MicrOmega on the ExoMars 2020 rover
Organic Compositional Analyzer (OCA)	<ul style="list-style-type: none"> Gas Chromatograph Mass Spectrometer (GC-MS) with both chirality analysis and Stable Isotope Analyzer (SIA) 	<ul style="list-style-type: none"> Quadrupole mass spectrometer (QMS) <ul style="list-style-type: none"> Electron ionization source Mass-to-charge (m/z) range: 2–550 Da Mass resolution: Δm ≤1 Da across m/z range Abundance sensitivity: >10⁶ LOD (for organics): 1 pmol g⁻¹ Sample oven max temperature: ≥600°C Stable Isotope Analyzer (SIA): <ul style="list-style-type: none"> LOD (for C1 compound at 1 pmol g⁻¹): 10 fmol g⁻¹ 	<ul style="list-style-type: none"> QMS and GC from the Sample Analysis at Mars (SAM) suite on MSL
Geophysical Sounding System (GSS)	<ul style="list-style-type: none"> Broad-band seismometer 	<ul style="list-style-type: none"> Frequency range: 0.1 to >100 Hz 3-axis arrival information 	<ul style="list-style-type: none"> SP seismometer from SEIS on In-Sight

Table 4.5.3: Europa Lander Threshold Model Payload. *Note that not all of the characteristics of the ‘similar instruments’ listed are relevant to the Europa Lander model instruments.

Instrument Class	Threshold Model Payload		
	Model Instrument	Characteristics	Similar Instruments*
Context Remote Sensing Instrument (CSRI)	<ul style="list-style-type: none"> Two identical RGB, fixed focus, stereo overlapping cameras 	<ul style="list-style-type: none"> RGB Bayer pattern CMOS detectors 14.7-mm fixed focal length, f/12 lenses with 45° x 45° FOV Camera heads: <ul style="list-style-type: none"> Mounted on the HGA, ≥1 m above the local european surface Spaced ≥20 cm apart with 2.5° toe-in Camera resolution: <ul style="list-style-type: none"> Minimum of 500 microns per pixel at distance of 2 m or more 	<ul style="list-style-type: none"> Navcam on MSL EECAM for Mars 2020
Microscope for Life Detection (MLD)	<ul style="list-style-type: none"> Atomic Force Microscope (AFM) with optical context imager 	<ul style="list-style-type: none"> Optical context imager: <ul style="list-style-type: none"> Fixed focus with 6x magnification FOV: 2 mm x 1 mm Atomic Force Microscope <ul style="list-style-type: none"> Scan area: 65 microns x 65 microns Resolution (x, y, z): 50 nm 	<ul style="list-style-type: none"> OM-AFM of the Phoenix Mars Lander MECA system Aspects of the MIDAS-AFM on Rosetta
Vibrational Spectrometer (VS)	<ul style="list-style-type: none"> Raman Laser Spectrometer (RLS) 	<ul style="list-style-type: none"> Raman infrared point spectrometer <ul style="list-style-type: none"> Adjustable optical focus (depth of field: ±1 mm) Raman shift: 150–3800 cm⁻¹ <ul style="list-style-type: none"> Sufficient range for minerals and organics Resolution: ~6 cm⁻¹ 	<ul style="list-style-type: none"> RLS on the ESA ExoMars 2020 rover VNIR+SWIR for SuperCam on Mars 2020
Organic Compositional Analyzer (OCA)	<ul style="list-style-type: none"> Gas Chromatograph Mass Spectrometer (GC-MS) with chirality analysis 	<ul style="list-style-type: none"> Quadrupole mass spectrometer (QMS) <ul style="list-style-type: none"> Electron ionization source Mass-to-charge (m/z) range: 2–550 Da Mass resolution: Δm ≤1 Da across m/z range Abundance sensitivity: >10⁶ LOD (for organics): 1 pmol g⁻¹ Sample oven max temperature: ≥600°C 	<ul style="list-style-type: none"> QMS and GC from the Sample Analysis at Mars (SAM) suite on MSL
Geophysical Sounding System (GSS)	<ul style="list-style-type: none"> 3-axis geophone 	<ul style="list-style-type: none"> Frequency range: 0.1–100 Hz 3-axis arrival information 	<ul style="list-style-type: none"> SISMO seismometer from the OPTIMISM instrument on the Russian Mars 96 spacecraft

Due to the mass and volume envelope constraints of the Europa Lander mission, it is important to note that the Context Remote Sensing Instrument (CRSI), described in **Table 4.5.1**, was, and could be, considered as possibly providing science-supporting engineering data for the mission. This engineering data could include, but is not limited to, imaging to facilitate precise positioning and monitoring of robotic arm placement and sample extraction, and assessment of lander operational safety relative to its interfaces with the ground after landing.

The mass and volume envelope constraints of the mission also drive use of data acquired by engineering subsystems and tools to address some of the science goals and objectives described in the STM (**Table 4.4.1**). These engineering instruments, described collectively as the Lander Infrastructure Sensors for Science (LISS), are captured in **Table 4.5.4** and section 4.5.7, below.

Table 4.5.4. Lander Infrastructure Sensors for Science (LISS); owing to mass and volume envelope constraints, the following engineering instrumentation data should be downlinked, calibrated, and archived for scientific use.

Engineering Sensor	Baseline	Threshold	Science Investigations
Descent Imaging (Powered Descent Vehicle nadir descent imaging)	✓	✓	1D1, 2B2, 3A1, 3A2 (see Table 4.5.10)
Descent LIDAR (Descent hazards imaging LIDAR)	✓	✓	
Telecom (HGA to CRO) (Europa Lander HGA to Carrier Relay Orbiter)	✓	✓	3B4 (see Table 4.5.11)
Engineering Thermal Sensor System (For thermal monitoring of the lander during surface operations)	✓	✓	2B2, 3A1, 3B3 (see Table 4.5.12)
Sampling System	✓	✓	3A1, 3B1, 3B3 (see Table 4.5.13)

4.5.1 SAMPLING STRATEGY & ALLOCATIONS

During lander mission operations, a minimum of five (three for Threshold) samples of at least 7 cubic centimeters (cc) of Europa surface material would be collected from a depth of at least 10 cm. The sampling system could also collect samples from shallower depths, including at the surface (e.g., if fresh material such as a plume deposit is identified). These samples may be collected from one or more distinct sampling sites within the accessible lander workspace volume (see **Chapter 5** for more details on sampling site selection). Each 7 cc sample would be allocated as follows:

- Microscope for Life Detection (MLD) [5 cc]
- Vibrational Spectrometer (VS) [1 cc]
- Organic Compositional Analyzer (OCA) [1 cc]

Each sample would be delivered raw and unprocessed to the designated instrument. The samples would most likely contain ice, salts, silicates, meteoritic material, and/or other insoluble material in unknown proportions and of a variety of grain sizes. To maintain sample integrity, each sample would be maintained at <150 K or within 10 K of the surface temperature at the time of collection, whichever is higher, until delivery to the instrument.

Model payload instruments are described in detail below, with examples based on flight hardware provided for each case. Implementation of the payload in terms of surface operations, and accommodation of the payload on the Europa Lander mission concept, are described further in **Chapters 9 and 10**.

4.5.2 CONTEXT REMOTE SENSING INSTRUMENT

The CRSI would be used to image the landscape and spatially resolve and characterize, in three dimensions and in color, the immediate landing area to determine the optimal locations for acquisition of samples from within the arm-accessible workspace volume. The CRSI would also acquire stereo, color images that are used, together with images from the EMFM and from the Europa Lander descent imaging system and LIDAR topographic mapper, to determine the geologic context of the collected samples. As outlined in **Table 4.5.5**, the CRSI would also be used to characterize any macroscale morphological biosignatures (section 4.1.2), as well any evidence of short-term dynamical phenomena at the landing site relevant to the habitability of Europa. In particular, the CRSI would be used to search for surface morphologies and textures indicative of biogenic activity and liquid water emplacement at the local landing site at a variety of scales, from millimeters to several meters. To support the search for evidence of fresh plumes, the CRSI would acquire multi-temporal horizon imaging at high phase angle to document any active plume discharge or surface change phenomena, and would seek geomorphic evidence for local deposition from plume materials.

To support future exploration, the CRSI would characterize millimeter-to-decameter scale textural and structural attributes of the European surface, including solid surface materials and loose or weakly indurated fine material exposed at the landing site and by the sample extraction tool. Any changes in the surface over the mission duration would also be monitored by the CRSI in both two and three dimensions, as well as in color. Finally, the CRSI would execute repeat stereo imaging to produce time-variable digital terrain models (DTMs) of the landing site, to quantify any topographic variability and/or characterize observed surface changes, ideally at centimeter horizontal scales. The full list of measurement requirements, both Baseline and Threshold, pertaining to the CRSI is shown in **Table 4.5.5**.

Table 4.5.5. Baseline and Threshold requirements for the Context Remote Sensing Instrument (CRSI). Gray cells indicate capabilities not included in the Threshold mission concept.

Investigation	Measurement Requirement
1B2: Resolve and characterize the landing site for any macroscale morphological evidence for life.	Identify objects as small as 1 mm within the lander workspace (~2 m), in color.
1D1: Determine the geological context from which samples are collected.	Identify features as small as 1 mm at the sampling sites, in color. Identify features as small as 1 mm in the lander workspace (~2 m), and as small as 1 cm in the landing zone (~5 m), in color.
2A2: Identify patterns of spatial variability (textural, compositional) that may relate to habitability, and inform sample collection.	Determine variations in morphology of the lander workspace (~2 m) at 2 mm per pixel or better. Determine variations in composition of the landing zone (~5 m) at better than 1 decimeter per pixel (e.g., with color or spectral information). Determine variations in composition of the sampled material at better than 1 mm per pixel.
2B2: Search for evidence of interactions with liquid water on the surface at any scale.	Identify any surface morphologies/textures indicative of liquid water emplacement in the landing zone, including any compositional indicators of liquid water emplacement, and any thermal signatures of recent endogenic activity associated with liquid water.
2B3: Search for evidence of active plumes and ejected materials on the surface.	Acquire multi-temporal horizon imaging (high phase angle) to search for active plume discharge or surface change, over mission duration. Characterize any geologic and geomorphic evidence for local deposition from plume materials, such as arrival of new surface material, sloughing, plume ejecta, and non-ice composition.
3A1: Characterize the physical properties of Europa's surface materials through interaction with the sampling and landing systems.	Measure physical and mechanical properties of surface "fines" and regolith (i.e., loose, unconsolidated or weakly indurated fine-grained surface materials). Characterize textural and structural attributes of this material at millimeter scales in the workspace, and as exposed by the sample extraction tool, and at decameter scales in the far-field (horizon). Measure physical and mechanical properties of solid surface materials (i.e., icy-shell material). Characterize textural and structural attributes of this material at millimeter-to-meter scales in the landing zone (~5 m), and at decameter scales in the far-field (horizon).
3A2: Identify geomorphic features and their quantitative relief (topography) characteristics in the landing zone.	Determine centimeter to decimeter slope and elevation distribution of the landing zone (~5 m). Characterize centimeter- to meter-scale geomorphic features (e.g., boulders, penitentes, frost deposits, sublimation residues, small impact craters, ejecta deposits, and pits) in the landing zone (~5 m).
3B1: Characterize the physical processes that affect materials on Europa (e.g., gardening).	Identify changes to textural and structural attributes of surface "fines" over mission duration. Identify changes to textural and structural attributes of solid ice and mineral ice shell materials over mission duration.
3B2: Characterize the chemical processes that affect materials on Europa (e.g., radiolysis).	Characterize changes in ice and other surface materials in the landing zone (~5 m) in response to landing and sample collection, over mission duration (e.g., color, morphology, and composition).
3B3: Characterize the magnitude of the thermal response at the landing site from the landing event and the lander surface operations (e.g., sampling).	Identify thermally-induced changes to the surface over mission duration. Monitor surface temperature to an accuracy of ± 5 K over mission duration.
3B4: Characterize the three-dimensional surface dynamics of Europa and the local dynamic variability (potentially indicative of activity) at the landing site.	Obtain repeated stereo imaging to produce time-variable digital terrain models.

To support critical engineering requirements, the CRSI may also be used to provide science-supporting engineering data for the Europa Lander mission, such as imaging to facilitate and monitor precise placement of the robotic arm and sample extraction, and assessment of lander operational safety by imaging its interfaces with the ground after landing. Due to the limited mass and volume resource envelopes of the lander, dual science and engineering roles

for instruments such as the CRSI, as well as the engineering sensors (LISS, see section 4.5.7), are strongly recommended by the SDT to best achieve the science goals of the mission.

Baseline Instrument

The Baseline model payload CRSI would consist of two multi-filter, focusable, visible to near infrared (350–1050 nm) cameras equipped with the same filters as are being developed for the EIS imaging system on the EMFM. Use of the EIS narrowband filter set is intended to provide a relatively mass/volume envelope-efficient solution to allow comparison of the lander-based imaging datasets to those from overhead flyby coverage. Both CRSI camera optical assemblies (instrument heads) would be mounted on the HGA to provide the required azimuth and elevation pointing while minimizing instrument mass (see **Chapter 8**). The camera heads would be spaced at least 20 cm apart (inter-ocular distance) with a 2.5° toe-in to provide stereo overlap for surface DTM generation (Malin et al., 2017). Positioning on the HGA would be at least 1 m above the nominal local Europa surface (i.e., potentially using a horizontal mounting bar attached to the HGA to ensure precise field of view stereo overlap). These geometric requirements are driven by the requirements for stereo overlap in order to produce stereogrammetric point-clouds, from which the DTMs can be generated at the scales described in the STM. Specifically, detailed geologic context requires the ability to measure 5-mm relief features at ranges beyond 2 m (potentially out to 3–4 m from the edge of the lander). This necessitates camera heads spaced at least 20 cm apart with instantaneous fields of view (IFOV) of approximately 200 microradians.

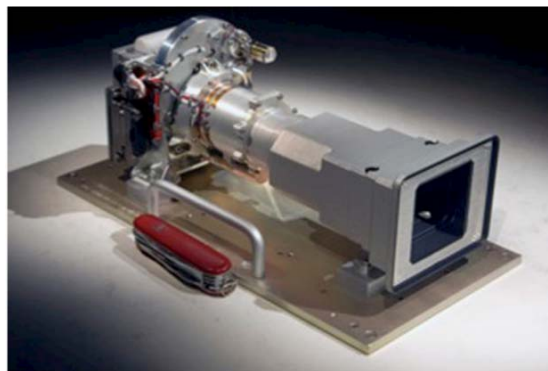


Figure 4.5.1. Example camera instrument head upon which the CRSI Baseline model payload instrument is based, the MSL Mastcam-34 (Grotzinger et al., 2012). Shown is one instrument head; the Baseline CRSI consists of two heads (in a stereo overlapping geometry) plus a calibration target and a digital electronics assembly located inside the lander vault.

Both of the Baseline CRSI model payload camera heads are functionally the same as the Mastcam-34 optical assemblies that are presently operating on Mars on the MSL Curiosity rover (Malin et al., 2017). Each of these 34-mm fixed focal length camera heads is a focusable, color, and multispectral camera. Each have f/8 lenses that illuminate a 21° × 15° field-of-view (FOV) using a 1600 wide by 1200 high charge coupled device (CCD) detector. Both of the camera heads use an RGB Bayer pattern color filter array with microlenses integrated with the detector and allow for imaging the surface of Europa via the RGB detector through a broadband filter or via one of 6 narrowband filters, arranged on a filter wheel, in the 350–1050 nm range, matching those on the JPL EMFM EIS camera passbands (Turtle et al., 2016).

This example of a CRSI imaging system meets the Baseline measurement goals outlined in the STM (and in **Table 4.5.5**) for spatial resolution, stereo-ranging precision (for DTM generation), and has an adequate FOV so that a 360° panorama could be acquired in a reasonable number of steps (and mosaicked) using rotation of the HGA/camera mount assembly on the Europa Lander. It would produce 0.44 mm (440 microns) per pixel resolution color images throughout the accessible workspace volume and the stereo imaging would permit a workspace volume DTM with <1 mm vertical precision under most landing geometry circumstances.

While other implementations that achieve this level of flight performance or better are clearly possible, this existence proof offers an already flight-tested version that meets all of the imaging-affiliated measurement goals with well-known resource allocations (mass, power, data-rate, etc.). As one example, the MSL Mastcam-34 1600 × 1200 CCD detector could be replaced with the 2048 × 2048 complementary metal oxide semiconductor (CMOS) detector that would be flown on the Mars 2020 Rover (EECAM/Navcams), which would improve the overall performance in spatial resolution and ranging precision by more than 10%. Such an implementation on the Europa Lander CRSI system may include slightly smaller pitch pixels for improved radiation tolerance*. Other implementation approaches could include imagers with detectors sensitive to longer wavelengths, combinations of imagers with point spectrometers (e.g., Wiens et al., 2016; Cook et al., 2016) or imaging spectrometers (e.g., Pilorget and Bibring, 2014).

The driving requirement for the Baseline CRSI model payload system is to identify objects as small as 1 mm (1000 microns) within ~2 meters of the lander in the robotic arm accessible sample workspace volume (2.2 m would be the maximum possible radial extension of the arm, see **Chapter 8**). This requirement drives a camera to be able to acquire images with a minimum resolution of 500 microns per pixel (in the cross-boresight direction) at a distance of approximately 2 m. The MSL Mastcam-34 optics provide an IFOV of 218 microradians, which yields an effective pixel scale of 0.44 mm at 2 m distance, and 22 cm at 1 km (horizon). This scale (440 microns) is finer than the required 500 microns per pixel described above. Replacement of the MSL Mastcam-34 optics with the M-100 (100 mm focal length) system would improve this spatial resolving power by a factor of three to 150 microns per pixel at 2 m and 300 microns per pixel at 4 m slant range, but at the expense of the projected angular field of view (FOV). Given SDT discussions about the tradeoffs between CRSI (camera) FOV and resolution associated with the required imaging of the workspace volume, the Mastcam-34 system is a useful representative example for the model payload.

An MSL Mastcam approach for the CRSI imaging system on the Europa Lander presents another option, in which one of the two camera heads would serve as a wider FOV but

*Radiation tolerance in CMOS detectors depends on pixel pitch. A smaller pitch reduces the distance that signal electrons have to travel by thermal diffusion, decreasing the chances of signal loss due to charge recombination.

moderate resolution system (i.e., Mastcam-34), while the other would offer a much more extreme telephoto capability, similar to the Remote Micro-Imager (RMI) that is part of the MSL ChemCam system (Maurice et al., 2012). An RMI-like second camera head on the HGA with the Mastcam-34-class primary camera could provide a factor of ten increased spatial resolution at the expense of the camera's angular FOV. This approach would produce better than 50 microns per pixel resolution imaging at the edge of the accessible workspace volume, allowing features as small as 100 microns to be resolved. However, in this configuration, the stereo imaging for DTM generation would require lander HGA azimuthal rotation and collection of more frames to achieve a given region of coverage. Other variations of this 'multi-head' approach are also possible, including improved spectral coverage associated with one of the camera heads to extend the compositional capability of the CRSI system.

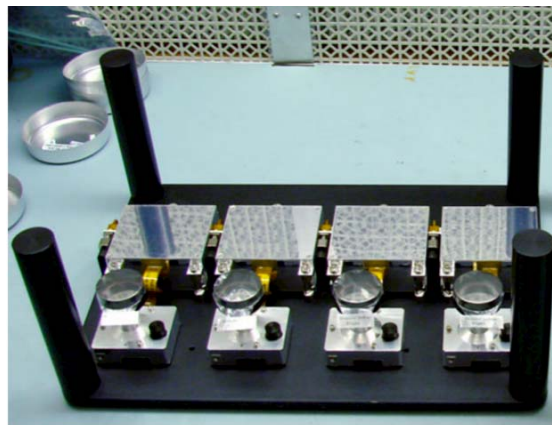


Figure 4.5.2. Example of the CRSI Threshold model payload instrument, the MSL Curiosity rover NavCams (Maki et al., 2012). The Europa Lander would use only two of the 4 cameras shown here.

Threshold Instrument

The Threshold model payload CRSI system must address all of the “science floor” measurements outlined in the STM (and **Table 4.5.5**), especially those associated with spatial resolution and with the ability to produce quantitative DTMs for multiple purposes, including both science (STM) and possibly engineering support (of the landed surface sampler system operations and precise arm positioning). The Threshold model payload CRSI would consist of two identical RGB (red, green, blue) Bayer pattern microfiltered fixed focus CMOS detector cameras. A reasonable point of reference for this instrument is a color version of the Navcam instruments of the MSL Curiosity rover currently operating on Mars (Maki et al., 2012). Enhanced navigation cameras in development at JPL for flight on the Mars 2020 caching rover (EECAMs; Maki et al., 2016) are an improvement and could also be considered, by virtue of their wider angular FOV, improved pixel pitch, and factor of two finer spatial resolution (350 microradians with 6.4 micron pixels and 0.7 mm per pixel at 2 m slant range).

The Threshold CRSI system is similar to the MSL Navcams with one exception – the Threshold CRSI would include a color Bayer pattern filter with each camera head to permit limited (RGB) color assessment at mm to cm scales of the accessible workspace volume. The Threshold CRSI cameras would be two identical fixed focal length (14.7 mm) f/12 optical systems, each with $45^\circ \times 45^\circ$ fields of view that would be mounted at least 20 cm apart on the

lander HGA (and at least 1 m above the local surface). Each of the camera heads would employ 2048×2048 CMOS detectors with a pixel scale of 0.400 milliradians per pixel.

While similar to the MSL Navcams in their architecture, the optics would need to be tailored to meet the requirements of the Europa Lander. The driving requirement for the Threshold CRSI cameras is to identify features as small as 1 mm (1000 microns) in the near-field, and as small as 1 cm in the far-field of the sample workspace volume. This requirement drives a camera to be able to acquire images with a minimum resolution of 500 microns per pixel (in the cross-boresight direction) at a distance of ~ 2 m. Each of these stereo-overlapping camera optical heads of the color MSL Navcams would provide a 1.6 mm per pixel resolution from a distance of 2 m, and 89 cm per pixel at 1 km (“horizon”); slightly modified versions with 2048×2048 CMOS detectors would deliver 0.8 mm per pixel resolution at a slant range distance of 2.2 m. The DTM quality from this Threshold instrument implementation is limited by ranging errors that would likely be ~ 0.2 cm at a 2 m slant range, but 0.1 cm in the nearfield of the accessible workspace volume. This 2048×2048 CMOS version of the dual-headed camera would also improve the spatial resolution by a factor of two, consistent with STM measurement goals. It should be further noted that the Mars 2020 EECAMS, now under flight development at JPL (Maki et al., 2016), would enable wider FOV imaging at spatial resolutions a factor of two finer than this Threshold CRSI system, and with more than two times the angular FOV coverage per frame. Once validated for flight (target - April 2017), this system would offer operational benefits by virtue of its finer resolution and wider FOV, presenting another option for consideration as a Threshold CRSI system. Finally, the pan-zoom approach now under development for the Mars 2020 Rover (Mastcam-Z) offers yet another possibility, with greater operational flexibility for stereo-coverage and/or fine-scale resolution (Bell et al., 2016).

Instrument Operations

The CRSI could be a dual-use instrument, supporting both Europa Lander science goals and engineering tasks. Engineering support could include imaging of sample extraction and delivery, inspection of sampling system hardware, and examination of the lander/european surface interfaces (e.g., to confirm lander stability). These engineering tasks would be performed on an as-needed basis as defined by the Europa Lander project engineering team. The operation of the CRSI system to meet the Europa Lander science goals and investigations is described below.

The concept of operations for the model payload CRSI system involves imaging phases designed to meet key science objectives and their required operations of the Europa Lander mission. These phases are as follows: landscape reconnaissance, sampling operations, spatio-temporal monitoring, and targets of opportunity. Each imaging phase would generate multiple data products in order of science and operations priority, as detailed below.

Landscape Reconnaissance:

- 1) Horizon-scanned near-360° panorama of the landing site, acquired as soon as possible after landing with a single CSRI instrument head to establish the lander location (relative to descent and EMFM images of the landing site) and context (for operations). This panorama should have sufficient resolution to identify key features within the workspace. If feasible within the lander concept of operations, this could be acquired in stereo to allow a time-zero DTM to be generated at whatever spatial sampling is possible with covering the full 360 degrees of azimuth around the landing zone.
- 2) Medium resolution imaging of the entire accessible workspace volume, with all color filters and using both cameras for complete stereo overlap, to allow the science team to begin sampling site selection on the basis of engineering-quality ranging and digital topography. A DTM with ≤ 1 cm per pixel local vertical precision would also be generated from these images with anticipated ground scale distance sampling of 1 cm or better. While not a requirement, this would allow engineering assessment of the surface sampling system operational safety and optimization in the event of challenging local terrain conditions.
- 3) Horizon-scanned 360° panorama with the second camera head, to generate a DTM of the entire landing site region, beyond the scale of the workspace volume. Spatial resolution and associated DTM spatial/vertical resolution should be the same as the time-zero panorama or better.
- 4) Highest resolution (≤ 500 microns per pixel in the workspace volume) imaging of candidate sampling sites identified by the Science Team within the accessible workspace volume in stereo (to enable refined local-area DTMs to be computed to document the sampling sites before and after (Goal 3, **Chapter 4**)).

Information sufficient to recognize compositional heterogeneities in the work volume should be acquired, in particular for (but not limited to) data products 2 and 4 above. Decimeter-scale and smaller properties of the surface will not be known prior to the EMFM; remote-sensing observations and the lander CRSI would sample at sub-pixel scale (of EIS flyby imaging). Understanding heterogeneities, if present, would be important for optimizing the locations of the multiple samples. CRSI color mosaics coupled with chemical measurements from the OCA and VS of sampled materials is the minimal means (Threshold) by which to discriminate heterogeneities in sample provenance, on the basis of analyses of the first sample.

Sampling Operations:

- 1) Image of each sampling site at highest resolution, in color, prior to sample collection in stereo with both camera optical heads (for 3-D context).
- 2) Close-up images of each site during excavation (sampling) is recommended. These images, collected periodically, could be used to generate an animation with stereo overlap, ideally involving multiple frames so that Shape from Motion (SfM) methods can be used to make specialized DTMs. These images would allow determination of the efficiency of excavation, observation of the material being moved outside of the trench (particle size, color, texture, stratigraphic relations, etc.), monitoring of the behavior of the material being moved (clumping), and determination of where the tailings are deposited (i.e., all as quantitatively as possible to constrain engineering boundary conditions).
- 3) Highest resolution images, in color, are desired of material inside the sample collection device on the arm (i.e., with the highest spatial resolution possible). The robotic arm may need to present the sample to the CRSI system in some fashion not yet fully determined by the Europa Lander project engineering team.
- 4) Images are desired of the sampling site at highest resolution after sample collection in stereo to enable computation of a post-sampling DTM. Note that if the bottom of the sampling site is not visible due to viewing geometry, the addition of a mirror (or mirrored surface) onto the arm could be explored by the Lander Project engineering team.

Spatio-Temporal Monitoring:

- 1) Full resolution near-360° panorama with both cameras (to generate DTMs from stereo overlapping images), performed episodically during and at the end of the mission, to search for any local relief changes in the landing site over the mission duration. As per Goal 3, it would be advantageous to conduct accessible workspace volume stereo imaging surveys every 3.5 days or diurnally, from which a time series of DTMs (at least 5 during the nominal surface mission) could be generated and analyzed in comparison with the time-zero DTM (just after landing). An instantaneous field of view (IFOV) of >70 microradians would permit identification of 0.5 m relief changes (assuming a 2-pixel wide point spread function) along faults located up to 3.5 km away from the lander (half of the average 7-km distance between ridges). A similar IFOV in each camera would permit vertical precisions of 0.2 mm in the near edge of the work volume and ~3 mm at the far edge.

- 2) Multi-temporal horizon imaging at high phase angle to search for active plume discharge. This also includes changes in color, albedo, or morphology of the field site, from lander surfaces to workspace to horizon, to seek any changes related to deposition of new plume material over mission duration. Horizon images should be obtained using the shortest wavelength filter (~0.35 micron filters in the near UV) during times that have been identified as favorable for plume activity (and using the EMFM datasets as a guide). These should be repeated as often as possible over the mission duration.

Targets of Opportunity:

- a) Images of trench post-excavation but before sample collection. The interior of the trench might be in shadow or obstructed from view of the CRSI system, which is why this type of image is not a requirement for the mission.
- b) During sampling phase, image delivery of sample to instruments, when observable, and potentially in stereo so that a range map can be computed.

Resource Estimates

To achieve payload point designs for use in the Europa Lander mission concept, existing instruments with flight heritage were used to construct Baseline and Threshold model payload resource allocations. These model payloads are notional, and utilized here only to provide estimates to define mission parameters such as payload mass/volume/power, surface operations timeline, and overall mission lifetime requirements.

The payload mass allocation for the CRSI system on the Europa Lander is 4.3 kg (including 2 camera heads, harness, electronics, and radiation shielding). Note that the CRSI is the **only model payload instrument outside of the lander vault**, and therefore, radiation shielding is included in this payload mass allocation.

Given that multispectral, stereo images typically comprise the majority of the science data return for landed missions in terms of data volume, the CRSI system would make use of as much data volume as can be provided by the Europa Lander downlink capability. On the basis of the Baseline CRSI model payload above (with the EIS filter positions) and the concept of operations described, gigabits of lossless compressed image data could be generated during the 20-day surface mission. It might be possible to reduce downlink data volume via onboard (lander or CRSI compute element) data product generation, such as production of DTMs.

4.5.3 MICROSCOPE FOR LIFE DETECTION

The model payload Microscope for Life Detection (MLD) is tasked with the search for cells, biogenic microstructures, and other biosignatures (Goal 1) over the mission duration. The Threshold instrument retains the search for cells and microstructures. To address habitability (Goal 2), the MLD would investigate textural patterns of spatial variability in the delivered sample. The MLD instrument would also characterize textural and structural properties of the sample to support the assessment of Europa surface material physical properties as outlined in Goal 3. Characterization of changes in ice and other surface materials in response to landing and sample collection would also be performed to search for chemical processes affecting materials on Europa.

The requirements for both the Baseline and Threshold MLD are given in **Table 4.5.6**. Microscopes can utilize optical, electron, or scanning probe technologies, depending on the resolution required for various science investigations. As described below, the Baseline and Threshold model instruments for MLD take advantage of multiple microscope architectures.

Baseline Instrument

The Baseline model payload MLD instrument is a system capable of coordinated (co-located, or simultaneous) microscopic imaging and spatially-resolved detection of chemical (spectroscopic) signatures at the single cell level. Spatially-resolved spectroscopic data could provide information on elemental and/or molecular composition on the same objects that a microscope observes (e.g., Harz et al., 2008), enhancing the ability to discriminate between abiotic and potentially biogenic features. Such an instrument would allow for spatially-resolved mapping of organic-mineral, mineral-mineral, and mineral-organic-ice associations as described in **Chapter 4**, while still meeting the requirements for the MLD (**Table 4.5.6**) and VS (**Table 4.5.7**) instruments.

Various combinations of microscope technology (Optical Microscopy, Fluorescence Microscopy, AFM or combinations therein, e.g., Aghayee et al., 2013) and spectroscopy (IR or Raman) have been built and integrated (e.g., AFM-Raman microscopy; Tang et al., 2013). Two microscope-IR spectrometers, Rosetta Philae CIVA-M/V (Bibring et al., 2007ab) and Phobos-Grunt Videospectrometer (Korbalev et al., 2010) were built, flight qualified, and flown on spaceflight missions, though they never operated due to other challenges to those missions. The optical microscope component of those systems provided resolutions down to approximately 4 to 7 microns, which is larger than the 0.2 μm capability required by the Europa Lander. However, both AFM (see description below) and a Deep UV (DUV) fluorescence microscope (range <250 nm; Bhartia et al., 2010) meet detection requirements (see Investigation 1B1) and could, in part, characterize SCF properties (see Investigation 1B3). The integration of DUV fluorescence (optical) microscopy to detect native fluorescence of aromatics with

Table 4.5.6. Baseline and Threshold requirements for the Microscope for Life Detection (MLD). Gray cells indicate capabilities not included in the Threshold mission concept.

Investigation	Measurement Requirement
1B1: Resolve and characterize microscale evidence for life in collected samples.	Search for cells and other microstructures in the sample that are 0.2 micron or larger in their longest dimension.
1B3: Detect structural, compositional, or functional indicators of life.	Measure structural, compositional, and/or functional properties such as biophysical or mechanical properties, native autofluorescence, or microspectroscopic signatures, associated with microscale particles in the sampled material.
3A1: Characterize the physical properties of Europa's surface materials through interaction with the sampling and landing systems.	Measure physical and mechanical properties of surface "fines" and regolith (i.e., loose, unconsolidated or weakly indurated fine-grained surface materials). Characterize textural and structural attributes of this material at millimeter scales in the workspace, and as exposed by the sample extraction tool. Measure physical and mechanical properties of solid surface materials (i.e., icy-shell material). Characterize textural and structural attributes of this material at millimeter-to-meter scales in the landing zone (~5 m).
3B2: Characterize the chemical processes that affect materials on Europa (e.g., radiolysis).	Characterize changes in ice and other surface materials in the landing zone (~5 m) in response to landing and sample collection, over mission duration (e.g., color, morphology, and composition).

DUV-Resonance Raman spectroscopy (see details in the Baseline Vibrational Spectrometer section below) would be a sensitive technology combination. In addition to the 0.2 micron resolution requirement, the MLD must be capable of detecting dilute particles (e.g., potential cells) at 100 per cc of sample on a 1 mm diameter surface.

For the purposes of mass, power, and volume allocation, estimates for the Baseline instrument were referenced to the SHERLOC instrument selected for the Mars 2020 mission (Beagle et al., 2015).

Threshold Instrument

A model payload microscope capable of detecting microscopic lifeforms (and even those that potentially contribute to macroscale morphology, if present) is a combined instrument system that incorporates both an atomic force microscope (AFM) and an optical microscope for wider-scale context imaging. Primary aspects of this combined technology that make it potentially well-suited as a conceptual Threshold instrument system are:

- a) An AFM could be used to characterize collected particles by size, shape, and texture. This includes structural and functional properties of microbial cell surfaces.
- b) A combined platform with an AFM and an optical context microscope could image the same sample across several orders of magnitude, from tens of microns to nanometer resolution.

The microscope component of the Microscopy, Electrochemistry, and Conductivity Analyzer (MECA) system of the Phoenix Mars Lander is used as an example of the model payload instrument (Hecht et al., 2008). Some specifications from the MIDAS-AFM (Riedler

et al., 2007) that flew on the ESA Rosetta Mission were also used as reference points for the model payload.

The MECA microscope system of the Phoenix Mars Lander (**Figure 4.5.3**) includes a fixed-focus 6× optical microscope (OM), a sample stage, and an AFM. The sample stage is capable of rotation (15-micron step) and translation (0.25-micron step). AFM is fundamentally different than optical and electron microscopy in that the surface relief of samples are physically probed to generate x, y, and z coordinates at scanned positions, allowing three-dimensional images to be constructed from the data (but only after sample preparation). This is accomplished at the sub-micron scale by a cantilever with a sharp tip, which responds to forces between the tip and specimen as it probes surfaces and supplies information on the sample position as well as textures. Slight deflections of the cantilever due to interactions between the tip and specimen can be measured precisely (e.g., 50 nm resolution for the MECA AFM and 0.16 nm for MIDAS), providing a height measurement for each x-y coordinate interrogated and precise measurement of particle/cell length, area, and abundance.

While there are distinct advantages in using AFM to determine the size and three-dimensional structure of putative european microbes in the samples, shortcomings of this approach include the limited scan field of regard (up to 65 μm for the MECA AFM and ~100 μm for MIDAS) and relatively long acquisition times required to obtain each scan. The time per scan for the MECA AFM was 25 minutes, or 2 hours for 4 images per substrate (the Phoenix sampling system used a number of substrates to examine dust/soil samples collected). The MECA microscope platform also included an optical microscope (OM) to image a larger field of view initially to identify zones of interest within the sample for AFM scanning. The OM resolution was ~8 μm on MECA (Hecht et al., 2008), which was optimized to image particles smaller than 0.1 mm on a substrate that was 3.0 mm in diameter. Images of this substrate were captured with a 512 × 256 CCD. The OM would enable rapid scanning of large areas of view, detection of larger particles, and identification of regions of interest for detailed imaging via AFM. It should be noted that the systems of Phoenix were designed and tested in the 2002–2006 timeframe for their 2007 launch to Mars. Many of these Phoenix-era OM-AFM limitations could be improved for a Threshold microscope on the Europa Lander.

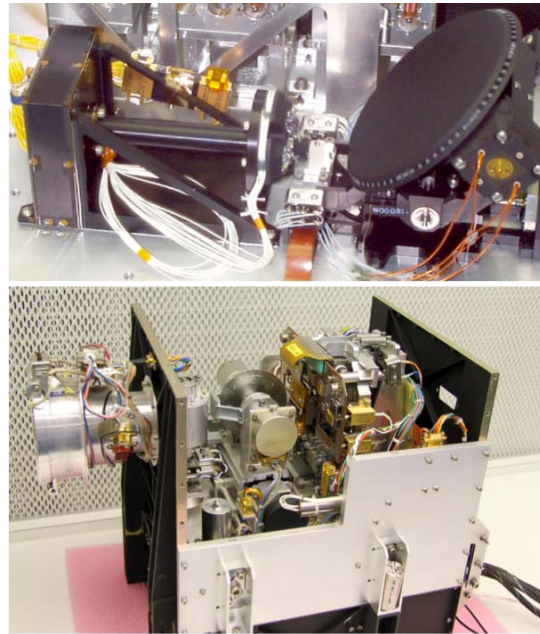


Figure 4.5.3. Examples of the MLD Threshold model payload instrument. **Top:** The Mars Phoenix Lander MECA optical microscope (OM) and atomic force microscope (AFM). **Bottom:** The MIDAS-AFM of the ESA Rosetta Mission.

There are several considerations that would need to be optimized for Europa samples. The nature of the sample, associated analysis conditions, and goal to search for signs of life (Goal 1), all differ from previous missions sampling Mars soils or comet-derived dust. The following details therefore focus not on the specifics employed on previous missions, but rather on the suite of parameters that would require optimization when searching for signs of life in low abundance (i.e. $100 \text{ cells mL}^{-1}$). Such parameters may include the AFM tip exchange system, topography sensing modes for particle characterization (static and dynamic), procedures for adhering sample to substrate for scanning, and vibration sensitivity, among others. For further details of the MECA AFM design, see Gautsch (2002) and Hecht et al. (2008).

Sample Handling and Analysis

For microscopic analysis, ice samples would need to be melted and potentially concentrated on a substrate, requiring a temperature/pressure controlled manifold. As described in **Chapter 4**, concentration of 5 cc of sampled material onto a 1-mm diameter filter would bring multiple cells into an imaging field of view, even if these cells were present at Lake Vostok (low biomass) concentrations (**Figure 4.1.12**). For filter concentration, the collected sample may need to be sealed within a container to a pressure of 6.1 mbar (vapor pressure of water at 273 K), melted, and kept liquid for the remainder of the analysis. The analytical time required for 1 sample is estimated at ~ 25 minutes, or ~ 2 hours if four images are generated per sample (Gautsch, 2002).

Resource Estimates

The payload mass allocation for the Threshold MLD on the Europa Lander is 5.4 kg (including sample handling and electronics). Size, power and data estimates for the Threshold model instrument are based on those for Phoenix's MECA OM-AFM (Gautsch, 2002). In the case of Phoenix, the total mass was 2.1 kg (not including electronics, which were shared). The optical microscope volume was 783 cm^3 . The peak power was 18.3 W, and the average 7.4 W, with an electronic circuit max power consumption of 3.3 W. Assuming 256×256 pixel images, 4 images per area and 2 images per substrate (nominal), MECA OM-AFM had a data volume of 8.4 Mbits per scanned area (uncompressed), and a total of 18.9 Mbits for a set of 9 substrates (with jpeg2000 compression). Assuming 512×512 pixel images, 4 images per area and 4 images per substrate (maximum), the data volume per area was 134.2 Mbits (uncompressed) with a total of 302 Mbits for set of 9 substrates (with jpeg2000 compression). Based on flight-ready CCDs using CMOS and other technologies, it would be possible to increase the image size to 1024×1024 or $2 \text{ K} \times 2 \text{ K}$ for the Europa Lander MLD payload element.

4.5.4 VIBRATIONAL SPECTROMETER

The model payload Vibrational Spectrometer (VS) instrument is tasked with the quantitative sensing of chemical bonds that indicate the nature of the ices, organics, salts, silicates, and other minerals present on the surface of Europa, as described in **Chapter 4**. The model payload VS instrument is sensitive to chemical structure rather than bulk chemistry. Either infrared (IR) or Raman spectrometers can fit this measurement requirement with the precise

Table 4.5.7. Baseline and Threshold requirements for the Vibrational Spectrometer (VS). Gray cells indicate capabilities not included in the Threshold mission concept.

Investigation	Measurement Requirement
1A1: Determine the abundances and patterns (i.e., population distributions) of organic compounds in the sampled material, with an emphasis on identifying potentially biogenic characteristics.	Determine the presence, identities, and relative abundances of amino acids, carboxylic acids, lipids, and other molecules of potential biological origin (biomolecules and metabolic products) at compound concentrations as low as 1 picomole in a 1 gram sample of european surface material. Determine the broad molecular weight distribution to at least 500 Da (Threshold) and bulk structural characteristics of any organics at compound concentrations as low as 1 picomole in a 1 gram sample of european surface material.
1A2: Determine the types, relative abundances, and enantiomeric ratios of any amino acids in the sampled material.	Detect and identify (at 1 nM LOD) at least four of the following amino acids: Ala, Asp, Glu, His, Leu, Ser, Val, Iva, Gly, β -Ala, GABA, and AIB, with at least one from each representative class (abiotic, biotic, proteinogenic). Note that for chiral amino acids, limit of detection is 1 nM for each of the two different chiral forms. Quantify abundances of all amino acids detected relative to glycine (Gly) at an accuracy of better than or equal to 2%.
1B3: Detect structural, compositional, or functional indicators of life.	Measure structural, compositional, and/or functional properties such as biophysical or mechanical properties, native autofluorescence, or microspectroscopic signatures, associated with microscale particles in the sampled material.
1C1: Detect and characterize any potential biominerals.	Identify potential biominerals, such as SiO_2 or carbonate filaments/structures, magnetite, and iron sulfides, at levels of a few to hundreds of parts per thousand (ppt) by mass.
1D2: Characterize the chemistry of the near-subsurface to determine the endogenous versus exogenous origin of the sample, and any surface processing of potential biosignatures.	Identify salts, radiation products (e.g., H_2O_2 , CO_2 , O_2 , SO_2 , S_n), silicates (anhydrous and hydrous), metals, and metal hydroxides, if present, at levels of a few to hundreds of ppt by mass.
2A1: Determine the extent to which the habitability of Europa's ocean and liquid water environments can be inferred from surface non-ice materials as sampled and imaged.	Determine the abundances of Cl-containing compounds, carbonates, sulfates, metal hydroxides, silica, and silicates, if present, at levels of a few to hundreds of ppt by mass.
2A2: Identify patterns of spatial variability (textural, compositional) that may relate to habitability, and inform sample collection.	Determine variations in composition of the sampled material at better than 1 mm per pixel.
3A3: Characterize the chemical and mineralogical composition of the surface to inform future site selection.	Identify salts, radiation products, silicates, metals, and metal hydroxides, if present, at levels of a few to hundreds of ppt by mass.
3B1: Characterize the physical processes that affect materials on Europa (e.g., gardening).	Identify changes to textural and structural attributes of surface "fines" over mission duration. Identify changes to textural and structural attributes of solid ice and mineral ice shell materials over mission duration.
3B2: Characterize the chemical processes that affect materials on Europa (e.g., radiolysis).	Characterize changes in ice and other surface materials in the landing zone (~5 m) in response to landing and sample collection, over mission duration (e.g., color, morphology, and composition).

technical specifications required to achieve the desired science measurements. In this payload implementation, the model spectrometer instrument is housed in the Europa lander vault for inspection of the sampled materials. The Threshold model payload instrument is a point spectrometer, nominally the Raman Laser Spectrometer (RLS) on the ExoMars 2020 rover (Edwards et al., 2012; Hutchinson et al., 2016). The Baseline model payload instrument is a 2-D imaging or rastering spectrometer, nominally SHERLOC on the Mars 2020 rover. As noted in the previous section, for the Baseline implementation the MLD and VS instruments could be combined in an instrument suite on a single platform to meet the science requirements (**Table 4.5.7**).

Baseline Instrument

The Baseline VS model payload instrument is referenced to the Scanning Habitable Environments with Raman & Luminescence for Organics & Chemicals (SHERLOC) instrument (**Figure 4.5.4**), competitively-selected for the Mars 2020 Rover. SHERLOC is a robotic arm-mounted, Deep UV (DUV) resonance fluorescence and Raman spectrometer utilizing a 248.6 nm DUV laser, integrated with an autofocusing/rastering optical system, and co-boresighted to a context imager (Beegle et al., 2015). The Mars 2020 SHERLOC combines two spectral phenomena: native fluorescence and DUV Raman scattering. In fluorescence, the incident photon is absorbed and re-emitted at a longer wavelength. SHERLOC makes measurements with a resolution of <1 nm over the 270–360 nm region, where spectral features indicative of fluorescent aromatic organic molecules occur. Raman shifts of 1000–3500 cm^{-1} from inelastic scattering are also measured with the same CCD over the fluorescence-free region of 250–270 nm to identify organics and select minerals. SHERLOC is being designed to detect and map organics and specific minerals over a 7×7 mm area with a fine-scale spatial resolution of 50 microns per laser spot, paired with a 30 micron per pixel context imager (similar to parts of the MSL Mars hand lens imager [MAHLI], but in the UV). The focused laser spot is rastered with a steering mirror over the field-of-view. The light is collected by a mirror and directed to a Mangin spectrometer and then onto the CCD. Separately, the co-boresighted context imager autofocuses on the sample and provides a color image. Another instrument module contains command and data handling and power and electronics units. The instrument also has a calibration target.

SHERLOC will be TRL 8 for the flight of the Mars 2020 Rover by 2020. For the Europa Lander, specific adaptations would be needed, including changes in the microscope optics, to achieve the higher spatial resolutions for compositional information required (see **Chapter 4**). Additionally, the instrument would be repackaged from its current arm-body unit configuration to a package within a single instrument inside the lander vault (no instruments would be mounted on the lander arm – see **Chapter 8**). A mechanism or solution for viewing of the calibration targets would have to be devised and thermal requirements assessed for the

warmer vault environment (compared to the surface of Mars). These are relatively straightforward engineering tasks, and thus, SHERLOC is an appropriate model payload instrument for the key VS role on the Europa Lander. Other spectrometer instruments for 2-D spatially-resolved composition at a similar TRL of 5/6 include:

- The Mars Microbeam Raman Spectrometer/Compact Integrated Raman Spectrometer (MMRS/CIRS), a 2-D rastering green Raman spectrometer (Wang et al., 2003).
- The infrared imaging spectrometer MicrOmega on the ExoMars 2020 Rover and JAXA's Hayabusa-2 (Pilorget and Bibring, 2014).
- The infrared Ultra Compact Imaging Spectrometer (UCIS), matured to TRL 6 under MatISSE funding (VanGorp et al., 2014).



Figure 4.5.4. Example of part of the joint MLD and VS Baseline model payload instrument, the SHERLOC prototype 2 (PT2). Source: Beegle et al., 2015.

Threshold Instrument

The suggested Threshold VS model payload example instrument is the Raman Laser Spectrometer (RLS) on the ESA ExoMars 2020 Rover. The ExoMars RLS instrument consists of three independent units connected via electrical and optical harnesses: a 532-nm laser source and control unit, an optical head, and a spectrometer (Rull et al., 2011a,b) (**Figure 4.5.5**). The collimated laser beam is conveyed via fiber optic cable to the optical head, which contains a mechanism to adjust the optical focus for ± 1 mm irregularities within the particulate sample. The Raman signal is collected through the same foreoptics, the excitation wavelength is filtered out, and the signal is transmitted via fiber optic cable to the spectrometer unit for capture and dispersion on a 2-D CCD, maintained at a temperature of -10°C to -40°C by thermoelectric cooling. In this implementation, the laser spot size is around $50\ \mu\text{m}$ on the target, and produces an irradiance on the target between 0.8 and $1.2\ \text{kW cm}^{-2}$. The laser light interacts with molecular vibrations, resulting in the energy of the laser photons being shifted up or down (the Raman shift), which is measured to $\sim 6\ \text{cm}^{-1}$ in the fingerprint spectral region below $2000\ \text{cm}^{-1}$. A calibration target is required for wavelength calibration with this system.

RLS is being readied for flight on the 2020 ExoMars Rover and will be TRL 8 for this launch opportunity by 2021. For the Europa Lander, alignments and fiber robustness would have to be validated for the different landing scenario, as well as any differences in radiation

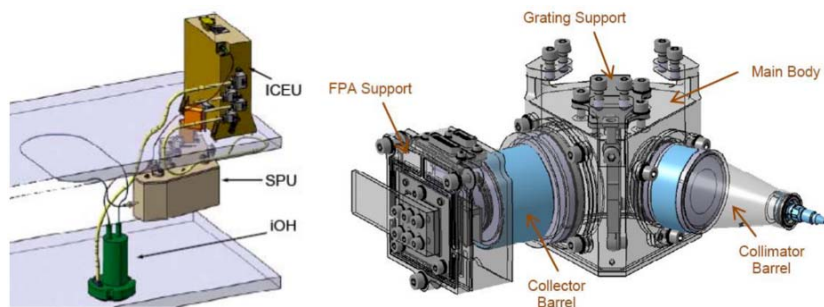


Figure 4.5.5. Example of the VS Threshold model payload instrument, the Raman Laser Spectrometer (RLS) of the ESA ExoMars 2020 Rover. **Left:** Schematic of the Instrument Control and Excitation Unit (ICEU), Spectrometer Unit (SPU) and internal optical head (iOH). **Right:** Mechanical design of the SPU. Sources: Rull et al. 2011(a) and (b).

exposure and/or thermal environments. Because the Threshold instrument would be inside the lander vault, the thermal controls would require re-evaluation for a higher temperature environment than for the martian environment anticipated for ExoMars. In contrast to the ExoMars rover scenario where a stage moves beneath the instrument, a Europa Lander-based RLS, if implemented as a point spectrometer, would have to include a sample manipulation system. A strategy would also need to be devised for the wavelength calibration target to be located beneath the instrument. A Europa Lander-based RLS might increase the spot size to collect more photons from the sample if being operated as a point spectrometer (versus the complexity of adding a mechanism to raster). Use of a different excitation wavelength to minimize interference from sample fluorescence might also be considered. These are relatively straightforward engineering tasks, and thus the RLS is an appropriate model payload instrument as the basis for a Threshold instrument on the Europa Lander.

Other point spectrometer instruments for bulk mineralogic composition at similar TRL 5/6 include: the Near-Infrared Volatile Spectrometer System (NIRVSS; Cook et al., 2016), a point infrared spectrometer package, and the visible near-infrared and short wavelength infrared (VNIR+SWIR) point spectrometers being developed for SuperCam on the Mars 2020 Rover (Wiens et al., 2016). These are landscape-viewing systems, but with modest optics engineering, all would be straightforwardly implementable to view small samples.

Sample Handling and Analysis

The Baseline VS instrument requires an accessible depth of field of ± 12.5 mm. For the Threshold instrument, the accessible depth of field is ± 1 mm. Accuracy of placement beneath the optical head, roughness of sample preparation, and loss due to sublimation or other mechanisms must be considered when designing suitable sample handling and optics.

A typical measurement timeline for the Baseline VS instrument, rastering 49 spots per target and including the context image and fluorescence measurement, would require 1 hour. For the Threshold VS instrument with RLS, a typical measurement would require approximately 10–30 minutes, depending on sample composition. Higher spatial resolution measurements with more complete spot coverage would require longer durations.

Resource Estimates

The payload mass allocation for the VS on the Europa Lander is 5.4 kg (including sample handling and electronics). Assuming a context image (40 Mbits), Raman, fluorescence, and dark signal CCD maps (12 Mbits each), and instrument housekeeping, 79.7 Mbits per observation is produced for a realistic allocation for the Baseline VS instrument. A likely protocol could consist of measurement of the calibration target, measurement of the ice sample, measurement of the sample residual following sublimation, re-measurement of the calibration target, and packetization of instrument state of health data over all the measurement for a minimum data volume of approximately 320 Mbits per sample.

Assuming 16-bit data for the 2048×512 CCD, 17 Mbits per spectrum is produced for a realistic allocation for the Threshold VS instrument. This would be the minimum data volume, assuming onboard averaging of shots. A protocol in this case might be measurement of calibration target, measurement of ice sample, measurement of sample residual following sublimation, re-measurement of the calibration target, and packetization of instrument state of health data during all of the measurements, for a minimum data volume of approximately 80 Mbits per sample.

The optical elements of the Threshold VS instrument are sensitive to alignment mismatching due to temperature variations and gradients. The CCD requires a specific cold temperature (-10°C to -40°C) to provide the required performance.

4.5.5 ORGANIC COMPOSITIONAL ANALYZER

The primary objective of the Organic Compositional Analyzer (OCA) is to determine the abundances and distributions of organic compounds of potential biological origin (amino acids, carboxylic acids, lipids, etc.), including resolving enantiomeric excess (ee). The OCA would also search for metabolic products in the gas and solid phases, and the Baseline instrument would assess the carbon isotopic distribution of both organic and inorganic carbon to compare against known examples of biology. The OCA would characterize the chemical composition of collected samples to assess the habitability of Europa and inform future site selection, in addition to searching for radiation byproducts that may affect the sample. The full list of measurement requirements for the OCA is given in **Table 4.5.8**.

Baseline Instrument

The Baseline model payload instrument for the OCA to implement the separation-mass spectrometry (S-MS) for compositional analysis measurements is a Gas Chromatograph Mass Spectrometer (GC-MS) with a Stable Isotope Analyzer (SIA) for carbon isotopic analysis capability. The GC-MS derives heritage primarily from the Sample Analysis at Mars (SAM) investigation on the MSL Curiosity rover (Mahaffy et al., 2012) (**Figure 4.5.4**), but also from other spaceflight MS and GC-MS instruments such as the Galileo Probe Neutral Mass Spectrometer (Niemann et al. 1992). SAM was designed to be able to conduct a wide range of reconfigurable experimental sequences, on a large number of individual solid samples (74 sample cups), over a long-duration Mars surface mission. SAM combines a multi-functional GC-MS with a tunable laser spectrometer (TLS) and an extensive associated gas processing system (GPS). The Europa Lander model GC-MS would comprise sensor, electrical, and mechanical modules that represent a subset of the GC-MS-specific hardware elements of a SAM-like suite. As such, the CBE mass of the Europa GC-MS is 16.4 kg, compared to approximately 40 kg for SAM, on the basis of selective removal of Mars-oriented SAM-subsystems that are not required for the Europa Lander.

The model Baseline mass spectrometer is the quadrupole mass spectrometer (QMS) from SAM, which ionizes gas using a filament-based electron ionization source. The quadrupole filter mass analyzer has a mass-to-charge (m/z) range of 1–550 Da with unit mass resolution and an abundance sensitivity of greater than 10^6 .

Threshold Instrument

In the case of the Organic Compositional Analyzer, the Threshold model instrument is the Baseline GC-MS without the carbon isotopic analysis capability. As this only affects the mass resolution of the instrument, we utilize SAM to define the sample handling parameters and provide resource estimates below.

Sample Handling and Analysis

In the model example case, particulate samples would be delivered to the Solid Sample Inlet Tube (SSIT), similar to that used in MSL SAM. The MSL SAM version uses a combination of gravity feed and piezo-electric vibration to transfer sample into cups supported in a 12-cup carousel-based Sample Manipulation System (SMS), which is

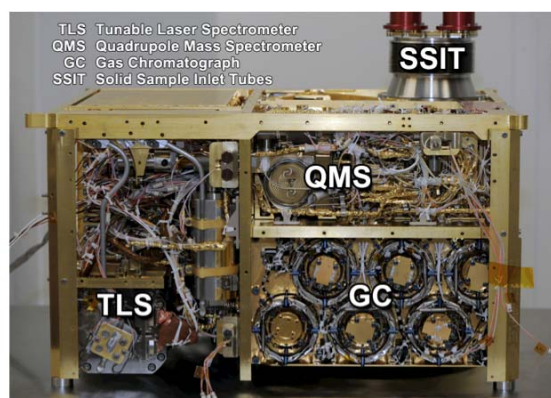


Figure 4.5.4. Example of a flight-qualified reference instrument for the OCA Threshold model payload instrument, the Sample Analysis at Mars (SAM) instrument of the MSL Curiosity Rover. (Credit: NASA-GSFC)

Table 4.5.8. Baseline and Threshold requirements for the Organic Compositional Analyzer (OCA). Gray cells indicate capabilities not included in the Threshold mission concept.

Investigation	Measurement Requirement
1A1: Determine the abundances and patterns (i.e., population distributions) of organic compounds in the sampled material, with an emphasis on identifying potentially biogenic characteristics.	Determine the presence, identities, and relative abundances of amino acids, carboxylic acids, lipids, and other molecules of potential biological origin (biomolecules and metabolic products) at compound concentrations as low as 1 picomole in a 1 gram sample of europan surface material. Determine the broad molecular weight distribution to at least 500 Da (Threshold) and bulk structural characteristics of any organics at compound concentrations as low as 1 picomole in a 1 gram sample of europan surface material.
1A2: Determine the types, relative abundances, and enantiomeric ratios of any amino acids in the sampled material.	Identify and detect (at 1 nM LOD) at least eight of the following amino acids: Ala, Asp, Glu, His, Leu, Ser, Val, Iva, Gly, β -Ala, GABA, and AIB, with at least one from each representative class (abiotic, biotic, proteinogenic). Note that for chiral amino acids, limit of detection is 1 nM for each of the two different chiral forms. Quantify abundances of all amino acids detected relative to glycine (Gly) at an accuracy of better than or equal to 2%. Quantify enantiomeric excess (ee) of at least three proteinogenic amino acids, one abiotic amino acid, and histidine, with an accuracy of 5% or better.
1A3: Determine whether the carbon stable isotope distribution among organic and inorganic carbon is consistent with biological activity.	Measure the carbon stable isotope composition of multiple compounds, compound classes, or pools of carbon with a relative standard deviation of no greater than 5‰ (5 per mille) in each measurement. Note that to achieve such measurements for organic compound concentrations as low as 1 picomol per gram, the LOD would need to be at most 10 fmol per gram to measure $^{13}\text{C}/^{12}\text{C}$ in a C1 compound.
1D2: Characterize the chemistry of the near-subsurface to determine the endogenous versus exogenous origin of the sample, and any surface processing of potential biosignatures.	Identify salts, radiation products (e.g., H_2O_2 , CO_2 , O_2 , SO_2 , S_n), silicates (anhydrous and hydrous), metals, and metal hydroxides, if present, at levels of a few to hundreds of ppt by mass.
2A1: Determine the extent to which the habitability of Europa's ocean and liquid water environments can be inferred from surface non-ice materials as sampled and imaged.	Determine the abundances of Cl-containing compounds, carbonates, sulfates, metal hydroxides, silica, and silicates, if present, at levels of a few to hundreds of ppt by mass. Determine the abundances of volatiles such as H_2S , CH_4 , O_2 , H_2O_2 , SO_2 , CO , CO_2 , CH_3SH , and dimethyl sulfide (DMS), if present, at levels of a few ppt by mass.
3A3: Characterize the chemical and mineralogical composition of the surface to inform future site selection.	Identify salts, radiation products, silicates, metals, and metal hydroxides, if present, at levels of a few to hundreds of ppt by mass.
3B2: Characterize the chemical processes that affect materials on Europa (e.g., radiolysis).	Characterize changes in ice and other surface materials in the landing zone (~5 m) in response to landing and sample collection, over mission duration (e.g., color, morphology, and composition).

included in the overall GC-MS mass estimate. (Note: the Europa Lander model payload would not rely on gravity feed for any sample collection or transfer activities.) The individual cups meet the sample vessel requirement, discussed above, for the GC-MS case. The set of multiple cups additionally enable pristine analyses of each new sample in the Baseline instrument. In the nominal approach, equal aliquots of sample from each 1-cc collection would be delivered into two cups. The first aliquot would be subjected to a “general survey” GC-MS analysis, while the second would be used either to repeat the first analysis, perhaps with tuned parameters, or to conduct a derivatization GC-MS run, discussed below. Data from the two aliquot analyses would be optimized, respectively for Investigations 1A1 and 1A2; however, these are not exclusive associations. Investigation 1A3 may be supported by analysis of either aliquot.

Each sample would be rotated, in turn, from the sample loading position to an analysis position where it would engage with the Gas Processing System (GPS) inlet via hermetic seal and microvalve. While at this stage the sample would remain under high vacuum conditions, the increasing temperature due to contact with the SSIT and SMS would induce release of trapped gases and sublimation of water ice. In the first phase of analysis, evolved light volatiles including CH₄, CO₂, CO, NH₃, and NO would be sampled from the sample cup headspace and analyzed directly (real-time evolved gas analysis, EGA) and/or after concentration in a hydrocarbon trap that serves to eliminate potential interferences. It is worth noting that, in the case of an ice-dominated sample, infrastructure and resources would exist in the Threshold GC-MS design to enable the sample vessel to be pressurized and the ice to be melted at this point in the sequence. A small liquid water-based sample would be drawn off through a flow valve and processed as may be required by complementary liquid analysis techniques sharing common resources with the GC-MS.

Continuing with general GC-MS, volatiles would then be further released via applied, stepwise heating. Water is expected to dominate the low-temperature evolution. While Objective 1A does not specifically call for analysis of the H₂O itself, potentially significant additional science return may be possible by sampling a small volume fraction with real-time EGA. For example, the D/H ratio in water could be an important indicator of provenance and processing of the near-surface ice, and could help calibrate carbon isotope studies if it is also measured in CH₄. However, due to subsequent potential interferences with derivatization chemistry, required for subsequent analysis of amino acids and some other compounds, the bulk of sample water would then be removed from the system by flushing with He through heated lines and venting to space.

The remaining sample (which could be bulk mineral phases including salts, or limited to a residue) would then be subjected to the primary GC-MS scan. In the scan, the sample would be heated over the oven's full range (up to at least 600°C), releasing organics and inorganic volatiles via thermal desorption from, and pyrolysis of, the mineral matrix. Real-time EGA would continue to operate during the full pyrolysis ramp, sampling a small gas fraction via a split into the ion source. Most organic compounds in the balance gas would be captured on a pair of hydrocarbon injection traps, in parallel. Each trap would contain a high-surface area molecular absorbant such as Carbosieve[®]. These serve to concentrate organic analyte that would be subsequently introduced to the GC.

The injection traps would be sequentially heated, with each product directed to a heated general-purpose column used to separate a wide range of volatile and semi-volatile organics by retention time, which would thus be introduced over a period of tens of minutes into the MS. Each several-second duration chromatographic peak corresponding to a small number of compounds with similar/identical retention times can be sampled multiple times by the MS, providing additional time (and compound) resolution and maximizing analytical

dynamic range, both required to resolve and identify isomers in a mixed sample. The analysis from the duplicate injection trap would provide opportunities for co-adding signals, extending the effective dynamic range, as well as conducting follow-up focus scans of selected m/z ranges, identified autonomously from the first “survey” scan. Such focus scans lower the limits of detection, and enable improved quantitative analysis, for tentatively detected species.

Data from the first sample aliquot would provide a general assay of organic content and key inorganics from EGA. This data would also guide the optimal tuning and mode parameters for analysis of the second aliquot. The subsequent sample would be added into a cup pre-loaded with a derivatization agent such as N,N-dimethylformamide dimethyl acetal (DMF-DMA), which would be mixed with the sample after removal of the bulk water. Through reactions under pressure and temperature control, nominally nonvolatile analytes are made more volatile (and converted to a specific heavier “derivatized” form) to enable their analysis via GC-MS. For example, DMF-DMA reacts with fatty acids, amines, and amino acids by replacing a labile hydrogen with a methyl group, reducing the polarity of the molecule. The more volatile product analyte can then be then processed as above with injection traps and column. For the second sample, the primary column would be one sensitive to chiral compounds – leading to separation of stereoisomers in support of Investigation 1A2. An additional benefit of parallel hydrocarbon traps in this case would be the ability to distinguish the baseline responses of separate columns, when processing the same derivatized analyte, which would provide an important cross calibration when looking for enantiomeric excesses of trace-concentration compounds.

The GC-MS readily analyzes individual organic compounds with concentration limits of detection of approximately 0.01 ppb by weight (ppbw), or one order of magnitude below the requirement noted above, corresponding to approximately 100 femtomoles (fmol) of analyte at 100 Da in a single aliquot of 1 cm³, or 1 g if primarily water ice.

Resource Estimates

The payload mass allocation for the OCA on the Europa Lander is 16.4 kg (including sample handling and electronics). Processing of each sample aliquot would require approximately 50 minutes on Europa. Multiple aliquots can either be processed during a single “run” (100 min total) or in subsequent tals. The total data volume from a total of four GC-MS scans is approximately 8 MB, uncompressed.

4.5.6 GEOPHYSICAL SOUNDING SYSTEM

Among the highest priorities regarding Europa’s habitability is the task of locating liquid in the subsurface. This water may be present in the ocean, in discrete water bodies, and/or distributed

Table 4.5.9. Baseline and Threshold requirements for the Geophysical Sounding System (GSS). Gray cells indicate capabilities not included in the Threshold mission concept.

Investigation	Measurement Requirement
2B1: Search for any subsurface liquid water within 30 km of the lander, including the ocean.	Measure the thickness of the ice shell and locate any subsurface water by observing reflected body and/or surface waves from seismic events with 3-axis arrival information over a range of frequencies from 0.1–100 Hz (Threshold), or 0.1 to >100 Hz or better (Baseline).
2B4: Determine the depth of Europa's ocean.	Measure the depth of the ocean by observing reflected body waves from seismic events covering frequencies from 0.1 to >100 Hz with 3-axis arrival information.
3A4: Characterize the internal structure of Europa including ice shell thickness and depth of the ocean.	Measure acoustic signals of reflecting body waves over the lifetime of the surface mission, covering frequencies from 0.1 to >100 Hz with 3-axis arrival information.

within the ice shell. To understand the evolution of the material sampled by the lander, including its provenance and any recent interactions with water, knowledge of the location of water around the lander is essential.

The Baseline Geophysical Sounding System (GSS) would measure the thickness of the ice shell, the depth of the ocean (i.e., three-dimensional vertical extent), and potentially characterize the internal structure of Europa by observing reflected body waves over the lander mission duration. The Threshold GSS would measure the thickness of the ice shell and locate any subsurface liquid water bodies, including the ocean, by observing reflected body and/or surface waves with from seismic events over a range of frequencies. These requirements are further outlined in **Table 4.5.9**.

The seismic investigations would enable ground truth for orbital measurements while also addressing the context of material sampled by the lander. The planned location for the Baseline and Threshold instruments is within the vault, however advancements in instrument technology may allow other implementations.

Baseline Instrument

The Baseline GSS model payload instrument is the short-period (SP) seismometer based on the SEIS instrument on the Mars InSight Lander,** planned for launch in 2018 (**Figure 4.5.7**). This instrument would consist of at least one broadband 3-axis seismometer in the vault, with a frequency range of 0.1 to 100 Hz, to detect reflected and transformed body waves generated by larger, possibly infrequent or more distant seismic events (100 to >250 m depth cracking events) from the background noise that is produced by surface waves from more frequent events (i.e., <50 m-depth cracking events). This range would capture the received energy from most sources of seismicity that could reach the Europa Lander (see **Figure 4.2.10**). Sensitivity to the higher frequency range would enable signal discrimination from an ambient noise floor

**The SEIS instrument onboard InSight consists of both the SP seismic probes and the Very Broad Band (VBB) seismic probes. Implementation of an SP-like instrument onboard the Europa Lander would be internal to the Lander vault and not require external deployment nor external mounting.

of 35 dB relative to 1 micron per second (see **Figure 4.2.6**). This Baseline GSS instrument provides the ability to detect reflections from the ice-ocean interface using shallow acoustic sources (cracks), and potentially reflections off the silicate interior, thereby sensing the full ocean depth.

Threshold Instrument

A three-axis geophone covering 0.1–100 Hz would have the capability to measure short period, nearby (<100 km), energetic seismic events on Europa, and could confirm both the period over which Europa is geologically active, as well as probe the ice shell thickness.

Seismic sensors such as geophones can observe polarization of the seismic signal to allow compressional, shear, and surface waves to be unambiguously identified, as well as potentially observe Love waves (Lee et al., 2003; Lorenz, 2012).

The model payload Threshold GSS instrument (**Figure 4.5.8**) is a three-axis geophone, based on the SISMO seismometer of the OPTIMISM (Observatoire Planétologique Magnétique et Sismique sur Mars) instrument on the Russian Mars 96 spacecraft (Lognonne et al., 1998). Though the Mars 96 mission failed during launch, the OPTIMISM instrument was a flight-qualified, fully tested, part of the science payload. The seismic instrument was designed to record long period waves (between 0.5 and 50 seconds) over a range of 0.2 to 2 Hz. The full seismic capability of the OPTIMISM probes extended to 100 Hz.

Instrument Operations

The Baseline model payload GSS instrument would monitor for acoustic events throughout the entire mission duration. The diurnal tide would be fully sampled several times across several European days. The highest priority times of operation for the GSS instrument are during maximum tension for the region of the surface surrounding the Europa Lander's position, in order to provide the largest number of potential cracking events.

Notably, an observation of opportunity would occur during the landing sequence. The lander could operate both the seismic instrument (GSS) and the onboard lander accelerometer throughout the landing event, after the Powered Descent Vehicle (PDV) stage delivers the lander to the

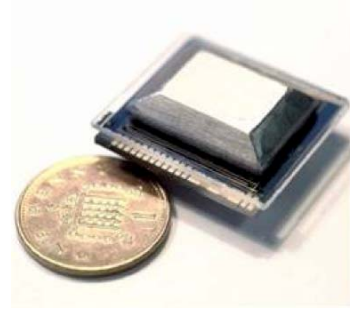


Figure 4.5.7. Example of the GSS Baseline model payload instrument, the short-period (SP) seismometer of SEIS from the Mars InSight 2018 Lander.



Figure 4.5.8. Example of the GSS Threshold model payload instrument, the three-axis geophone of the OPTIMISM instrument from the Mars 96 mission.

surface and flies away, and throughout the impact of the PDV stage. Such an impact event would provide a specific source-receiver direction and magnitude that would be discretely known in space and time. Such an implementation would require further Phase A evaluation.

Finally, if resources allow, more than one GSS (SP or 3-axis geophone) should be carried so as to remove any ambiguity in localization of any acoustic sources.

Resource Estimates

The payload mass allocation for the GSS instrument on the Europa Lander is 1.2 kg (including electronics). For the Baseline model payload GSS, which is a three-axis microseismometer, this is easily met. For the Threshold model payload GSS, the resource estimates are derived from the SISMO seismometer, which was designed to operate on 5 mW (with 45 mW for the microprocessor and electronics). The mass was 405 g (Lognonne et al. 1998), also well below the payload mass allocation.

Seismometer data volumes will vary significantly depending on the mode of operations and would be tuned to maximize science return. The arrival of a surface wave would trigger recording of individual events, recorded for 30, 60, or 180 seconds depending on the amplitude of the arriving signal. Sampling rates can be varied for individual measurements. Expected data rates would be expected to range from 1 kbit per second for long duration monitoring to tens of kbits per second for triggered high resolution measurements. A preliminary concept of operations of the GSS instrument would require 1.1 Gbits total. For the Threshold GSS, the maximum data produced by the entire OPTIMISM instrument (which included a magnetometer and inclinometer in addition to the seismometer) was 1 Mb per day.

4.5.7 LANDER INFRASTRUCTURE SENSORS FOR SCIENCE (LISS)

In order to optimize the science return of the Europa Lander mission, the SDT strongly recommends a close partnership between science and project engineering. Use of data from several subsystems (e.g., descent stage, thermal management, sampling system) could serve their primary engineering roles while also yielding useful science results. This is particularly relevant for Goal 3 investigations, which are largely applied science investigations that feed forward into solving future engineering challenges. Reliance on these data to achieve science measurements does not drive or impose requirements on the design and operation of those sensors.

To implement this dual-use application of engineering sensors for science, integration of scientists and subject-matter experts should be performed early enough during mission development such that supporting science team members could participate in determining the configuration, calibration, downlink prioritization, and archiving of the relevant engineering

data from such LISS systems (especially for PDV nadir descent imaging and LIDAR topographic imaging systems). Interaction between science and engineering teams has been demonstrated on previous missions (e.g., MER and MSL) and set a strong precedent for the Europa Lander mission.

The engineering sensors that could service science are part of the Powered Descent Vehicle (PDV) and the lander spacecraft. Termed the Lander Infrastructure Sensors for Science (LISS), they include, but are not limited to, the following:

- PDV spacecraft nadir descent imaging (part of the TRN system for deorbit, descent and landing)
- Descent hazards imaging LIDAR topographic mapper (DTM of the immediate landing zone during descent)
- Telecom of Europa Lander HGA to the Carrier Relay Orbiter (CRO)
- Sampling system (robotic arm and sample extraction tool)

The science contributions for each component of LISS are described below. These contributions are also outlined in the STM, and in several of the investigations within Goals 2 and 3 (see also **Table 4.5.4**).

Descent Imaging

Descent imaging (panchromatic) is provided by nadir-viewing engineering cameras designed to meet descent and landing engineering requirements as part of terminal Deorbit, Descent, and Landing (DDL) operations. The Europa Lander investigations that utilize descent images are listed in **Table 4.5.10**, and primarily involve placing surface observations into a multiscale geologic context. As described in **Goal 3**, the coupled orbiter–lander observations of Mars enabled discoveries that were synergistic between the two missions (e.g., HiRISE and MSL) and not attainable with the individual datasets alone. Similar discoveries could be enabled by coupling of Europa Lander descent imaging data to the CRSI and MLD data, and ultimately to the regional and global datasets of the EMFM. Of particular importance for the geomechanics investigations (Goal 3) are:

- a) Sub-meter-scale observations of the surface (spatial distributions of fine-grained materials versus icy shell substrate), and especially those at feature identification resolutions finer than that which could be achieved with the Narrow Angle EIS imaging from the Europa Multiple Flyby Mission (i.e., <50–60 cm per pixel). Note that vertical baseline stereo methods involving new Shape from Motion (SfM) computer vision algorithms could be used to compute DTMs from such

images, thereby providing further three-dimensional constraints on the sub-meter scale geology of the immediate landing zone.

- b) Images that capture the impingement and effects of impingement, including particle entrainment and motion, of Europa Lander descent engines on the surface. Such images provide information about the state of properties of the regolith and substrate at the time of descent and landing (e.g., Moore et al. 1987; Moores et al. 2016).

Recent analysis of the MSL Mars Descent Imager (MARDI) data from ~2.5 km to the surface by the imaging team has demonstrated the quality of DTMs that can be constructed from nested, vertical baseline stereo images for geological interpretation, which can exceed those from orbital stereo (Garvin et al., 2017). Descent images can also be utilized to localize the lander and link image data from the EMFM, and other coarser-scale compositional and thermophysical data, to the lander workspace. This is accomplished by acquiring multiple descent images, including those at sub-decameter scale (e.g., from 1–10 cm/pixel).

The current Europa Lander engineering concept for descent imaging calls for a 1 megapixel camera with 90° FOV that images 1 frame per second between altitudes of 5 km and 30 m during the terminal descent (**Chapter 8**). Assuming 1 megapixel requires a 1000 × 1000 pixel square detector, then at 5 km altitude, a typical nadir descent image would be at about 10 m per pixel and thus cover 10 × 10 km; at 30 m altitude, it would be at about 6 cm per pixel and, thus, cover 600 × 600 m.

Table 4.5.10. Baseline and Threshold investigations which require downlink, calibration, study and archiving of descent images and LIDAR topographic mapping products.

Investigation	Measurement Requirement
1D1: Determine the geological context from which samples are collected.	Identify features in the landing zone (~5 m) as small as 50 cm, in color, to bridge the gap between lander and flyby resolutions.
2B2: Search for evidence of interactions with liquid water on the surface at any scale.	Identify any surface morphologies/textures indicative of liquid water emplacement in the landing zone, including any compositional indicators of liquid water emplacement, and any thermal signatures of recent endogenic activity associated with liquid water.
3A1: Characterize the physical properties of Europa's surface materials through interaction with the sampling and landing systems.	Measure physical and mechanical properties of surface "fines" and regolith (i.e., loose, unconsolidated or weakly indurated fine-grained surface materials). Characterize textural and structural attributes of this material at millimeter scales in the workspace, and as exposed by the sample extraction tool, and at decameter scales in the far-field (horizon). Measure physical and mechanical properties of solid surface materials (i.e., icy-shell material). Characterize textural and structural attributes of this material at millimeter-to-meter scales in the landing zone (~5 m), and at decameter scales in the far-field (horizon).
3A2: Identify geomorphic features and their quantitative relief (topography) characteristics in the landing zone.	Determine centimeter to decimeter slope and elevation distribution of the landing zone (~5 m). Characterize centimeter- to meter-scale geomorphic features (e.g., boulders, penitentes, frost deposits, sublimation residues, small impact craters, ejecta deposits, and pits) in the landing zone (~5 m).

Such data would bridge the scale gap from the CRSI landed images with their ~ 1 mm (near-field) to ~ 10 cm (far-field) resolution by providing images and derived DTMs with < 50 cm resolution for a wider region around the final touchdown position of the Europa Lander.

Descent LIDAR

Descent Light Detection and Ranging (LIDAR) “topographic imaging” (in the form of point clouds and derived DTMs) is provided by a sensor designed to meet descent and landing engineering requirements during terminal DDL associated with landing safety (**Chapter 10**). The anticipated LIDAR topographic imaging product (DTM) obtained during landing would aid in the geomorphic interpretation of the landing site, as described in **Goal 3**. The Europa Lander investigations that depend on descent LIDAR are listed in **Table 4.5.10**.

The Europa Lander project engineering calls for a single descent LIDAR product with ~ 5 cm post (i.e., 5 cm ground scale distance uniform sampling), ~ 5 cm elevation precision (i.e., relative vertical locations for each of the $5 \text{ cm} \times 5 \text{ cm}$ grid cells are measured with vertical statistical noise less than 5 cm), and a 100×100 m DTM of the area that includes the final landing site.

These requirements, driven by engineering constraints, would be sufficient for assessment of sub-meter-scale landing and mobility hazards (relevant for future landed or roving missions), and address multiple Goal 2 and 3 measurement requirements, as listed in the STM. Having a synoptic 3-D view of the landing zone from which to place all other descent and landed measurements in precise three-dimensional context would allow the Europa Lander (and supporting LISS observations) to tie to the EMFM remote sensing regional to global context, further enhancing the science return of both missions.

Telecom (HGA to CRO)

The primary means by which Investigation 3B4 is conducted is via the telecommunications link between the lander and the Carrier Relay Orbiter (CRO). To determine the time-variable position of the lander over the surface mission duration, the x, y, z position of the lander would be monitored via the telecom link between the lander and the CRO, as well as from the CRO to Earth. A Baseline requirement includes monitoring this link for 10 seconds or longer at 0.1 mm per second via X-band. The Baseline Investigation that requires this engineering data is listed in **Table 4.5.11**.

Table 4.5.11. Investigation Baseline measurement that uses engineering data from the HGA to CRO, and CRO to Earth.

Investigation	Measurement Requirement
3B4: Characterize the three-dimensional surface dynamics of Europa and the local dynamic variability (potentially indicative of activity) at the landing site.	Determine the time variable position of the lander over the surface mission duration by tracking the x,y,z position of the lander from the Carrier Relay Orbiter spacecraft (CRO) as well as from the CRO to Earth (e.g., via X-Band at 0.1 mm per s over 10 s or longer).

Engineering Thermal Sensor System

The engineering thermal sensor system (lander-required temperature point measurement sensors) would provide temperature measurements of the euroman surface throughout the Europa Lander mission duration. Measuring the temperature of the surface is an important part of characterizing the physical properties of Europa's surface materials, as described in the STM and in **Table 4.5.12**.

Table 4.5.12. STM Investigations that require downlink, calibration, study and archiving of temperature measurements from the lander.

Investigation	Measurement Requirement
2B2: Search for evidence of interactions with liquid water on the surface at any scale.	Identify any surface morphologies/textures indicative of liquid water emplacement in the landing zone, including any compositional indicators of liquid water emplacement, and any thermal signatures of recent endogenic activity associated with liquid water.
3A1: Characterize the physical properties of Europa's surface materials through interaction with the sampling and landing systems.	Determine the temperature of the euroman surface at the landing site, to an accuracy of ± 5 K.
3B3: Characterize the magnitude of the thermal response at the landing site from the landing event and the lander surface operations (e.g., sampling).	Identify thermally-induced changes to the surface over mission duration. Monitor surface temperature to an accuracy of ± 5 K over mission duration.

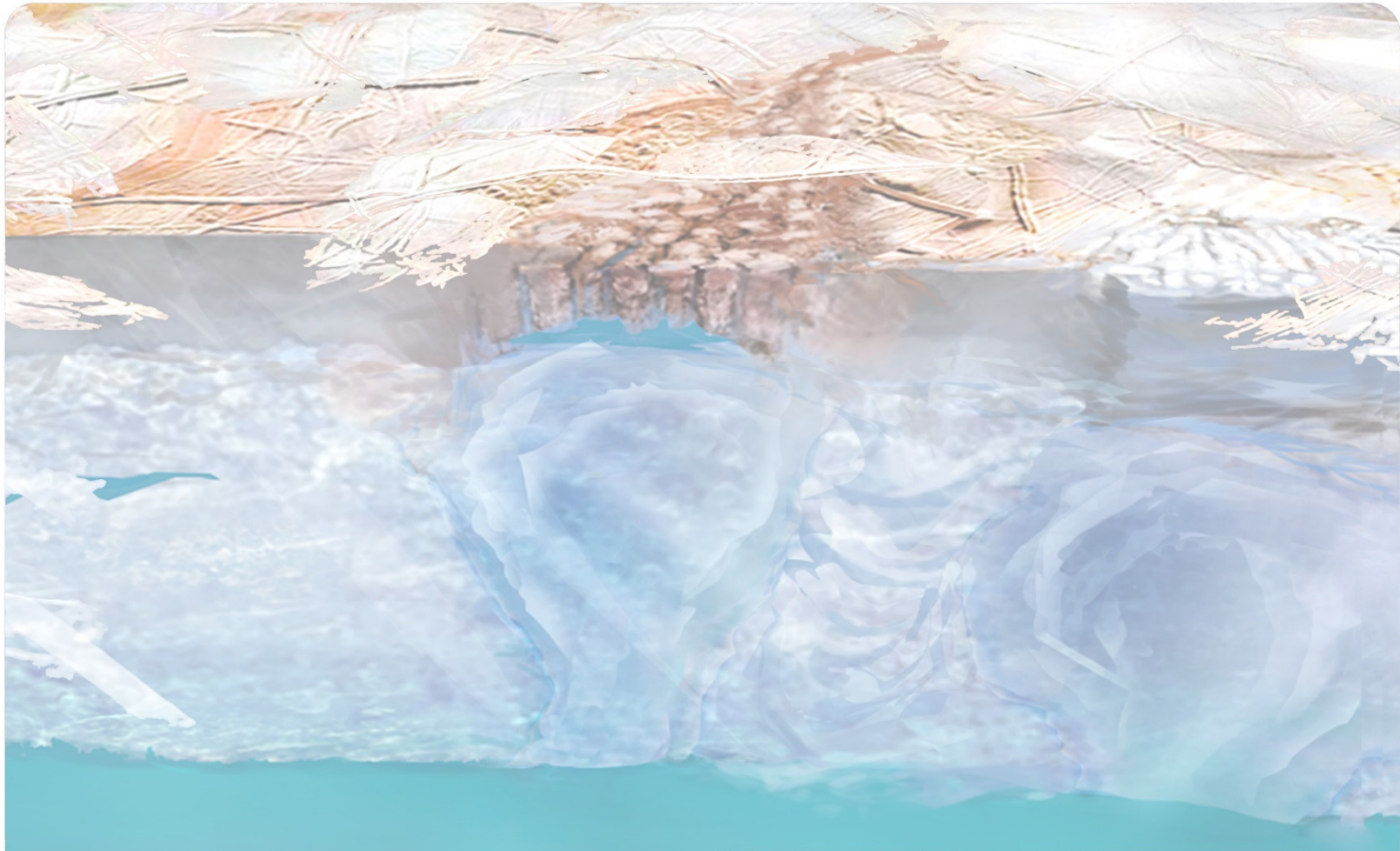
Sampling System

As with previous in situ missions (Viking, MER, Phoenix, MSL Curiosity), robotic arms and sampling systems offer the potential to yield valuable data on surface properties. The SDT recommends that the Europa Lander mission follow this model, maximizing the use of engineering measurements of the robotic arm and sample extraction system to obtain knowledge of physical properties of the surface.

Calibrated engineering data collected by the robotic arm and sample extraction tool would enhance the science return related to surface geomechanical properties and hazards investigations, as detailed in the STM and in **Table 4.5.13**. As with the other LISS systems, these measurements would involve interaction between the science team and the engineering team early in the development of the mission to ensure pre-launch calibration and post-landing archiving of data.

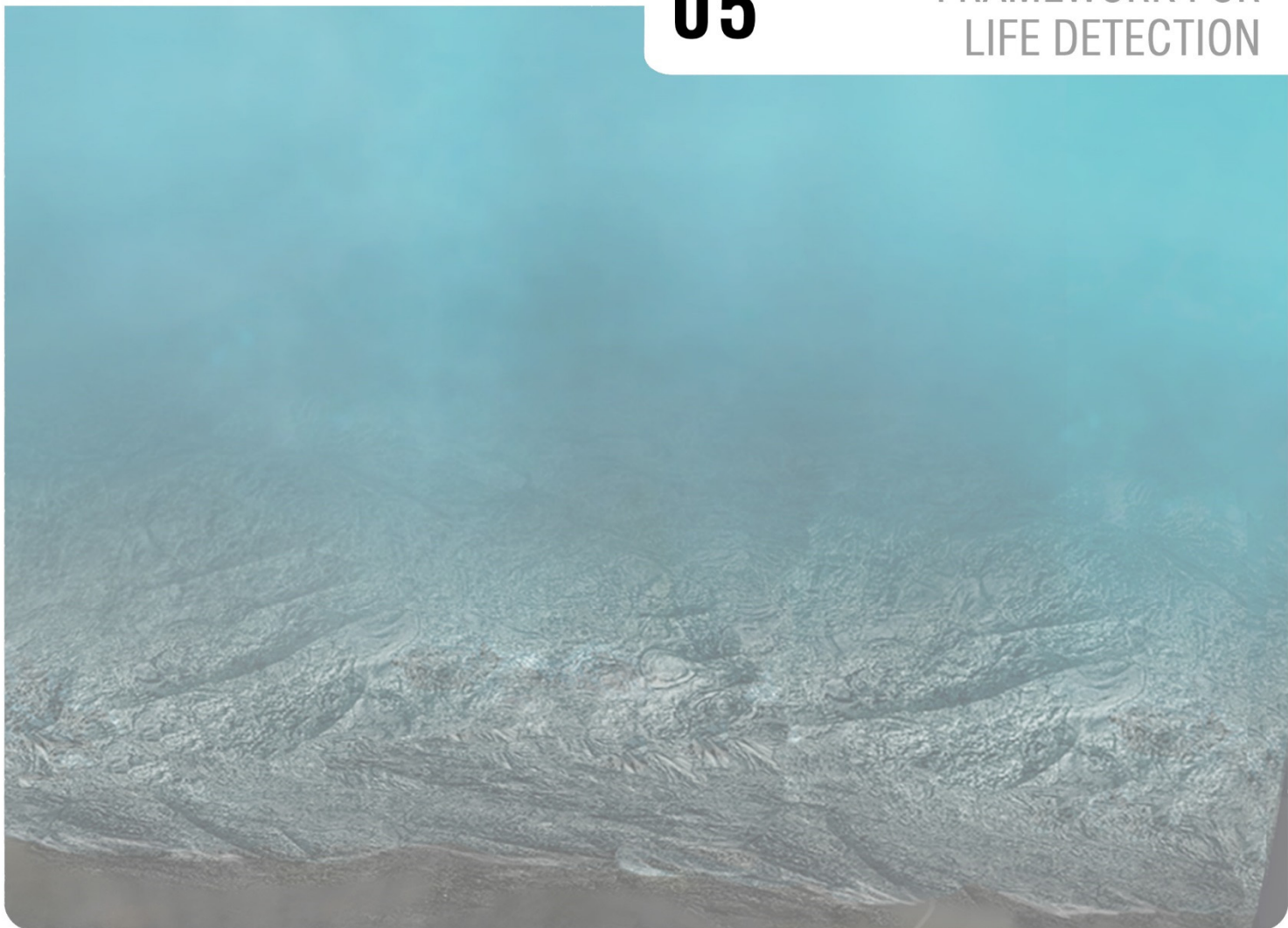
Table 4.5.13. Baseline and Threshold investigations that require downlink, calibration, study and archiving of engineering data from the sampling system.

Investigation	Measurement Requirement
<p>3A1: Characterize the physical properties of Europa's surface materials through interaction with the sampling and landing systems.</p>	<p>Measure physical and mechanical properties of surface "fines" and regolith (i.e., loose, unconsolidated or weakly indurated fine-grained surface materials). Characterize textural and structural attributes of this material at millimeter scales in the workspace, and as exposed by the sample extraction tool. Measure physical and mechanical properties of solid surface materials (i.e., icy-shell material). Characterize textural and structural attributes of this material at millimeter-to-meter scales in the landing zone (~5 m).</p>
<p>3B1: Characterize the physical processes that affect materials on Europa (e.g., gardening).</p>	<p>Identify changes to textural and structural attributes of surface "fines" over mission duration. Identify changes to textural and structural attributes of solid ice and mineral ice shell materials over mission duration.</p>
<p>3B3: Characterize the magnitude of the thermal response at the landing site from the landing event and the lander surface operations (e.g., sampling).</p>	<p>Identify thermally-induced changes to the surface over mission duration. Monitor surface temperature to an accuracy of ± 5 K over mission duration.</p>



05

FRAMEWORK FOR
LIFE DETECTION





5 FRAMEWORK FOR LIFE DETECTION & ASSESSING POTENTIAL BIOSIGNATURES

The challenge of searching for life on another world is in part the burden of proof for a positive detection of life, and the challenge of interpreting an ambiguous result. Furthermore, a null result for life on Europa – or any world for that matter – is clearly impossible to prove without an armada of spacecraft that explore every possible niche. Despite these challenges it was critical to the Science Definition Team’s effort that a framework for assessment of biosignatures and sample analyses be considered. In this chapter, we present components of that framework that could help minimize ambiguous or otherwise conflicting interpretations of potential biosignatures.

Each of the measurements described in **Chapter 4** constitutes a potential biosignature or an important part of the environmental context for understanding potential biosignatures. As a guide for assessing the utility of a variety of measurements and techniques, the NASA Astrobiology Program has created the “Ladder of Life” (NASA, 2017b). Each row, or ‘rung’, on the ladder represents a phenomenon or measurable parameter that can be observed, and which may serve as a biosignature. The lowest rungs correspond to measurements that aid in assessing habitability, while with each move up the ladder the observable is generally considered a stronger sign of life.

Critically, features in each rung have an associated ambiguity and potential for false positives and false negatives; no single row is, for the most part, a definitive measurement of life. To arrive at a positive detection of life requires a coordinated measurement approach that employs several different, and ideally complementary, potential biosignatures. The Europa Lander Science Definition Team used the Ladder of Life as guide for assembling a suite of measurements, and a model payload, that could yield a high degree of confidence in biosignature detection.

To assess the type, redundancy, and complementary nature of the potential biosignature measurements available to the model payload, the Science Definition Team (SDT) discussed which set of measurements, when combined, would yield a strong “potential biosignature” interpretation of the sampled material. In other words, for a given sample, if a subset of measurements indicated biological activity (e.g., detection of chirality and observation of cell-like structures), would the combination of evidence merit a positive biosignature result and justify sampling the same site again for further confirmation?

The SDT’s model payload offers at least four investigations for possible organic biosignatures (abundance of organics, patterns of complexity, chirality, and isotopic fractionation). Morphology presents at least two strong lines of evidence – observation of cell-like

structures using microscopy, and interrogating any putative cells for additional evidence of biogenicity. Macroscale evidence in the surrounding terrain could also provide another line of evidence, but for the sake of the present discussion, such evidence was book-kept under landing site context. Inorganic biominerals serve as a seventh independent potential biosignature. Finally, both the sample context, and the endogenous versus exogenous determination of the sample are key factors for the biosignature framework.

The above list leads to a set of permutations for the collection of biosignatures of 2⁹, or 512, possible combinations. Of these combinations, the question then becomes: **Which of these combinations lead to a net positive result for a potential biosignature?** Or framed another way: **What combination of evidence would lead to the decision to sample the same site again to get a second, and ultimately third, confirmation of biosignatures (and ultimately the possibility of claiming a detection of life)?** Table 5.1 shows a subset of these permutations. For each row, a “1” in the column indicates that the measurement yielded evidence for that specific biosignature, and a “0” indicates that the evidence was insufficient to claim as evidence for life. At the far right a “1” indicates that for that particular set of measurements, the accumulated evidence supports the interpretation of the sample having evidence of life. A “0” indicates that the combination of evidence is insufficient.

Table 5.1. A possible framework for biosignature detection based on the measurements included in the Europa Lander model payload. For a given sample, a “1” indicates that the evidence supports a biosignature interpretation, while a “0” indicates that the evidence is insufficient as a biosignature. The combined set of evidence may then lead to a “1” or “0” in the far-right column. A “1” in the far-right column indicates that a second sample should be collected from the same site for a repeat measurement. Many more permutations are possible than what is shown here. Additional detail on this framework is provided in the text.

Sample #1 Analysis Results	GCMS				Microscope		Raman	CRS		Biosignature Result
	Raman				Raman	GCMS	GCMS	GCMS, Raman		
	Abundance	Pattern	Chirality	Isotopes	Microscopy	Cellular properties	Biominerals	Context	Endo vs Exo	
	1	1	1	1	1	0	1	1	1	1
	1	1	1	0	1	0	1	1	1	1
	1	1	1	0	1	0	0	1	1	1
	1	1	0	0	1	0	0	1	1	1
	1	0	1	0	1	0	0	1	1	1
	1	1	0	0	0	0	0	1	1	1
	1	0	1	0	0	0	0	1	1	1
	1	0	0	1	0	0	0	1	1	0
	1	1	0	0	0	0	1	1	1	1
	1	0	0	0	0	0	1	1	1	0
	1	0	0	0	0	0	1	1	1	1
	1	0	1	0	0	0	1	1	1	1
	1	0	0	0	1	0	1	1	1	1
	1	0	0	0	1	0	0	1	1	0
	0	0	0	0	1	0	1	1	1	0

The SDT treated this matrix as a useful exercise and thought experiment to help develop a surface mission phase and sampling sequence. A key driving consideration being the need to analyze three independent samples (Threshold mission), each of which would need to show multiple lines of evidence for biosignatures, in order to then have repeated measurements that corroborate the conclusion that signs of life have been detected. The conservative approach here, of course, echoes back to the need for “life [to be] the hypothesis of last resort” (Sagan et al., 1993).

With five samples as part of the Baseline, the first two samples could yield a negative result and yet if the third sampling site generated a net positive biosignature there would still be the capability for two additional samples, and the possibility of having a biosignature result repeated in triplicate.

Interestingly, out of the 512 possibilities available from the nine different lines of evidence, only about ten to twenty combinations consistently lead to a “1” in the far-right column, as judged by SDT members. No attempt was made to formalize a specific set of biosignature permutations as definitive, but the scientific community should continue to examine this issue as it is relevant to all missions pursuing evidence of life beyond Earth.

To address the operational issue of sampling sites and repeat measurements, the team considered a scenario in which the landing site workspace was divided into five different regions and samples were acquired from any of the five regions. If the first sample revealed a net positive biosignature result, then the second sample would be acquired from the same region. If no biosignatures were revealed, then the second sample would be acquired from a different region. For each subsequent sample the same logic applies – if biosignatures are detected, sample the same site again; if not, move to a new site. **Figure 5.1** illustrates this sampling sequence. The vertical axis indicates the sampling region and the horizontal axis denotes a positive or negative biosignature result: if the sample reveals biosignatures then sampling continues at that site and the sequence moves to the right, collecting the next sample at the same site. If no biosignatures are discovered – or if the sample generates an ambiguous result – the sequence moves downward to start the process over in the next sampling region. Any path that leads to three or more moves to the right, i.e., “positive detections”, could result in a possible claim of life detection, based on evidence collected during the mission.

Another component of the mission that is important to consider for resolving any biosignature ambiguities is the total number of samples analyzed. Though the SDT developed a mission concept that has three samples as the Threshold, and five samples as the Baseline, the mission, as designed, could potentially analyze more than five samples. The battery powered lander provides a minimum of 45 kWh for surface operations. In the 20-day mission scenario described in **Chapters 6** and **7**, the Baseline sampling utilizes approximately 24 hours

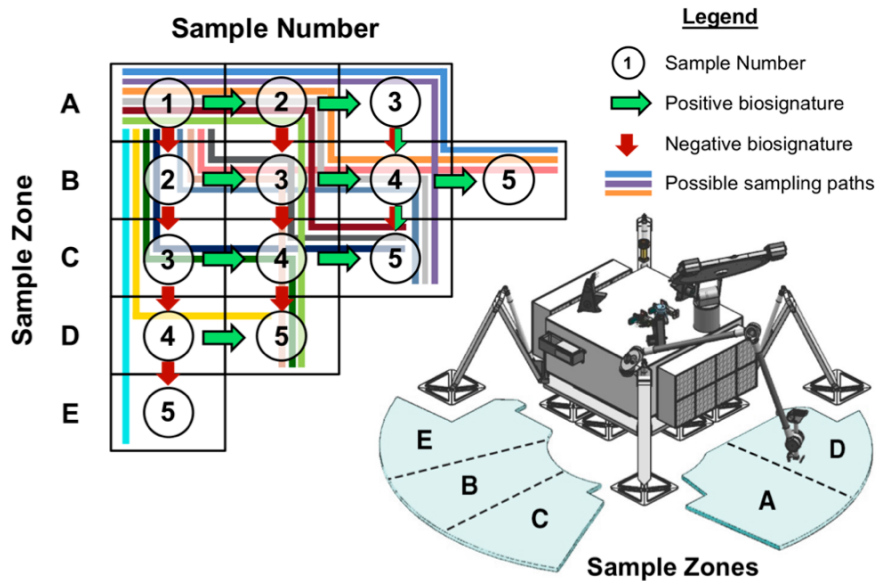


Figure 5.1. Example sampling sequence for generating repeat measurements for potential biosignatures. The chart shows the sample number as collected in a given sampling region. If a sufficient collection of biosignatures are measured in the sample (see **Table 5.1**), then that site is sampled again (move to the right). If the evidence for biosignatures is insufficient, then the robotic arm moves to a new region and collects a new sample. A minimum of three repeat measurements, in three discrete samples, are needed for the possibility of concluding that life has been detected. Additional detail provided is the text.

per sample acquisition and analysis sequence, leaving a total of nearly 15 days (Earth days) for additional monitoring (e.g., with geophone), imaging, and schedule margin.

If the mission proceeded such that five samples were collected and successfully analyzed (regardless of biosignature results), additional samples could be collected and processed. The only key consequence is that the sampling and analyses would use part of the remaining kWh stored in the primary batteries. The total mission duration would be shortened by approximately 48 hours of monitoring capabilities for each additional sample processed.

Figure 5.2 shows several examples of mission scenarios for sampling, monitoring, and survival. As described above, the Baseline mission scenario results in a minimum of 20 days of surface operations. Energy margin is included in the battery design to guarantee a 20-day Baseline mission against design and unexpected growth in power consumption. However, if some of this margin is unutilized for its intended purpose, it could lead to additional time on the surface, so that the Baseline mission could continue for as long as 34 days. The Threshold mission scenario is defined by descopes in monitoring, image collection, and data return. These changes could grow the mission duration to at least 24 days, and up to 37 days if energy margin is available. In the event that the mission requires going into safe mode, or “survival”, the mission could last for between 26 and 41 days (depending on available margin), if exclusively in this mode.

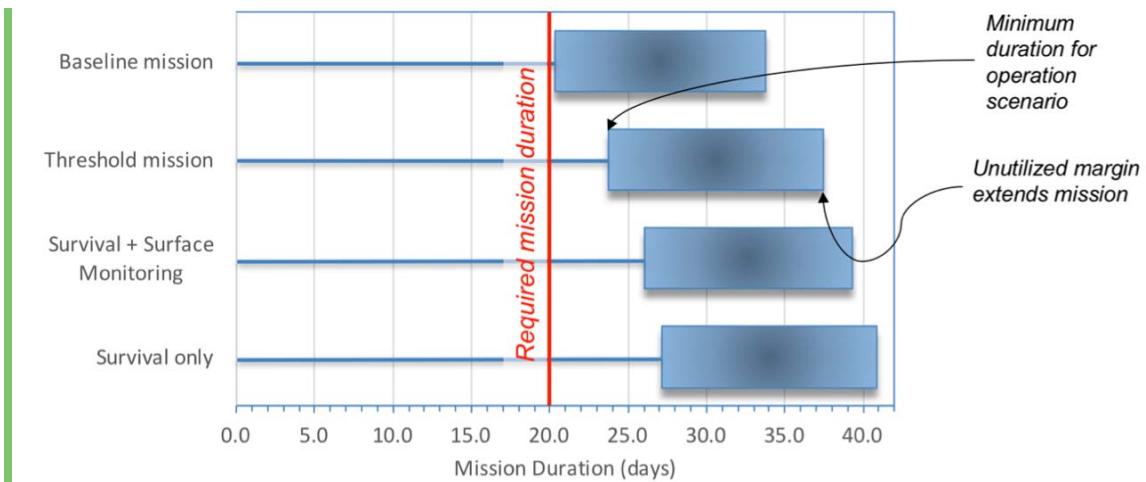
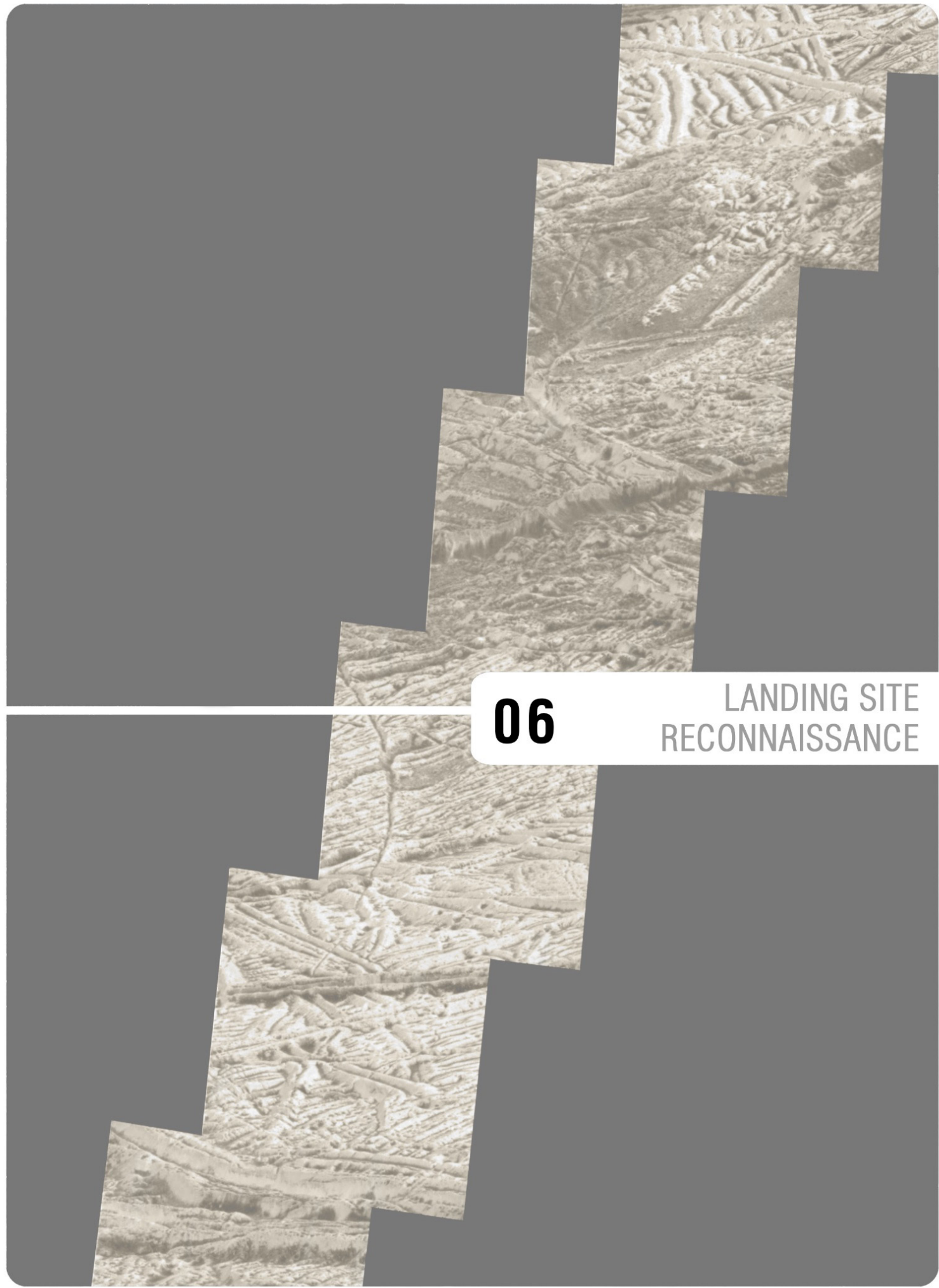


Figure 5.2. Mission concept scenarios for the Europa Lander. The total primary battery allocation is 45 kWh. Sampling, analyses, monitoring, data uplink, and spacecraft survival use this energy throughout the mission, e.g. more sampling and analyses uses the available energy in a shorter period. Blue rectangles indicate energy margin from the batteries. Durations are in Earth days. See text for additional detail on each scenario shown above.

The combination of at least nine lines of evidence for biosignatures, an adaptable sampling sequence that accommodates at least five samples, and the incorporation of significant margin in the surface phase of operations, leads to a mission concept that offers a robust approach to resolving ambiguities associated with searching for life beyond Earth. Additional detail on the mission concept and surface phase of operation can be found in Chapters 8, 9, and 10.



06

LANDING SITE
RECONNAISSANCE



6 LANDING SITE RECONNAISSANCE AND ACCESS CONSIDERATIONS

Selection of a landing site on Europa requires consideration of two main factors: scientific value, and landing site safety and access. The primary goals of the Europa Lander mission are to seek evidence of life and characterize Europa's habitability. Scientific value is therefore correlated to a site's potential for interaction with liquid water in the geologically recent past, interaction with radiation and geologic processing. Radiation is a concern as it would be detrimental to biosignature preservation (Hand et al., 2009, and references therein). Geologic processing of the surface could also obscure or destroy biomarkers, thus careful selection of a landing site should consider the presumed history of the surface. Assessment of the safety of the landing site requires observations at high enough resolution to characterize hazards, including meter-scale boulders, steep slopes, and pits. Below, we present the expected data to be returned by the Europa Multiple Flyby Mission (EMFM) and short discussions on scientific value, radiation, and landing site safety. Together, these considerations describe the reconnaissance necessary to access the locations on Europa that have high scientific values and provide the best opportunity for life detection.

Europa's surface will be investigated by the EMFM instruments at a resolution and spectral range adequate to characterize at least 40 sites, $\geq 2 \text{ km} \times 4 \text{ km}$ in area, at $\leq 1 \text{ m/pixel}$ spatial resolution, as described in the project requirements document (EMFM Project Requirements Document) with additional stereo coverage planned up to 0.5 m/pixel . Ultraviolet, visual, infrared, and thermal imaging, along with radar (sounding, reflectometry, and altimetry), and in-situ particle composition data would all be collected over these sites to aid interpretation of scientifically interesting locations. Stereo images would enable digital terrain models (DTMs) to be produced, providing high-resolution 3-D models of the sites. Especially interesting features may be places of active or recent geologic activity including venting, exotic surface composition, sites of ocean-surface or shallow water-surface interactions, and/or proximal water bodies in the ice shell. The data would also aid evaluation of safe landing sites by informing interpretation of slope angles, block abundance, thermal anomalies, and slope stability. Plume activity would be sought through imaging and in situ fields and particle analyses. If plumes are detected, they would be correlated to geologic features to the degree possible. **Table 6.1** lists the EMFM instruments, a high-level summary of the data that would be collected by each, and the applications to scientific value and landing site safety. The data, along with consideration of engineering constraints, would enable the selection of a scientifically interesting and technologically viable landing site.

Scientific Value

The scientific value of a landing site will necessarily be assessed upon the potential for interactions between the surface and water at or near the surface as well as young surface. These sites may be chosen via evidence of high material mobility (i.e., ocean-surface interactions) or local enrichments of non-ice materials, especially organics. This

narrows sites of interest to those with features that are likely to have formed in the presence of liquid water.

Table 6.1. The instruments of the EMFM, the data they would collect, and the applications of that data to assessing the scientific value and landing safety of regions on Europa’s surface.

Europa Flyby Mission instrument	Data	Applications
EIS	Mid- to high- resolution visible imaging	<ul style="list-style-type: none"> • Image geologic features, slopes, blocks, fractures • Detect possible plumes
REASON	Subsurface sounding Altimetry	<ul style="list-style-type: none"> • Proximity of water to the surface • Surface topography • Permittivity
E-THEMIS	Thermal infrared imaging	<ul style="list-style-type: none"> • Block abundance, hot spots, slope stability
MISE	IR spectroscopic imaging	<ul style="list-style-type: none"> • Surface composition • Detect possible plumes
Europa-UVS	Ultraviolet spectroscopic imaging	<ul style="list-style-type: none"> • Surface composition • Detect possible plumes
SUDA, MASPEX	Composition of dust and gas	<ul style="list-style-type: none"> • Detect possible plumes and determine dust and gas composition
ICEMAG, PIMS	Composition of plasma	<ul style="list-style-type: none"> • Detect possible plumes and determine plasma composition

Ridges, ridge complexes, and chaos terrain (including smaller lenticulae) rise to the top of the list of scientifically valued targets given their possible formation scenarios (e.g., Greenberg et al., 1999; Pappalardo et al., 1998; Spaun et al., 1999; Figueredo et al., 2003; Greenberg et al., 2003; Prockter and Patterson, 2009; Hand et al., 2009; Collins and Nimmo, 2009; Schmidt et al., 2011; Pappalardo et al., 2015). Although morphological evidence does not directly support widespread cryovolcanism on Europa, limited extrusive volcanism may be possible (Fagents, 2003; Quick et al., 2016) and recent observations of putative plume activity increase the potential that subsurface material may emanate from active plume sources (Roth et al., 2014; Sparks et al., 2016). Several compelling theories for ridge and ridge complex formation include mechanisms that produce fresh or exposed materials: the constant working of surface materials (e.g., Pappalardo et al., 1998; Prockter and Schenk, 2005) that would break down ice – either exposing or destroying biomarkers; squeezing up of fresh ice; and eruption of water directly through the ice from the ocean or from subsurface injection (e.g., Ojakangas and Stevenson, 1989ab; Pappalardo et al., 1998; Greenberg et al., 1999; Craft et al., 2016). On the other hand, all formation scenarios for chaos terrain involve the production of liquid water, either: complete melt-through of the ice shell (O’Brien et al., 2002); diapirism with partial melting (e.g., Pappalardo and Barr, 2004; Schenk and Pappalardo, 2004); or significant melting within the ice shell (Schmidt et al., 2011). In these scenarios, recent or current water at or near the subsurface is likely. Chaos materials are generally stratigraphically young (Figueredo and Greeley, 2004). All of these observations place chaos features amongst the highest scientific

value both for habitability and for the search for life. Thera Macula (50°S, 180°E) is an interesting site for both scientific and radiation concerns as, based on its morphology, the chaos feature has been suggested to contain a substantial subsurface reservoir active at the time of the Galileo mission (Schmidt et al., 2011) and is expected to remain so today. Also, Thera Macula receives lower radiation exposure being located outside of the 10 cm radiation depth envelopes (see **Figure 6.1**)

and is influenced less by the deposition of sulfur-rich material ejected from Io as it resides on the anti-jovian hemisphere. As such, this region was selected by the 2012 Europa Lander study as the prime target, with two other chaos sites as backup targets (Pappalardo et al., 2013). This region is also a prime study target for both the EMFM and ESA JUICE missions. Several large ridge systems as well as

Thera Macula are within the region of Europa's surface where putative plumes could have their source (Roth et al., 2014; Sparks et al., 2016); whether there is any correlation between chaos terrains or ridges and eruptions is currently unknown.

Considerations of scientific value imply that a lander would aim to sample geologically young sites, specifically with a stable or gradually changing environment and liquid water interactions. Site types that achieve high marks based on these criteria are described in Figueredo et al. (2003), including chaos regions. The planned coverage by the EMFM will open new areas for consideration as landing sites that will be assessed for scientific value, allowing for a robust selection process.

Radiation

Paranicas et al. (2002), and more recently Nordheim et al. (2016; 2017a) and Patterson et al. (2012), modeled and mapped radiation levels at Europa's surface. Nordheim et al. (2016; 2017a) found that low latitude regions at both the leading and trailing hemispheres are the most heavily irradiated. **Figure 6.1** shows the locations on the surface where charged particle bombardment is expected to process surface material to a radiation dose of 100 eV per 16 amu down to a depth of 10 cm on a timescale of approximately 10 Myr. Such a dose, equivalent to approximately 60 Grad, is generally considered sufficient to fully process material by breaking

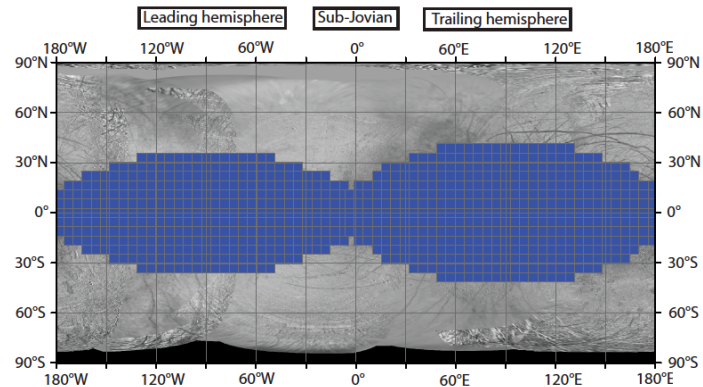


Figure 6.1. In blue, locations where charged particles process surface material to depths of 10 cm or greater. (A significant radiation dose is defined as reaching 100 eV/16 amu in less than 10 My). Depth estimates are given for water ice with a density of 1 g/cm³. From Nordheim et al. (2017a).

most chemical bonds at least once (Paranicas et al., 2009). Thus, within the blue region, samples should be acquired from a depth of at least 10 cm. For landing sites not in the blue region, the lander could access material that has been significantly less processed by radiation at depths shallower than 10 cm. In other words, the requirement to sample to a depth of at least 10 cm is derived from ensuring that the region in blue is permissible from a sampling standpoint. Critically, these calculations are for a globally averaged surface age of 10 Myr. Thus, if the EMFM identifies younger surfaces the radiation depth, and sampling depth requirement, would scale accordingly. Radiation effects on the surface are discussed in more detail in **Chapter 4** (Objective 1D).

Site Characterization

The EMFM will provide excellent scientific reconnaissance for the selection of landing sites. The synergistic investigations of that mission will combine to characterize the science value of potential landing sites. The REASON ice penetrating radar would be able to confirm or detect both large scale water masses like the ocean (if shallow enough), and water lenses within the shell. Additionally, any localized body of water with dimensions larger than the wavelength (5 m) of the Very High Frequency (VHF) radar signal, could be detected, providing a direct measurement of the location of water in Europa's subsurface. MISE would search for regions of non-ice materials, including organics, which likely exist within dark regions on the surface. These regions could be imaged further by EIS. The MASPEX and SUDA instruments would characterize the composition of materials within the europian environment that have been ejected off the surface by sputtering, micrometeoroid impacts, or active plumes, large or small.

The EMFM's Europa Imaging System (EIS) plans to acquire visual imaging of ≥ 40 surface "sites" (site = surface area $\geq 2 \text{ km} \times 4 \text{ km}$, with $2 \text{ km} \times 10 \text{ km}$ swath coverage planned) at a pixel scale of ≤ 1 up to $\sim 0.5 \text{ m/pixel}$ to build DTMs with a post spacing of $\sim 3 \text{ m}$ and vertical precision of $\leq 0.3 \text{ m}$. These DTMs would support slope measurements of $\leq 1^\circ$ accuracy for baselines $\geq 6 \text{ m}$ (*EMFM Project Requirements Document*). These datasets could substantially improve upon the highest resolution imaging ($\sim 6\text{--}12 \text{ m/pixel}$) previously acquired by Galileo (**Figure 6.2**), which is only available for a small fraction of the surface ($10^{-4}\%$).



Figure 6.2. Example of the highest resolution imaging available, across $\ll 1\%$ of the surface, from Galileo at 6 m/pixel .

Landing Site Safety & Access

Site characteristics most important for landing site safety are slope angle, vertical topography relief, block abundance and shadowing. **Table 6.2** describes constraint values for the Europa Lander mission concept. Also, important to landing is the ability of the lander Deorbit, Decent and Landing (DDL) team to employ a Terrain Relative Navigation (TRN) strategy to approach and land at a selected site within an approximately 100 m diameter area. Shadows constrain the landing site to within $\pm 60^\circ$ of equator for TRN requirements. Further, current trajectory design for the EMFM is such that the relative surface-to-spacecraft velocity is too high for EIS Narrow Angle Camera (NAC) high-resolution imaging over parts of the leading and trailing hemispheres. Therefore, high latitudes and regions at the leading and trailing hemispheres are restricted for landing site planning (see **Figure 6.3**).

DTMs derived from Europa Multiple Flyby data would enable characterization of geologically interesting terrains as well as provide input for landing site safety. **Figure 6.4** shows the expected coverage by the EIS NAC stereo imaging for the 15F10 and 16F11 trajectories at the highest resolutions of up to 0.5 m per pixel that would inform the assessment of scientific value and landing site safety for potential landing sites. Colors denote the ground sample distance (GSD). Red hash areas are regions where radiation could be processed to a depth of 10 cm or greater for material 10 Myr old or older (see **Figure 6.1**).

A sampling of regions of scientific interest is denoted by white circles in **Figure 6.4**. Many other interesting features have also been observed, and many more are expected to be revealed with the improved imaging resolution and coverage that the EMFM will produce. In the Northern hemisphere lies Conamara Chaos, and in the Southern hemisphere lies Thrace and Thera Macula, which are chaos regions. Other candidate landing sites as suggested by Figueredo et al. (2003), Prockter and Schenk (2005), Lipps and Rieboldt (2005), and Ivanov et

Table 6.2. Landing site constraints for Europa Lander mission concept.

Constraint	Value
Landing area diameter	• 100 m
Slopes within landing area	• $<25^\circ$
Vertical relief at lander scale	• 0.5 m
Latitude of landing site	• within $\pm 60^\circ$ of equator

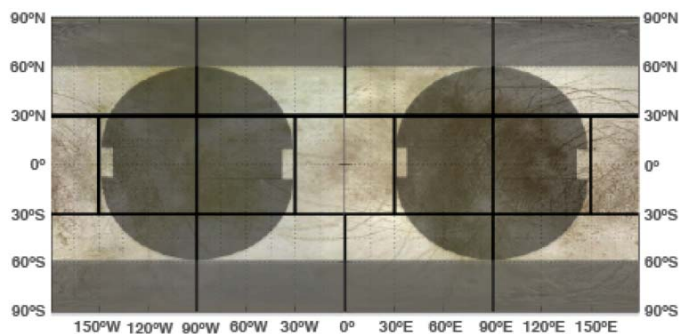


Figure 6.3. Landing site constraints due to TRN technique shadow sensitivities (excludes latitudes poleward of 60°) and the EMFM mission design constraints (circular shaded regions are excluded) (*Mission Design Team, EMFM*).

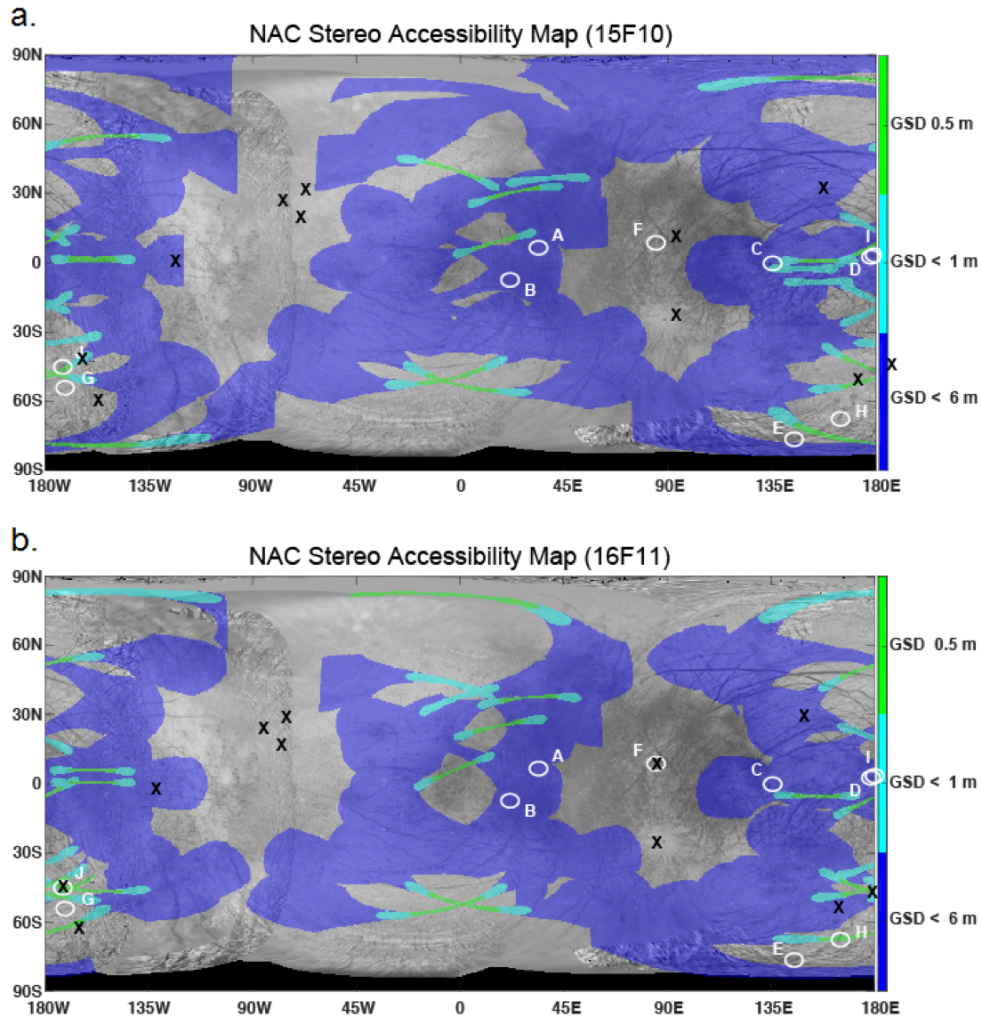


Figure 6.4. Maps of locations accessible for stereo imaging by the EMFM EIS NAC for trajectories: **a.** 15F10 and **b.** 16F11. Colors depict ground sample distance (GSD) resolution: dark blue GSD < 6 m, light blue GSD < 1 m and green GSD of ~ 0.5 m (although stereo images cannot be obtained below a spacecraft altitude of 50 km). Black X's denote the approximate locations of selected Chaos terrains known to exist across the surface, including Thera Macula shown at 50°S and ~180°E. **Table 6.3** lists a sampling of areas described as potentially scientifically interesting landing sites, denoted by white circles on the map.

al. (2011) are also denoted in **Figure 6.4** and **Table 6.3**. As coverage and engineering constraints allow, these and others sites can be considered. As trajectory development for the EMFM continues, changes in the latitude coverage could be considered, although at a potential cost of additional fuel depending on the delta-v required. Latitude changes or repeat coverage would also change the downstream flyby ground track locations. This mission design flexibility, as described by the EMFM, Mission Design Team, is limited, but may provide a means to react to new findings, such as plume observations or discovery of recent geologic activity. A future discovery of recent geologic activity, and therefore potentially also a younger surface,

Table 6.3. Proposed scientifically interesting landing sites.

Feature #	Feature Name	References
A	Smooth plains ("puddle" 6° N, 323° W)	Greeley et al., 1998
B	Smooth bands (Band D, 6° S, 240° W)	Prockter et al., 2002; Figueredo et al., 2003
C	Castalia Macula (~ 0°, 135° E)	Figueredo et al., 2002; Prockter and Schenk, 2005
D	Cilix (2° N, 182° W)	Lipps and Rieboldt, 2005
E	Astypalaea Linea and surrounding ridges (76.5° S, 220.3° W)	Lipps and Rieboldt, 2005; Johnson, 2001
F	Conamara Chaos (9.5° N, 273.3° W)	Figueredo et al., 2003; Lipps and Rieboldt, 2005; Schmidt et al., 2011
G	Pull-apart zone (51.8° S, 177.2° W)	Ivanov et al., 2011
H	Pull-apart zone (68.1° S, 196.7° W)	Ivanov et al., 2011
I	Dark and likely smooth plains (2.4° N, 181° W)	Ivanov et al., 2011
J	Thera Macula (50°S, 180° E)	Schmidt et al., 2011; Pappalardo et al., 2013

could be cause to land in higher radiation areas on Europa’s surface if the activity is deemed to have occurred in the last 10 Myr.

There are no landing location constraints due to radiation on the engineering components, as the baseline shielding would be adequate to protect the instruments and spacecraft electronics from expected levels, even for a low-latitude landing site. **Figure 6.5** shows the calculated spacecraft radiation dose rates due to photons, electrons, protons and total dosage vs. aluminum shielding thickness at Europa’s trailing hemisphere. Although the shielding may

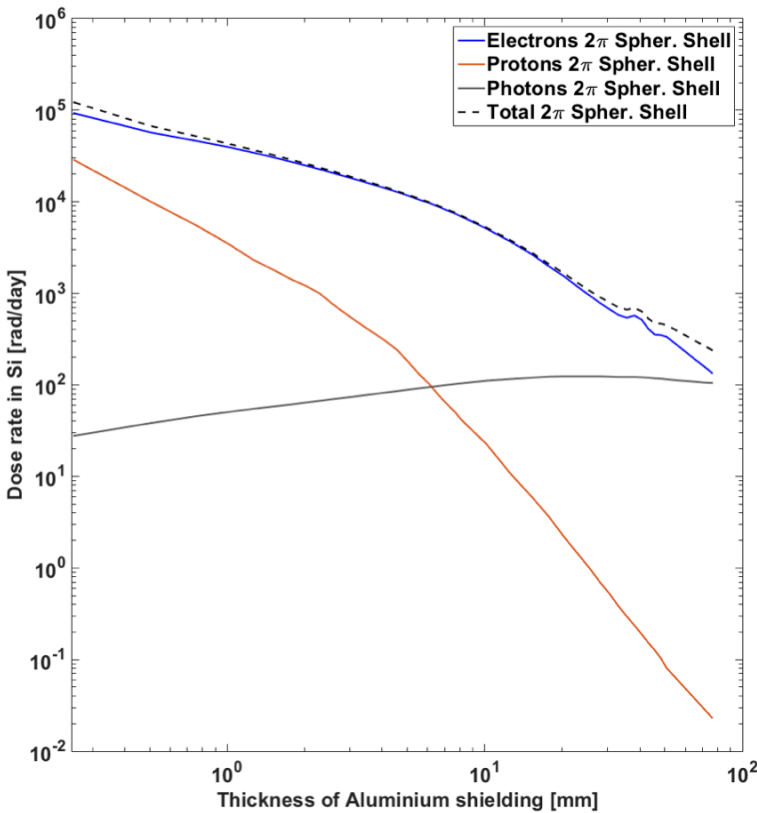


Figure 6.5. Dose rate in Silicon (Si) for different shielding thicknesses at the trailing hemisphere of Europa. This dose is representative of that received by spacecraft hardware behind a 2π aluminum shell. The dose at the trailing hemisphere is estimated by determining the dose in Jupiter's radiation belt when Europa is not present and then dividing that by a factor of two to account for self-shielding by the moon.

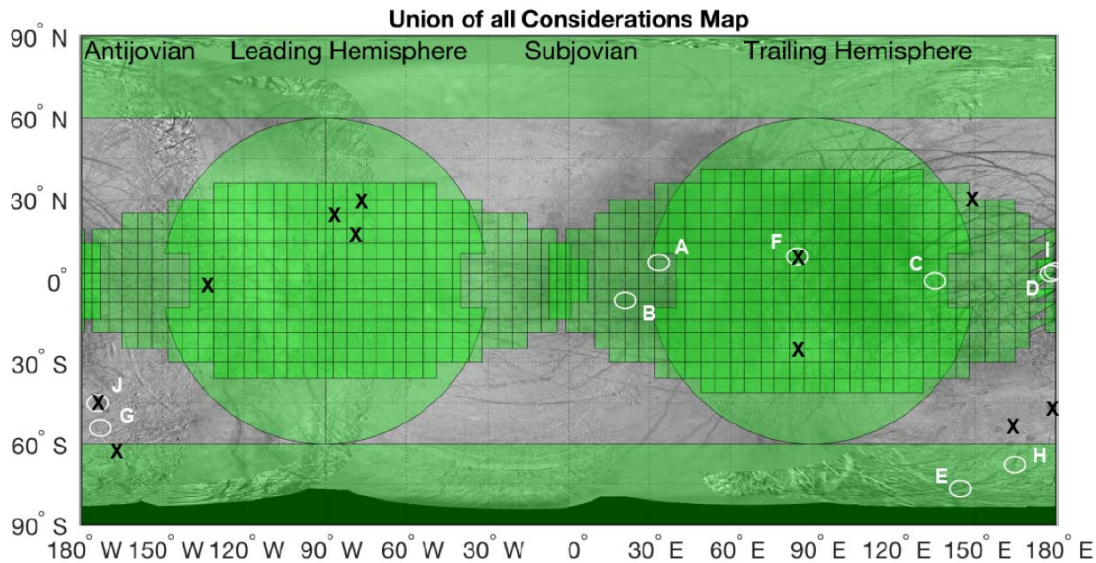


Figure 6.6. Preliminary summary of landing site selection and sampling depth considerations shown in green. These are due to EMFM trajectory constraints (circular areas), shadowing at high latitudes ($\geq 60^\circ$ Lat), and sampling considerations due to the radiation dose from deeply penetrating (up to 10 cm depth) electrons (pixelated lens-shaped regions). Black X's denote the approximate locations of selected Chaos terrains. White circles denote potentially scientifically interesting sites described in **Table 6.3**.

enable a low-latitude landing site, achieving the science objectives means a preference to sample in regions where radiation has not processed surface material all the way down to the 10 cm sampling depth. **Figure 6.6** shows a synthesis of all constraints for landing site selection.

Landing Site Selection

The strategy to characterize 40 sites with the EMFM, and the downselect process based on the landing safety requirements and scientific criteria, would serve to provide at least two viable landing sites. Selection of a landing site on another world is a matter of finding the balance between meeting landing (DDL) and landed (surface operations) subsystem engineering requirements and achieving mission science goals. For example, the processes followed for landed missions on Mars have varied, with some primarily involving the engineering and science team members who work directly on that specific mission; other missions add to this an outside science working group/steering committee; and still others add a series of public/scientific community workshops for site suggestion and analysis (Masursky and Crabill, 1976; Masursky and Crabill, 1981; Golombek et al., 1997; Vasavada et al., 2000; Bridges et al., 2003; Golombek et al., 2003; Arvidson et al., 2008; Grant et al., 2011; Golombek et al., 2012; Golombek et al., 2013; Golombek et al., 2014; Flahaut et al., 2014; Ori et al., 2015; Bridges et al., 2016; Golombek et al., 2016). For the Europa Lander mission, the process would leverage

lessons learned from previous missions, and solicit community-wide input. **Figure 6.7** depicts a proposed general pathway to landing site selection, from data acquisition to site selection.

For the NASA Mars missions of the past two decades, a chief discriminant regarding how the process was conducted was whether the mission was PI-led (Scout- or Discovery-class missions, specifically Mars Polar Lander, Phoenix, and InSight) – for which the landing site candidates and evaluation process are a key component of the proposed mission science – or whether the mission was a Program-directed (Strategic) mission for which the choice of landing site was undefined until late in the mission development effort (Mars Pathfinder, Mars Exploration Rovers, Mars Science Laboratory, Mars 2020). Similar permutations of these processes have been applied for landing site selection on other worlds, as well, going back to the Surveyor/Apollo efforts of the 1960s (e.g., El-Baz, 1968). For NASA landed missions in recent decades, it is ultimately the NASA Associate Administrator responsible for overseeing planetary science who is briefed and makes the final decision on where to land, taking into account the combination of engineering and science risk as well as the potential for scientific reward.

The SDT advocates for an open, inclusive, and publicly visible landing site selection process and believes that this would be a benefit to the achievement of the Europa Lander

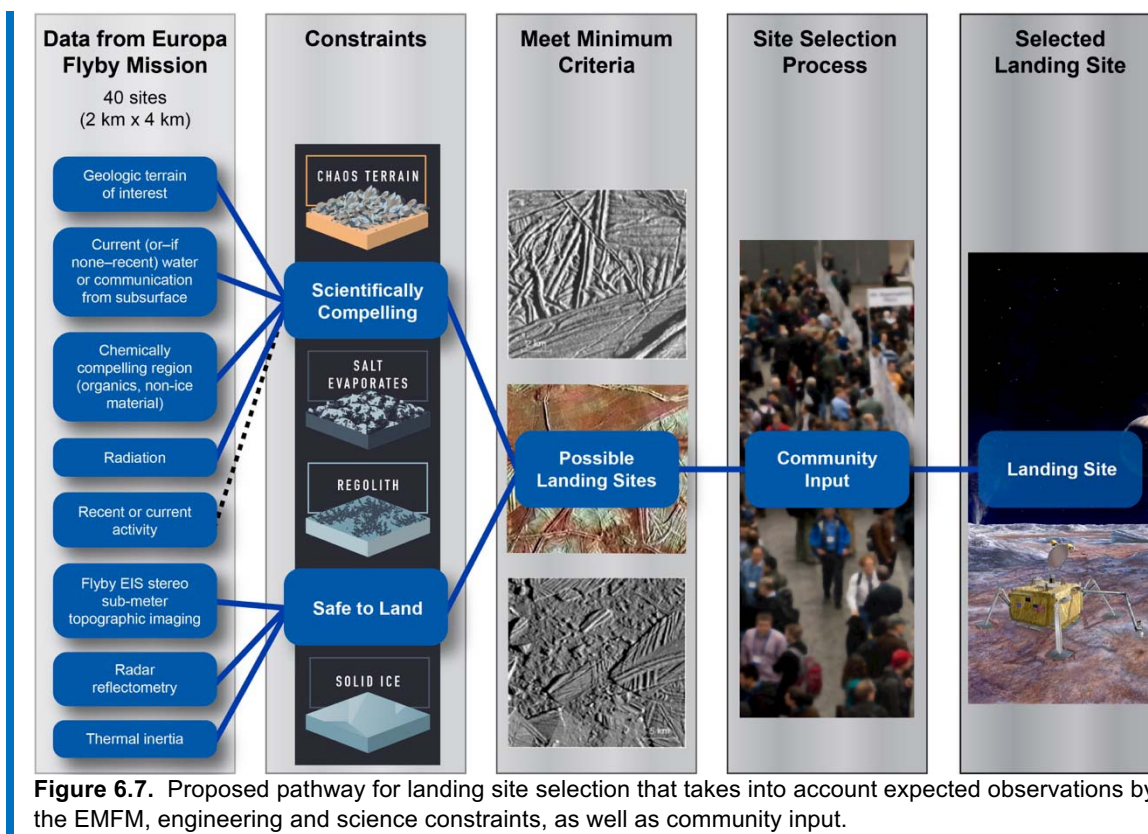
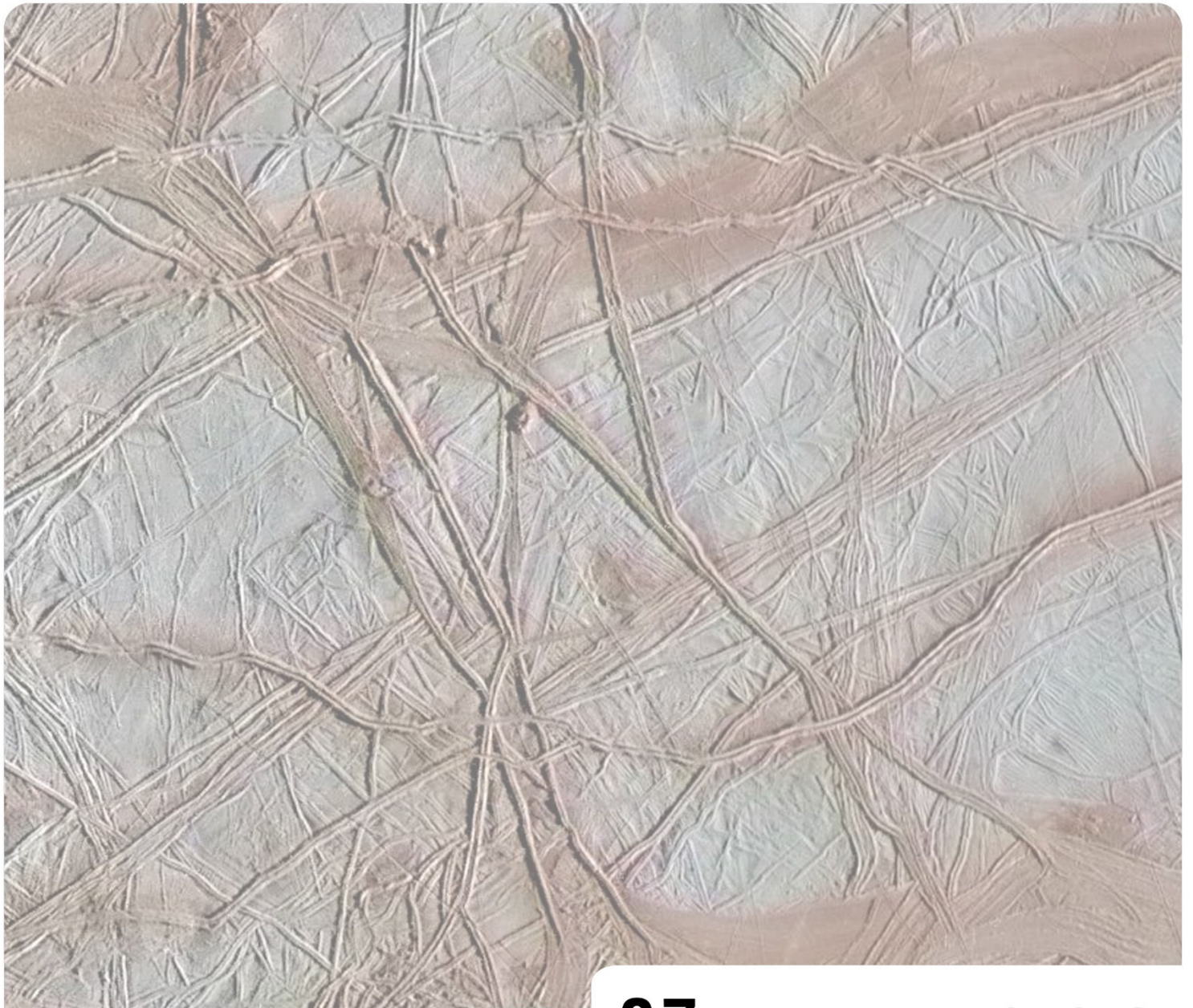


Figure 6.7. Proposed pathway for landing site selection that takes into account expected observations by the EMFM, engineering and science constraints, as well as community input.

mission science goals. A series of site selection workshops, perhaps held annually, would provide a forum for project engineers, science team members, the interested scientific community, and interested members of the public to gather and update each other on landing site engineering constraints, mission science goals, landing and landed hardware subsystems, science payload, and observations of candidate landing site science and engineering properties obtained by any means (e.g., Europa flyby mission instruments, Earth-orbiting and ground-based telescopes, ESA's JUICE mission). Such workshops would provide the Europa Lander team an opportunity to update the science community and public on mission development progress and ensure that no stone is left unturned in the effort to identify a primary and backup landing site that would optimize between engineering and scientific risk and science return. These workshops would further provide a forum to share any critical new findings from the broader scientific community that might impact the search for life on Europa (e.g., new lessons learned from investigation of life in Earth extreme environments, preservation of organisms in ice, etc.). These workshops could be developed in two phases. Early workshops, based solely on existing Galileo datasets could identify notional landing sites but also focus on overall site selection criteria and engineering constraints as well as identify other key trades. Once new data from the EMFM becomes available, the community will have a relatively shorter period of time to study the new images using previously defined criteria and methodologies and to propose actual candidate landing sites that would be vetted and ultimately downselected.

In the SDT's experience, such workshops also provide opportunities for students and early career colleagues to get involved with lander mission science – potentially informing concepts for Participating Scientist and Data Analysis proposals – and can even create opportunities for education and public engagement (e.g., Edgett, 2000).



07 PLANETARY PROTECTION



7 PLANETARY PROTECTION

The potential habitability of Europa confers a great responsibility on our future exploration of the european surface and subsurface.

Preventing the forward contamination of Europa by microorganisms from Earth contained on, or within, a robotic spacecraft, is paramount to the highest-level goals of the Europa Lander mission. Success of the mission requires strict adherence to planetary protection protocol and requirements.

All elements of the Europa Lander mission will comply with planetary protection requirements, policies, and procedures. The following documents, or the latest approved versions, are applicable:

- NPD 8020.7G Biological Contamination Control for Outbound and Inbound Planetary Spacecraft (Revalidated 11/25/08).
- NPR 8020.12D, Planetary Protection Provisions for Robotic Extraterrestrial Mission, Rev. D, April 20, 2011 (Requirements, including guideline on planetary protection categorizations).
- Committee on Space Research (COSPAR) Planetary Protection Policy, 20 October 2002 (as amended 3/24/2011).

The mission design of Europa Lander (**Chapter 10**), as a spacecraft that will land and also potentially impact the european surface prior to landing, should be compliant with the requirements of PP mission classification Category IV under current COSPAR and NASA planetary protection policy, i.e., *less than 1×10^{-4} probability of contaminating the european ocean by a viable Earth microorganism*. The ultimate landing, a relatively low-velocity impact of Europa Lander onto Europa's surface without the benefit of atmospheric heating, drives the derived requirement for bioburden reduction processing of the spacecraft hardware.

The importance of preventing forward contamination is two-fold, first as a legal and ethical consideration to protect potentially viable organisms and ecosystems beyond Earth, and second as a scientific imperative to ensure that false positives are minimized (NAS, 1958; COSPAR, 1964; Rummel and Billings, 2004; UNOOSA, 1966; and see Hand et al., 2009 for a more detailed discussion). The specific language to which the United States, and therefore NASA, committed to in 1967 is that of the Outer Space Treaty, Article IX: "States Parties to the Treaty shall pursue studies of outer space, including the moon and other celestial bodies,

and conduct exploration of them so as to avoid their harmful contamination ... and, where necessary, shall adopt appropriate measures for this purpose.”

Over the past two decades the National Research Council has conducted several studies at NASA’s request to consider in detail the planetary protection risks and challenges associated with the exploration of Europa (NRC, 2000; NRC, 2011). These studies have further emphasized the need for sterilization and bioburden reduction, and have advocated for the continued development of tools and techniques to improve pre- and post-launch capabilities for achieving the $<1 \times 10^{-4}$ probability of contaminating the Europa’s ocean.

In addition, work for both the Mars Science Laboratory (Curiosity) and the upcoming Mars 2020 mission have advanced NASA’s understanding of, and capabilities for, protecting the science of the mission through planetary protection requirements. The Europa Lander mission must leverage NASA’s ongoing investment in these efforts to ensure that both Europa and the science of the lander mission are protected. Additional consideration on this topic, and the mission design, are provided in **Chapter 10**.

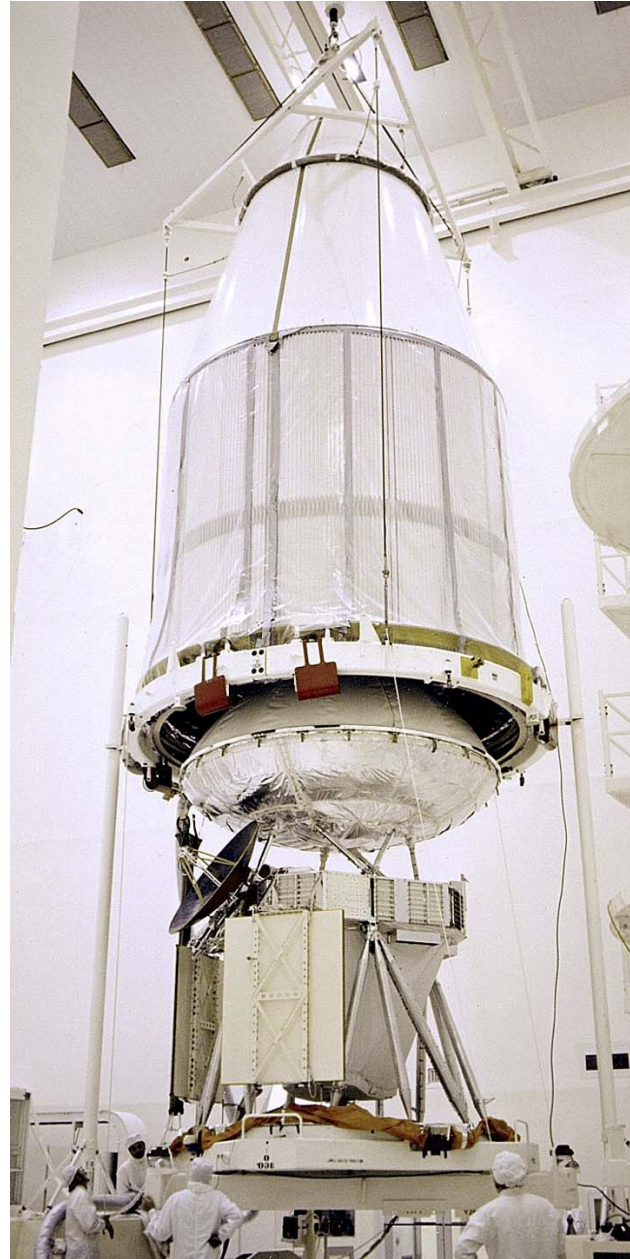
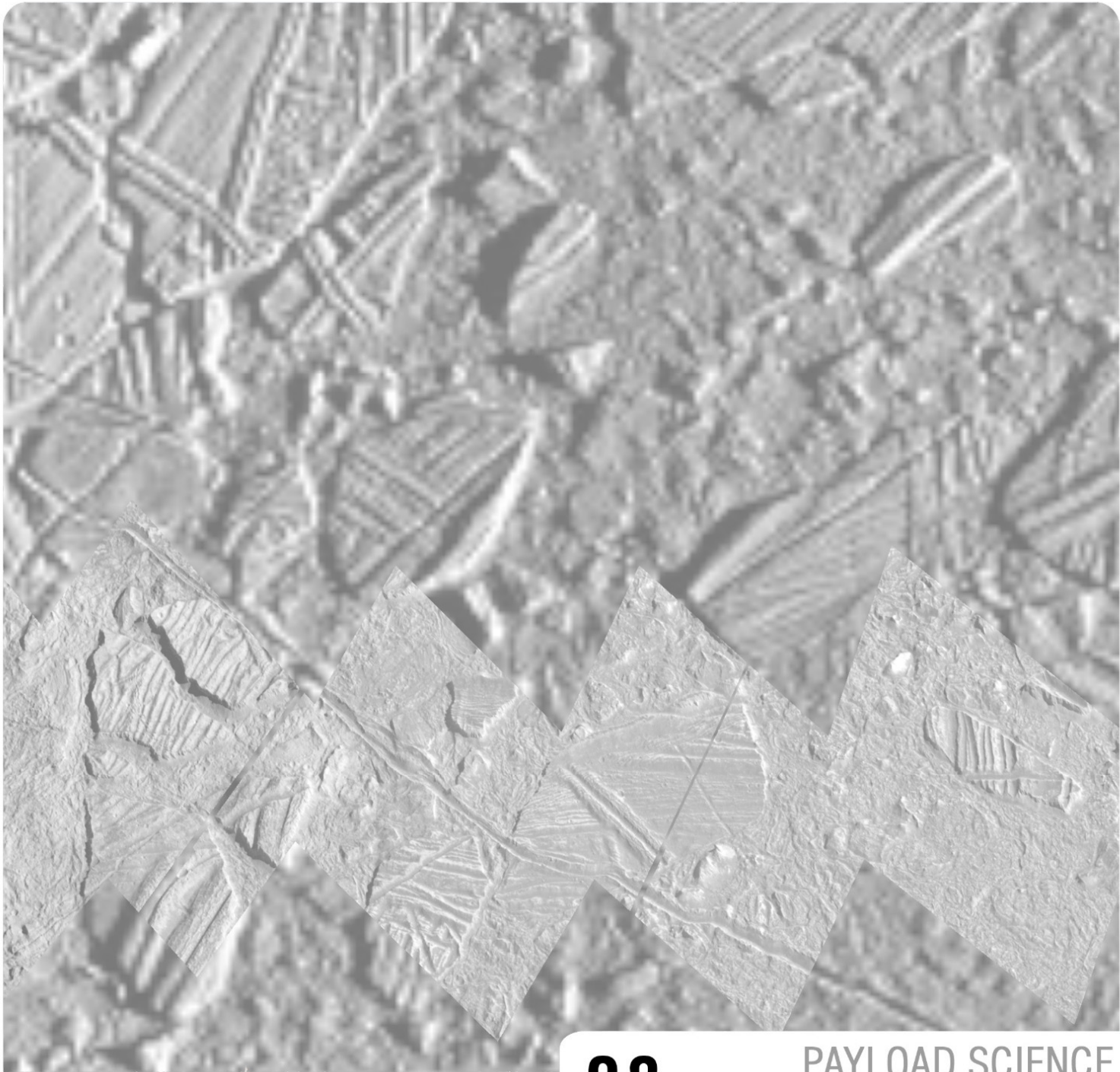
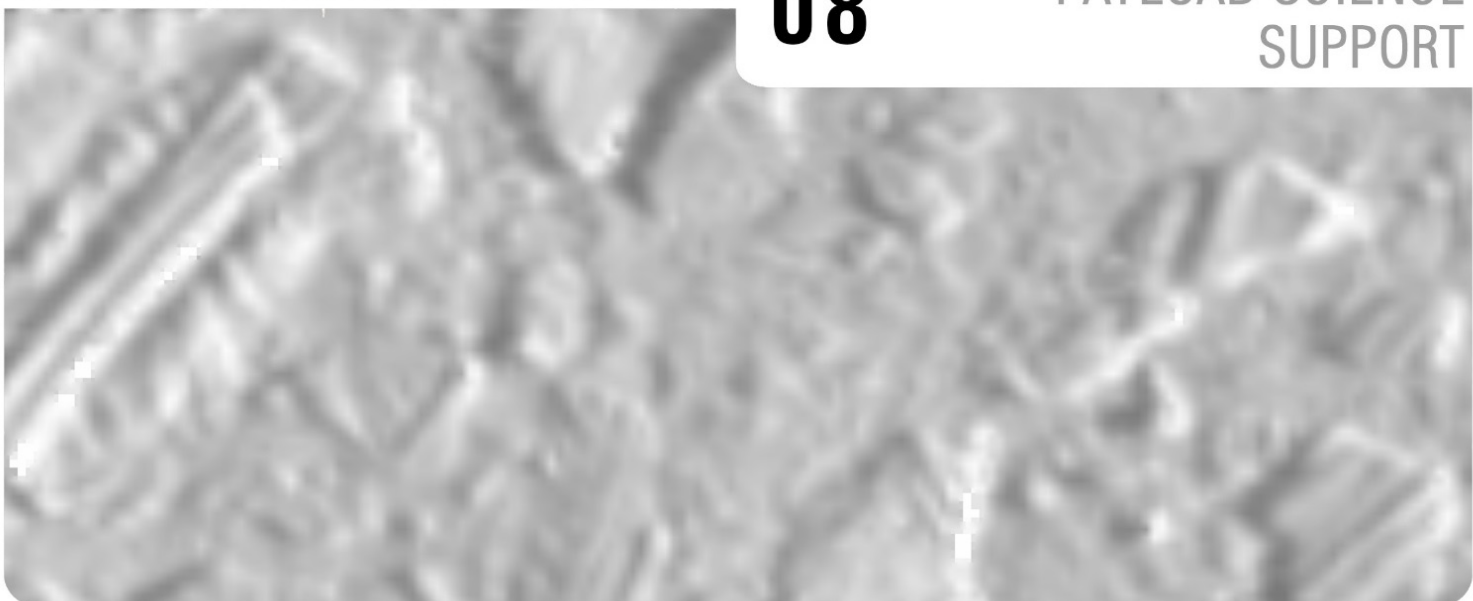


Figure 7.1. A Viking spacecraft (Orbiter plus Lander) being covered by the Centaur rocket nose fairing at Kennedy Space Center on July 3rd, 1975. The lander (near center of image) was encapsulated in a bioshield after bakeout for planetary protection. Below the lander, the orbiter with its black high-gain antenna and folded solar panels can be seen.



08

PAYLOAD SCIENCE
SUPPORT



8 PAYLOAD SCIENCE SUPPORT CAPABILITY

8.1 INTRODUCTION

8.1.1 DESIGN DRIVERS AND UNIQUE CHALLENGES COMPARED TO PAST MISSIONS

Compared with past surface sampling missions such as the Mars missions Viking, Phoenix, and Curiosity, the Europa Lander sampling system is faced with several distinct challenges:

- Less-understood terrain features at sampling-system scale (~10 cm)
- Shorter mission duration
- Greater target depth for sampling
- Tighter requirements on temperature increase of sample before delivery
- High-radiation environment

The first of these – poorly-characterized terrain at small scales – motivates adoption of a sampling end effector designed for robustness and effectiveness against a wide variety of terrain types and shapes. Similar to the Viking and Phoenix Landers, but different than the rover Curiosity, the terrain immediately in front of the landing spot must suffice for sampling locations; there is no mobility system that can be used to search for a better site. Furthermore, a shorter mission duration argues for a mechanically robust end-effector.

8.1.2 SAMPLING SYSTEM OUTPUT CHARACTERISTICS

The sampling system would present or deliver to the instruments a container of raw, unprocessed sample at <150 K (or, 10 K above the surface temperature if the surface starts at >150 K). This temperature requirement is set so as to allow the composition of the natural ice and materials trapped within (e.g., gases) to be analyzed or captured prior to sublimation or melting within the warmer vault. The sample could consist of a range of particle sizes and may contain ice, salts, and dust and/or other insoluble material in proportions that are, a priori, unknown. From each site, the 7 cc sample would be portioned into 3 separate containers that

would be passed to the Vibrational Spectrometer (1 cc), Organic Compositional Analysis instrument (1 cc), and Microscope for Life Detection (5 cc).

8.1.3 INSTRUMENT SAMPLE PROCESSING FRONT ENDS

Individual sample analysis instruments may require additional sample processing after receiving a container from the sampling system. For the mission concept study conducted in coordination with the Europa Lander Science Definition Team, several past missions served as useful analogues for the Organic Compositional Analysis (OCA) and Vibrational Spectrometer (VS) instruments. Here, we focus on the Microscope for Life Detection (MLD) as the driving case for sample processing front end.

The MLD front end must first ensure that the sample is dissolved in enough liquid water to enable effective filtering. Although the sample may have enough native European water ice to suffice, there is no a priori guarantee – e.g., the sample may be mostly or entirely salts. To handle this unknown, the front end would need to warm the sample and add liquid water (see MLD Model Payload discussion in section 4.5). A lab rule of thumb calls for a volume of water 5× the volume of sample to be dissolved. Next the sample would need to pass through a 2-stage filter. The use of a ~20–50 micron filter during the first stage is intended to strain out insoluble particles that are larger than typical terrestrial single-cell organisms so that such particles neither clog a fine filter nor optically block the microscope from discerning organism-scale particles. The second stage 0.2 micron filter would trap particles of the desired size range to search for the possible presence of cells. This sample derivative could then be presented to the microscope for analysis.

Analogues can be found for each step in the sample processing from flight instruments or, in some cases, automated marine sampling systems. Further, for resource (mass, volume, and power) scoping purposes, it is assumed that the front end would have an individual processing hardware chain for each sample as a conservative estimate. The mass would include the processing chain, as well as key ancillary hardware that the overall front end would require (e.g., reservoir tanks for water or post-analyses samples).

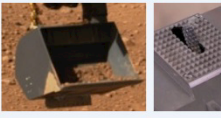
8.2 SAMPLING SYSTEM

This section provides information on the sampling system conceptual design and operations for the Europa Lander mission. This information includes requirements and constraints that will be levied on proposed instruments that intend to examine surface samples, as well as information regarding the interfaces between the sampling system and proposed instruments.

8.2.1 SAMPLING SYSTEM HERITAGE MISSIONS

Past Mars surface missions with the analogous need of collecting and analyzing bulk samples (i.e., ~1 cc) serve as a useful comparison point for the lander sampling system. **Figure 8.1** provides a qualitative assessment. Both the Viking and Phoenix missions used scoops as the primary method to excavate and collect bulk samples of unconsolidated soil-type material. However, against hard material, like cryogenic water ice, scoop blades tend to be poor in achieving depth. The Phoenix Rapid Acquisition Sampling Package (RASP) successfully generated sample against hard ice material with minimal thermal modification to the sample, although only to a depth limited to approximately less than 1 cm. Percussion drills, like MSL, have an advantage excavating hard material to depth, but tend to be less robust against complex terrain shapes and less amenable to minimizing thermal input to the sample.

The current architecture for Europa Lander sampling combines a counter-rotating saw for bulk excavation to depth, with the flight-proven Phoenix approach (i.e., scoop + RASP) for ice sample collection (see **Figure 8.1**).

Mission	Tool	Excavation	Excavation to >> 1cm		Topography Robustness*	Sample Volume	Sample Temperature	Mass / Power
			Hard	Soft / Loose				
Viking Scoop			Red	Green	Red	Green	Green	Green
Phoenix Scoop + Rasp			Red	Green	Yellow	Green	Green	Green
MSL Drill			Green	Green	Yellow	Green	Yellow	Red
Europa Lander Saw + Scoop + Rasp			Green	Green	Green	Green	Green	Green

* i.e., robust to surfaces such as hard cryo-ice rough/broken at all scales

Tool Efficacy: Poor Challenge Good

Figure 8.1. Sampling Heritage. The Europa Lander sampling system combines a counter-rotating saw (robust for excavation in rugged terrain) with a Phoenix-derived RASP for sample collection. Tool efficacy in each case is evaluated against the original requirements for that mission.

8.2.2 SAMPLING SYSTEM OVERVIEW

The Europa Lander would provide a sampling system as a spacecraft capability. The sampling system would be critical to the mission's scientific investigations that require evaluation of the surface material. The sampling system is responsible for excavation, collection, and presentation (or transfer) of samples to scientific instruments for observation and analysis. The sampling system is also responsible for the integrity of the sample from excavation until physical transfer into any instrument. The principal elements of the sampling system, as summarized in **Table 8.1** and shown in **Figure 8.2**, include a lander-mounted robotic arm, a tool for sample excavation, a sample collection device, a sample transfer dock, and a mechanism for moving, presenting and transferring samples to instruments. Each element is described below.

Table 8.1. Sampling System Infrastructure.

Mechanical Element	Brief Description
Robotic Arm (RA)	Lander mounted arm with end-effectors for excavation and collection of surface samples. The arm is not intended to accommodate in situ placement of science instruments for contact science or proximity observations of the surface.
Sample Excavation Tool	Primary tool mounted to the end of the robotic arm for sample excavation.
Sample Collection Device	Primary device mounted to the end of the robotic arm to collect the excavated sample. Also responsible for packing sample into containers for presentation/delivery to instruments.
Sample Transfer Dock	Hardware mounted on the lander where the robotic arm docks to unload sample containers from the sample collection device.
Sample Transfer Mechanism	Lander-mounted mechanism for handling sample containers for presentation/delivery to scientific instruments.

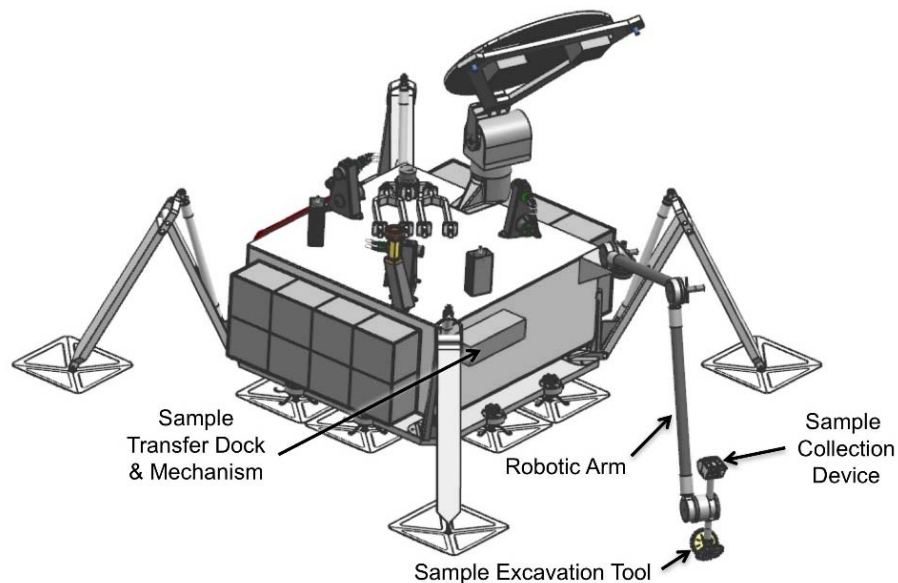


Figure 8.2. Europa Lander surface configuration showing the sampling system. Additional detail can be found in **Figure 8.3**. For scale, the central chassis is about 1 meter square.

8.2.3 DESCRIPTION OF THE SAMPLING SYSTEM

Robotic Arm

The sampling system would include a robotic arm (RA) for acquisition of surface samples from within a defined workspace. The RA would be approximately 1.4–2.2 m in length (**Figure 8.2** shows a 1.6 m arm) when fully extended. The arm would be capable of 5-DOF (degrees of freedom) motion and would have two end effectors. These end effectors would be responsible for extracting and collecting surface samples from a depth of at least 10 cm and transferring them back to the lander for close observation by the science payload.

Sample Excavation Tool

The current configuration for the sample excavation tool is a combination of two counter-rotating, offset saw blades. Prototypes of this tool have demonstrated excavation of cryogenic water ice materials from depths greater than 10 cm in a laboratory setting. Saw tools have advantages over drills, including: 1) effectiveness over a wide range of mechanical orientations, 2) limited requirements for pre-loading on the cutting target, and 3) being largely agnostic to local surface topography (Berisford et al., 2016).

Despite the above limitations, coring could prove useful for several reasons. An intact core retains the spatial concentration of chemical species in a heterogeneous sample enabling 1) extremely low limits of detection via local chemical probes, and 2) association of organics with mineral phases to help determine their provenance. A core of length 10 cm or more captures a range of environmental exposure effects from the uppermost processed surface to the well-protected interior, allowing gradients to be quantified via spatially-resolved analyses. Moreover, following surface examination, a core could be actively and cleanly delivered to a sealable sample vessel, and analyzed as a bulk sample if required.

Sample Collection Device

The sample collection device would be responsible for aggregating sample excavated from the surface at the target depth. It would also play a role in packaging the material into containers for presentation (or delivery) to the science instruments. The sample collection device would pack the sample in the canister to ensure an adequate amount of sample has been collected. Once sample has been collected from the target depth and packaged for delivery, it would be transferred back to the lander via the sample transfer dock.

Sample Transfer Dock

The sample transfer dock would be mounted on the lander vault and used to accommodate docking of the robotic arm. Once the arm is docked to the lander, this would allow the sample

collection device to transfer sample containers to the lander. The dock may also serve as a reset location for the collection device and/or as a storage area for additional sample containers.

Sample Transfer Mechanism

The sample transfer mechanism would receive the sample from the sample collection device via the dock and provide it to the instruments. The mechanism would preserve the sample integrity (volume, temperature) while presenting it to instruments for observations, or until physical transfer of the sample into an instrument is completed.

8.3 SAMPLING WORKSPACE

The exact shape of the accessible workspace is dependent on the shape of the terrain and the final lander configuration geometry, as well as the final length of the arm. A notional workspace is shown below for an RA of approximately 1.6 m in length, shown in **Figure 8.3**. There would likely be a region of surface terrain close to the lander that is not available for sampling due to kinematic constraints of the arm. The sampling workspace would also be limited by potential interference of the angular sweep of the arm with other elements of the lander. The sampling workspace would have a minimum required area of approximately 1.8 m^2 for a nominal landing condition. This workspace size would support excavation of the minimum required number of samples (5 for Baseline, 3 for Threshold). Workspace sizing also includes area to distribute additional materials either excavated but not collected (e.g., “tailings” from the sampling system), or collected but not delivered (dumped sample). These tailings and any dumped sample would potentially be observable by the CRSI. See **Figure 8.3** for visualization of the sampling workspace available for a nominal landing condition. In the case where the lander body rests on a local protrusion, for example, the extent of the arm’s

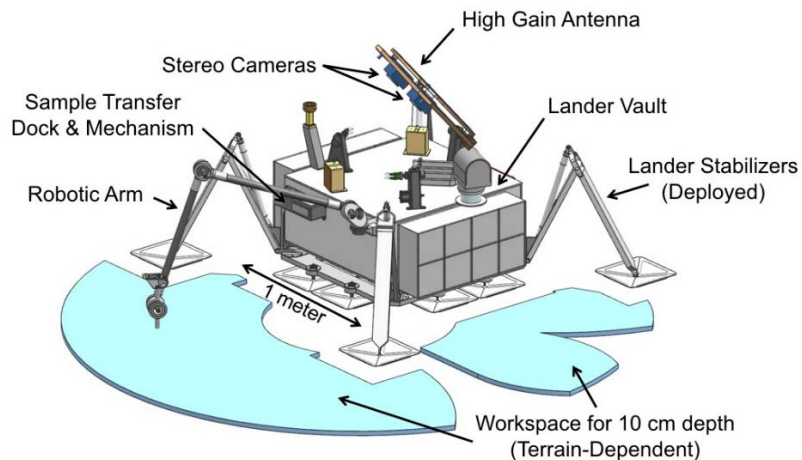


Figure 8.3. Sampling Workspace, Flat Terrain. The area accessible for sampling (shown in blue) will be terrain-dependent, with generally the widest reach being available on relatively flat terrain. The 1-meter width of the lander is indicated for scale.

Table 8.2. Sampling System Requirements and Sample Characteristics.

Requirement	Baseline
Number of surface samples to be acquired	5
Minimum amount of each sample delivered to each instrument	5 cc (MLD), 1 cc (OCA), 1 cc (VS)
Minimum target depth for delivered sample	10 cm (below horizontal surface)
Minimum fraction of delivered sample from target depth	80% (by volume)
Maximum fraction of sample-to-sample cross-contamination	No requirement but will characterize
Maximum temperature of sample prior to presentation or delivery to science instrument	150 K or <10 K above surface temperature, whichever is greater

reach to the surrounding lower terrain would be relatively reduced, as shown in **Figure 10.3**. In general, the largest workspace is expected to be in a flat-terrain case.

8.4 SAMPLE CHARACTERISTICS

The Europa Lander nominal mission would include the capability to acquire, present and transfer five distinct samples to the science instruments. The sampling system would be responsible for excavating, collecting, and delivering samples to the scientific payload, as well as for maintaining the sample integrity until final delivery into an instrument. The hardware and the energy are sized for achieving ≥ 10 cm sampling depth. Samples would be obtained and preserved with the characteristics outlined in **Table 8.2**. Note that each sampling site selected would have 7 cc of material excavated from the target depth (or greater) and delivered back to the instruments. This 7 cc of material would be portioned into three containers of sizes 1 cc, 1 cc, and 5 cc for the OCA, the VS, and the MLD, respectively.

There could be some unavoidable mixing of materials from different depths during sampling; the requirement is currently that $>80\%$ of material within a delivered sample originates from ≥ 10 cm depth. Cross contamination from sample to sample would depend on the final design of the sample handling components, the surface material composition, and the ability to discard excess material between samples. Cross contamination would be characterized during development and minimized through operational procedures. The sampling system would be capable of acquiring samples from both consolidated and unconsolidated mixtures of cryogenic ice and non-ice materials. The sampling system lifetime and capability will meet the requirements for total desired number of samples to be acquired (see **Table 8.2**).

8.5 SAMPLING SYSTEM OPERATIONS

The lander flight computer would control placement of the arm and end-effector for sample acquisition. Samples would be collected after excavation at selected sample sites within the

workspace and then delivered one at a time for observation/analyses by the science instruments in the vault. Note that the sampling system would be capable of having sample sites selected by either ground operators or by onboard algorithm. In the case of the latter, the sampling system would be capable of conducting a sampling cycle in a fully autonomous fashion with no input from ground operators, from target selection to sample delivery. This autonomous capability is to guard against a prolonged telecommunications fault during the short mission lifetime, and will be in place to provide added assurance that the mission threshold science would be met. **Figure 8.4** presents a storyboard of operations for a single sampling cycle.

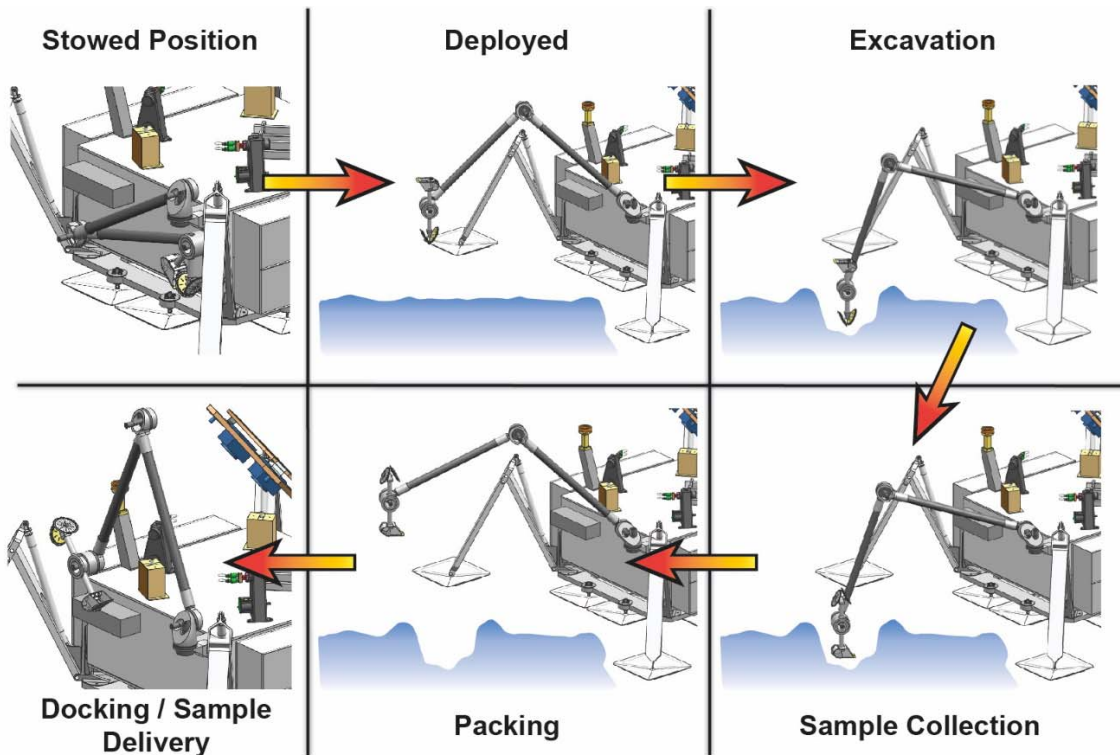


Figure 8.4. Sampling system storyboard shows the sequence (represented by the arrows) starting in the stowed position of the arm and end-effector operation.



09

SURFACE OPERATIONS
CONCEPT



9 SURFACE OPERATIONS CONCEPT

9.1 INTRODUCTION

The Surface Phase is the primary segment of the Europa Lander mission for science activities; key requirements are summarized in **Table 9.1**.

Table 9.1. Key requirements and constraints on landed operations.

Requirement or Constraint	Value	Comment
Landed mission duration	20 days nominal	Battery energy is the limiting factor
Number of sampling cycles	5 (Baseline)	Additional sampling possible if energy permits
Tactical Command cycle duration	10 hours	Driven by the telecom relay carrier orbit

The Surface Phase is expected to last at least 20 days, during which time the lander is expected to complete a total of at least 5 sample acquisitions. During this mission phase, resources such as energy, thermal, and data would be tightly constrained and, as a result, surface operations would be highly automated. As noted in the table, the key constraint on mission life is the total energy available for the mission.

9.2 SURFACE ENERGY

Figure 9.1 shows a breakdown of how energy would be sub-allocated to particular functions for a sampling cycle. During an operational cycle where sampling is carried out, approximately half of the energy utilized would be for background engineering functions (avionics, communications, survival heating, etc.), and for continuous science monitoring of the surface (e.g. with the GSS), while the other half of the energy would be used for sample acquisition (robotic arm and excavation) and analyses activities (science payload). During an operational cycle where no sampling is carried out, only the background engineering and monitoring portion of the energy would be utilized. Over a 20-day surface mission scenario, including 5 sample cycles, 4/5 of the total energy would be allocated to background engineering and

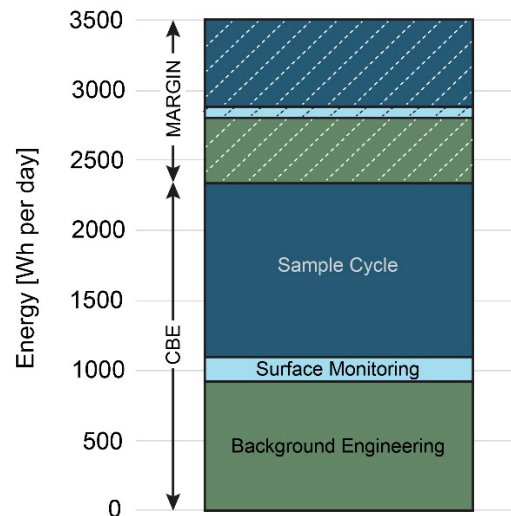


Figure 9.1. Surface mission energy allocation by function for an example sampling tal.

Table 9.2. Estimated energy usage per tal for Engineering and Science operations. Surface monitoring tals and sampling tals both require the energy needed for Spacecraft Minimal Operations.

Activity	Energy Required per Tal (Whr, estimated)	Comments
Spacecraft Minimal Operations	1100	Includes minimal communications for background engineering and survival heater energy
Surface Monitoring	210 (1310 total)	Includes additional lander awake-time and communications
Single Sample Acquisition, Transfer, and Analysis tal (with Monitoring)	1250 (2560 total)	Analysis by all three instruments and associated additional communications. (1250+210+1100 = 2560 Whr total)

monitoring, and 1/5 to sample acquisition and analysis. As a point of reference, the estimated energy required for primary activities is shown in **Table 9.2**. Note that the energy required for sampling is roughly equivalent to the energy required for a monitoring tal (as defined in **Table 9.3**). For example, an operational choice to analyze only 4 samples would result in 1 full additional tal of monitoring science. Conversely, more than 5 samples could be acquired and analyzed if fewer monitoring and margin tals were needed.

9.2.1 TERMINOLOGY

The surface operations approach for Europa Lander is derived from experience gained on Phoenix and Mars Science Laboratory. Terms are defined within **Table 9.3**.

Table 9.3. Europa Lander Surface Phase Key Terminology.

Terms	Definitions
Tal	The period of performance on Europa defined from the rise of the CRO over the european horizon through the next rise (24 hr). <i>Etymology: Talos</i> was a bronze automaton presented to Europa by Zeus as a protector on Crete. As part of its duties, Talos circled Crete three times daily. "Tal" is short for "talosian period" (similar to "sol", short for "solar day", in Mars surface operations).
Ground planning cycle ("ground cycle", for short)	The working shift for the operations teams in tactical operations, starting with the receipt of the first bit of return link (telemetry) in the Mission Support Area (MSA), through uplink of the command sequences to the relay spacecraft for transmission to the lander. Generally, the products of a ground planning cycle would cover one tal of operations. Figure 9.2 shows a notional ground planning cycle timeline.
Sample Cycle	A sample cycle is a sequence of sampling and science activities that include the sample acquisition and operation of the non-destructive and destructive science payloads.
Sample Tal	The <i>sample tal</i> template exemplifies tals where the primary activity is sampling and associated sample science. A secondary activity is to perform environmental monitoring. A sample tal is composed of a sample cycle and a specially constrained ground cycle.
Monitoring Tal	The <i>monitoring tal</i> template is exemplary of tals where the primary activity is remote sensing instrument science. This tal template type will nominally be the default lander operating mode and serve as the primary low power state for the lander.
Decisional data	Engineering and science data that is critical for decision-making in the immediately following ground planning cycle. Examples include data required to assess the state of instrument and spacecraft health and the current arm attitude, and data needed for selecting targets and instrument modes or safely maneuvering the sampling system into position.
Non-decisional data	All other telemetry to be returned, but which is not required to feed into decision-making for the immediately following ground planning cycle. Data from individual science observations may or may not be decisional, depending on whether the selection or targeting of activities planned for the next ground planning cycle depends on the observation results.
Tactical operations	Refers to the daily rapid turnaround of data analysis, science and engineering activity planning, resource modeling, and the generation and review of the integrated set of commands and sequences necessary to support the daily operation of the Europa Lander.

9.3 SURFACE MISSION TIMELINE

Figures 9.2 and **9.3** represent two elements of the baseline surface timeline. The surface mission is broken into tals that represent an orbital period of the carrier, nominally 24 Earth hours. There are primarily two types of tals in the surface mission: monitoring tals and sampling tals (**Table 9.3**). A monitoring tal is the default operational tal for the lander; a sampling tal is composed of a sample cycle overlaid on a monitoring tal. A baseline sampling tal is shown in **Figure 9.2** and in the bottom left corner of **Figure 9.3**. The tal would start at hour 00:00 and conclude at hour 24:00, which is the CRO orbital period. During each tal, there would be a period when the carrier is “In View of the Lander”; nominally this would be 10 hours and covers the duration of a sample cycle. This is in contrast to Mars operations where the relay orbits enable short but frequent communication periods. There are 5 Sampling Tals planned over the 20-day mission; they are nominally tals 1, 3, 5, 7, and 9 as shown in **Figure 9.3**.

On a notional sampling tal, as the carrier rises above the horizon, and comes into view of the lander, the commands to perform a sample cycle would be sent from the carrier High Gain Antenna (HGA) to the lander at 01:00 hours, as shown in **Figure 9.2**. Once the commands are received on the lander, the sample acquisition process would begin with the carrier in view and listening for the lander. The sample acquisition is anticipated to last 5 hours. At the conclusion of the sample acquisition process the sample would be transferred to the science instruments and decisional engineering data would be transmitted to the carrier at 06:00 hours in **Figure 9.2**.

The data transmitted from the carrier would be immediately relayed to Earth to start the engineering ground in the loop process. This is best shown in the enlargement in a “Typical Sampling Tal” in **Figure 9.3**, where the orange boxes indicate communication periods and the red lines indicate the transfer of data. The data rates from the lander to the carrier are anticipated to be extremely large resulting in very small transmit times. Once the data are received on the carrier, the carrier would slew and transmit the data to Earth. Data transmission to Earth is subject to one-way-light-time of 1 hour. The carrier to Earth visibility is not expected to be a driving constraint in the transmission of data. However, the data rate from the carrier to Earth of 80 kbps could represent the biggest bottleneck in the timely return of decisional data. Once the data are transmitted to Earth, the carrier would slew back to point the HGA at the lander.

The science instruments would analyze the data over the course of the next 5 hours. At the conclusion of the sample analysis period, science decisional data would be transmitted from the lander to the carrier for relay. This would represent the end of a sample cycle and the lander would transition to the monitoring, low-power state.

Once the decisional data are received on the ground, the science and engineering teams have 8 and 16 hours, respectively, to plan and generate commands for the subsequent tal, which includes making the decision on the activities for the next tal. The ground-in-the-loop (GITL) is represented by the dark green bands in **Figure 9.3** and the green band in **Figure 9.2**.

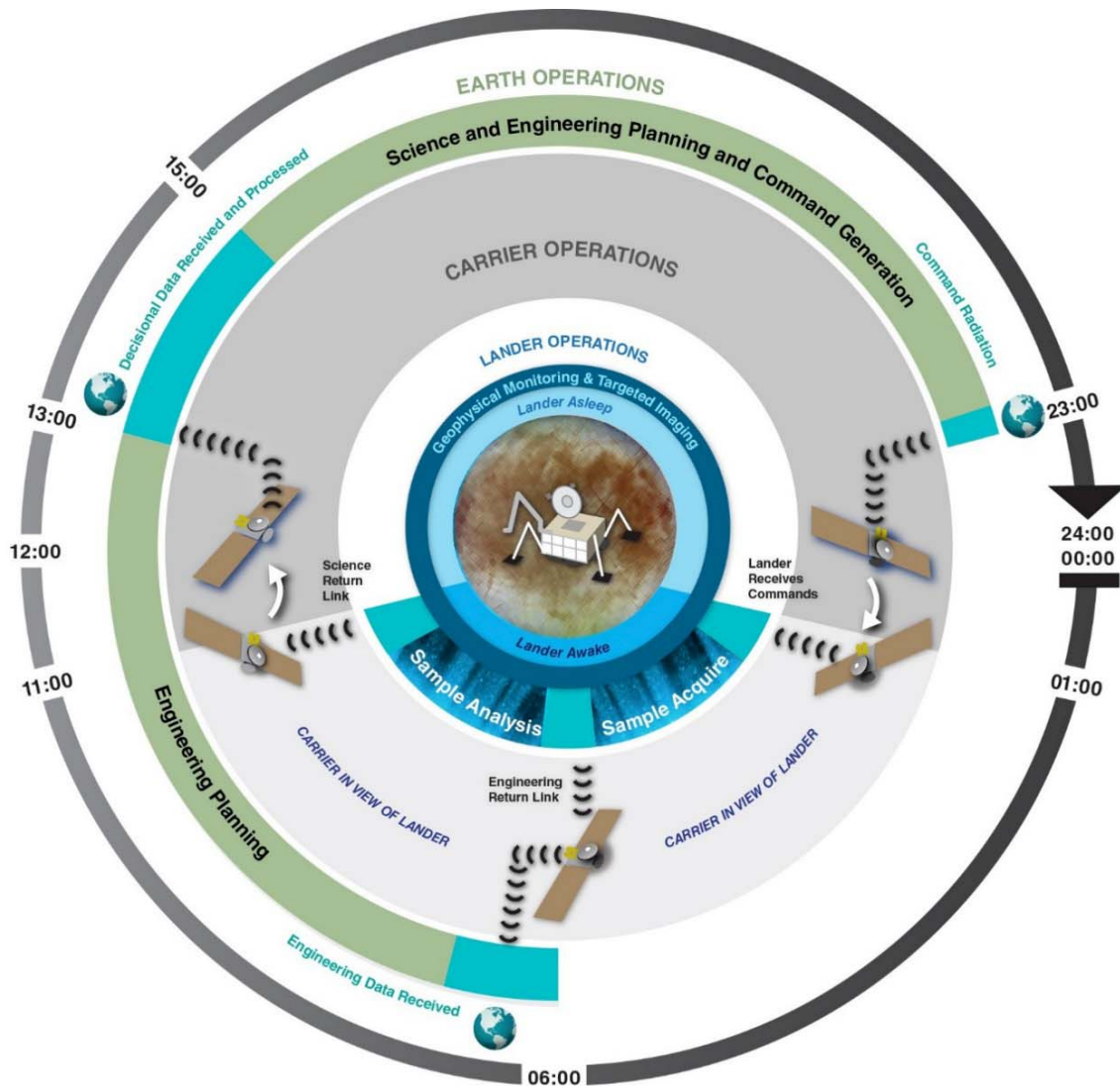


Figure 9.2. Europa Lander Sample Tal: A Sample Tal represents the tal during which samples would be acquired and analyzed by the lander. A Sample Tal would start at 00:00 hours with the carrier ready to transmit commands to the lander and would end with the Command Radiation from the Earth to the carrier in preparation for the next tal.

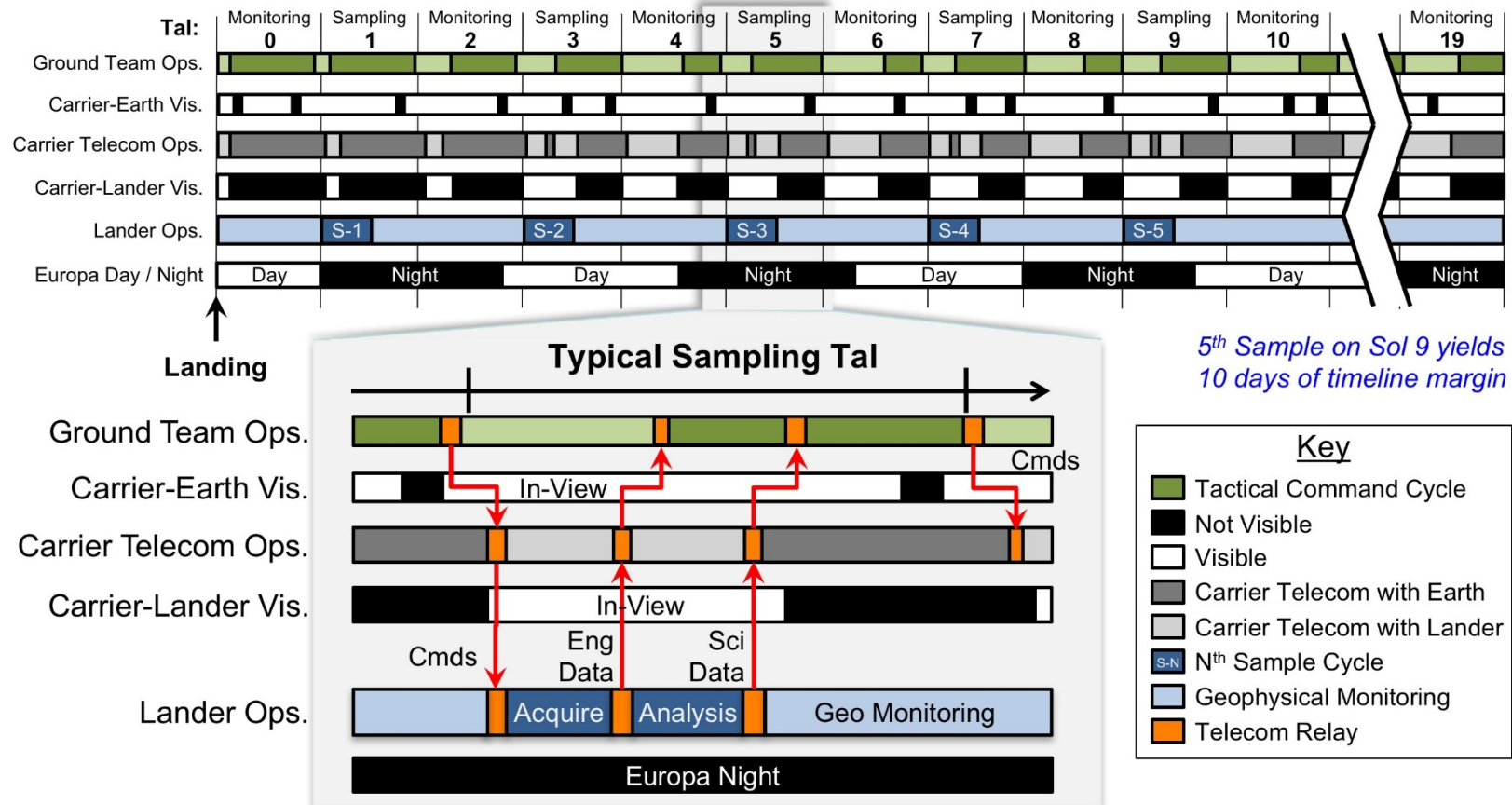


Figure 9.3. The Nominal Surface Mission plan includes completion of final sample analysis on Tal 9, with 10 tals of time margin bookkept as Monitoring Tals.

On a monitoring tal, the geophysical instruments would be kept on and generate data over the course of the tal. Additionally, there could be some targeted imaging that can occur on these tals. Nominally, as the carrier rises, the lander would be commanded to stay in a monitoring mode and take a small number of images. These data would nominally be transmitted to the carrier at the end of the overflight just prior to the carrier setting over the horizon.

A Tal is: the period of performance, on Europa defined by the rise of the CRO over the european horizon. *Etymology:* Talos was a bronze automaton, presented to Europa by Zeus as a protector on Crete. As part of its duties, Talos circled Crete three times daily. “Tal” is short for “talosian period” (similar to “sol”, short for “solar day”, in Mars surface operations).

Nominally, the sample tals would be executed every other day for the first 10 days, leaving 10 days of timeline margin as shown in dark blue in **Figure 9.3**. Sampling at night would be technically possible, though requirements for imaging before and after collection would need to be considered. Early in the mission, when the visibility from carrier to lander is subject to change due to trajectory maneuvers, the first 3 tals represent the period of time between landing and the establishment of a steady-state relay orbit by the carrier.

All critical deployments are intended to occur during the pass that would occur immediately post-landing on tal 0. That pass is anticipated to be at least 15 mins in length and is part of the Transition phase of the mission. At the beginning of the second pass, the sampling system and instruments would be ready for use and, nominally, would perform the first sample cycle.

The surface mission timeline is primarily driven by the sampling strategy employed. Short mission duration motivates an aggressive strategy wherein (a) successful delivery of sample is available for ground confirmation prior to initiating the next sampling cycle, but (b) only partial, not full, sample analysis data is available on the ground to inform the next sample cycle. This strategy results in sampling every other tal, and the net resulting mission profile is shown in **Figure 9.3**. As can be seen, this results in 10 tals of timeline margin for Sampling Science bookkept at the end of the prime mission.

9.4 STRATEGY FOR SCIENCE-IN-THE-LOOP

9.4.1 MONITORING TAL

The monitoring tal template is exemplary of tals where the primary activity is remote sensing instrument science. This tal template type would nominally be the default lander operating mode and serve as the primary low power state for the lander. The lander may acquire, for example, a panorama, geophysical measurements, and thermal measurements. The heat generated by the instruments in this tal would be used to keep the remaining instruments above their minimum allowable flight temperatures. Pre-scheduled communication opportunities would ensure that the data is nominally downlinked during the next ground cycle.

9.4.2 SAMPLE TAL

The sample tal template exemplifies tals where the primary activity is sampling and associated sample science. A secondary activity is to perform environmental monitoring. A sample tal is composed of a sample cycle and a specially constrained ground cycle.

A sample cycle is a sequence of sampling and science activities that include the sample acquisition and operation of the non-destructive and destructive science payloads.

The sample cycle would commence with commanding the lander and conclude with the uplink of data from the lander to the carrier. A significant part of the sample cycle is the sample acquisition period, which is described in more detail in section 10.5. The sample cycle represents the most active period of time for the lander throughout the lander mission. There are several constraints that affect the sample cycle.

1. Thermal: During this period, there would be significant heat dissipated inside the vault from electrical components, which results in a sharp rise in vault temperature. In order to manage the temperature rise, instruments that operate longer than 1 hour must be able to operate without lander Computer and Data Handling (CDH). In addition, deviations from instrument power allocations may result in violations of allowable flight temperatures.
2. Autonomy: A sample cycle is expected to be a fully autonomous sequence of events and performed with no real-time interaction with Earth. Once begun, the sample cycle would go through each of the defined steps, with the sample provided to each instru-

- ment in turn, without an intervening ground cycle. Consequently, within a sample cycle, instruments are expected to perform all activities without ground intervention and within their time allocation.
3. **Time:** The most constraining class of trajectories for the carrier relay orbit results in approximately 10 hours of line-of-sight coverage per tal between the carrier and lander. To support ground-in-the-loop commanding, each over-flight would need to include both forward and return links for the lander, which in turn could limit the duration of a sample cycle to 10 hours. Data considered decisional must be ready to transmit by the end of the sample cycle. Instruments that are not producing decisional data may continue to operate subject to their thermal, data, and power constraints. (Refer to **Table 9.3** for the definition of decisional data.)

The ground cycle would start with the receipt of decisional data transmitted from carrier to Earth (return link) and end with the transmission of spacecraft commands to the carrier (forward link). Taking one-way light time, lander–carrier data rates and carrier–Earth data rates into account could result in 8–9 hours on Earth for the entirety of the ground cycle, including making the decision whether to sample on the next tal. During the ground cycle, the lander would be in a monitoring mode similar to a monitoring tal. This period of time would also allow the lander to cool down following the activities of the sample cycle.

9.5 FAULT TOLERANCE, AUTOMATION, AND ROBUSTNESS OF SURFACE PHASE

The challenge of fault management for the surface mission is the containment of both transient and permanent errors while at the same time maximizing science return for the limited mission duration. The overall Fault Management philosophy is therefore biased toward continuing operations in the presence of faults. This means that both the spacecraft and instruments will be designed to mask or detect, identify, and recover from anomalies autonomously as the first tenet of that philosophy.

9.5.1 LANDER FAULT TOLERANCE

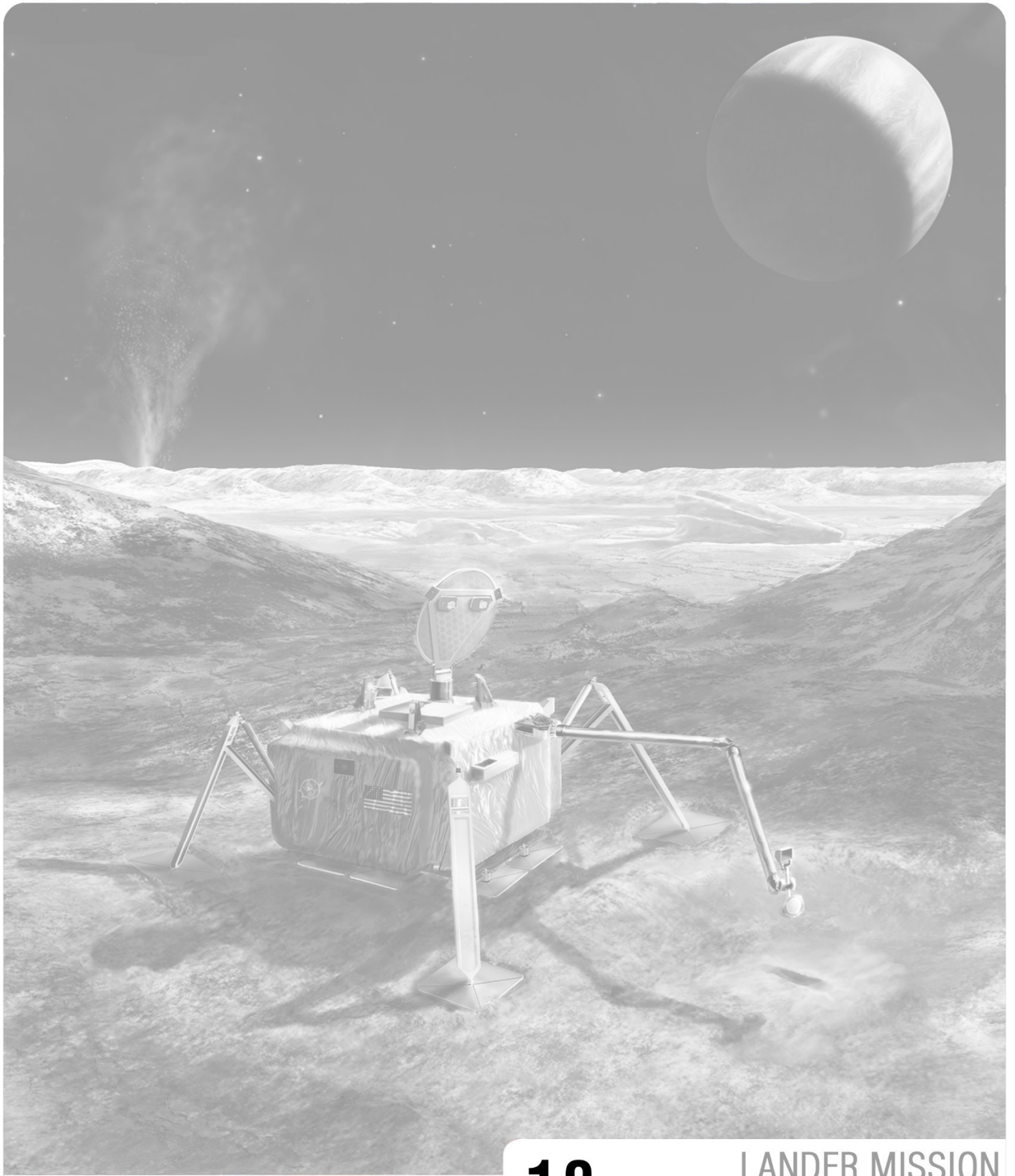
The lander is responsible for its overall health and, based on ground direction and autonomous actions, for conducting the activities that constitute the surface mission. This includes communication with the orbiter, acquisition of samples, conveyance of samples, sequence-of-events coordination, management of communication between the lander and the instruments, data collection from the instruments, power/energy management, and the autonomous and

automated actions/reactions to faults, errors, and anomalies. The lander will be designed to recover and continue its activities without interrupting instrument activities, if possible. The shared goal between the lander and the instruments is the continuation of science activities in the presence of faults and must be a cooperative effort.

9.5.2 INSTRUMENT FAULT TOLERANCE

The preservation of energy is a significant factor in surface mission lifetime. The instruments will be required to nominally operate both when the lander avionics are on and also while the spacecraft avionics are off (i.e., asleep). Since the spacecraft cannot provide the same command and data handling functions, safety net, or monitoring functions while asleep that can be achieved when the spacecraft is awake, each instrument must be self-sufficient in regards to its internal actions and activities, data storage, anomalies, and self-commanded activities.

Instruments need to be designed to execute high-level behaviors/actions as well as produce state, status, and results that can be examined to affect the overall plan. This is most obviously required for the coordination of sampling and for the initial activities post-landing. First actions after landing would be automatically executed, and instruments must be designed so that any releases, checkout, and first use/analysis could be performed without requiring a GITL cycle. Plans will contain primary and alternative logical paths to maximize the science return in the limited lifetime. For example, onboard logic may need to stop and/or restart actions or sequences of events in response to possible, but non-optimal, execution (e.g., insufficient sample volume may require a discard action and a reacquisition). For instruments that ingest or otherwise process samples, the instrument should be designed so that it would be ready for a second or subsequent sample (if no explicit fault occurs) without any need for a time consuming GITL cycle. Similarly, an instrument should be capable of autonomously recovering from a fault, or a spacecraft-commanded stop or abort, so that the plan logic could continue operations with a subsequent sample delivery to the instrument.



10

LANDER MISSION
CONCEPT



10 LANDER MISSION CONCEPT

10.1 MISSION OVERVIEW

The Europa Lander mission would place a robotic lander onto the surface of Europa as early as the 2031 timeframe. The lander will be equipped with an instrument suite designed to analyze samples acquired by the lander's sampling system. The battery-powered lander would nominally operate for twenty Earth days before depleting its batteries.

The overall Mission approach is depicted in **Figure 10.1**. The mission would require a single launch on an SLS and could be launched as early as 2024. An Earth gravity assist would be used, resulting in a ~5-year cruise to Jupiter Orbit Insertion. A series of jovian moon flybys over the course of ~1.5 years would set up the trajectory required for Deorbit, Descent, and Landing (DDL). The deorbit vehicle would separate from the carrier (also known as the Carrier Relay Orbiter [CRO]) and execute a guided deorbit burn. After jettisoning the deorbit

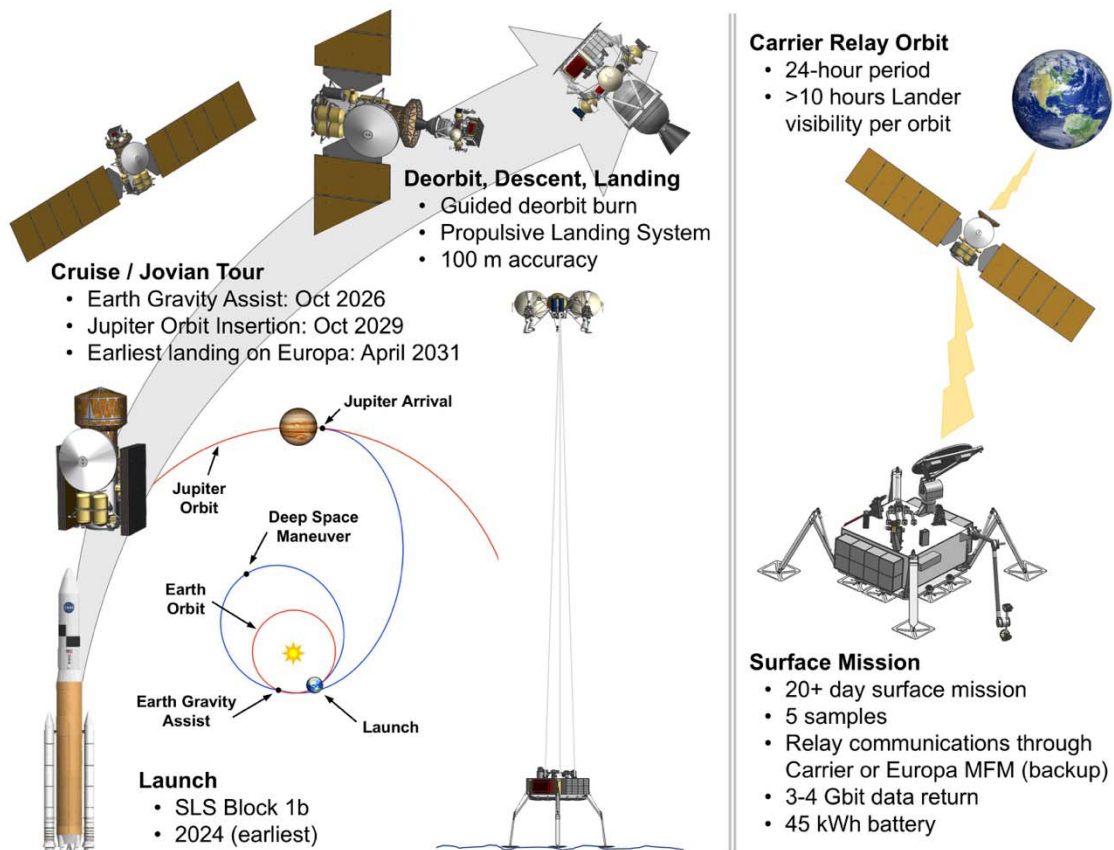


Figure 10.1. Key Features of Europa Lander mission design, from launch to landing.

stage with its solid rocket, the Powered Descent Vehicle liquid propulsion system would cancel out relative velocity and lower the lander to the surface via tethers with an MSL-derived Sky Crane system. The CRO would establish an orbit around Europa and serve as a communications relay for the 20+ day surface mission, during which five samples would be acquired and analyzed by the science instruments.

10.2 INTEGRATED SPACECRAFT AND CARRIER ELEMENT OVERVIEW

The spacecraft in its stowed launch configuration would be comprised of five primary elements. These elements are the Carrier Relay Orbiter stage, the Deorbit Stage, the Descent Stage, the Lander, and the Bio-Barrier (see **Figure 10.2**). In its launch configuration, the Deorbit Stage, Descent Stage, and Lander would be fully enclosed within the Bio-Barrier, and the Lander inverted with respect to its landed orientation. The Carrier includes propellant tanks used for the Deep Space Maneuver (DSM tanks), which would be jettisoned after use during cruise.

Electronics on all elements of the spacecraft that are sensitive to radiation are shielded within protective vaults on the CRO, Descent Stage, and Lander. Electronic parts would be selected to be compatible with the resulting shielded environment. Cameras such as star trackers on the CRO, descent imagers on the Descent Stage, and cameras located on the lander would be mounted external to the primary vault with localized shielding.

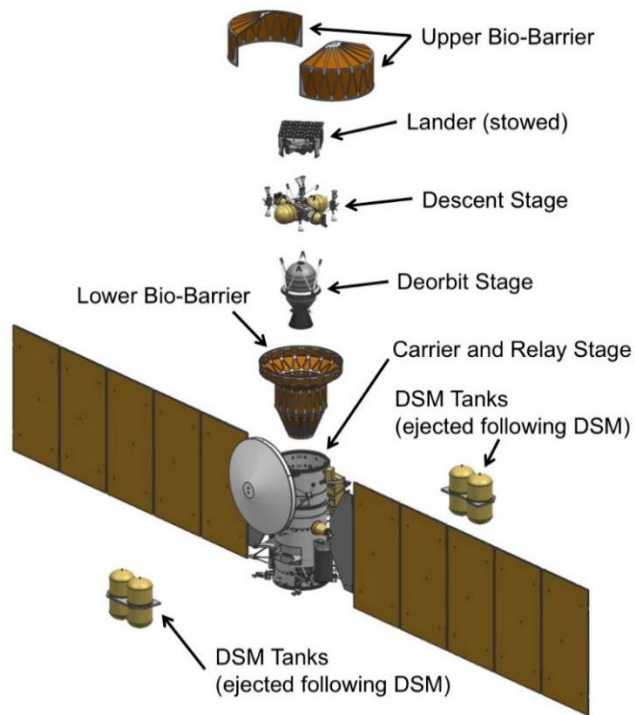


Figure 10.2. Europa Lander Hardware Configuration (exploded view).

10.3 LANDER SPACECRAFT CONCEPTUAL DESIGN

The lander configuration (see **Figure 8.2**) is driven by several considerations:

- 1) Stable landed platform robust to a variety of terrains;
- 2) Enable a work area of the terrain to be accessible both to the Sampling System and to the Stereo Camera field of view;
- 3) Provide full sky coverage for a High Gain Antenna;
- 4) Enclose science instruments, electronics, and other subsystems within a thermally-efficient, radiation-shielded vault;
- 5) Provide access ports for science instruments to receive samples.

In the landed configuration, the stabilizers are only attached to the bellypan structure (see **Figure 10.3**), and the bellypan structure is thermally isolated from the lander vault in order to minimize the thermally conductive path to Europa's surface. The stabilizers are designed to individually extend, conforming to local terrain features in order to achieve a level lander body in a range of possible surface topographies.

The sample analysis instruments are co-located on one side of the vault, each with external access to receive samples from the sampling system. The lander conceptual design provides a payload volume resource envelope that allows for potential rearrangement in the layout and shape of the individual instruments.

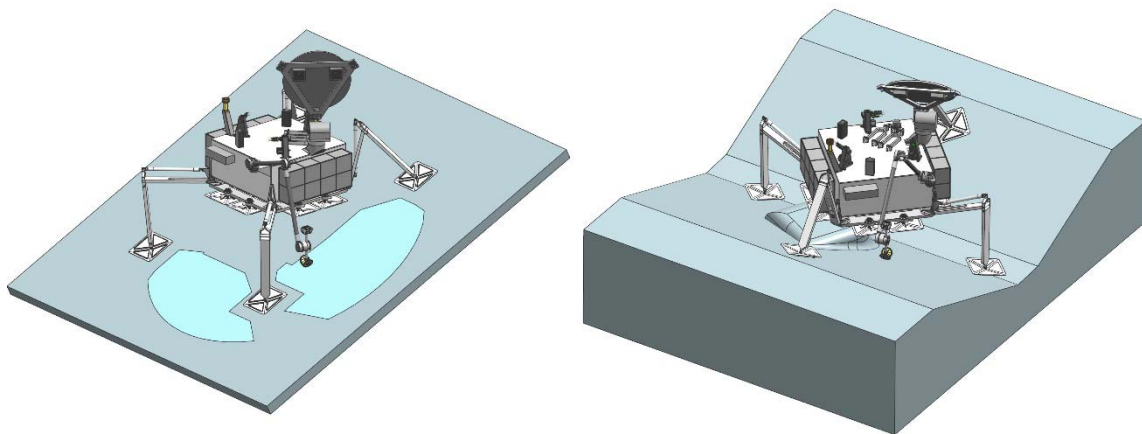


Figure 10.3. Lander Stabilizers (the four leg-like structures and pads on the underside of the lander) enable landing and sampling in a variety of terrains. The 'bellypan' of pads on the underside of the lander serves to provide thermal isolation of the lander body.

The lander vault internal walls would be thermally controlled by the flight system to within the range $-40/+50^{\circ}\text{C}$ (Allowable Flight Temperature [AFT]) at the vault-wall interfaces, and they would be qualified to operate over the wider temperature range of -55°C to $+70^{\circ}\text{C}$. Thermal control of the vault would be achieved through several strategies, including MLI blankets, electrical heaters, thermostats, heat spreaders, and thermo-optical coatings. The vault walls would serve as the thermal sink and interface for the instruments. The instruments would be mounted and coupled (mechanically and thermally) directly on the lander vault walls, or be isolated (mechanically and thermally), from the walls via structural supports that have the necessary levels of thermal isolation.

10.4 MISSION OPERATIONS

10.4.1 LAUNCH/CRUISE

Following the EMFM's projected launch in 2022, the Europa Lander Mission would launch on a separate launch vehicle as early as 2024. Due to the large spacecraft mass at launch, the Space Launch System (SLS) launch vehicle is likely required to provide sufficient performance and is expected to be available by 2024.

Baseline Cruise scenario: The flight system would be launched from Kennedy Space Center and follow a ΔV -leveraged Earth Gravity Assist (ΔV -EGA) trajectory to Jupiter. Two ΔV -EGA launch opportunities to Jupiter open within approximately two months of each other and repeat roughly every thirteen months with the synodic period between Jupiter and Earth. **Figure 10.4** shows an example trajectory with launch in 2025. Following a Deep Space Maneuver (DSM), the spacecraft would encounter Earth for a gravity assist and arrive at Jupiter.

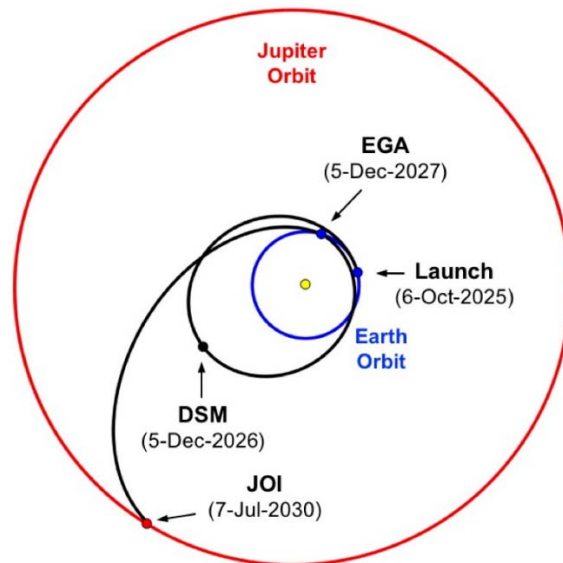


Figure 10.4. An example 2025 launch with a ΔV -EGA trajectory and a 4.8-year transfer time.

10.4.2 JOI AND JUPITER TOUR

The tour trajectory would begin with a Ganymede gravity assist prior to the Jupiter Orbit Insertion (JOI) maneuver, capturing the spacecraft into a 200-day orbit. At apoapsis, a Peri-Jove Raise (PJR) maneuver would set up the next gravity assist at Ganymede. This example tour trajectory is designed to reduce the spacecraft velocity relative to Europa, which enables an efficient landing while also minimizing the fuel requirements and the spacecraft's exposure to Jupiter's radiation. Consequently, the tour would consist of a series of gravity assists from Callisto and Ganymede and would only encounter Europa at the very end of the tour, more than 18 months after JOI. **Figure 10.5** shows a representative trajectory for the Jupiter tour of the mission (trajectory 12L4, Campagnola et al. (2013)).

10.4.3 DEORBIT, DESCENT, AND LANDING

The first Europa gravity assist would mark the beginning of the final mission phase before landing, and the spacecraft would now be exposed to much higher daily radiation doses than before. The first Europa gravity assist would be designed to insert the spacecraft into a Europa-resonant orbit, and ΔV -leveraging maneuvers would further reduce the spacecraft's velocity relative to Europa (Campagnola and Russell, 2010). This velocity reduction would make the low-energy (or three-body) regime accessible to the spacecraft, in which the gravitational interplay of Europa and Jupiter would enable the carrier to reside in the vicinity of Europa for

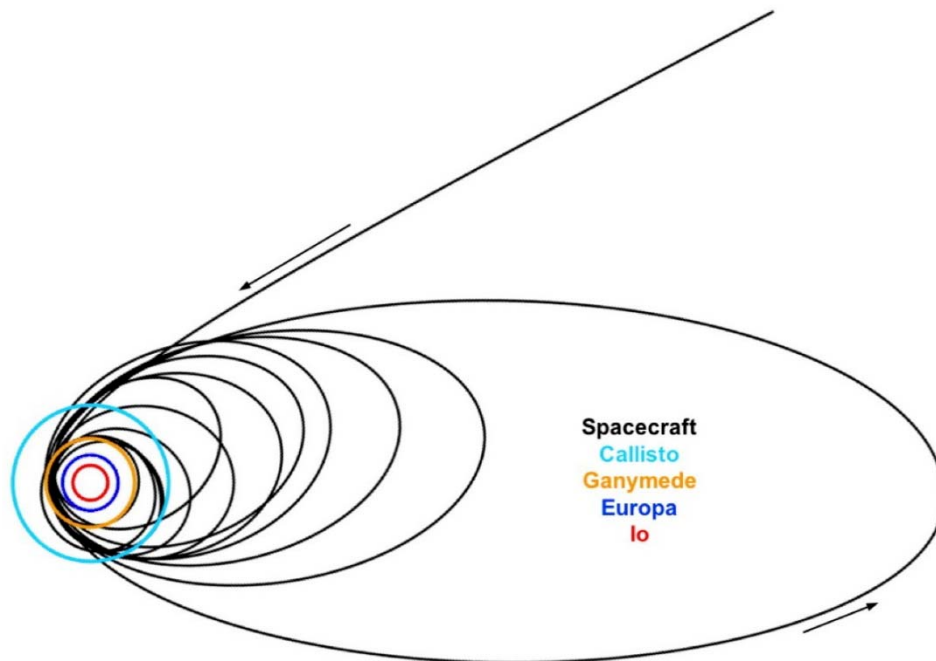


Figure 10.5. Example tour trajectory showing Jupiter arrival and transition to Europa.

the full duration of the surface mission. This final part of the tour trajectory, from first Europa flyby to landing, would take approximately one month and would set up the lander delivery to a 5 km periapsis altitude at a target state relative to the landing site.

The Deorbit, Descent, and Landing (DDL) system (see **Figure 10.6**) utilizes cameras that require lighting with low shadows of the surface, i.e., specific local times at the potential landing site. Since Europa is tidally locked with Jupiter, one Europa day equals Europa’s period of 3.55 Earth days, and a local time at a given landing site can be directly translated into a true longitude along Europa’s orbit. The tour trajectory would need to set up the lander delivery to coincide with this true longitude.

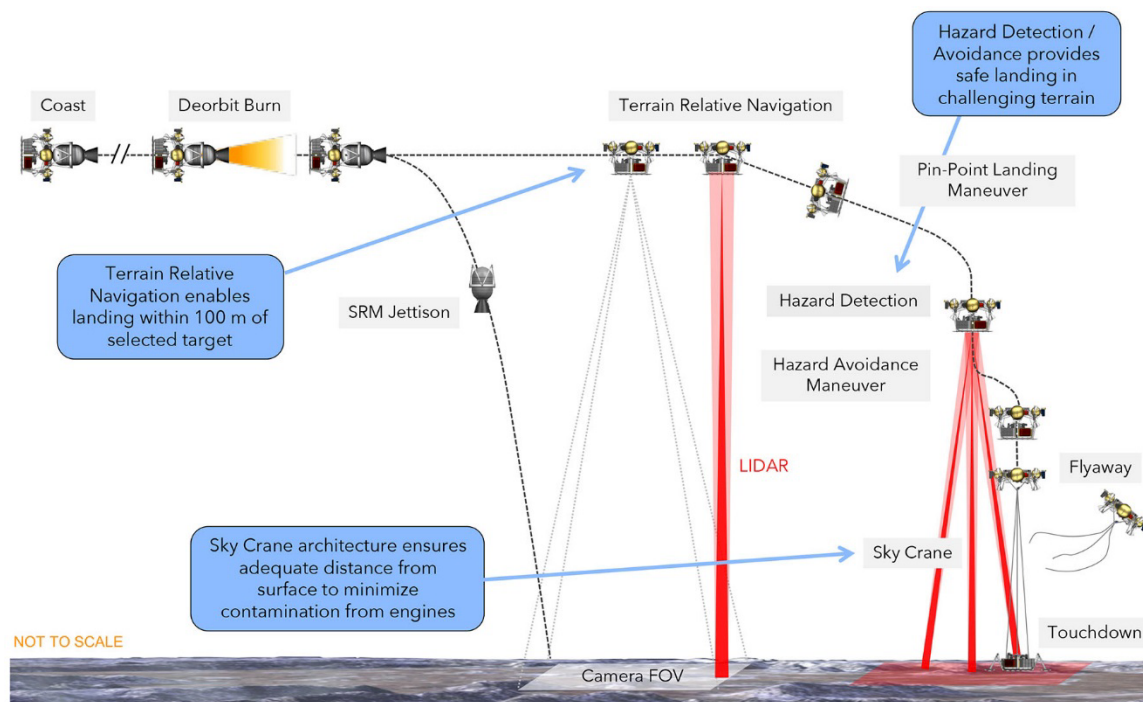


Figure 10.6. Deorbit, Descent, and Landing sequence showing the final stages before touchdown on Europa’s surface.

The final DDL would be completely autonomous due to the long light-time between Europa and Earth and the fast sequence of events during DDL. The lander would use a solid rocket motor for deorbiting and rely, while using computer vision for terrain-relative navigation and hazard avoidance during its subsequent powered descent. In the last stage of landing, the lander would be lowered on tethers from the descent stage in a sky crane configuration before final touchdown, after which the descent stage would fly away and impact at a safe distance from the lander.

Prior to touchdown, the lander stabilizers would be deployed. As the lander is set onto the terrain, the stabilizer legs would contract as needed to both maintain contact with the ground and enable the lander body to remain flat. Contact of the lander body with the surface would trigger release of the bridle. The stabilizers would then be locked in position to yield a stable lander configuration for science operations.

After landing, the CRO would function as a telecom asset to relay the lander data to Earth. Various carrier relay orbits are currently under study, and the selection would balance landing site accessibility, post-landing telecom visibility, range between carrier and lander, as well as fuel requirements, radiation exposure, and planetary protection considerations. **Figure 10.7** shows an example trajectory for final approach to Europa, lander delivery, CRO transfer, and relay orbit in the Jupiter–Europa rotating frame.

10.4.4 LANDER AND CARRIER DURING SURFACE PHASE

Figure 10.7 shows the view onto Europa’s north pole in a Jupiter–Europa rotating reference frame. The combined lander-carrier spacecraft would follow the green trajectory until the divert maneuver. After the divert, the lander would continue to the landing site. The carrier would execute several transfer orbits (red) over the course of 48 hours to reach the final relay orbit. Line-of-sight durations with the lander during the Transition orbits would be limited (see section 9.3 for operational implications), but the final relay orbit would achieve >10 hours of communications coverage every tal (24-hour period).

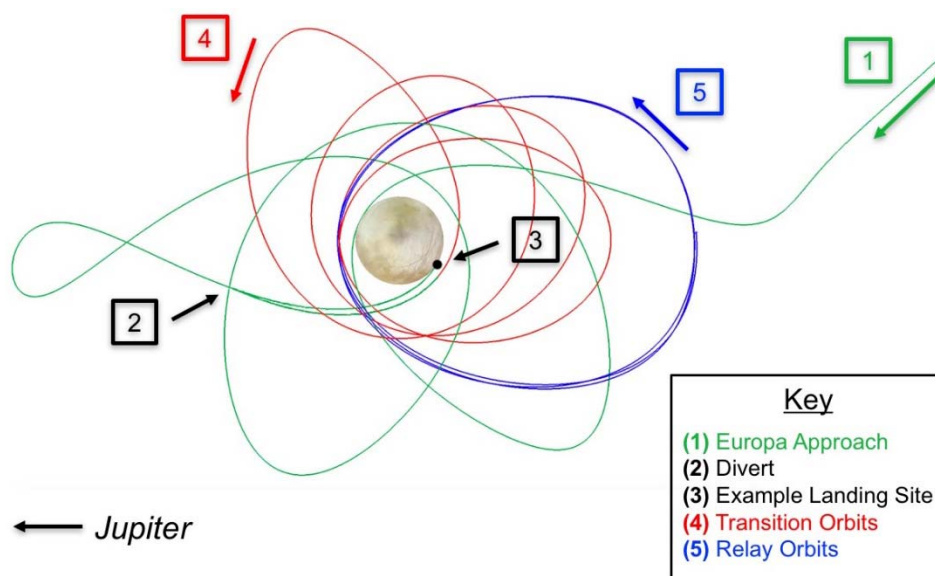


Figure 10.7. The Carrier and Relay Orbiter (CRO) delivers the lander to the surface, after which it transitions to a relay orbit for science mission communications support.

The lander telecommunications subsystem would be used to send commands to the lander and would return engineering telemetry and science data to the Earth using relay communications with either the Europa Lander Carrier (primary relay asset) or EMFM spacecraft (only as backup). Lander transmit capability (telemetry and science) is in the 2 kbps to 1024 kbps range. The subsystem does not support traditional Direct-to-Earth (DTE) or Direct-from-Earth (DFE) communications with the DSN. Surface operations once the lander is on the ground are covered in detail in **Chapter 9**.

10.5 SYSTEMS ENGINEERING

10.5.1 ENVIRONMENTS

Radiation Environment

The jovian radiation environment represents a uniquely challenging risk to mission performance and lifetime. Based on the current mission design trajectories and GIRE-2p jovian radiation model, the lander would experience a total ionizing dose (TID) of ~1.7 Mrad behind 100 mil Al (Si equivalent), primarily from electrons.

The local lander radiation environment would be mitigated with a combination of hardened technology and shielding. To attenuate the expected lander dose to 150 krad (Si), most lander and payload electronics are housed in a radiation vault similar to that used on Juno, and planned for the EMFM. Shielding by the lander vault would decrease the expected TID to 150 krad (Si). All electronics within the vault must be rated to 300 krad in order to maintain a radiation design factor of two (RDF = 2).

Standard radiation shielding would meet the same requirement of 150 krad (Si) for instruments with electronics and sensors outside of the vault at designated locations. Any additional mass required for openings in shield boxes to make scientific observations (e.g., a camera shutter) should be included in the mass of the instrument.

Descent Stage Plume Contamination

Contamination of the surface by rocket engine exhaust during DDL was examined by the project during this study. During descent, the descent stage thrusters would use hydrazine. The thruster nozzles would nominally be angled away from the lander to minimize direct exhaust contamination. However, at the end of descent, during the Sky Crane maneuver, the hydrazine exhaust would likely deposit at least some material on the surface near the landing

site (Lorenz, 2016). All scientific instruments should expect that hydrazine exhaust constituents would be present at some level on the surface as a result of landing.

The primary exhaust constituents of decomposed hydrazine are nitrogen, ammonia, and hydrogen with smaller amounts (<1% by weight) of water, carbon dioxide, aniline, iron, chloride, and unburnt hydrazine. The condensation temperatures in vacuum of hydrogen and nitrogen are 4 K and 26 K, respectively. Ammonia has a condensation temperature of 101 K. Initial expectations are that of the primary exhaust constituents, ammonia would remain largely present on Europa's surface near the lander. All of the lesser constituents should be assumed to remain present as well.

To mitigate against contamination, the Sky Crane design contains three features that would serve to minimize the impact of the propulsion system on the terrain that science instruments would sample and analyze. First, the Sky Crane tethers are of a length (~10 m) such that the minimum altitude of the descent engine nozzles over Europa's surface is 12 meters. In addition, the descent stage has two sets of four thrusters, one set canted 5 degrees, the other canted 30 degrees. During the terminal descent and Sky Crane phases of DDL (starting at 30 m above the surface down to 12 m), the descent stage would only use the engines that are canted 30 degrees off nadir, thus further minimizing contamination of the landing site. Finally, ultrapure hydrazine would be used to minimize the impact of residual propellant contamination. Ongoing studies will continue to examine this issue in detail. The requirement that the lander be able to acquire samples from at least 10 cm beneath the surface (due to radiation processing), would also help ensure that sampled materials are not contaminated by DDL exhaust.

Contamination Control

The baseline cleanliness and contamination control requirements for the Europa Lander would assume a contamination control program implemented for the flight system, engineering systems, and science payloads, which is designed to be complementary to the EMFM. The contamination control program would be designed to achieve a particulate cleanliness level based on IEST-STD-CC1246E for all hardware. These cleanliness levels are intended to enable science investigations conducted by possible contact with the surface of Europa, including those with organic and/or extant life detection, and optical imaging for engineering and science purposes. Additional requirements, or the identification of limitations on specific contaminant compounds, may be imposed after payloads and the associated science investigations are selected.

Contamination control will be an ongoing process, addressed throughout the mission lifetime by:

- Initial delivery of clean science instrument hardware,
- Initial delivery of clean spacecraft hardware, and
- Operational methods that apply standard best-practice contamination control techniques.

Instruments would be integrated with the spacecraft in a Class 100,000 (ISO 8) or better facility. Instrument components such as MLI, electronics, cabling, and other designated instrument hardware would require thermal vacuum bake-out to remove out-gassing contaminants prior to instrument integration. Instrument design would preclude lubricated hardware from contaminating other adjacent Europa Lander hardware (e.g., other instruments) and any critical internal items (e.g., lenses, mirrors, detectors). Dry nitrogen purge, more stringent clean-room facilities, or other special integration procedures may be required. Instruments would need to address requirements for any sample blanks as part of their calibration strategy. After instrument selection, a detailed assessment of sample handling chain would be completed for contamination control to identify any additional considerations.

10.5.2 PLANETARY PROTECTION IMPLEMENTATION

An overview of Planetary Protection requirements, policies, and procedures is provided in Chapter 7. In this section, we provide information on implementation approaches.

Bioburden Reduction Processing

Pre-launch, dry-heat microbial reduction (DHMR) and heat microbial reduction (HMR) processing of the spacecraft prior to integration with the launch vehicle would be the principal techniques used for bioburden reduction. DHMR is a bake-out process in which the hardware is held at an elevated temperature (typically $>125^{\circ}\text{C}$) for many hours to days in a controlled humidity ($<25\%$ relative humidity) environment, such as partial vacuum or dry nitrogen.

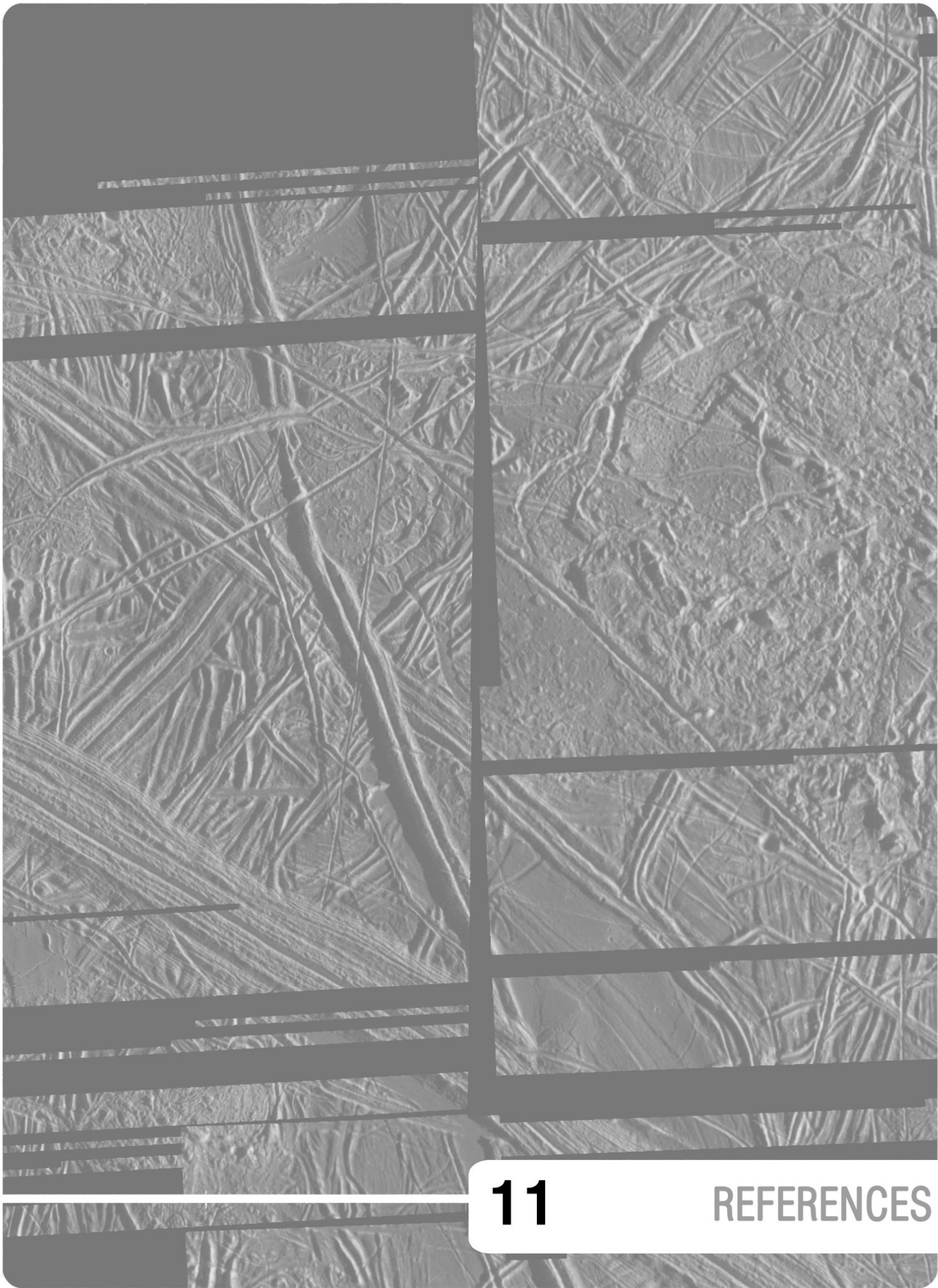
The lander would be enclosed in a biobarrier and would undergo a system-level DHMR bioburden reduction process prior to launch. As a backup, some lander hardware may undergo penetrating irradiation microbial reduction and then be aseptically assembled. Batteries would be irradiated instead of DHMR to achieve Planetary Protection requirements. Finally, an incendiary device design option is being explored for the vault. This device would potentially be triggered just prior to the end of the lander surface phase so as to further sterilize the space craft.

Planetary Protection Contamination and Recontamination Control

Recontamination control is key to maintaining cleanliness to the level required for the spacecraft to meet microbial cleanliness requirements at Europa. Pre-launch techniques that may be used for recontamination management include (but are not limited to) HMR/DHMR, chemical agents (e.g., vapor hydrogen peroxide [VHP]), and ultraviolet (UV) or gamma irradiation. Steps taken to prevent recontamination would include specialized handling procedures, seals, covers, filters, and/or other techniques incorporated into the design. Instrument apertures without windows, or with windows unable to withstand alcohol wipe cleaning, would be protected by a biobarrier, flight covers, or removable preflight covers to prevent recontamination of the interior of the instrument or window. Post-launch (en route) guidelines for radiation-induced bioburden reduction prior to first Europa encounter are:

- Hardware seeing more than or equal to 10 Mrad is generally considered to have achieved the microbial cleanliness target en route (mostly external surfaces).
- Hardware seeing less than 10 Mrad would require protection from any possible recontamination (most hardware).

Ongoing studies will continue to examine and develop the Planetary Protection protocols for the Europa Lander mission.



11 REFERENCES

- Alonso-Saez, L., P. E. Galand, E. O. Casamayor, C. Pedros-Alio, and S. Bertilsson. (2010) "High bicarbonate assimilation in the dark by Arctic bacteria." *The ISME Journal* 4(12): 1581–1590.
- Alsteens, D. (2012) "Microbial cells analysis by Atomic Force Microscopy." In *Imaging and Spectroscopic Analysis of Living Cells: Imaging Live Cells in Health and Disease*, edited by P. M. Conn., p. 3–17.
- Anderson, J. D., G. Schubert, R. A. Jacobson, E. L. Lau, W. B. Moore, and W. L. Sjogren. (1998) "Europa's differentiated internal structure: Inferences from four Galileo encounters." *Science* 28(5385): 2019–2022.
- Arvidson, R., D. Adams, G. Bonfiglio, P. Christensen, S. Cull, M. Golombek, J. Guinn, *et al.* (2008) "Mars Exploration Program 2007 Phoenix landing site selection and characteristics." *Journal of Geophysical Research: Planets* 113(E00A03). doi:10.1029/2007JE003021.
- Arvidson, R. E., K. D. Iagnemma, M. Maimone, A. A. Fraeman, F. Zhou, M. C. Heverly, P. Bellutta, *et al.* (2016) "Mars Science Laboratory Curiosity Rover megaripple crossings up to sol 710 in Gale Crater." *Journal of Field Robotics*. doi:10.1002/rob.21647.
- Arvidson, R. E., S. W. Squyres, J. F. Bell III, J. G. Catalano, B. C. Clark, L. S. Crumpler, P. A. de Souza Jr., *et al.* (2014) "Ancient aqueous environments at Endeavor Crater, Mars." *Science* 343(6169): Article #1248097.
- Aubrey, A. D. (2008) "Implications for the detection of extinct or extant microbial communities on Mars." Ph.D. thesis, University of California, San Diego.
- Bada, J. L. (1997) "Meteoritics - Extraterrestrial Handedness?" *Science* 275(5302): 942-943.
- Bada, J. L., and G. D. McDonald. (1996) "Detecting amino acids on Mars." *Analytical Chemistry* 68(21): A668-A73.
- Bagenal, F., R. L. McNutt Jr., J. W. Belcher, H. S. Bridge, and J. D. Sullivan. (1985) "Revised ion temperatures for Voyager plasma measurements in the Io plasma torus." *Journal of Geophysical Research* 90(A2): 1755–1757.
- Balkwill, D. L., F. R. Leach, J. T. Wilson, J. F. McNabb, and D. C. White. (1988) "Equivalence of microbial biomass measures based on membrane lipid and cell wall components, adenosine triphosphate, and direct counts in subsurface aquifer sediments." *Microbial Ecology* 16: 73-84.
- Banfield, J. F., and K. H. Nealson, eds. (1997) *Geomicrobiology: Interactions between Microbes and Minerals*. Vol. 35, edited by P. H. Ribbe. Reviews in Mineralogy: Mineralogical Society of America, 448 p.
- Banfield, J. F., S. A. Welch, H. Zhang, T. T. Ebert, and R. L. Penn. (2000) "Aggregation-based crystal growth and microstructure development in natural iron oxyhydroxide biomineralization products." *Science* 289(5480): 751–754.

- Baross, J., J. I. Lunine, L. Becker, S. Chang, D. W. Deamer, M. L. Fogel, N. R. Pace, and D. A. Stahl. (2002) *Signs of Life: A Report Based on the April 2000 Workshop on Life Detection Techniques*. Edited by The National Research Council Committee on the Origins and Evolution of Life, Washington, D.C.: The National Academies Press.
- Bascomb, C. L. (1968) "Distribution of pyrophosphate-extractable iron and organic carbon in soils of various groups." *Journal of Soil Science* 19(2): 251–268.
- Beegle, L. W., R. Bhartia, M. White, L. DeFlores, W. Abbey, Y.-H. Wu, B. Cameron, *et al.* (2015) "SHERLOC: Scanning Habitable Environments with Raman & Luminescence for Organics and Chemicals." *IEEE Aerospace Conference*. Big Sky, MT. doi:10.1109/AERO.2015.7119105.
- Belton, M. J. S., J. W. Head III, A. P. Ingersoll, R. Greeley, A. S. McEwen, K. P. Klaasen, D. Senske, *et al.* (1996) "Galileo's first images of Jupiter and the Galilean satellites." *Science* 274(5286): 377–385.
- Bentley, M. S., R. Schmied, T. Mannel, K. Torkar, H. Jeszenszky, J. Romstedt, A. C. Levasseur-Regourd, *et al.* (2016) "Aggregate dust particles at Comet 67P/Churyumov-Gerasimenko." *Nature* 537(7618): 73-75.
- Benzerara, K., N. Menguy, P. López-García, T. H. Yoon, J. Kazmierczak, T. Tyliszczak, F. Guyot, and G. E. Brown. (2006) "Nanoscale detection of organic signatures in carbonate microbialites." *Proceedings of the National Academy of Sciences USA* 103(25): 9440–9445.
- Berisford, D. F., J. Foster, M. J. Poston, and K. P. Hand. (2016) "Cryogenic ices under vacuum: Preliminary tests related to sampling material on Europa's surface." *47th Lunar and Planetary Science Conference*. The Woodlands, TX: Lunar and Planetary Institute. Abstract #2298.
- Berney, M., F. Hammes, F. Bosshard, H. U. Weilenmann, and T. Egli. (2007) "Assessment and interpretation of bacterial viability by using the Live/Dead BacLight Kit in combination with flow cytometry." *Applied and Environmental Microbiology* 73(10): 3283–3290.
- Bhartia, R., E. C. Salas, W. F. Hug, R. D. Reid, A. L. Lane, K. J. Edwards, and K. H. Nealon. (2010) "Label-free bacterial imaging with deep-UV-laser-induced native fluorescence." *Applied and Environmental Microbiology* 76(21): 7231–7237.
- Bibring, J. P., P. Lamy, Y. Langevin, A. Soufflot, M. Berthe, J. Borg, F. Poulet, and S. Mottola. (2007a) "CIVA." *Space Science Reviews* 128(1-4): 397–412.
- Bibring, J. P., H. Rosenbauer, H. Boehnhardt, S. Ulamec, J. Biele, S. Espinasse, B. Feuerbacher, *et al.* (2007b) "The Rosetta Lander ("Philae") investigations." *Space Science Reviews* 128(1-4): 205–220.
- Bidle, K. D., S. Lee, D. R. Marchant, and P. G. Falkowski. (2007) "Fossil genes and microbes in the oldest ice on Earth." *Proceedings of the National Academy of Sciences USA* 104(33): 13455–13460.

- Biemann, K. (2007) “On the ability of the Viking gas chromatograph–mass spectrometer to detect organic matter.” *Proceedings of the National Academy of Sciences USA* 104(25): 10310–10313.
- Biemann, K., J. Óro, P. Toulman III, L. E. Orgel, A. O. Nier, D. M. Anderson, D. Flory, *et al.* (1977) “The search for organic substances and inorganic volatile compounds in the surface of Mars.” *Journal of Geophysical Research* 82(28): 4641–4658.
- Bierhaus, E. B., C. R. Chapman, and W. J. Merline. (2005) “Secondary craters on Europa and implications for cratered surfaces.” *Nature* 437: 1125–1127.
- Bierhaus, E. B., K. Zahnle, and C. R. Chapman. (2009) “Europa's Crater Distributions and Surface Ages.” In *Europa*, edited by R. T. Pappalardo, W. B. McKinnon and K. K. Khurana. Tucson, AZ: University of Arizona Press, p. 161–180.
- Billings, S. E., and S. A. Kattenhorn. (2005) “The great thickness debate: Ice shell thickness models for Europa and comparisons with estimates based on flexure at ridges.” *Icarus* 177(2): 397–412.
- Bills, B. G., F. Nimmo, Ö. Karatekin, T. Van Hoolst, N. Rambaux, B. Levrard, and J. Laskar. (2009) “Rotational Dynamics of Europa.” In *Europa*, edited by R. T. Pappalardo, W. B. McKinnon and K. K. Khurana. Tucson, AZ: University of Arizona Press, p. 119–134.
- Bligh, E. G., and W. J. Dyer. (1959) “A rapid method of total lipid extraction and purification.” *Canadian Journal of Biochemistry and Physiology* 37(8): 911–917.
- Boetius, A., A. M. Anesio, J. W. Deming, J. A. Mikucki, and J. Z. Rapp. (2015) “Microbial ecology of the cryosphere: Sea ice and glacial habitats.” *Nature Reviews Microbiology* 13(11): 677–690.
- Böttcher, T. (2016) “An additive definition of molecular complexity.” *Journal of Chemical Information and Modeling* 56(3): 462–470.
- Bowman, J. P., M. V. Brown, and D. S. Nichols. (1997) “Biodiversity and ecophysiology of bacteria associated with Antarctic sea ice.” *Antarctic Science* 9(2): 134–142.
- Bowman, J. S., S. Rasmussen, N. Blom, J.W. Deming, S. Rysgaard, and T. Sicheritz-Ponten. (2012) “Microbial community structure of Arctic multiyear sea ice and surface seawater by 454 sequencing of the 16S RNA gene.” *The ISME Journal* 6(1): 11–20.
- Braterman, P. S., Z. P. Xu, and F. Yarberr. (2004) “Layered Double Hydroxides (LDHs).” Chap. 8 In *Handbook of Layered Materials*, edited by S. M. Auerbach, K. A. Carrado and P. K. Dutta. New York: Marcel Dekker, Inc., p. 373–474.
- Bridges, J. C., R. A. Henson, J. L. Vago, D. Loizeau, R. M. E. Williams, H. Hauber, E. Sefton-Nash, and the ExoMars Landing Site Selection Working Group. (2016) “ExoMars landing site characterization and selection.” *47th Lunar and Planetary Science Conference*. The Woodlands, TX: Lunar and Planetary Institute. Abstract #2170.
- Bridges, J. C., A. M. Seabrook, D. A. Rothery, J. R. Kim, C. T. Pillinger, M. R. Sims, M. P. Golombek, *et al.* (2003) “Selection of the landing site in Isidis Planitia of Mars probe Beagle 2.” *Journal of Geophysical Research: Planets* 108(E1). doi:10.1029/2001JE001820.

- Brilliantov, N. V., J. Schmidt, and F. Spahn. (2008) “Geysers of Enceladus: Quantitative analysis of qualitative models.” *Planetary and Space Science* 56(12): 1596–1606.
- Brinkmeyer, R., K. Knittel, J. Jurgens, H. Weyland, R. Amann, and E. Helmke. (2003) “Diversity and structure of bacterial communities in Arctic vs. Antarctic pack ice.” *Applied and Environmental Microbiology* 69(11): 6610–6619.
- Brown, M. E. “Potassium in Europa’s atmosphere.” (2001) *Icarus* 151(2): 190–195.
- Brown, M. E., and K. P. Hand. (2013) “Salts and radiation products on the surface of Europa.” *The Astronomical Journal* 145(4). doi:10.1088/0004-6256/145/4/110.
- Brown, M. E., and R. E. Hill. (1996) “Discovery of an extended sodium atmosphere around Europa.” *Nature* 380: 229–231.
- Butler, H. J., L. Ashton, B. Bird, G. Cinque, K. Curtis, J. Dorney, K. Esmonde-White, *et al.* (2016) “Using Raman spectroscopy to characterize biological materials.” *Nature Protocols* 11(4): 664–687.
- Cady, S. L. (2002) “Formation and Preservation of Bona Fide Microfossils.” In *Signs of Life: A Report Based on the April 2000 Workshop on Life-Detection Techniques*, edited by The National Academies Space Studies Board and Board on Life Sciences. Washington, D.C.: National Academies Press, p. 149–155.
- Campagnola, S., R. P. Russell. (2010) “The endgame problem Part 1: V-infinity leveraging technique and leveraging graph.” *Journal of Guidance, Control, and Dynamics* 33(2): 463–475. doi:10.2514/1.44258.
- Campagnola, S., B. B. Buffington, A. E. Petropoulos. (2013) “Jovian tour design for orbiter and lander missions to Europa.” *23rd AAS/ALAA Space Flight Mechanics Meeting*. Kauai, HI. AAS 13-494.
- Carlson, R. W., M. S. Anderson, R. E. Johnson, W. D. Smythe, A. R. Hendrix, C. A. Barth, L. A. Soderblom, *et al.* (1999a) “Hydrogen peroxide on the surface of Europa.” *Science* 283(5410): 2062–2064.
- Carlson, R. W., R. E. Johnson, and M. S. Anderson. (1999b) “Sulfuric acid on Europa and the radiolytic sulfur cycle.” *Science* 286(5437): 97–99.
- Carlson, R. W., M. S. Anderson, R. E. Johnson, M. B. Schulman, and A. H. Yavrouian. (2002) “Sulfuric acid production on Europa: The radiolysis of sulfur in water ice.” *Icarus* 157(2): 456–463.
- Carlson, R. W., W. M. Calvin, J. B. Dalton, G. B. Hansen, R. L. Hudson, R. E. Johnson, T. B. McCord, and M. H. Moore. (2009) “Europa's Surface Composition.” In *Europa*, edited by R. T. Pappalardo, W. B. McKinnon and K. K. Khurana. Tucson, AZ: University of Arizona Press, p. 283–328.
- Carlson, R. W., K. P. Hand, D. F. Berisford, and D. Keymeulen. (2013) “The Compositional Infrared Interferometric Spectrometer (CIRIS) for assessing the habitability of Europa.” *American Geophysical Union 2013 Fall Meeting*. San Francisco, CA. Abstract #P43A-2008.

- Cassidy, T., P. Coll, F. Raulin, R. W. Carlson, R. E. Johnson, M. J. Loeffler, K. P. Hand, R. A. Baragiola. (2009) "Radiolysis and photolysis of icy satellite surfaces: Experiments and theory." *Space Science Reviews*. doi:10.1007/s11214-009-9625-3.
- Christner, B. C., E. Mosley-Thompson, L. G. Thompson, and J. N. Reeve. (2003) "Bacterial recovery from ancient glacial ice." *Environmental Microbiology* 5(5): 433–436.
- Christner, B. C., G. Royston-Bishop, C. M. Foreman, B. R. Arnold, M. Tranter, K. A. Welch, W. B. Lyons, *et al.* (2006) "Limnological conditions in Subglacial Lake Vostok, Antarctica." *Limnology and Oceanography* 51(6): 2485–2501.
- Christner, B. C., M. L. Skidmore, J. C. Priscu, M. Tranter, and C. M. Foreman. (2008) "Bacteria in subglacial environments." In *Psychrophiles: From Biodiversity to Biotechnology*, edited by R. Margensin, F. Schinner, J.-C. Marx and C. Gerday. New York: Springer.
- Christner, B. C., J. C. Priscu, A. M. Achberger, C. Barbante, S. P. Carter, K. Christianson, A. B. Michaud, *et al.* (2014) "A microbial ecosystem beneath the West Antarctic ice sheet." *Nature* 512(7514): 310–313.
- Church, M. (2006) "Bed material transport and the morphology of alluvial river channels." *Annual Review of Earth and Planetary Sciences* 34(325-354): 325–354.
- Chyba, C. F. (2000) "Energy for microbial life on Europa: A radiation-driven ecosystem on Jupiter's moon is not beyond the bounds of possibility." *Nature* 403(6768): 381–382.
- Chyba, C. F., and G. D. McDonald. (1995) "The origin of life in the Solar System: Current issues." *Annual Review of Earth and Planetary Sciences* 23: 215–249.
- Chyba, C. F., and C. B. Phillips. (2001) "Possible ecosystems and the search for life on Europa." *Proceedings of the National Academy of Sciences USA* 98: 801–804.
- . (2002) "Europa as an abode of life." *Origins of Life and Evolution of the Biosphere* 32(1): 47–67.
- Clarke, A. (2014) "The thermal limits to life on Earth." *International Journal of Astrobiology* 13(2): 141–154.
- Cleland, C. E., and C. F. Chyba. (2002) "Defining 'Life'." *Origins of Life and Evolution of the Biosphere* 32(4): 387–393.
- Cobb, A. K., and R. E. Pudritz. (2014) "Nature's Starships. I. Observed abundances and relative frequencies of amino acids in meteorites." *The Astrophysical Journal* 783(2). doi:10.1088/0004-637x/783/2/140.
- Cockell, C. S., G. R. Osinski, N. R. Banerjee, K. T. Howard, I. Gilmour, and J. S. Watson. (2010) "The microbe-mineral environment and gypsum neogenesis in a weathered polar evaporite." *Geobiology* 8(4): 293–308.
- Cohen, C. M. S., E. C. Stone, and R. S. Selesnick. (2001) "Energetic ion observations in the middle jovian magnetosphere." *Journal of Geophysical Research: Space Physics* 106(A12): 29871–29881.
- Collins, G., and F. Nimmo. (2009) "Chaotic Terrain on Europa." In *Europa*, edited by R. T. Pappalardo, W. B. McKinnon and K. K. Khurana. Tucson, AZ: University of Arizona Press, p. 259–282.

- Collins, G. C., J. W. Head III, R. T. Pappalardo, and N. A. Spaun. (2000) “Evaluation of models for the formation of chaotic terrain on Europa.” *Journal of Geophysical Research: Planets* 105(E1): 1709–1716.
- Collins, R. E., S. D. Carpenter, and J. W. Deming. (2008) “Spatial heterogeneity and temporal dynamics of particles, bacteria, and peeps in Arctic winter sea ice.” *Journal of Marine Systems* 74: 902–917.
- Committee on Space Research [COSPAR]. (1964) “COSPAR Resolution No. 26, COSPAR Information Bulletin, No. 20.” Paris: COSPAR.
- Committee on Space Research [COSPAR]. (2002) “Planetary Protection Policy” (*Amended 24 March 2011*).
- Cook, A. M., A. Colaprete, T. L. Roush, J. E. Benton, J. B. Forcione, B. White, R. Bielawski, and E. Fritzier. (2016) “NIR spectroscopy and multi-wavelength imaging for volatile prospecting.” *3rd International Workshop on Instrumentation for Planetary Missions*. Pasadena, CA. Abstract #4023.
- Cooper, J. F., R. E. Johnson, B. H. Mauk, H. B. Garrett, and N. Gehrels. (2001) “Energetic ion and electron irradiation of the icy Galilean satellites.” *Icarus* 149(1): 133–159.
- Cosmidis, J., K. Benzerara, E. Gheerbrant, I. Esteve, B. Bouya, and M. Amaghazaz. (2013) “Nanometer-scale characterization of exceptionally preserved bacterial fossils in Paleocene phosphorites from Ouled Abdoun (Morocco).” *Geobiology* 11(2): 139–153.
- Cosmidis, J., and A. S. Templeton. (2016) “Self-assembly of biomorphic carbon/sulfur microstructures in sulfidic environments.” *Nature Communications*. doi:10.1038/ncomms12812.
- Costello, A. M., A. J. Auman, J. L. Macalady, K. M. Scow, and M. E. Lidstrom. (2002) “Estimation of methanotroph abundance in a freshwater lake sediment.” *Environmental Microbiology* 4: 443–450.
- Craft, K. L., G. W. Patterson, R. P. Lowell, and L. Germanovich. (2016) “Fracturing and flow: Investigations on the formation of shallow water sills on Europa.” *Icarus* 274: 297–313.
- Crawford, G. D., and D. J. Stevenson. (1988) “Gas-driven water volcanism and the resurfacing of Europa.” *Icarus* 73: 66–79.
- Creamer, J. S., M. F. Mora, and P. A. Willis. (2017) “Enhanced resolution of chiral amino acids with capillary electrophoresis for biosignature detection in extraterrestrial samples.” *Analytical Chemistry* 89(2): 1329–1337.
- Cronin, J. R., and S. Pizzarello. (1983) “Amino acids in meteorites.” *Advances in Space Research* 3(9): 5–18.
- Cronin, L. (2016) “A probabilistic intrinsically calibrated framework for recognising complex molecules as biosignatures.” Paper presented at the *Proceedings of the National Academy of Sciences Workshop: Searching for Life Across Space and Time*. Irvine, CA.
- Culha, C., A. G. Hayes, M. Manga, and A. M. Thomas. (2014) “Double ridges on Europa accommodate some of the missing surface contraction.” *Journal of Geophysical Research: Planets* 119(3): 395–403.

- Dalton, J. B., O. Prieto-Ballesteros, J. S. Kargel, C. S. Jamieson, J. Jolivet, and R. C. Quinn. (2005) "Spectral composition of heavily hydrated salts with disrupted terrains on Europa." *Icarus* 177(2): 472–490.
- Dalton III, J. B., J. H. Shirley, and L. W. Kamp. (2012) "Europa's icy bright plains and dark linea: Exogenic and endogenic contributions to composition and surface properties." *Journal of Geophysical Research: Planets* 117(E3). doi:10.1029/2011JE003909.
- De Angelis, M., J. R. Petit, J. Savarino, R. Souchez, and M. H. Thiemens. (2004) "Contributions of an ancient evaporitic-type reservoir to Subglacial Lake Vostok chemistry." *Earth and Planetary Science Letters* 222(3-4): 751–765.
- Des Marais, D. J. (2001) "Isotopic evolution of the biogeochemical carbon cycle during the Precambrian." In *Stable Isotope Geochemistry*, edited by J. W. Valley and D. Cole. Reviews in Mineralogy and Geochemistry. Washington, D.C.: Mineralogical Society of America, p. 555–578.
- Decho, A. W. (2010) "Overview of biopolymer-induced mineralization: What goes on in biofilms?" *Ecological Engineering* 36(2): 137–144.
- Domagal-Goldman, S. D., K. E. Wright, K. Adamala, L. A. de la Rubia, J. Bond, L. R. Dartnell, A. D. Goldman, *et al.* (2016) "The Astrobiology Primer V2.0." *Astrobiology* 16(8): 561–653.
- Dombard, A. J., G. W. Patterson, A. P. Lederer, and L. M. Prockter. (2013) "Flanking fractures and the formation of double ridges on Europa." *Icarus* 223: 74–81.
- Dorn, E. D., G. D. McDonald, M. C. Storrie-Lombardi, and K. H. Nealson. (2003) "Principal component analysis and neural networks for detection of amino Acid biosignatures." *Icarus* 166(2): 403–409.
- Dorobantu, L. S., G. G. Goss, and R. E. Burrell. (2012) "Atomic Force Microscopy: A nanoscopic view of microbial cell surfaces." *Micron* 43(12): 1312–1322.
- Douglas, S. (2005) "Mineralogical footprints of life." *American Journal of Science* 305: 503–525.
- Douglas, S., and H. Yang. (2002) "Mineral biosignatures in evaporites: Presence of rosickyite in an endoevaporitic microbial community from Death Valley, California." *Geology* 30: 1075–1078.
- Downs, R. T. (2006) "The RRUFF Project: An integrated study of the chemistry, crystallography, Raman, and infrared spectroscopy of minerals." *19th General Meeting of the International Mineralogical Association*. Kobe, Japan. Abstract #O03-13.
- Dugan, H. A., P. T. Doran, B. Wagner, F. Kenig, C. H. Fritsen, S. A. Arcone, E. Kuhn, *et al.* (2015) "Stratigraphy of Lake Vida, Antarctica: Hydrologic implications of 27 m of Ice." *The Cryosphere* 9(2): 439–450.
- Edgett, K. S. (2000) "K-12 educator involvement in the Mars Pathfinder field trips in the Channeled Scablands of Washington and Idaho." *Journal of Geoscience Education* 48(2): 150–160.
- Edgett, K. S., R. A. Yingst, M. A. Ravine, M. A. Caplinger, J. N. Maki, F. T. Ghaemi, J. Schaffner, *et al.* (2012) "Curiosity's Mars Hand Lens Imager (MAHLI) Investigation." *Space Science Reviews* 170(1-4): 259–317.

- Edwards, H. G. M., I. Hitchinson, and R. Ingley. (2012) “The ExoMars Raman spectrometer and the identification of biogeological spectroscopic signatures using a flight-like prototype.” *Analytical and Bioanalytical Chemistry* 404(6-7): 1723–1731.
- Ehrenfreund, P., and S. B. Charnley. (2000) “Organic molecules in the interstellar medium, comets, and meteorites: A voyage from dark clouds to the early Earth.” *Annual Review of Astronomy and Astrophysics* 38: 427–483.
- Eigenbrode, J. L. (2008) “Fossil lipids for life-detection: A case study from the early Earth record.” In *Strategies of Life Detection*, edited by O. Botta, J. Bada, J. Gómez Elvira, E. Javaux, F. Selsis and R. Summons. Space Sciences Series of Issi. Springer, p. 161–185.
- El-Baz, F. (1968) “Geologic characteristics of the nine lunar landing mission sites recommended by the Group for Lunar Exploration Planning.” Bellcomm, Inc.. Document #TR-68-340-1.
- Elsila, J. E., J. C. Aponte, D. G. Blackmond, A. S. Burton, J. P. Dworkin, and D. P. Glavin. (2016) “Meteoritic amino acids: Diversity in compositions reflects parent body histories.” *ACS Central Science* 2(6): 370–379.
- Fagents, S. A. (2003) “Considerations for effusive cryovolcanism on Europa: The post-Galileo perspective.” *Journal of Geophysical Research: Planets* 108(E12). doi:10.1029/2003JE002128.
- Fagents, S. A., R. Greeley, R. J. Sullivan, R. T. Pappalardo, L. M. Prockter, and The Galileo SSI Team. (2000) “Cryomagmatic mechanisms for the formation of Rhadamanthys Linea, triple band margins, and other low-albedo features on Europa.” *Icarus* 144(1): 54–88.
- Farmer, J. D., and D. J. Des Marais. (1999) “Exploring for a record of ancient martian life.” *Journal of Geophysical Research: Planets* 104(E11): 26977–26995.
- Figueredo, P. H., and R. Greeley. (2004) “Resurfacing history of Europa from pole-to-pole geological mapping.” *Icarus* 167(2): 287–312.
- Figueredo, P. H., F. C. Chuang, J. Rathbun, R. L. Kirk, and R. Greeley. (2002) “Geology and origin of Europa’s “Mitten” feature (Murias Chaos).” *Journal of Geophysical Research: Planets* 107(5). doi:10.1029/JE001591.
- Figueredo, P. H., R. Greeley, S. Neuer, L. Irwin, and D. Schulze-Makuch. (2003) “Locating potential biosignatures on Europa from surface geology observations.” *Astrobiology* 3(4): 851–861.
- Fischer, M., G. J. Triggs, and T. F. Krauss. (2016) “Optical sensing of microbial life on surfaces.” *Applied and Environmental Microbiology* 82(5): 1362–1371.
- Fischer, P. D., M. E. Brown, and K. P. Hand. (2015) “Spatially resolved spectroscopy of Europa: The distinct spectrum of large-scale chaos.” *The Astronomical Journal* 150(5). doi:10.1088/0004-6256/150/5/164.
- Fitzsimmons, J. N., S. G. John, C. M. Marsay, C. L. Hoffman, S. L. Nicholas, B. M. Toner, C. R. German, and R. M. Sherrell. (2017) “Iron persistence in a distal hydrothermal plume supported by dissolved-particulate interactions.” *Nature Geoscience*, accepted manuscript.

- Flahaut, J., D. Loizeau, J. L. Vago, and The ExoMars Landing Site Selection Working Group. (2014) “Where to land with ExoMars 2018: The candidate landing sites.” *8th International Conference on Mars*. Pasadena, CA. Abstract #1194.
- Flombaum, P., J. L. Gallegos, R. A. Gordillo, J. Rincon, L. L. Zabala, N. A. Z. Jiao, D. M. Karl, *et al.* (2013) “Present and future global distributions of the marine cyanobacteria *Prochlorococcus* and *Synechococcus*.” *Proceedings of the National Academy of Sciences USA* 110(24): 9824–9829.
- Forte, E., M.D. Fratte, M. Azzaro, and M. Guglielmin. (2016) “Pressurized brines in continental Antarctica as a possible analogue of Mars.” *Scientific Reports* 6: 33158.
- Fu, L., S. W. Li, Z. W. Ding, J. Ding, Y. Z. Lu, and R. J. Zeng. (2016) “Iron reduction in the DAMO/*Shewanella oneidensis* MR-1 coculture system and the fate of Fe(II).” *Water Research* 88: 808–815.
- Gaidos, E. J., K. H. Nealson, and J. L. Kirschvink. (1999) “Life in ice-covered oceans.” *Science* 284(5420): 1631–1633.
- Garvin, J.B., M. C. Malin, and M. A. Ravine. (2017) “Descent imaging of sub-meter topography from vertical baseline stereo analysis of Curiosity MARDI images, Gale Crater, Mars.” *48th Lunar and Planetary Science Conference*. The Woodlands, TX. Abstract #2526.
- Garvin, J.B., M. C. Malin, M. A. Ravine, R. Dotson, and J. Frawley. (2017) “Geologic terrain analysis of topography measured from descent imaging of Mars from the Mars Descent Imager (MARDI) on the Curiosity Rover at Gale Crater, Mars.” *Geophysical Research Letters*, submitted manuscript.
- Gaskin, J. A., T. Abbott, S. Medley, K. Patty, D. Gregory, K. Thaisen, B. Ramsey, *et al.* (2010) “Miniaturized scanning electron microscope for in-situ planetary studies.” In *Earth and Space 2010: Engineering, Science, Construction, and Operations in Challenging Environments*, edited by G. Song and R. B. Malla: American Society of Civil Engineers, p. 1246–1257.
- Gaskin, J. A., G. Jerman, D. Gregory, and A. R. Sampson. (2012) “Miniature variable pressure scanning electron microscope for in-situ imaging and chemical analysis.” *2012 IEEE Aerospace Conference*. doi:10.1109/AERO.2012.6187064.
- Gautsch, S. (2002) “Development of an Atomic Force Microscope and measurement concepts for characterizing martian dust and soil particles.” Ph.D. thesis, University of Neuchâtel.
- Geissler, P. E., R. Greenberg, G. Hoppa, P. Helfenstein, A. McEwen, R. Pappalardo, R. Tufts, *et al.* (1998) “Evidence for non-synchronous rotation of Europa.” *Nature* 391: 368–370.
- Ghosh, K. K., L. D. Burns, E. D. Cocker, A. Nimmerjahn, Y. Ziv, A. El Gamal, and M. J. Schnitzer. (2011) “Miniaturized integration of a fluorescence microscope.” *Nature Methods* 8: 871–878.
- Giovannoni, S. J. (2017) “SAR11 bacteria: The most abundant plankton in the oceans.” *Annual Review of Marine Science* 9: 231–255.

- Glavin, D. P., J. E. Elsila, A. S. Burton, M. P. Callahan, J. P. Dworkin, R. W. Hilts, and C. D. K. Herd. (2012) “Unusual nonterrestrial L-proteinogenic amino acid excesses in the Tagish Lake meteorite.” *Meteoritics & Planetary Science* 47(8): 1347–1364.
- Gleeson, D. F., C. Williamson, S. E. Grasby, R. T. Pappalardo, J. R. Spear, and A. S. Templeton. (2011) “Low temperature S⁰ biomineralization at a supraglacial spring system in the Canadian High Arctic.” *Geobiology* 9(4): 360–375.
- Gleeson, D. F., R. T. Pappalardo, M. S. Anderson, S. E. Grasby, R. E. Mielke, K. E. Wright, and A. S. Templeton. (2012) “Biosignature detection at an Arctic analog to Europa.” *Astrobiology* 12(2): 135–150.
- Glein, C. R., J. A. Baross, and Jr. J. H. Waite. (2015) “The pH of Enceladus’ ocean.” *Geochimica et Cosmochimica Acta* 162: 202–219.
- Goetz, W., W. T. Pike, S. F. Hviid, M. B. Madsen, R. V. Morris, M. H. Hecht, U. Staufer, *et al.* (2010) “Microscopy analysis of soils at the Phoenix landing site, Mars: Classification of soil particles and description of their optical and magnetic properties.” *Journal of Geophysical Research: Planets* 115(E8). doi: 10.1029/2009je003437.
- Golombek, M. P., and D. Rapp. (1997) “Size-frequency distributions of rocks on Mars and Earth analog sites: Implications for future landed missions.” *Journal of Geophysical Research: Planets* 102(E2): 4117–4129.
- Golombek, M. P., R. A. Cook, H. J. Moore, and T. J. Parker. (1997) “Selection of the Mars Pathfinder landing site.” *Journal of Geophysical Research: Planets* 102(E2): 3967–3988.
- Golombek, M. P., J. A. Grant, T. J. Parker, D. M. Kass, J. A. Crisp, S. W. Squyres, A. F. C. Haldemann, *et al.* (2003) “Selection of the Mars Exploration Rover landing sites.” *Journal of Geophysical Research: Planets* 108(E12). doi:10.1029/2003JE002074.
- Golombek, M., J. Grant, D. Kipp, A. Vasavada, R. L. Kirk, R. Fergason, P. Bellutta, *et al.* (2012) “Selection of the Mars Science Laboratory landing site.” *Space Science Reviews* 170: 641–737.
- Golombek, M., L. Redmond, H. Gengl, C. Schwartz, N. Warner, B. Banerdt, and S. Smrekar. (2013) “Selection of the InSight landing site: Constraints, plans, and progress.” *44th Lunar and Planetary Science Conference*. The Woodlands, TX. Abstract #1691.
- Golombek, M., N. Warner, N. Wigton, C. Bloom, C. Schwartz, S. Kannan, D. Kipp, A. Huertas, and B. Banerdt. (2014) “Final four landing sites for the InSight geophysical lander.” *45th Lunar and Planetary Science Conference*. The Woodlands, TX. Abstract #1499.
- Golombek, M. P., J. A. Grant, K. A. Farley, K. Williford, A. Chen, R. E. Otero, and J. W. Ashley. (2016) “Downselection of landing sites proposed for the Mars 2020 Rover Mission.” *47th Lunar and Planetary Science Conference*. The Woodlands, TX. Abstract #2324.
- Goodman, J. C., G. C. Collins, J. Marshall, and R. T. Pierrehumbert. (2004) “Hydrothermal plume dynamics on Europa: Implications for chaos formation.” *Journal of Geophysical Research: Planets* 109(E3). doi:10.1029/2003JE002073.

- Gramling, C. (2012) “A tiny window opens into Lake Vostok, while a vast continent awaits.” *Science* 335(6070): 788–789.
- Grant, J. A., M. P. Golombek, J. P. Grotzinger, S. A. Wilson, M. M. Watkins, A. R. Vasavada, J. L. Griffes, and T. J. Parker. (2011) “The science process for selecting the landing site for the 2011 Mars Science Laboratory.” *Planetary and Space Science* 59: 1114–1127.
- Greeley, R., R. Sullivan, J. Klemaszewski, K. Homan, J. W. Head III, R. T. Pappalardo, J. Veverka, *et al.* (1998) “Europa: Initial Galileo geological observations.” *Icarus* 135(1): 4–24.
- Greeley, R., C. F. Chyba, J. W. Head, T. McCord, W. B. McKinnon, R. T. Pappalardo, and P. Figueredo. (2004) “Geology of Europa.” In *Jupiter: The Planet, Satellites and Magnetosphere*, edited by F. Bagenal, T. E. Dowling and W. B. McKinnon. Cambridge: Cambridge University Press, p. 329–362.
- Greenberg, R., P. Geissler, G. Hoppa, B. R. Tufts, D. R. Durda, R. Pappalardo, J. W. Head, R. Greeley, R. Sullivan, and M. H. Carr. (1998) “Tectonic processes on Europa: Tidal stresses, mechanical response, and visible features.” *Icarus* 135: 64–78.
- Greenberg, R., G. V. Hoppa, B. R. Tufts, P. Geissler, J. Riley, and S. Kadel. (1999) “Chaos on Europa.” *Icarus* 141(2): 263–286.
- Greenberg, R., M. A. Leake, G. V. Hoppa, and B. R. Tufts. (2003) “Pits and uplifts on Europa.” *Icarus* 161(1): 102–126.
- Grotzinger, J. P., J. Crisp, A. R. Vasavada, R. C. Anderson, C. J. Baker, R. Barry, D. F. Blake, *et al.* (2012) “Mars Science Laboratory mission and science investigation.” *Space Science Reviews* 170(1): 5–56.
- Groussin, O., L. Jorda, A.-T. Auger, E. Kührt, R. Gaskell, C. Capanna, F. Scholten, *et al.* (2015) “Gravitational slopes, geomorphology, and material strengths of the nucleus of Comet 67P/Churyumov-Gerasimenko from Osiris observations.” *Astronomy and Astrophysics* 583: Article #A32. doi:10.1051/0004-6361/201526379.
- Grundy, W. M., B. J. Buratti, A. F. Cheng, J. P. Emery, A. Lunsford, W. B. McKinnon, J. M. Moore, *et al.* (2007) “New Horizons mapping of Europa and Ganymede.” *Science* 318(5848): 234–237.
- Gutiérrez-Preciado, A., H. Romero, and M. Peimbert. (2010) “An evolutionary perspective on amino acids.” *Nature Education* 3(9): 29.
- Hall, D. T., G. R. Gladstone, H. W. Moos, F. Bagenal, J. T. Clarke, P. D. Feldman, M. A. McGrath, *et al.* (1994) “Extreme Ultraviolet Explorer satellite observation of Jupiter's Io plasma torus.” *The Astrophysical Journal* 426(1): L51–L54.
- Halpern, B. (1969) “Optical activity for exobiology and exploration of Mars.” *Applied Optics* 8(7): 1349–1353.
- Hand, K. P., and M. E. Brown. (2013) “Keck II observations of hemispherical differences in H₂O₂ on Europa.” *The Astrophysical Journal Letters* 766(2): L21.
- Hand, K. P., and R. W. Carlson. (2012) “Laboratory spectroscopic analyses of electron irradiated alkanes and alkenes in Solar System ices.” *Journal of Geophysical Research: Planets* 117(E3). doi:10.1029/2011JE003888.

- . (2015) “Europa’s surface color suggests an ocean rich with sodium chloride.” *Geophysical Research Letters* 42: 3174–3178.
- Hand, K. P., and C. F. Chyba. (2007) “Empirical constraints on the salinity of the European ocean and implications for a thin ice shell.” *Icarus* 189(2): 424–438.
- Hand, K. P., R. W. Carlson, and C. F. Chyba. (2007) “Energy, chemical disequilibrium, and geological constraints on Europa.” *Astrobiology* 7(6): 1–18.
- Hand, K. P., C. F. Chyba, J. C. Priscu, R. W. Carlson, and K. H. Nealson. (2009) “Astrobiology and the potential for life on Europa.” In *Europa*, edited by R. T. Pappalardo, W. B. McKinnon and K. K. Khurana. Tucson, AZ: University of Arizona Press, p. 529–544.
- Hand, K. P. (2010) “The ocean of Europa and implications for habitability and the origin of life.” In *Astrobiology: From Simple Molecules to Primitive Life*, edited by V. A. Basiuk and R. Navarro-González. American Scientific Publishers.
- Hansen, G. B., and T. B. McCord. (2004) “Amorphous and crystalline ice on the Galilean satellites: A balance between thermal and radiolytic processes.” *Journal of Geophysical Research: Planets* 109(E1). doi:10.1029/2003JE002149.
- . (2008) “Widespread CO₂ and other non-ice Compounds on the anti-jovian and trailing sides of Europa from Galileo/NIMS observations.” *Geophysical Research Letters* 35(1). doi:10.1029/2007GL031748.
- Hansen, G., T. McCord, R. Clark, D. Cruikshank, R. Brown, K. Baines, G. Bellucci, *et al.* (2005) “Ice grain size distribution: Differences between jovian and saturnian icy satellites from Galileo and Cassini measurements.” *37th Annual Meeting of the Division for Planetary Sciences of the American Astronomical Society*. Cambridge, UK. Abstract #729.
- Hartgers, W. A., S. Schouten, J. F. Lopez, J. S. S. Damsté, and J. O. Grimalt. (2000) “¹³C contents of sedimentary bacterial lipids in a shallow sulfidic monomictic lake (Lake Cisó, Spain).” *Organic Geochemistry* 31(9): 777–786.
- Hayes, A. G., J. P. Grotzinger, L. A. Edgar, S. W. Squyres, W. A. Watters, J. Sohl-Dickstein. (2011) “Reconstruction of eolian bedforms and paleocurrents from cross-bedded strata at Victoria Crater, Meridiani Planum, Mars.” *Journal of Geophysical Research: Planets* 116(E7): doi:10.1029/2010JE003688.
- Hayes, J. M. (2001) “Fractionation of carbon and hydrogen isotopes in biosynthetic processes.” In *Stable Isotope Geochemistry*, edited by J. W. Valley and D. Cole. Reviews in Mineralogy and Geochemistry, Washington, D.C.: Mineralogical Society of America, p. 225–277.
- Head, J., R. Pappalardo, G. Collins, M. J. S. Belton, B. Giese, R. Wagner, H. Breneman, N. Spaun, B. Nixon, G. Neukum, and J. Moore. (2002) “Evidence for Europa-like tectonic resurfacing styles on Ganymede.” *Geophysical Research Letters* 29(24): 4-1–4-4.
- Hecht, M. H., J. Marshall, W. T. Pike, U. Staufer, D. Blaney, D. Braendlin, S. Gautsch, *et al.* (2008) “Microscopy capabilities of the Microscopy, Electrochemistry, and

- Conductivity Analyzer.” *Journal of Geophysical Research: Planets* 113(E3). doi:10.1029/2008je003077.
- Hedman, M. M., C. M. Gosmeyer, P. D. Nicholson, C. Sotin, R. H. Brown, R. N. Clark, K. H. Baines, B. J. Buratti, and M. R. Showalter. (2013) “An observed correlation between plume activity and tidal stresses on Europa.” *Nature* 500: 182–184.
- Heijnen, J. J., and J. P. Van Dijken. (1992) “In search of a thermodynamic description of biomass yields for the chemotrophic growth of microorganisms.” *Biotechnology and Bioengineering* 39(8): 833–858.
- Higgs, P. G., and R. E. Pudritz. (2009) “A thermodynamic basis for prebiotic amino acid synthesis and the nature of the first genetic code.” *Astrobiology* 9(5): 483–490.
- Hobley, D. E. J., J. M. Moore, and A. D. Howard. (2013) “How rough is the surface of Europa at lander scale?” *44th Lunar and Planetary Science Conference*. The Woodlands, TX. Abstract #2432.
- Hoefs, J. (2004) *Stable Isotope Geochemistry*. Berlin: Springer-Verlag, 244 pp.
- Hoehler, T. M., and B. B. Jørgensen. (2013) “Microbial life under extreme energy limitation.” *Nature Reviews Microbiology* 11: 83–94.
- Hoehler, T. M., M. J. Alperin, D. B. Albert, and C. S. Martens. (2001) “Apparent minimum free energy requirements for methanogenic Archaea and sulfate-reducing bacteria in an anoxic marine sediment.” *FEMS Microbiology Ecology* 38(1): 33–41.
- Holland, H. D. (1984) *The Chemical Evolution of the Atmosphere and Oceans*. Princeton Series in Geochemistry. Princeton: Princeton University Press, 598 pp.
- Hoppa, G. V., B. R. Tufts, R. Greenberg, and P. E. Geissler. (1999) “Formation of cycloidal features on Europa.” *Science* 285(5435): 1899–1902.
- Horita, J. (2005) “Some perspectives on isotope biosignatures for early life.” *Chemical Geology* 218(1–2): 171–186.
- Hörst, S. M., and M. E. Brown. (2013) “A search for magnesium in Europa’s atmosphere.” *The Astrophysical Journal Letters* 764(2). doi:10.1088/2041-8205/764/2/L28.
- Howard, A. D., and J. M. Moore. (2008) “Sublimation-driven erosion on Callisto: A landform simulation model test.” *Geophysical Research Letters* 35(3). doi:10.1029/2007GL032618.
- Hsu, H.-W., F. Postberg, Y. Sekine, T. Shibuya, S. Kempf, M. Horányi, A. Juhász, *et al.* (2015) “Ongoing hydrothermal activities within Enceladus.” *Nature* 519: 207–210.
- Hussmann, H., and T. Spohn. (2004) “Thermal-orbital evolution of Io and Europa.” *Icarus* 171(2): 391–410.
- Ingalls, A. E., S. R. Shah, R. L. Hansman, L. I. Aluwihare, G. M. Santos, E. R. M. Druffel, and A. Pearson. (2006) “Quantifying Archaeal community autotrophy in the mesopelagic ocean using natural radiocarbon.” *Proceedings of the National Academy of Sciences USA* 103(17): 6442–6447.
- Ivanov, M. A., L. M. Prockter, and B. Dalton. (2011) “Landforms of Europa and selection of landing sites.” *Advances in Space Research* 48(4): 661–677.

- Johnson, R. E., and T. I. Quickenden. (1997) “Photolysis and radiolysis of water ice on outer Solar System bodies.” *Journal of Geophysical Research: Planets* 102(E5): 10985–10996.
- Johnson, R. E., F. Leblanc, B. V. Yakshinskiy, and T. E. Madey. (2002) “Energy distributions for desorption of sodium and potassium from ice: The Na/K ratio at Europa.” *Icarus* 156(1): 136–142.
- Johnson, R. E., R. W. Carlson, J. F. Cooper, C. Paranicas, M. H. Moore, and M. C. Wong. (2004) “Radiation effects on the surfaces of the Galilean satellites.” In *Jupiter: The Planet, Satellites and Magnetosphere*, edited by F. Bagenal, T. E. Dowling and W. B. McKinnon. Cambridge: Cambridge University Press, p. 485–512.
- Johnson, R. E., M. H. Burger, T. A. Cassidy, F. Leblanc, M. Marconi, and W. H. Smyth. (2009) “Composition and detection of Europa’s sputter-induced atmosphere.” In *Europa*, edited by R. T. Pappalardo, W. B. McKinnon and K. K. Khurana. Tucson, AZ: University of Arizona Press, p. 507–528.
- Johnson, W. R. (2001) “Named surface features on Europa.” <http://www.johnstonsarchive.net/astro/europaname.html>. Accessed 23 December 2016.
- Johnston, S. A., and L. G. J. Montesi. (2014) “Formation of ridges on Europa above crystallizing water bodies inside the ice shell.” *Icarus* 237: 190–201.
- Jorgensen, B. B., and I. P. G. Marshall. (2016) “Slow microbial life in the seabed.” *Annual Review of Marine Science* 8: 311–332.
- Jouzel, J., J. R. Petit, R. Souchez, N. I. Barkov, V. Y. Lipenkov, D. Raynaud, M. Stievenard, *et al.* (1999) “More than 200 meters of lake ice above Subglacial Lake Vostok, Antarctica.” *Science* 286(5447): 2138–2141.
- Joyce, G. F. (1994) “Foreward.” In *Origins of Life: The Central Concepts*, edited by D. W. Deamer and G. R. Fleischaker. Boston: Jones & Bartlett Publishers.
- Joye, S. B., I. R. MacDonald, J. P. Montoya, and M. Peccini. (2005) “Geophysical and geochemical signatures of Gulf of Mexico brines.” *Biogeosciences* 2: 295–309.
- Junge, K., H. Eicken, and J. W. Deming. (2004) “Bacterial activity at –2 to –20°C in Arctic wintertime sea ice.” *Applied And Environmental Microbiology* 70(1): 550–557.
- Kaiser, K., and R. Benner. (2008) “Major bacterial contribution to the ocean reservoir of detrital organic carbon and nitrogen.” *Limnology and Oceanography* 53(1): 99–112.
- Kapitsa, A. P., J. K. Ridley, G. D. Robin, M. T. Sieger, and I. A. Zotikov. (1996) “A large deep freshwater lake beneath the ice of Central East Antarctica.” *Nature* 381: 684–686.
- Kargel, J. S., J. Z. Kaye, J. W. Head III, G. M. Marion, R. Sassen, J. K. Crowley, O. Prieto-Ballesteros, S. A. Grant, and D. L. Hogenboom. (2000) “Europa’s crust and ocean: Origin, composition and the prospects for life.” *Icarus* 148(1): 226–265.
- Karl, D. M., D. F. Bird, K. Björkman, T. Houlihan, R. Shakelford, and L. Tupas. (1999) “Microorganisms in the accreted ice of Lake Vostok, Antarctica.” *Science* 286(5447): 2144–2147.

- Karner, M. B., E. F. DeLong, and D. M. Karl. (2001) "Archaeal dominance in the mesopelagic zone of the Pacific Ocean." *Nature* 409: 507–510.
- Kasas, S., F. S. Ruggeri, C. Benadiba, C. Maillard, P. Stupar, H. Tourneu, G. Dietler, and G. Longo. (2015) "Detecting nanoscale vibrations as signature of life." *Proceedings of the National Academy of Sciences USA* 112(2): 378–381.
- Kaspar, H., K. Dettmer, W. Gronwald, and P. J. Oefner. (2008) "Automated GC-MS analysis of free amino acids in biological fluids." *Journal of Chromatography B: Analytical Technologies in the Biomedical and Life Sciences* 870(2): 222–232.
- Kattenhorn, S. A., and T. Hurford. (2009) "Tectonics of Europa." In *Europa*, edited by R. T. Pappalardo, W. B. McKinnon and K. K. Khurana. Tucson, AZ: University of Arizona Press, 199-236.
- Kattenhorn, S. A., and L. M. Prockter. (2014) "Evidence for subduction in the ice shell of Europa." *Nature Geoscience* 7: 762–767.
- Kellogg, C. A. (2010) "Enumeration of viruses and prokaryotes in deep-sea sediments and cold seeps of the Gulf of Mexico." *Deep-Sea Research Part II: Topical Studies in Oceanography* 57(21-23): 2002–2007.
- Khurana, K. K., M. G. Kivelson, K. P. Hand, and C. T. Russell. (2009) "Electromagnetic induction from Europa's ocean and the deep interior." In *Europa*, edited by R. T. Pappalardo, W. B. McKinnon and K. K. Khurana. Tucson, AZ: University of Arizona Press, 571-88.
- Killawee, J. A., I. J. Fairchild, J.-L. Tison, L. Janssens, and R. Lorrain. (1998) "Segregation of solutes and gases in experimental freezing of dilute solutions: Implications for natural glacial systems." *Geochimica et Cosmochimica Acta* 62(23–24): 3637–3655.
- Kivelson, M. G., K. K. Khurana, C. T. Russell, M. Volwerk, R. J. Walker, and C. Zimmer. (2000) "Galileo Magnetometer measurements: A stronger case for a subsurface ocean at Europa." *Science* 289(5483): 1340–1343.
- Klein, H. P. (1978) "The Viking biological experiments on Mars." *Icarus* 34(3): 666–674.
- Klein, H. P., J. Lederberg, and A. Rich. (1972) "Biological experiments: The Viking Mars Lander." *Icarus* 16(1): 139–146.
- Könneke, M., A. E. Bernhard, J. R. de la Torre, C. B. Walker, J. B. Waterbury, and D. A. Stahl. (2005) "Isolation of an autotrophic ammonia-oxidizing marine Archaeon." *Nature* 437: 543–546.
- Korablev, O. I., A. V. Bondarenko, I. V. Dokuchaev, A. Y. Ivanov, O. E. Kozlov, V. A. Kottsov, A. B. Kiselev, J. P. Bibring, and J. J. Fourmond. (2010) "Microscope spectrometer for the Phobos-Grunt mission." *Solar System Research* 44(5): 403–408.
- Kramer, C., and G. Gleixner. (2006) "Variable use of plant- and soil-derived carbon by microorganisms in agricultural soils." *Soil Biology and Biochemistry* 38(11): 3267–3278.
- Krauskopf, K. B., and D. K. Bird. (1995) *Introduction to Geochemistry*. New York: McGraw-Hill, 647 pp.

- Kuhn, E., A. S. Ichimura, V. Peng, C. H. Fritsen, G. Trubl, P. T. Doran, and A. E. Murray. (2014) “Brine assemblages of ultrasmall microbial cells within the ice cover of Lake Vida, Antarctica.” *Applied and Environmental Microbiology* 80(12): 3687–3698.
- Kvenvolden, K. A. (1973) “Criteria for distinguishing biogenic and abiogenic amino acids: Preliminary considerations.” *Space Life Sciences* 4(1): 60–68.
- Lamarche-Gagnon, G., R. Comery, C. W. Greer, and L. G. Whyte. (2015) “Evidence of in situ microbial activity and sulphidogenesis in perennially sub-0°C and hypersaline sediments of a High Arctic permafrost spring.” *Extremophiles* 19(1): 1–15.
- Lee, S., M. Zanolin, A. M. Thode, R. T. Pappalardo, and N. C. Makris. (2003) “Probing Europa’s interior with natural sound sources.” *Icarus* 165(1): 144–167.
- Leith, A. C., and W. B. McKinnon. (1996) “Is there evidence for polar wander on Europa?” *Icarus* 120(2): 387–398.
- Lester, E. D., M. Satomi, and A. Ponce. (2007) “Microflora of extreme arid Atacama Desert soils.” *Soil Biology and Biochemistry* 39(2): 704–708.
- Li, J., and M. D. Eastgate. (2015) “Current Complexity: A tool for assessing the complexity of organic molecules.” *Organic & Biomolecular Chemistry* 13(26): 7164–7176.
- Liebes, S., and A. A. Schwartz. (1977) “Viking 1975 Mars Lander interactive computerized video stereophotogrammetry.” *Journal of Geophysical Research* 82: 4421–4429.
- Lipps, J. H., and S. Rieboldt. (2005) “Habitats and taphonomy of Europa.” *Icarus* 177: 515–527.
- Litchfield, C. D. (1998) “Survival strategies for microorganisms in hypersaline environments and their relevance to life on early Mars.” *Meteoritics & Planetary Science* 33(4): 813–819.
- Liu, S. Y., and Y. F. Wang. (2010) “Application of AFM in microbiology: A Review.” *Scanning* 32(2): 61–73.
- Lobry, J. R. (1996) “Asymmetric substitution patterns in the two DNA strands of bacteria.” *Molecular Biology and Evolution* 13(5): 660–665.
- Lobry, J. R., and C. Gautier. (1994) “Hydrophobicity, expressivity and aromaticity are the major trends of amino-acid usage in 999 *Escherichia coli* chromosome-encoded genes.” *Nucleic Acids Research* 22(15): 3174–3180.
- Lodders, K., and B. Fegley. (1998) *The Planetary Scientist's Companion*. Oxford: Oxford University Press, 400 pp.
- Lognonné, P., V. N. Zharkov, J. F. Karczewski, B. Romanowicz, M. Menvielle, G. Poupinet, B. Brient, et al. (1998) “The Seismic OPTIMISM Experiment.” *Planetary and Space Science* 46(6-7): 739–747.
- Lollar, B. S., G. Lacrampe-Couloume, G. F. Slater, J. Ward, D. P. Moser, T. M. Gihring, L. H. Lin, and T. C. Onstott. (2006) “Unravelling abiogenic and biogenic sources of methane in the Earth’s deep subsurface.” *Chemical Geology* 226(3-4): 328–339.
- Lorenz, R. D. (2012). Planetary seismology—Expectations for lander and wind noise with application to Venus. *Planetary and Space Science*, 62(1), 86-96.

- Lorenz, R. D. (2016). Lander rocket exhaust effects on Europa regolith nitrogen assays. *Planetary and Space Science*, 127, 91-94.
- Lovelock, J. E. (1965) "A physical basis for life detection experiments." *Nature* 207(4997): 568–570.
- Lowe, D. G. (2004) "Distinctive image features from scale-invariant keypoints." *International Journal of Computer Vision* 60: 91–110.
- Lowenstam, H. A., and S. Weiner. (1989) *On Biomineralization*. New York: Oxford University Press, Inc., 336 pp.
- Lu, Y., and S. Freeland. (2006) "On the evolution of the standard amino-acid alphabet." *Genome Biology* 7. doi:10.1186/gb-2006-7-1-102.
- Mahaffy, P. R., C. R. Webster, M. Cabane, P. G. Conrad, P. Coll, S. K. Atreya, R. Arvey, *et al.* (2012) "The Sample Analysis at Mars investigation and instrument suite." *Space Science Reviews* 170(1): 401–478.
- Maki, J., D. Thiessen, A. Pourangi, P. Kobzeff, T. Litwin, L. Scherr, S. Elliott, A. Dingizian, and M. Maimone. (2012) "The Mars Science Laboratory engineering cameras." *Space Science Reviews* 170(1): 77–93.
- Maki, J. N., C. M. McKinney, R. G. Sellar, R. G. Willson, D. S. Copley-Woods, D. C. Gruel, D. L. Nuding, M. Valvo, T. Goodsall, J. McGuire, J. Kempenaar, T. E. Litwin. (2016) "Enhanced Engineering Cameras (EECAMs) for the Mars 2020 Rover." 3rd *International Workshop on Instrumentation for Planetary Missions*. Pasadena, CA. Abstract #4132.
- Malin, M. C., *et al.* (2017) "The Mars Science Laboratory mast and descent cameras. I. Investigation and instrument descriptions." *Journal of Geophysical Research: Planets*. In review.
- Malfatti, F., T. J. Samo, and F. Azam. (2010) "High-resolution imaging of pelagic bacteria by atomic force microscopy and implications for carbon cycling." *The ISME Journal* 4: 427–439.
- Martin, A., J. A. Hall, R. O'Toole, S. K. Davy, and K. G. Ryan. (2008) "High single-cell metabolic activity in Antarctic sea ice bacteria." *Aquatic Microbial Ecology* 52(1): 25–31.
- Martins, Z., C. M. O. Alexander, G. E. Orzechowska, M. L. Fogel, M. A. Sephton, and P. Ehrenfreund. (2007a) "Indigenous amino acids present in CR primitive meteorites." *Meteoritics & Planetary Science* 42(12): 2125–2136.
- Martins, Z., B. A. Hofmann, E. Gnos, R. C. Greenwood, A. Verchovsky, I. A. Franchi, A. J. T. Jull, *et al.* (2007b) "Amino acid composition, petrology, geochemistry, ¹⁴C terrestrial age and oxygen isotopes of the Shisr 033 CR chondrite." *Meteoritics & Planetary Science* 42(9): 1581–1595.
- Masursky, H., and N. L. Crabill. (1976) "The Viking landing sites: Selection and certification." *Science* 193: 809–812.
- . (1981) "Viking Site Selection and Certification." Washington, D.C.: National Aeronautics and Space Administration, Report #NASA SP-429, 34 pp.

- Maurice, S., R. C. Wiens, M. Saccoccio, B. Barraclough, O. Gasnault, O. Forni, N. Mangold, *et al.* (2012) “The ChemCam instrument suite on the Mars Science Laboratory (MSL) Rover: Science objectives and mast unit description.” *Space Science Reviews* 170(1): 95–166.
- Mazur, P., E. S. Barghoon, H. O. Halvorson, T. H. Jukes, I. R. Kaplan, and L. Margulis. (1978) “Biological implications of the Viking mission to Mars.” *Space Science Reviews* 22(1): 3–34.
- McCarthy, C., and R. F. Cooper. (2016) “Tidal dissipation in creeping ice and the thermal evolution of Europa.” *Earth and Planetary Science Letters* 443: 185–194.
- McCarthy, M. D., J. I. Hedges, and R. Benner. (1998) “Major bacterial contribution to marine dissolved organic nitrogen.” *Science* 281: 231–234.
- McCullom, T. M. (1999) “Methanogenesis as a potential source of chemical energy for primary biomass production by autotrophic organisms in hydrothermal systems on Europa.” *Journal of Geophysical Research: Planets* 104(E12): 30729–30742.
- McCullom, T. M., and J. P. Amend. (2005) “A thermodynamic assessment of energy requirements for biomass synthesis by chemolithoautotrophic micro-organisms in oxic and anoxic environments.” *Geobiology* 3(2): 135–144.
- McCullom, T. M., and J. S. Seewald. (2007) “Abiotic synthesis of organic compounds in deep-sea hydrothermal environments.” *Chemical Reviews* 107(2): 382–401.
- McCord, T. B., G. B. Hansen, D. L. Matson, T. V. Johnson, J. K. Crowley, F. P. Fanale, R. W. Carlson, *et al.* (1999) “Hydrated salt minerals on Europa’s surface from the Galileo Near-Infrared Mapping Spectrometer (NIMS) investigation.” *Journal of Geophysical Research: Planets* 104(E5): 11827–11851.
- McEwen, A. S., L. Keszthelyi, J. R. Spencer, G. Schubert, D. L. Matson, R. Lopes-Gautier, K. P. Klaasen, *et al.* (1998) “High-temperature silicate volcanism on Jupiter's moon Io.” *Science* 281(5373): 87–90.
- McKay, C. P. (2004) “What is life—and how do we search for it in other worlds?” *PLOS Biology* 2(9). doi:10.1371/journal.pbio.0020302.
- Ménez, B., V. Pasini, and D. Brunelli. (2012) “Life in the hydrated suboceanic mantle.” *Nature Geoscience* 5(2): 133–137.
- Michaut, C., and M. Manga. “Domes, pits, and small chaos on Europa produced by water sills.” *Journal of Geophysical Research: Planets* 119(3): 550–573.
- Mikucki, J. A., A. Pearson, D. T. Johnston, A. V. Turchyn, J. Farquhar, D. P. Schrag, A. D. Anbar, J. C. Priscu, and P. A. Lee. (2009) “A contemporary microbially maintained subglacial ferrous ‘ocean’.” *Science* 324: 397–400.
- Miltner, A., H.-H. Richnow, F.-D. Kopinke, and M. Kästner. (2004) “Assimilation of CO₂ by soil microorganisms and transformation into soil organic matter.” *Organic Geochemistry* 35(9): 1015–1024.
- Moore, H. J., R. E. Hutton, C. D. Clow, and C. R. Spitzer. (1987) “Physical properties of the surface materials at the Viking landing sites on Mars.” *U.S. Geological Survey Professional Paper, Report #1389*. Washington, D.C.: U.S. Government Printing Office, 222 pp.

- Moore, J. M., M. T. Mellon, and A. P. Zent. (1996) “Mass wasting and ground collapse in terrains of volatile-rich deposits as a Solar System-wide geological process: The pre-Galileo view.” *Icarus* 122: 63–78.
- Moore, J. M., G. Black, B. Buratti, C. B. Phillips, J. Spencer, and R. Sullivan. (2009) “Surface properties, regolith, and landscape degradation.” In *Europa*, edited by R. T. Pappalardo, W. B. McKinnon and K. K. Khurana. Tucson, AZ: University of Arizona Press, p. 329–349.
- Moore, M. H., and R. L. Hudson. (1998) “Infrared study of non-irradiated water-ice mixtures with hydrocarbons relevant to comets.” *Icarus* 135: 518–527.
- Moore, M. H., R. L. Hudson, and R. W. Carlson. (2007) “The radiolysis of SO₂ and H₂S in water ice: Implications for the icy jovian satellites.” *Icarus* 189(2): 409–423.
- Moore, M. H., R. F. Ferrante, R. L. Hudson, and J. N. Stone. (2007) “Ammonia–water ice laboratory studies relevant to outer Solar System surfaces.” *Icarus* 190(1): 260–273.
- Moores, J. E., J. Schieber, A. M. Kling, R. M. Haberle, C. A. Moore, M. S. Anderson, I. Katz, *et al.* (2016) “Transient atmospheric effects of the landing of the Mars Science Laboratory rover: The emission and dissipation of dust and carbazic acid.” *Advances in Space Research* 58(6): 1066–1092.
- Murray, A. E., and J. J. Grzymalski. (2007) “Diversity and genomics of Antarctic marine micro-organisms.” *Philosophical Transactions Of The Royal Society B: Biological Sciences* 362(1488): 2259–2271.
- Murray, A. E., F. Kenig, C. H. Fritsen, C. P. McKay, K. M. Cawley, R. Edwards, D. M. McKnight, *et al.* (2012) “Microbial life at –13°C in the brine of an ice-sealed Antarctic lake.” *Proceedings of the National Academy of Sciences USA* 109: 20626–20631.
- Mustard, J. F., M. Adler, A. Allwood, D. S. Bass, D. W. Beaty, J. F. Bell III, W. B. Brinckerhoff, *et al.* (2013) “Report of the Mars 2020 Science Definition Team.” Mars Exploration Program Analysis Group (MEPAG), 154 pp.
- Mykytczuk, N. C. S., J. R. Lawrence, C. R. Omelon, G. Southam, and L. G. Whyte. (2016) “Microscopic characterization of the bacterial cell envelope of *Planococcus Halocryophilus* Or1 during subzero growth at –15°C.” *Polar Biology* 39(4): 701–712.
- NASA (2014) “2014 Science Plan (Section 4.3).” https://smd-prod.s3.amazonaws.com/science-green/s3fs-public/atoms/files/2014_Science_Plan_PDF_Update_508_TAGGED.pdf. Accessed 9 January 2017.
- (2015) “NASA Astrobiology Strategy 2015.” Edited by L. Hays. https://nai.nasa.gov/media/medialibrary/2015/10/NASA_Astrobiology_Strategy_2015_151008.pdf.
- (2017a) “Science Mission Directorate.” <https://science.nasa.gov/>. Accessed 10 January 2017.
- (2017b) “Life Detection Ladder.” <https://astrobiology.nasa.gov/research/life-detection/ladder/>. Edited by J. Fletcher. Accessed 22 January 2017.

- NASA Policy Directive [NPR] 8020.7G (2013) “Biological Contamination Control for Outbound and Inbound Planetary Spacecraft.” (*Updated and Revalidated 17 May 2013*).
- NASA Procedural Requirements [NPR] 8020.12D (2011) “Planetary Protection Provisions for Robotic Extraterrestrial Missions.” (*Effective 20 April 2011*).
- National Academy of Sciences [NAS]. (1958) “Resolution Adopted by the Council of the NAS, February 8, 1958.” In *Addendum to Minutes of the Meeting of the National Academy of Sciences, February 8, 1958*.
- National Research Council [NRC]. (2000) *Preventing the Forward Contamination of Europa*. Washington, D.C.: The National Academy Press. doi:10.17226/9895.
- . (2003) *New Frontiers in the Solar System: An Integrated Exploration Strategy*. Washington, D.C.: The National Academies Press. doi:10.17226/10432.
- . (2011) *Vision and Voyages for Planetary Science in the Decade 2013-2022*. Washington, D.C.: The National Academies Press. doi:10.17226/13117.
- Navarro-González, R., K. F. Navarro, J. de la Rosa, E. Iñiguez, P. Molina, L. D. Miranda, P. Morales, *et al.* (2006) “The limitations on organic detection in Mars-like soils by Thermal Volatilization-Gas Chromatography-MS and their implications for the Viking results.” *Proceedings of the National Academy of Sciences USA* 103(44): 16089–16094.
- Navarro-González, R., E. Vargas, J. de la Rosa, A. C. Raga, and C. P. McKay. (2010) “Reanalysis of the Viking results suggests perchlorate and organics at midlatitudes on Mars.” *Journal of Geophysical Research: Planets* 115: E12010. doi:10.1029/2010JE003599
- Nealson, K. H. (1997) “The limits of life on Earth and searching for life on Mars.” *Journal of Geophysical Research: Planets* 102(E10): 23675–23686.
- Nedwell, D. B. (2006) “Effect of low temperature on microbial growth: Lowered affinity for substrate limits growth at low temperature.” *FEMS Microbiology Ecology* 30(2): 101–111.
- Ngwenya, B. T. (2016) “Bacterial Mineralization.” In *Reference Module in Materials Science and Materials Engineering*, edited by S. Hashmi, Elsevier. doi:10.1016/B978-0-12-803581-8.02248-7.
- Niederberger, T. D., N. N. Perreault, J. R. Lawrence, J. L. Nadeau, R. E. Mielke, C. W. Greer, D. T. Andersen, and L. G. Whyte. (2009) “Novel sulfur-oxidizing streamers thriving in perennial cold saline springs of the Canadian High Arctic.” *Environmental Microbiology* 11(3): 616–629.
- Niederberger, T. D., N. N. Perreault, S. Tille, B. S. Lollar, G. Lacrampe-Couloume, D. Andersen, C. W. Greer, W. Pollard, and L. G. Whyte. (2010) “Microbial characterization of a subzero, hypersaline methane seep in the Canadian High Arctic.” *The ISME Journal* 4(10): 1326–1339.
- Niemann, H. B., D. N. Harpold, S. K. Atreya, G. R. Carignan, D. M. Hunten, and T. C. Owen. (1992) “Galileo Probe Mass Spectrometer Experiment.” *Space Science Reviews* 60(1): 111–142.

- Nimmo, F. (2004) “Stresses generated in cooling viscoelastic ice shells: Application to Europa.” *Journal of Geophysical Research: Planets* 109(E12001): doi:10.1029/2004JE002347.
- Nimmo, F., and B. Giese. (2005) “Thermal and topographic tests of Europa chaos formation models from Galileo E15 observations.” *Icarus* 177(2): 327–340.
- Nimmo, F., and M. Manga. (2009) “Geodynamics of Europa's icy shell.” In *Europa*, edited by R. T. Pappalardo, W. B. McKinnon and K. K. Khurana. Tucson, AZ: University of Arizona Press, 529-44.
- Nishikawa, K., and T. Ooi. (1982) “Correlation of the amino-acid-composition of a protein to its structural and biological characters.” *Journal of Biochemistry* 91(5): 1821–1824.
- Nordheim, T., K. P. Hand, C. Paranicus, C. Howett, and A. R. Hendrix. (2016) “Energetic charged particle interactions at icy satellites.” *American Geophysical Union 2016 Fall Meeting*. San Francisco, CA. Abstract #SM34A-08.
- Nordheim, T. A., K. P. Hand, and C. Paranicus. (2017a) “Europa’s surface radiation environment and considerations for in situ sampling.” *In preparation*.
- Nordheim, T. A., K. P. Hand, C. Paranicus, C. J. A. Howett, A. R. Hendrix, G. H. Jones, and A. J. Coates. (2017b) “The near surface electron radiation environment of Saturn’s moon Mimas.” *Icarus* 286: 56–68.
- Northrup, D. (1981) “The expression of isotope effects on enzyme-catalyzed reactions.” *Annual Review of Biochemistry* 50: 103–131.
- O'Brien, D., P. Geissler, and R. Greenberg. (2002) “A melt-through model for chaos formation on Europa.” *Icarus* 156(1): 152–161.
- Ojakangas, G. W., and D. J. Stevenson. (1989a) “Polar wander of an ice shell on Europa.” *Icarus* 81(2): 242–270.
- . (1989b) “Thermal state of an ice shell on Europa.” *Icarus* 81: 220–241.
- Orcutt, B. N., J. B. Sylvan, N. J. Knab, and K. J. Edwards. (2011) “Microbial ecology of the dark ocean above, at, and below the seafloor.” *Microbiology and Molecular Biology Reviews* 75(2): 361–422.
- Ori, G. G., A. Aboudan, A. Pacifici, F. Cannarsa, A. Murana, S. Portigliotti, A. Marcer, and L. Lorenzoni. (2015) “The ExoMars 2016 landing site.” *European Planetary Science Congress 2015*. Nantes, France. Abstract #EPSC2015-764-1.
- Paganini, L., M. J. Mumma, T. Hurford, L. Roth, and G. L. Villanueva. (2016) “‘Sniffing’ Jupiter’s moon Europa through ground-based IR observations.” *48th Annual Meeting of the Division for Planetary Sciences of the American Astronomical Society*. Pasadena, CA. Abstract #517.03
- Pappalardo, R. T., and A. C. Barr. (2004) “The origin of domes on Europa: The role of thermally induced compositional diapirism.” *Geophysical Research Letters* 31(1): L01701.
- Pappalardo, R. T., W. B. McKinnon, and K. K. Khurana, eds. (2009) *Europa*. Tucson, AZ: University of Arizona Press, 720 pp.

- Pappalardo, R. T., J. W. Head, R. Greeley, R. J. Sullivan, C. Pilcher, G. Schubert, W. B. Moore, *et al.* (1998) “Geological evidence for solid-state convection in Europa’s ice shell.” *Nature* 391(6665): 365–368.
- Pappalardo, R. T., S. Vance, F. Bagenal, B. G. Bills, D. L. Blaney, D. D. Blankenship, W. B. Brinckerhoff, *et al.* (2013) “Science potential from a Europa Lander.” *Astrobiology* 13(8): 740–773.
- Pappalardo, R., D. Senske, L. M. Prockter, B. Paczkowski, S. Vance, B. Goldstein, T. Magner, and B. Cooke. (2015) “Science and reconnaissance from the Europa Clipper Mission concept: Exploring Europa’s habitability.” *EGU General Assembly 2015*. Vienna, Austria. Abstract #EGU2015-8155.
- Paranicas, C., J. F. Cooper, H. B. Garrett, R. E. Johnson, and S. J. Sturmer. (2009) “Europa’s radiation environment and its effects on the surface.” In *Europa*, edited by R.T. Pappalardo, W. B. McKinnon and K. K. Khurana. Tucson, AZ: University of Arizona Press, p. 529–544.
- Paranicas, C., J. M. Ratliff, B. H. Mauk, C. Cohen, and R. E. Johnson. (2002) “The ion environment of Europa and its role in surface energetics.” *Geophysical Research Letters* 29(5): 18-1–18-4.
- Parenteau, M. N., and S. L. Cady. (2010) “Microbial biosignatures in iron-mineralized phototrophic mats at Chocolate Pots Hot Springs, Yellowstone National Park, United States.” *Palaios* 25(2): 97–111.
- Parnell, J., D. Cullen, M. R. Sims, S. Bowden, C. S. Cockell, R. Court, P. Ehrenfreund, *et al.* (2007) “Searching for life on Mars: Selection of molecular targets for ESA’s Aurora ExoMars Mission.” *Astrobiology* 7(4): 578–604.
- Partensky, F., W. R. Hess, and D. Vaultot. (1999) “Prochlorococcus, a marine photosynthetic prokaryote of global significance.” *Microbiology and Molecular Biology Reviews* 63(1): 106–127.
- Pasek, M. A., and R. Greenberg. (2012) “Acidification of Europa’s subsurface ocean as a consequence of oxidant delivery.” *Astrobiology* 12: 151–159.
- Patterson, G. W., C. Paranicas, and L. M. Prockter. (2012) “Characterizing electron bombardment of Europa’s surface by location and depth.” *Icarus* 220(1): 286–290.
- Perreault, N. N., D. T. Andersen, W. H. Pollard, C. W. Greer, and L. G. Whyte. (2007) “Characterization of the prokaryotic diversity in cold saline perennial springs of the Canadian High Arctic.” *Applied and Environmental Microbiology* 73(5): 1532–1543.
- Peters, K. E., C. C. Walters, and J. M. Moldowan. (2005) *The Biomarker Guide: Biomarkers and Isotopes in the Environment and Human History*. Vol. 1, Cambridge: Cambridge University Press, 492 pp.
- Phillips, C. B., A. S. McEwen, G. V. Hoppa, S. A. Fagents, R. Greeley, J. E. Klemaszewski, R. T. Pappalardo, K. P. Klaasen, and H. H. Breneman. (2000) “The search for current geologic activity on Europa.” *Journal of Geophysical Research* 105(E9): 22579–22597.
- Pilcher, C. B. (2004) “Biosignatures of early Earths.” *Astrobiology* 3(3): 471–486.

- Phoenix, V. R., K. O. Konhauser, D. G. Adams, and S. H. Bottrell (2001) "Role of biomineralization as an ultraviolet shield: Implications for Archean life." *Geology* 29(9): 823–826.
- Pierazzo, E., and C. F. Chyba. (2002) "Cometary delivery of biogenic elements to Europa." *Icarus* 157(1): 120–127.
- Pike, W. T., U. Staufer, M. H. Hecht, W. Goetz, D. Parrat, H. Sykulska-Lawrence, S. Vijendran, and M. B. Madsen. (2011) "Quantification of the dry history of the martian soil inferred from in situ microscopy." *Geophysical Research Letters* 38(24). doi:10.1029/2011gl49896.
- Pinkerton, H., S. A. Fagents, L. Prockter, P. Schenk, and D. A. Williams. (2000) "Exotic Lava Flows." In *Environmental Effects on Volcanic Eruptions: From Deep Oceans to Deep Space*, edited by J. R. Zimbelman and T. K. P. Gregg. New York: Springer Science + Business Media, LLC, p. 207–241.
- Pizzarello, S. (2006) "The chemistry of life's origin: A carbonaceous meteorite perspective." *Accounts of Chemical Research* 39(4): 231–237.
- Pizzarello, S., and W. Holmes. (2009) "Nitrogen-containing compounds in two CR2 meteorites: ¹⁵N composition, molecular distribution and precursor molecules." *Geochimica et Cosmochimica Acta* 73(7): 2150–2162.
- Porco, C., D. DiNino, and F. Nimmo. (2014) "How the geysers, tidal stresses, and thermal emission across the South Polar Terrain of Enceladus are related." *The Astronomical Journal* 148(3). doi:10.1088/0004-6256/148/3/45.
- Porter, J. R. (1976) "Antony Van Leeuwenhoek: Tercentenary of His Discovery of Bacteria." *Bacteriological Reviews* 40(2): 260–269.
- Postberg, F., J. Schmidt, J. Hillier, S. Kempf, and R. Srama (2011) "A salt-water reservoir as the source of a compositionally stratified plume on Enceladus." *Nature* 474: 620–622.
- Potter-McIntyre, S. L., M. A. Chan, and B. J. McPherson. (2014) "Textural and mineralogical characteristics of microbial fossils associated with modern and ancient iron (oxyhydr)oxides: Terrestrial analogue for sediments in Gale Crater." *Astrobiology* 14(1): 1–14.
- Price, P. B., and T. Sowers. (2004) "Temperature dependence of metabolic rates for microbial growth, maintenance, and survival." *Proceedings of the National Academy of Sciences USA* 101(13): 4631–4636.
- Price, P. B., R. A. Rohde, and R. C. Bay. (2009) "Fluxes of microbes, organic aerosols, dust, sea-salt Na ions, non-sea-salt Ca ions, and methanesulfonate onto Greenland and Antarctic ice." *Biogeosciences* 6(3): 479–486.
- Priscu, J. C., and K. P. Hand. (2012) "Microbial habitability of icy worlds." *Microbe* 7: 167–172.
- Priscu, J. C., E. E. Adams, W. B. Lyons, M. A. Voytek, D. W. Mogk, R. L. Brown, C. P. McKay, *et al.* (1999) "Geomicrobiology of subglacial ice above Lake Vostok, Antarctica." *Science* 286: 2141–2144.

- Prockter, L. M., and G. W. Patterson. (2009) “Morphology and evolution of Europa’s ridges and bands.” In *Europa*, edited by R. T. Pappalardo, W. B. McKinnon and K. K. Khurana. Tuscon, AZ: University of Arizona Press, p. 237–258.
- Prockter, L., and P. Schenk. (2005) “Origin and evolution of Castalia Macula, an anomalous young depression on Europa.” *Icarus* 177(2): 305–326.
- Prockter, L. M., J. W. Head III, R. T. Pappalardo, R. J. Sullivan, A. E. Clifton, B. Giese, R. Wagner, and G. Neukum. (2002) “Morphology of european bands at high resolution: A mid-ocean ridge-type rift mechanism.” *Journal of Geophysical Research* 107(E5): 5028.
- Quick, L. C., O. S. Barnouin, L. M. Prockter, and G. W. Patterson. (2013) “Constraints on the detection of cryovolcanic plumes on Europa.” *Planetary and Space Science* 86: 1–9.
- Quick, L. C., L. S. Glaze, and S. M. Baloga. (2017) “Cryovolcanic emplacement of domes on Europa.” *Icarus* 284: 477–488.
- Rappe, M. S., S. A. Connon, K. L. Vergin, and S. J. Giovannoni. (2002) “Cultivation of the ubiquitous SAR11 marine bacterioplankton clade.” *Nature* 418(6898): 630–633.
- Rathbun, J. A., N. J. Rodriguez, and J. R. Spencer. (2010) “Galileo PPR observations of Europa: Hotspot detection limits and surface thermal properties.” *Icarus* 210(2): 763–769.
- Raulin, F., K. P. Hand, C. P. McKay, and M. Viso. (2010) “Exobiology and planetary protection of icy moons.” *Space Science Reviews* 153(1): 511–535.
- Resing, J. A., P. N. Sedwick, C. R. German, W. J. Jenkins, J. W. Moffett, B. M. Sohst, and A. Tagliabue. (2015) “Basin-scale Transport of hydrothermal dissolved metals across the South Pacific Ocean.” *Nature* 523: 200–203.
- Rhoden, A. R., and T. A. Hurford. (2013) “Lineament azimuths on Europa: Implications for obliquity and non-synchronous rotation.” *Icarus* 226(1): 841–859.
- Rhoden, A. R., B. Militzer, E. M. Huff, T. A. Hurford, M. Manga, and M. A. Richards. (2010) “Constraints on Europa’s rotational dynamics from modeling of tidally-driven fractures.” *Icarus* 210(2): 770–784.
- Rhoden, A. R., G. Wurman, E. M. Huff, M. Manga, and T. A. Hurford. (2012) “Shell tectonics: A mechanical model for strike-slip displacement on Europa.” *Icarus* 218(1): 297–307.
- Riedler, W., K. Torkar, H. Jeszenszky, J. Romstedt, H. S. C. Alleyne, H. Arends, W. Barth, *et al.* (2007) “MIDAS - the Micro-Imaging Dust Analysis System for the Rosetta Mission.” *Space Science Reviews* 128(1-4): 869–904.
- Rosch, P., M. Harz, M. Schmitt, and J. Popp. (2005) “Raman spectroscopic identification of single yeast cells.” *Journal of Raman Spectroscopy* 36(5): 377–379.
- Roszak, D. B., and R. R. Colwell. (1987) “Survival strategies of bacteria in the natural environment.” *Microbiology and Molecular Biology Reviews* 51(3): 365–379.
- Roth, L., K. D. Retherford, J. Saur, D. F. Strobel, P. D. Feldman, M. A. McGrath, and F. Nimmo. (2014a) “Orbital apocenter is not a sufficient condition for HST/STIS

- detection of Europa's water vapor aurora." *Proceedings of the National Academy of Sciences USA* 111(48): 5123–5132.
- Roth, L., J. Saur, K. D. Retherford, D. F. Strobel, P. D. Feldman, M. A. McGrath, and F. Nimmo. (2014b) "Transient water vapor at Europa's south pole." *Science* 343(6167): 171–174.
- Rothschild, L. J., and R. L. Mancinelli. (2001) "Life in extreme environments." *Nature* 409(6823): 1092–1101.
- Røy, H., J. Kallmeyer, R. R. Adhikari, R. Pockalny, B. B. Jørgensen, and S. D'Hondt. (2012) "Aerobic microbial respiration in 86-million-year-old deep-sea red clay." *Science* 336(6083): 922–925.
- Royston-Bishop, G., J. C. Priscu, M. Tranter, B. Christner, M. J. Siegert, and V. Lee. (2005) "Incorporation of particulates into accreted ice above Subglacial Vostok Lake, Antarctica." *Annals of Glaciology* 40(1): 145–150.
- Rull, F., S. Maurice, E. Díaz, C. Tato, A. Pacros, *et al.* (2011a) "The Raman Laser Spectrometer (RLS) on the ExoMars 2018 Rover Mission." *42nd Lunar and Planetary Science Conference*. The Woodlands, TX. Abstract #2400.
- Rull, F., A. Sansano, E. Díaz, C. P. Canora, A. G. Moral, C. Tato, M. Colombo, *et al.* (2011b) "ExoMars Raman Laser Spectrometer for ExoMars." *Proceedings of the SPIE Conference*. San Diego, CA. In *Instruments, Methods, and Missions for Astrobiology XIV*. doi:10.1117/12.896787.
- Rummel, J., and L. Billings. (2004) "Issues in planetary protection: Policy, protocol, and implementation." *Space Policy* 20: 49–54.
- Sagan, C. "Life." In *Encyclopedia Britannica*, 1970.
- Sagan, C., W. R. Thompson, R. Carlson, D. Gurnett, and C. Hord. (1993) "A search for life on Earth from the Galileo spacecraft." *Nature* 365: 715.
- Salas, E. C., R. Bhartia, L. Anderson, W. F. Hug, R. D. Reid, G. Iturrino, and K. J. Edwards. (2015) "In situ detection of microbial life in the deep biosphere in igneous ocean crust." *Frontiers in Microbiology* 6: 1260.
- Santibáñez, P. A., J. R. McConnell, and J. C. Priscu. (2016) "A flow cytometric method to measure prokaryotic records in ice cores: An example from the West Antarctic Ice Sheet Divide drilling site." *Journal of Glaciology* 62(234): 655–673.
- Schenk, P. M. (2002) "Thickness constraints on the icy shells of the Galilean satellites from a comparison of crater shapes." *Nature* 417: 419–421.
- . (2009) "Slope characteristics of Europa: Constraints for landers and radar sounding." *Geophysical Research Letters* 36(15). doi:10.1029/2009GL039062.
- Schenk, P. M., and R. T. Pappalardo. (2004) "Topographic variations in chaos on Europa: Implications for diapiric formation." *Geophysical Research Letters* 31(16): L16703.
- Schilling, N., F. M. Neubauer, and J. Saur. (2007) "Time-varying interaction of Europa with the jovian magnetosphere: Constraints on the conductivity of Europa's subsurface ocean." *Icarus* 192(1): 41–55.

- Schmerr, N. C., K. M. Brunt, F. Cammarano, T. A. Hurford, V. Lekic, M. P. Panning, A. Rhoden, and J. M. Sauber. (2013) "Seismometers on Europa: Insights from modeling and Antarctic ice shelf analogs." *American Geophysical Union 2013 Fall Meeting*. San Francisco, CA. Abstract #P54A-01.
- Schmidt, B. E., D. D. Blankenship, G. W. Patterson, and P. M. Schenk. (2011) "Active formation of 'chaos terrain' over shallow subsurface water on Europa." *Nature* 479: 502–505.
- Schmidt, J., N. Brilliantov, F. Spahn, and S. Kempf. (2008) "Slow dust in Enceladus" plume from condensation and wall collisions in Tiger Stripe fractures." *Nature* 451: 685–688.
- Schmitt, J., and H. C. Flemming. (1998) "FTIR-spectroscopy in microbial and material analysis." *International Biodeterioration & Biodegradation* 41(1): 1–11.
- Schmitt-Kopplin, P., Z. Gabelica, R. D. Gougeon, A. Fekete, B. Kanawati, M. Harir, I. Gebefuegi, G. Eckel, and N. Hertkorn. (2010) "High molecular diversity of extraterrestrial organic matter in Murchison meteorite revealed 40 years after its fall." *Proceedings of the National Academy of Sciences USA* 107(7): 2763–2768.
- Serrano, P., D. Wagner, U. Bottger, J.-P. de Vera, P. Lasch, and A. Hermelink. (2014) "Single-cell analysis of the methanogenic archaeon *Methanosarcina soligelidi* from Siberian permafrost by means of confocal Raman microspectroscopy for astrobiological research." *Planetary and Space Science* 98: 191–197.
- Shen, Y., R. Benner, A. E. Murray, C. Gimpel, B. G. Mitchell, E. L. Weiss, and C. Reiss. (2017) "Bioavailable dissolved organic matter and biological hot spots during austral winter in Antarctic waters." *Journal of Geophysical Research: Oceans*. doi:10.1002/2016JC012301.
- Shimoyama, A., K. Harada, and K. Yanai. (1985) "Amino-acids from the Yamato-791198 carbonaceous chondrite from Antarctica." *Chemistry Letters*, no. 8: 1183–1186.
- Shirley, J. H., J. B. Dalton III, L. M. Prockter, and L. W. Kamp. (2010) "Europa's ridged plains and smooth low albedo plains: Distinctive compositions and compositional gradients at the leading side–trailing side boundary." *Icarus* 210(1): 358–384.
- Shock, E. L., and E. S. Boyd. (2015) "Principles of Geobiochemistry." *Elements* 11(6): 395–401.
- Shorthill, R. W., R. E. Hutton, H. J. Moore, and R. F. Scott. (1972) "Martian physical properties experiments: The Viking Mars Lander." *Icarus* 16: 217–222.
- Simo, C., V. Garcia-Canas, and A. Cifuentes. (2010) "Chiral CE-MS." *Electrophoresis* 31(9): 1442–1456.
- Simões, J. C., J. R. Petit, R. Souchez, V. Y. Lipenkov, M. De Angelis, L. B. Liu, J. Jouzel, and P. Duval. (2002) "Evidence of glacial flour in the deepest 89 m of the Vostok Ice Core." *Annals of Glaciology* 35(1): 340–346.
- Soderlund, K. M., B. E. Schmidt, J. Wicht, and D. D. Blankenship. (2014) "Ocean-sriven heating of Europa's icy shell at low latitudes." *Nature Geoscience* 7: 16–19.

- Sotin, C., and G. Tobie. (2004) "Internal structure and dynamics of the large icy satellites." *Comptes Rendus Physique* 5(7): 769–780.
- Sotin, C., J. W. Head, and G. Tobie. (2002) "Europa: Tidal heating of upwelling thermal plumes and the origin of lenticulae and chaos melting." *Geophysical Research Letters* 29(8). doi:10.1029/2001gl013844.
- Souchez, R., J.-R. Petit, J. Jouzel, J. Simões, M. de Angelis, N. Barkov, M. Stiévenard, *et al.* (2002) "Highly deformed basal ice in the Vostok Core, Antarctica." *Geophysical Research Letters* 29(7): 40-1–40-4.
- Sparks, W. B., K. P. Hand, M. A. McGrath, E. Bergeron, M. Cracraft, and S. E. Deustua. "Probing for Evidence of Plumes on Europa with Hst/Stis." *The Astrophysical Journal* 829 (2016).
- Sparks, W. B., M. McGrath, K. Hand, H. C. Ford, P. Geissler, J. H. Hough, E. L. Turner, C. F. Chyba, R. Carlson, and M. Turnbull. (2010) "Hubble Space Telescope observations of Europa in and out of eclipse." *International Journal of Astrobiology* 9(4): 265–271.
- Spaun, N. A., L. M. Prockter, J. W. Head, R. T. Pappalardo, G. C. Collins, A. Antman, R. Greeley, and The Galileo SSI Team. (1999) "Spatial distribution of lenticulae and chaos on Europa." *30th Lunar and Planetary Science Conference*. The Woodlands, TX. Abstract #1847.
- Spencer, J. R. (1987) "Thermal segregation of water ice on the Galilean satellites." *Icarus* 69: 297–313.
- Spencer, J. R., and W. M. Calvin. (2002) "Condensed O₂ on Europa and Callisto." *The Astronomical Journal* 124(6): 3400–3403.
- Squyres, S. W., R. E. Arvidson, J. F. Bell III, J. Brückner, N. A. Cabrol, W. Calvin, M. H. Carr, *et al.* (2004a) "The Spirit Rover's Athena Science Investigation at Gusev Crater, Mars." *Science* 305(5685): 794–799.
- Squyres, S. W., J. P. Grotzinger, R. E. Arvidson, J. F. Bell III, W. Calvin, P. R. Christensen, B. C. Clark, *et al.* (2004b) "In situ evidence for an ancient aqueous environment at Meridiani Planum, Mars." *Science* 306(5702): 1709–1714.
- Stack, K. M., C. S. Edwards, J. P. Grotzinger, S. Gupta, D. Y. Sumner, F. J. Calef III, L. A. Edgar, *et al.* (2016) "Comparing orbiter and rover image-based mapping of an ancient sedimentary environment, Aeolis Palus, Gale Crater, Mars." *Icarus* 280: 3–21.
- Stalport, F., D. P. Glavin, J. L. Eigenbrode, D. Bish, D. Blake, P. Coll, C. Szopa, *et al.* (2012) "The influence of mineralogy on recovering organic acids from Mars analogue materials using the 'One-Pot' derivatization experiment on the Sample Analysis at Mars (SAM) instrument suite." *Planetary and Space Science* 67(1): 1–13.
- Steger, K., K. Premke, C. Gudas, I. Sundh, and L. J. Tranvik. (2011) "Microbial biomass and community composition in boreal lake sediments." *Limnology and Oceanography* 56(2): 725–733.
- Stevens, E. W. N., J. V. Bailey, B. E. Flood, D. S. Jones, W. P. Gilhooly III, S. B. Joye, A. Teske, and O. U. Mason. (2015) "Barite encrustation of benthic sulfur-oxidizing bacteria at a marine cold seep." *Geobiology* 13: 588–603.

- Stevenson, A., J. A. Cray, J. P. Williams, R. Santos, R. Sahay, N. Neuenkirchen, C. D. McClure, *et al.* (2015) “Is there a common water-activity limit for the three domains of life?” *The ISME Journal* 9(6): 1333–1351.
- Stevenson, D. J. (2000) “Limits on the variation of thickness of Europa’s ice shell.” *31st Lunar and Planetary Science Conference*, The Woodlands, TX. Abstract #1506.
- Studinger, M., R. E. Bell, and A. A. Tikku. (2004) “Estimating the depth and shape of Subglacial Lake Vostok’s water cavity from aerogravity data.” *Geophysical Research Letters* 31(12). doi:10.1029/2004gl019801.
- Stumm, W., and J. J. Morgan. (1996) *Aquatic Chemistry: Chemical Equilibria and Rates in Natural Waters*. New York: John Wiley & Sons, Inc., 1022 pp.
- Sullivan, R., R. Greeley, J. Klemaszewski, J. Moreau, B. R. Tufts, J. W. Head III, R. Pappalardo, and J. Moore. (1999) “High resolution geological mapping of ridged plains on Europa. *30th Lunar and Planetary Science Conference*. The Woodlands, TX. Abstract #1925.
- Summons, R. E., P. Albrecht, G. McDonald, and J. M. Moldowan. (2008) “Molecular Biosignatures.” *Space Science Reviews* 135(1-4): 133–159.
- Summons, R. E., J. P. Amend, D. Bish, R. Buick, G. D. Cody, D. J. Des Marais, G. Dromart, *et al.* (2011) “Preservation of Martian organic and environmental records: Final Report of the Mars Biosignature Working Group.” *Astrobiology* 11(2): 157–181.
- Sundararaman, P., and J. E. Dahl. (1993) “Depositional environment, thermal maturity and irradiation effects on porphyrin distribution: Alum Shale, Sweden.” *Organic Geochemistry* 20(3): 333–337.
- Swalwell, J. E., F. Ribalet, and E. V. Armbrust. (2011) “Seaflow: A novel underway flow-cytometer for continuous observations of phytoplankton in the ocean.” *Limnology and Oceanography: Methods* 9(10): 466–477.
- Tang, M. J., G. D. McEwen, Y. Z. Wu, C. D. Miller, and A. H. Zhou. (2013) “Characterization and analysis of Mycobacteria and Gram-Negative Bacteria and co-culture mixtures by Raman microspectroscopy, FTIR, and Atomic Force Microscopy.” *Analytical and Bioanalytical Chemistry* 405(5): 1577–1591.
- Tarcea, N., M. Harz, P. Rosch, T. Frosch, M. Schmitt, H. Thiele, R. Hochleitner, and J. Popp. (2007) “UV Raman Spectroscopy: A technique for biological and mineralogical in situ planetary studies.” *Spectrochimica Acta, Part A: Molecular and Biomolecular Spectroscopy* 68(4): 1029–1035.
- Templeton, A., and K. Benzerara. (2015) “Emerging Frontiers in Geomicrobiology.” *Elements* 11(6): 423–429.
- Teolis, B. D., D. Y. Wyrick, A. Bouquet, B. A. Magee, and J. H. Waite (2017) “Plume and surface feature structure and compositional effects on Europa's global exosphere: Preliminary Europa mission predictions.” *Icarus* 284(1): 18–29.
- Thomas, N., B. S. Luthi, S. F. Hviid, H. U. Keller, W. J. Markiewicz, T. Blumchen, A. T. Basilevsky, *et al.* (2004) “The Microscope for Beagle 2.” *Planetary and Space Science* 52(9): 853–866.

- Tuorto, S. J., P. Darais, L. R. McGuinness, N. Panikov, T. Zhang, M. M. Haggblom, and L. J. Kerkhof. (2014) "Bacterial genome replication at subzero temperatures in permafrost." *The ISME Journal* 8: 139–149.
- Turtle, E. P., A. S. McEwen, G. C. Collins, L. Fletcher, C. J. Hansen, A. G. Hayes, T. A. Hurford, *et al.* (2016) "The Europa Imaging System (EIS): High-resolution imaging and topography to investigate Europa's geology, ice shell, and potential for current activity." *47th Lunar and Planetary Science Conference*. The Woodlands, TX. Abstract #1626.
- Tuschel, D. (2013) "Raman Spectroscopy of Oil Shale." *Spectroscopy* 28(3).
- United Nations Office for Outer Space Affairs [UNOOSA]. (1966) "Treaty on Principles Governing the Activities of States in the Exploration and Use of Outer Space, Including the Moon and Other Celestial Bodies."
<http://www.unoosa.org/oosa/ourwork/spacelaw/treaties/outerspacetreaty.html>
- van der Wielen, P. W., H. Bolhuis, S. Borin, D. Daffonchio, C. Corselli, L. Giuliano, G. D'Auria, *et al.* (2005) "The enigma of prokaryotic life in deep hypersaline anoxic basins." *Science* 307(5706): 121–123.
- Van Gorp, B., P. Mouroulis, D. Blaney, R. O. Green, B. L. Ehlmann, and J. I. Rodriguez. (2014) "Ultra-Compact Imaging Spectrometer for remote, in situ, and microscopic planetary mineralogy." *Journal of Applied Remote Sensing* 8(1).
doi:10.1117/1.JRS.8.084988.
- van Leewenhoek, A. (1677) "Observations, Communicated to the Publisher by Mr. Antony Van Leewenhoek, in a Dutch Letter of the 9th of Octob. 1676, Here English'd: Concerning Little Animals by Him Observed in Rain-, Well-, Sea and Snow-Water; as Also in Water Wherein Pepper Had Lain Infused." *Philosophical Transactions* 12(133-142): 821–831.
- Vance, S., L. E. Christensen, C. R. Webster, K. Sung. (2011) "Volatile organic sulfur compounds as biomarkers complementary to methane: Infrared absorption spectroscopy of CH₃SH enables in situ measurements on Earth and Mars." *Planetary and Space Science* 59(2-3): 299–303.
- Vance, S. D., K. P. Hand, and R. T. Pappalardo. (2016) "Geophysical controls of chemical disequilibria in Europa." *Geophysical Research Letters* 43(10): 4871–4879.
- Vasavada, A. R., J. P. Williams, D. A. Paige, K. E. Herkenhoff, N. T. Bridges, R. Greeley, B. C. Murray, D. S. Bass, and K. S. McBride. (2000) "Surface properties of Mars' polar layered deposits and polar landing sites." *Journal of Geophysical Research: Planets* 105(E3): 6961–6969.
- Vincent, J.-B., N. Oklay, M. Pajola, S. Höfner, H. Sierks, X. Hu, C. Barbieri, *et al.* (2016) "Are fractured cliffs the source of cometary dust jets? Insights from OSIRIS / Rosetta at 67P/Churyumov-Gerasimenko." *Astronomy and Astrophysics* 587. doi:10.1051/0004-6361/201527159.
- Vindedahl, A. M., J. H. Strehlau, W. A. Arnold, and R. L. Penn. (2016) "Organic matter and iron oxide nanoparticles: Aggregation, interactions, and reactivity." *Environmental Science: Nano* 3(3): 494–505.

- Wackett, L. P., A. Dodge, and L. B. M. Ellis. (2004) "Microbial genomics and the periodic table." *Applied and Environmental Microbiology* 70: 647–655.
- Wahr, J. M., M. T. Zuber, D. E. Smith, and J. I. Lunine. (2006) "Tides on Europa, and the thickness of Europa's icy shell." *Journal of Geophysical Research: Planets* 111(E12). doi:10.1029/2006JE002729.
- Waldhier, M. C., K. Dettmer, M. A. Gruber, and P. J. Oefner. (2010) "Comparison of derivatization and chromatographic methods for GC-MS analysis of amino acid enantiomers in physiological samples." *Journal of Chromatography B: Analytical Technologies in the Biomedical and Life Sciences* 878(15-16): 1103–1112.
- Wang, A., L. A. Haskin, A. L. Lane, T. J. Wdowiak, S. W. Squyres, R. J. Wilson, L. E. Hovland, *et al.* (2003) "Development of the Mars Microbeam Raman Spectrometer (MMRS)." *Journal of Geophysical Research: Planets* 108(E1). doi:10.1029/2002JE001902.
- Watanabe, K., H. Satoh, and T. Hoshiai. (1990) "Seasonal variation in ice algal assemblages in the fast ice near Syowa Station in 1983/84." In *Antarctic Ecosystems: Ecological Change and Conservation*, edited by K. R. Kerry and G. Hempel. Berlin: Springer-Verlag, p. 136–148.
- Webb, H. K., V. K. Truong, J. Hasan, R. J. Crawford, and E. P. Ivanoya. (2011) "Physico-mechanical characterisation of cells using Atomic Force Microscopy: Current research and methodologies." *Journal of Microbiological Methods* 86(2): 131–139.
- Westall, F., F. Foucher, N. Bost, M. Bertrand, D. Loizeau, J. L. Vago, G. Kminek, *et al.* (2015) "Biosignatures on Mars: What, Where, and How? Implications for the search for martian life." *Astrobiology* 15(11): 998–1029.
- White, O. L., O. M. Umurhan, and J. M. Moore. (2016) "Modeling of ice pinnacle formation on Callisto." *Journal of Geophysical Research: Planets* 121(1): 21–45.
- Whitman, W. B., D. C. Coleman, and W. J. Wiebe. (1998) "Prokaryotes: The unseen majority." *Proceedings of the National Academy of Sciences USA* 95: 6578–6583.
- Wiens, R. C., S. Maurice, K. McCabe, P. Cais, R. B. Anderson, O. Beyssac, L. Bonal, *et al.* (2016) "The SuperCam remote sensing instrument suite for Mars 2020." *47th Lunar and Planetary Science Conference*. The Woodlands, TX. Abstract #1322.
- Winters, Y. D., T. K. Lowenstein, and M. N. Timofeeff. (2013) "Identification of carotenoids in ancient salt from Death Valley, Saline Valley, and Searles Lake, California, using laser Raman spectroscopy." *Astrobiology* 13(11): 1065–1080.
- Wright, A., and M. Siegert. (2012) "A fourth inventory of Antarctic subglacial lakes." *Antarctic Science* 24(6): 659–664.
- Wüest, A., and E. Carmack. (2000) "A Priori estimates of mixing and circulation in the hard-to-reach water body of Lake Vostok." *Ocean Modelling* 2(1–2): 29–43.
- Yakimov, M. M., V. La Cono, G. L. Spada, G. Bortoluzzi, E. Messina, F. Smedile, E. Arcadi, *et al.* (2015) "Microbial community of the deep-sea brine Lake Kryos seawater-brine interface is active below the chaotropicity limit of life as revealed by recovery of mRNA." *Environmental Microbiology* 17(2): 364–382.

- Yingst, R. A., K. S. Edgett, M. R. Kennedy, G. M. Krezoski, M. J. McBride, M. E. Minitti, M. A. Ravine, and R. M. E. Williams. (2016) "MAHLI on Mars: Lessons learned operating a geoscience camera on a landed payload robotic arm." *Geoscientific Instrumentation, Methods and Data Systems* 5: 205–217.
- Zahnle, K., P. Schenk, H. Levison, and L. Dones. (2003) "Cratering rates in the outer Solar System." *Icarus* 163: 263–289.
- Zampolli, M. G., G. Basaglia, F. Dondi, R. Sternberg, C. Szopa, and M. C. Pietrogrande. (2007) "Gas Chromatography-Mass Spectrometry analysis of amino acid enantiomers as methyl chloroformate derivatives: Application to Space analysis." *Journal of Chromatography A* 1150(1-2): 162–172.
- Zegeye, A., G. Ona-Nguema, C. Carteret, L. Huguet, M. Abdelmoula, and F. Jorand. (2005) "Formation of hydroxysulphate Green Rust 2 as a single iron (II-III) mineral in microbial culture." *Geomicrobiology Journal* 22(7-8): 389–399.
- Zimmer, C., K. K. Khurana, and M. G. Kivelson. (2000) "Subsurface oceans on Europa and Callisto: Constraints from Galileo magnetometer observations." *Icarus* 147(22): 329–347.
- Zolotov, M. Y. (2007) "An oceanic composition on early and today's Enceladus." *Geophysical Research Letters* 34(23). doi:10.1029/2007GL031234.
- Zolotov, M. Y., and E. L. Shock. (2001) "Composition and stability of salts on the surface of Europa and their oceanic origin." *Journal of Geophysical Research: Planets* 106(E12): 32815–32827.
- . (2003) "Energy for biologic sulfate reduction in a hydrothermally formed ocean on Europa." *Journal of Geophysical Research: Planets* 108(E4). doi:10.1029/2002JE001966.
- . (2004) "A model for low-temperature biogeochemistry of sulfur, carbon, and iron on Europa." *Journal of Geophysical Research: Planets* 109(E6). doi:10.1029/2003JE002194.

APPENDICES

A.	Acronyms and Abbreviations	A-1
B.	Science Definition Team Findings	B-1

A. ACRONYMS AND ABBREVIATIONS

AA	amino acids
AFM	atomic force microscopy (technique) or atomic force microscope (instrument)
AFT	allowable flight temperature
AWI	Alfred Wegener Institute
CAPS	Committee on Astrobiology and Planetary Science
CBE	current best estimate
CCD	charge-coupled device
CDH	computer and data handling
CDW	Circumpolar Deep Water
CE	Common Era (or Current Era)
CE-MS	capillary electrophoresis mass spectrometry
CIRS	Compact Integrated Raman Spectrometer
CIVA	Comet Infrared and Visible Analyzer
CIVA-M	Comet Infrared and Visible Analyzer microscope
CMOS	complementary metal-oxide semiconductor
COSPAR	Committee on Space Research
CRISM	Compact Reconnaissance Imaging Spectrometer
CRO	Carrier Relay Orbiter
CRS	Context Remote Sensing
CRSI	Context Remote Sensing Instrument
CS	chiral selectors
CSIA	compound-specific isotope analysis
DDL	Deorbit, Descent, and Landing
DFAA	dissolved free amino acids
DFE	direct-from-Earth
DHMR	dry heat microbial reduction
DI	descent imaging
DMF-DMA	N,N-dimethylformamide dimethyl acetal

DNA	deoxyribonucleic acid
DOC	dissolved organic carbon
DOF	degrees of freedom
DRI	Desert Research Institute
DSM	Deep Space Maneuver
DSN	Deep Space Network
DTE	direct-to-Earth
DTM	digital terrain model OR digital topographic map
DUV	deep-ultraviolet
EECAM	Enhanced Engineering Camera
EGA	evolved gas analysis (science) OR Earth Gravity Assist (engineering)
EIS	Europa Imaging System
EMFM	Europa Multiple Flyby Mission
EPS	extracellular polymeric substances
ESA	European Space Agency
E-THEMIS	Europa Thermal Emission Imaging System
FOV	field of view
FTT	Fischer-Tropsch Type
GC	gas chromatograph
GC-MS	gas chromatograph mass spectrometer (the instrument) OR Gas Chromatography Mass Spectrometry (the technique)
GEANT4	Radiation modeling software
GITL	ground-in-the-loop
GIRE-2p	Galileo Interim Radiation Electron model
GPS	gas processing system
GSD	ground scale distance or ground sample distance
GSFC	Goddard Space Flight Center
GSS	Geophysical Sounding System
HGA	High-Gain Antenna
HiRISE	High-Resolution Imaging Science Experiment
HMR	heat microbial reduction
HQ	headquarters

HST	Hubble Space Telescope
ICBAO	International Bathymetric Chart of the Arctic Ocean
ICEMAG	Interior Characterization of Europa Using Magnetometry
ICEU	Instrument Control and Excitation Unit
IFOV	instantaneous field of view
iOH	internal optical head
IR	infrared
ISO	International Organization for Standardization
JAXA	Japan Aerospace Exploration Agency
JOI	Jupiter orbit insertion
JPL	Jet Propulsion Laboratory
JUICE	Jupiter Icy Moons Explorer
LC-MS	liquid chromatography mass spectrometry
LIDAR	Light Detection and Ranging
LISS	Lander Infrastructure Sensors for Science
LOD	limit of detection
LOQ	limit of quantitation
MAHLI	Mars Hand Lens Imager
MARDI	Mars Descent Imager
MASPEX	Mass Spectrometer for Planetary Exploration
MatISSE	Maturation of Instruments for Solar System Exploration
MECA	Microscopy, Electrochemistry, and Conductivity Analyzer
MER	Mars Exploration Rover
MIDAS	Micro-Imaging Dust Analysis System
MISE	Mapping Imaging Spectrometer for Europa
MISS	microbially-induced sedimentary structures
MLD	Microscope for Life Detection
MLI	multi-layer insulation
MMRS	Mars Microbeam Raman Spectrometer
MODIS	Moderate Resolution Imaging Spectroradiometer
MS	mass spectrometry – p. 56

MSA	Mission Support Area
MSL	Mars Science Laboratory
MTBSTFA	<i>N</i> -Methyl- <i>N</i> -tert-butyltrimethylsilyltrifluoroacetamide
NAC	Narrow Angle Camera
NAS	National Academy of Sciences
NASA	National Aeronautics & Space Administration
NIRVSS	Near-Infrared Volatile Spectrometer System
NPD	NASA Policy Directive
NPOC	non-purgeable organic carbon
NPR	NASA Procedural Requirements
NRC	National Research Council
OCA	Organic Compositional Analyzer
OM	optical microscope (instrument) or optical microscopy (technique)
OPAG	Outer Planets Assessment Group
OPTIMISM	Observatoire Planétologique Magnétisme et Sismique sur Mars
PAH	polycyclic aromatic hydrocarbon
PDS	Planetary Data System
PDV	Powered Descent Vehicle
PI	principal investigator
PIMS	Plasma Instrument for Magnetic Sounding
PJR	Peri-Jove Raise
PLFA	phospholipid fatty acid
PP	planetary protection
PRT	platinum resistance thermometer
QMS	quadrupole mass spectrometer
RA	robotic arm
RASP	rapid acquisition sampling package
RDF	radiation design factor
REASON	Radar for Europa Assessment and Sounding: Ocean to Near-surface
RGB	Red, Green, Blue
RLS	Raman Laser Spectrometer

RMI	Remote Micro-Imager
RNA	ribonucleic acid
RSD	relative standard deviation
SAM	Sample Analyzer at Mars
S/B	signal-to-baseline
SCF	structural, compositional, or functional
SD	standard deviation
SDT	Science Definition Team
SEIS	Seismic Experiment for Interior Structure
SEM	scanning electron microscopy
SfM	shape-from-motion
SHERLOC	Scanning Habitable Environments with Raman and Luminescence for Organics and Chemicals
SIA	Stable Isotope Analyzer
SISMO	Seismic instrument for Mars (part of OPTIMISM)
SLS	Space Launch System
SLV	Subglacial Lake Vostok
S-MS	separation mass spectrometer
SMS	Sample Manipulation System
SP	short-period
SPU	Spectrometer Unit
SRM	solid rocket motor
SSI	Solid State Imager
SSIT	Solid Sample Inlet Tube
STM	science traceability matrix
STScI	Space Telescope Science Institute
SUDA	Surface Dust Mass Analyzer
SWIR	short wavelength infrared
TID	total ionizing dose
TLS	tunable laser spectrometer
TRL	technology readiness level
TRN	Terrain Relative Navigation

UCIS	Ultra-Compact Imaging Spectrometer
UNOOSA	United Nations Office for Outer Space Affairs
USSR	Union of Soviet Socialist Republics
UV	ultraviolet
UVS	ultraviolet spectroscopic imaging
VBB	very broad band
VHF	very high frequency
VHP	vapor hydrogen peroxide
VNIR	visible near-infrared
VS	Vibrational Spectrometer

DEFINITIONS

Landing Zone	10 meter x 10 meter area around the lander
Workspace robotic arm	region within approximately 2 meters of lander accessible by the

UNITS

amu	atomic mass unit
cc	cubic centimeter (also cm ³)
cm	centimeter
cm ⁻¹	wavenumber
cm ²	square centimeter
cm ⁻²	per square centimeter
Da	Dalton
dB	decibel
dm	decimeter
eV	electron-volt
fmol	femtomole (10 ⁻¹⁵ moles)
g	gram
Gbit	gigabit (10 ⁹ bits)
Grad	gigarad (10 ⁹ rads)
Gyr	billion years

h/hr/hrs	hour(s)
Hz	hertz (equivalent to s^{-1})
J	joule
K	Kelvin
Kbps	kilobits per second
keV	kiloelectron-volt (10^3 eV)
kg	kilogram
kJ	kilojoule
km	kilometer
km ²	square kilometer
km ³	cubic kilometer
krad	kilorad (10^3 rads)
kW	kilowatt (10^3 watts)
kWh	kilowatt-hour
kyr	thousand years
L ⁻¹	per liter
<i>M</i>	molarity
m	meter
m ²	square meter
m ⁻²	per square meter
MB	megabyte (10^6 bytes)
mbar	millibar (10^{-3} bar)
Mbit	megabit (10^6 bits)
MeV	mega electron-volt (10^6 eV)
min	minute
mL	milliliter
mL ⁻¹	per milliliter
mm	millimeter
mmol	millimole (10^{-3} moles)
mol	mole
mol ⁻¹	per mole

MPa	megapascal (10^6 pascals)
Mrad	megarad (10^6 rads)
mW	milliwatt (10^{-3} watts)
Myr	million years
nm	nanometer
nM	nanomolar (10^{-9} M)
nmol	nanomole (10^{-9} moles)
Pa	pascal
per mille (‰)	parts per thousand (1×10^{-3} ; isotope geochemistry nomenclature)
pg	picogram (10^{-12} grams)
pmol	picomole (10^{-12} moles)
ppb	parts per billion (1×10^{-9})
ppbw	parts per billion by weight
ppm	parts per million (1×10^{-6})
ppt	parts per thousand (1×10^{-3})
pptr	parts per trillion (1×10^{-12})
px	pixel
rad	equivalent to absorbed radiation dose
s	second (also sec)
s ⁻¹	per second
W	watt
Wh	watt-hour
μm	micrometer (micron)
μM	micromolar (10^{-6} M)
μmol	micromole (10^{-6} moles)

B. SCIENCE DEFINITION TEAM FINDINGS

- **The SDT strongly recommends early coordination and integration of the instrument payload.** Sample handling, processing, and analyses would benefit significantly from optimization of sample-related operations, which could yield more efficient energy expenditure, resource allocation (mass, power, volume), and ultimately increase science return of the mission.
- **The SDT strongly recommends a close coupling between the Europa Lander Science Team, Project Science, and Project Engineering so as to optimize the potential science return from engineering subsystems and sensors on the Europa Lander mission spacecraft.** Engineering data from the Powered Descent Vehicle (during DDL landing operations), and from the lander engineering instruments and subsystems (during and after landing), supports multiple SDT goals and should be captured and returned to Earth as scientific datasets (which eliminates the need for additional science payload mass). A Deorbit, Descent and Landing (DDL) working group of scientists could be assembled to work closely with the Europa Lander Project to optimize science return from these assets.
- **NASA’s in situ search for life in our solar system would benefit from increased investments in advancing miniaturized microscope technologies for robotic spaceflight missions, specifically targeting evidence for life.**
- The SDT emphasizes that multi-scale connections from analyzed samples to local lander geology, to sub-regional context, and on to regional to global scales, are essential in the search for life on Europa. As a result, ensuring the collection and downlink of data from the different mission phases relevant to such scales should be prioritized (e.g., DDL-phase, Surface phase, and linking to the EMFM).
- The SDT emphasizes that interpretation of data collected from Europa’s near-subsurface optimally requires knowledge of sample heritage, emplacement mechanisms, and duration of surface exposure (radiation and ice crystallization state), as well as knowledge of the geologic context of samples (e.g., proximity to liquid water).
- The SDT recommends continued investment in establishing Earth-based ‘benchmark’ biosignatures to advance NASA’s capabilities for searching for life beyond Earth.
- The SDT recommends investment in establishing Europa surface reference materials so as to enable testing and refinement of processes for sample handling and analysis conducted by payload instruments that would operate on the surface of Europa.